Volume 30 / Issues 2,3 1991

CRITICAL REVIEWS

in

FOOD SCIENCE AND NUTRITION

Editor:

Fergus M. Clydesdale

CRC PRESS, INC.

Critical Reviews™ in Food Science and Nutrition

Volume 30 / Issues 2,3 1991

TABLE OF CONTENTS

Harry Levine
Louise Slade
14 July 2003

Critical Reviews in Food Science and Nutrition is published bi-monthly by CRC Press, Inc., 2000 Corporate Blvd., N.W., Boca Raton, FL 33431 USA. For 6 issues, U.S. rates are $99.50 to individuals; $295.00 to institutions; add $7.50 per issue foreign shipping and handling fees to all orders not shipped to a United States or Canada zip code. For immediate service and charge card sales, call our toll-free number: **1-800-272-7737** Monday through Friday (Continental U.S. only). Or send orders to: **CRC PRESS, INC., P.O. Box 750, Pearl River, NY 10965-0750.**

ISSN 1040-8398

Critical Reviews™ in

Food Science and Nutrition

Volume 30 / Issues 2,3 1991

Critical Reviews in Food Science and Nutrition, 30(2-3):115—360(1991)

Beyond Water Activity: Recent Advances Based on an Alternative Approach to the Assessment of Food Quality and Safety

Louise Slade and Harry Levine

Nabisco Brands, Inc., Fundamental Science Group, P.O. Box 1944, East Hanover, New Jersey 07936-1944.

Referee: **David S. Reid, Dept. of Food Science and Technology, Cruess Hall, University of California at Davis, Davis, California 95616.**

ABSTRACT: Water, the most abundant constituent of natural foods, is a ubiquitous plasticizer of most natural and fabricated food ingredients and products. Many of the new concepts and developments in modern food science and technology revolve around the role of water, and its manipulation, in food manufacturing, processing, and preservation. This article reviews the effects of water, as a near-universal solvent and plasticizer, on the behavior of polymeric (as well as oligomeric and monomeric) food materials and systems, with emphasis on the impact of water content (in terms of increasing system mobility and eventual water "availability") on food quality, safety, stability, and technological performance. This review describes a new perspective on moisture management, an old and established discipline now evolving to a theoretical basis of fundamental structure-property principles from the field of synthetic polymer science, including the innovative concepts of "water dynamics" and "glass dynamics". These integrated concepts focus on the non-equilibrium nature of all "real world" food products and processes, and stress the importance to successful moisture management of the maintenance of food systems in kinetically metastable, dynamically constrained glassy states rather than equilibrium thermodynamic phases. The understanding derived from this "food polymer science" approach to water relationships in foods has led to new insights and advances beyond the limited applicability of traditional concepts involving water activity. This article is neither a conventional nor comprehensive review of water activity, but rather a critical overview that presents and discusses current, usable information on moisture management theory, research, and practice applicable to food systems covering the broadest ranges of moisture content and processing/storage temperature conditions.

KEY WORDS: water activity, water relationships, moisture management, water as plasticizer, food polymer science, glass transition, water dynamics, glass dynamics

I. INTRODUCTION

Before 1950, many of the attributes of water-based food products were expressed in terms of water content, as was the ability of living cells to function optimally. In 1952, Scott[1] suggested that the (equilibrium thermodynamic) water activity (Aw), rather than water content, provided the true measure of physiological functioning and technological performance and quality. In recent years, more perceptive studies have shown that neither water content nor water activity can adequately account for the observed behavior of most moist, semi-moist, or almost-dry food systems.[2] Processes such as "water binding" and osmoregulation have been invoked in several empirical descriptions of food product stability or biological viability,[3] but none of these descriptions can be correlated with product safety or performance.[4-8]

In response to these shortcomings, a discussion conference, Water Activity: A Credible Measure of Technological Performance and Physiological Viability?, was convened at Girton

1040-8398/91/$.50

College, Cambridge, July 1 to 3, 1985, by the Industrial Physical Chemistry Group of the Faraday Division of the Royal Society of Chemistry, in association with the Food Chemistry Group (Industrial Division). Its main purpose was to clarify the significance and relevance of water activity as a measure of food product performance or the ability of living organisms to survive and function. A subsidiary objective was to arrive at recommendations for a more credible quality standard beyond water activity, still based on the properties of water. This conference was the genesis of this review.

The conference was divided into 4 half-day sessions on the basis of a "map of water regimes", defined by temperature and moisture content: very dilute systems near room temperature, steady-state systems at physiological temperatures, dry systems at and above room temperature, and concentrated systems over the broad range from subzero to elevated temperatures. The sessions emphasized the topics of the equilibrium thermodynamic basis of water activity, salting-in/salting-out phenomena, and specific molecular/ionic effects in dilute solutions near room temperature;[9,10] "compatible solutes" and osmoregulation in microbiological systems as complex dilute systems at physiological temperatures;[11] low-moisture food systems at room temperature and above, water vapor sorption, and sorption hysteresis as an indication of the inappropriate use of vapor pressure as a measure of water activity;[12,13] and intermediate-moisture, concentrated, and supersaturated glassy and rubbery food systems over a broad range of temperatures from subzero to over 200°C, water as plasticizer, and the mystique of "bound water".[14] In each session, an introductory critical review, by the speakers cited above,[9-14] was followed by a discussion among the participants (including industrial and academic scientists from the U.K., the Netherlands, France, Scotland, Switzerland, the U.S., Canada, and China; see Appendix) to develop a consensus of opinion. The final session was devoted to the drafting of a set of guidelines and recommendations for criteria of food quality and safety, more consistent with the current state of our knowledge of the physics and chemistry of aqueous systems.

The consensus of the meeting was that neither the equilibrium thermodynamic water activity nor its use as a parameter in water vapor sorption experiments should be used any longer as a criteria for performance and functioning of nonequilibrium food and biological systems in limited water.[2,15] Moreover, the concept of "bound water" is neither useful nor correct.[7,15] Discussion of alternative experimental approaches and interpretations for prediction of stability and biological behavior was based largely on the dynamically constrained behavior of polymers at different levels of plasticization. The consensus led to the adoption of a "water dynamics map" to describe the "map of water regimes" categorized by the speakers and to the recommendation of "water dynamics"[15,16] as a concept to serve as the next step in the evolution of criteria for food quality and safety.

This review describes the concept of water dynamics and its basis as a central element of a framework based on a "food polymer science" approach to the study of structure-property relationships in food products and processes.[8,14-39] The depth, breadth, and utility of this new research approach is contrasted with the limited scope and practical and technological shortcomings of the concept of water activity. In a critical rather than comprehensive fashion, this article reviews recent advances in the field of water relationships and moisture management in food systems during the decade of the 1980s, with emphasis on the period from the 1985 Faraday conference to the present. These advances have resulted in part from new interpretations and insights derived from the understanding provided by water dynamics and related elements of the food polymer science approach.

II. HISTORICAL BACKGROUND: SHORTCOMINGS OF THE TRADITIONAL APPROACH BASED ON THE CONCEPT OF Aw

It has been known for thousands of years that the quality and safety of naturally high-moisture foods are best preserved by storage at low moisture content and/or low temperature. Since the time of the Pharoahs, the shelf-lives of natural foods have been extended by removing water and

making foods dryer and/or by lowering the temperature and making foods colder. Ancient methods of food preservation were based on the generally correct assumption that the dryer and/or colder, the better, in terms of longer shelf-life. However, in modern times economic considerations regarding drying and refrigeration processes require us to ask the question: How dry is dry enough and how cold is cold enough to ensure optimum product quality and safety? Since the answers to these questions are not universal but rather specific to individual foods, we must be able to determine these answers, either empirically or, preferably, theoretically and predictively, based on fundamental physicochemical properties, which are both meaningful and measurable, of specific food materials.[40-42]

In recent decades, the concept of water activity advanced by Scott has become the traditional approach used universally to try to answer these questions. Because Aw (actually in terms of the relative vapor pressure of water in the headspace above a food) is an easily measured physicochemical property that can be empirically related to product shelf-life, Aw has become a strongly entrenched concept in the food science and technology literature. Despite this fact, the Aw concept is not universally useful or applicable, and an alternative, technologically practical approach is needed. A number of workers[2,16,43] have pointed out shortcomings and described serious problems that can arise when Aw is used as a predictor of food quality and safety. An alternative approach to the technological challenges of moisture management should emphasize three fundamental principles.[8,30] The first is that real food systems are never equilibrium systems, so that one must always deal with kinetics. Another is that there are interrelationships among the moisture content of a food sample, the time of an experiment or of a storage study, and the temperature, and that one can make manipulations or transformations among these three variables, so that one can predict shelf-life by interchanging the moisture and temperature parameters. Lastly, with respect to the question of just how cold and/or dry is good enough, one can establish reference conditions of temperature and moisture content to be measured for each solute or blend of solutes in an aqueous food system, so that one can begin to say, for example, that a particular freezer temperature is low enough, and closer to that temperature is better than farther above it for a given food material whose specific extent of maximal freeze-concentration in a realistic time frame (the process whereby the water-compatible solutes in a high-moisture food are maximally concentrated, due to the maximal phase separation of some portion of the total water in a food as *pure* ice, as the food is frozen by cooling to a sufficiently low subzero temperature[4]) can be measured quantitatively.[27,31-34,40-42]

The genesis of an alternative approach to moisture management based on these three principles dates back at least to 1966 and a seminal review by White and Cakebread[44] of glassy states in certain sugar-containing food products. They recognized (1) the importance of the glassy state, and of the glass transition temperature (Tg) and its location relative to the temperature of storage (either ambient or subzero), in a variety of aqueous food systems, including but not limited to boiled sugar candies, and (2) the critical role of water as a plasticizer of food glasses and the quantitative Tg-depressing effect of increasing content of plasticizing moisture, whereby Tg of a particular glass-forming solute-water mixture depends on the corresponding content of plasticizing water (Wg) in that glass at its Tg.[15] Tg and Wg represent the reference conditions of temperature and moisture content mentioned earlier.[16,30,40,41] White and Cakebread were apparently the first food scientists to allude to the broader implications of non-equilibrium glassy and rubbery states to the quality, safety, and storage stability of a wide range of glass-forming aqueous food systems. Evidently, outside a small community of candy technologists, the work of White and Cakebread, and its broader relevance to the field of moisture management and water relationships in foods, went largely unnoticed until the early 1980s. Since that time, other workers have helped to advance, with increasing momentum, concepts and approaches based on a similar recognition and ap-

plication of the principles underlying the importance of non-equilibrium glassy and rubbery states to food quality and safety.[4-8,14-43,45-66]

A. Intermediate Moisture Foods — Chemical, Physical, and Microbiological Stability

1. Intermediate Moisture Systems — Definitions

Most composite materials derived from naturally occurring molecules are subject to chemical, physical, and/or microbiological degradation and deterioration. As alluded to earlier, it was realized quite early on that such systems can be stabilized to some extent via the control of the moisture content. The role of water in processes that take place in semi-dry (or semi-moist) systems is complex: it can act as continuous phase (solvent, dispersion medium), as reactant (hydrolysis, protonation, etc.), and as plasticizer of biopolymer structures.

As already noted, in 1952 Scott[1] put forward the concept that it is the water activity, Aw, rather than the water content, that controls the various deterioration processes. (It should be clearly noted that the definition used by Scott was not actually the thermodynamic activity, but rather a steady-state relative vapor pressure.) This view has since been universally (and uncritically) adopted by the food industry and regulatory authorities,[67] and food products are labeled "intermediate moisture" when they are so formulated that their stabilities (physical, chemical, microbiological) depend on a critical value of Aw that must not be exceeded. The remainder of Section II.A reviews the factors that limit the utility of Aw as a measure of food quality and safety and as a predictive tool for the development of new "intermediate moisture foods" (IMFs).

2. Equilibrium Water Activity

Basic equilibrium thermodynamics teaches that the sign of the Fibbs free energy change, ΔG, determintes whether a given chemical reaction *can* proceed or not. Thus, chemical equilibrium is associated with the condition

$$\Delta G = 0 \text{ (at constant T and P)}$$

but the equilibrium is of a dynamic nature, i.e., the rates of the forward and backward reaction are equal. In an ideal aqueous system, the partial free energy (chemical potential) μ_i of any one component i is proportional to its mol fraction concentration x_i, which is itself proportional to its partial vapor pressure (Raoult's law). In a mixture where water is the only volatile component, its chemical potential is expressed in terms of the vapor pressure p by the equation

$$\mu_1 = \mu_1^\circ + RT \ln p \qquad (1)$$

where it is also assumed that the vapor above the system behaves as an ideal gas ($pV = RT$). For a real system, which deviates from Raoult's law and Henry's law, Equation 1 becomes increasingly approximate. Lewis and Randall[68] advanced the device of activity (Aw) to replace vapor pressure in Equation 1, such that Aw is proportional to p and becomes equal to p in the infinite dilution limit where the solution is ideal. This device makes it possible to retain simple, compact equations for the various thermodynamic properties even for nonideal systems. (The alternative would have been to add a series of correction terms.) Equation 1 is now rewritten in terms of Aw and contains a vapor pressure (p) term and an activity coefficient (f) term:

$$\begin{aligned} \mu_w &= \mu_w^\circ + RT \ln Aw \\ &= \mu_w^\circ + \underset{\text{ideal}}{RT \ln p} + \underset{\text{nonideal}}{RT \ln f} \end{aligned} \qquad (2)$$

The last term is a correction to allow for nonideal behavior in the system. In the limit of infinite dilution, $f = 1$ and

$$Aw = p/p^\circ \qquad (3)$$

where p° is the vapor pressure of pure *liquid* water under the same external conditions. Equation 3 is the expression usually found in the technical literature.

In many situations, other related quantities are used to express water activity, e.g., osmotic coefficients, water potential, relative humidity. Examples for ideal solutions (f = 1) are illustrated in Table 1.[9]

As described by Lilley,[9] reasons for departure from ideal behavior (shown in Figure 1)[9] include

1. Solute size (excluded volume).
2. Solvation effects; it is assumed that some solvent molecules, presumably those closest to the solute molecule, can be distinguished from the other solvent molecules by their interactions with the solute or their unique configurations — hence, the concept of "bound" water.
3. Intermolecular forces (between solute species); these might be modified as a result of specific solvation effects, see above.

Volume exclusion: for a binary aqueous solution

$$\ln Aw = 1 - [1/(x_w + Rx_s)] + \ln[x_w/(x_w + Rx_s)]$$

where x_i is the mol fraction of component i and R is the molar volume ratio solute:water. The effect on Aw is shown in Figure 2[9] for a 0.1 m solution; it can be significant.

Solvation: if a solute has a fixed hydration number h (water binding), then the effect on Aw is given by

$$Aw = (x_w - x_s h)/(x_w - x_s[h - 1])$$

The effect is shown in Figure 3[9] for 0.1 and 1.0 m solutions; note the marked dependence of Aw on h for high values of h.

Solute-solute interactions (association, aggregation, etc.): a simple example is given by the dimerization equilibrium

$$2S \Leftrightarrow S_2$$

In the limit where the association goes to completion and the dimerization constant becomes infinite, then

$$Aw = 2x_w/(2x_w + x_s)$$

This is illustrated in Figure 4.[9]

Cautionary note: for many aqueous systems, free energy-related functions such as Aw can be adequately fitted to one or more of the above

TABLE 1
Values of Some Properties, Related to Water Activity, of Ideal Aqueous Solutions at 25°C[9]

		Osmotic coefficients		Water potential	
Aw (= x_w)	m (mol kg^{-1})	g (ln Aw = g ln x_w)	ϕ (ln Aw = $-mM\phi$)	$-\Psi$ (Mpa) (ln Aw = $(\bar{v}_w/RT)\Psi$)	RH (Aw = RH/100)
0.9999	0.006	1	0.9999	0.0138	99.99
0.999	0.056	1	0.9995	0.138	99.9
0.99	0.561	1	0.994	1.38	99.0
0.90	6.17	1	0.948	14.5	90
0.80	13.8	1	0.898	30.7	80
0.70	23.8	1	0.832	40.1	70
0.60	37.0	1	0.766	70.3	60
0.50	55.5	1	0.693	95.4	50
0.40	83	1	0.613	126	40
0.30	130	1	0.514	165	30
0.20	222	1	0.402	221	20
0.10	500	1	0.256	317	10
0.01	5495	1	0.047	634	1

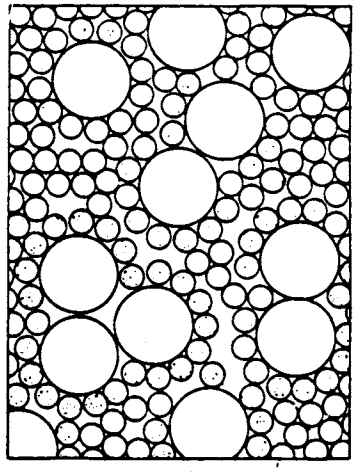

FIGURE 1. Schematic representation of a solution that would behave non-ideally, due to effects of volume exclusion, solvation, and solute-solute interactions. (Reproduced with permission from Reference 9.)

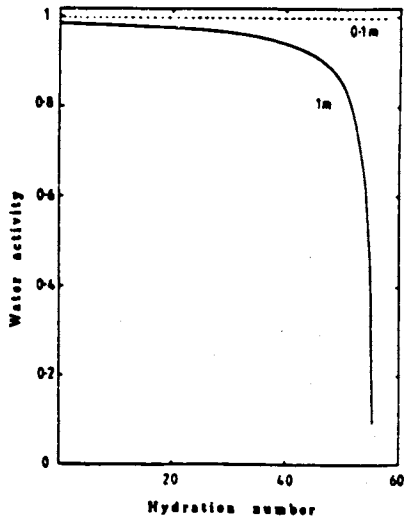

FIGURE 3. The effect of solute hydration number on the water activity of 0.1 and 1.0 molal solutions. (Reproduced with permission from Reference 9.)

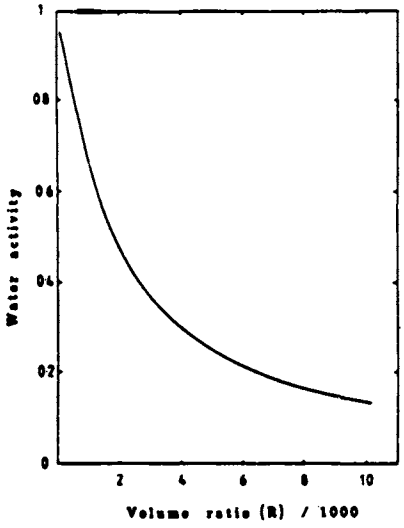

FIGURE 2. The effect of the molar volume ratio solute:water on the water activity of a non-ideal, binary aqueous solution. (Reproduced with permission from Reference 9.)

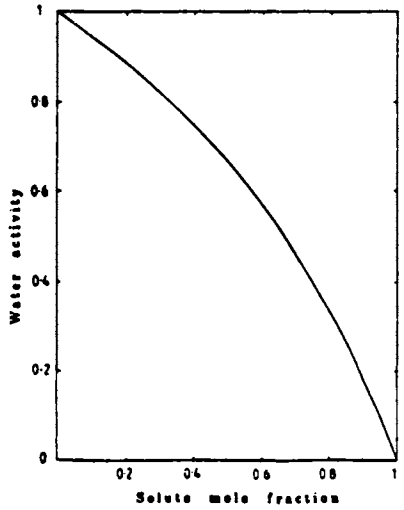

FIGURE 4. Variation of water activity with solute mole fraction. (Reproduced with permission from Reference 9.)

equations with only one parameter: R, h, or K (equilibrium constant). However, a good fit to the experimental data is not necessarily evidence of physical reality. A good test is the calculation of the effect of temperature on Aw and comparison with experiment. For instance, Aw of aqueous sugar solutions can usually be fitted by simple hydration equilibria of the type

$$S_{i-1} + H_2O \overset{K_{i-1}}{\Longleftrightarrow} S_i \quad i = 1,2,\ldots n$$

Assuming that all hydration sites i and all equilibrium constants K_{i-1} are equivalent, an average hydration number h can be calculated that depends only on Aw. Alternatively, Aw can be calculated by assigning a hydration number to

the sugar (usually equal to the number of $-OH$ groups). At 25°C the glucose data can be fitted up to saturation by putting $h = 6$ and $K = 0.789$ and the sucrose data ($h = 11$ and $K = 0.994$) up to 6 *M*! The fallacy of the model becomes apparent when the temperature dependence of K is considered. In both cases the model predicts that the equilibrium is shifted to the right by an increase in temperature, which is contrary to chemical common sense.

All of the previous equations only apply to ideal mixtures, i.e., Aw has been expressed without the introduction of activity coefficients (i.e., $Aw = p$). It is, of course, most unlikely that any real food system behaves ideally in the thermodynamic sense, especially at high concentrations (low Aw). It is also most unlikely that Aw can be realistically expressed in terms of any one of the described effects only. Probably Aw and its change with composition depend on the resultant of the molecular features of the particular system and its deviations from the laws that govern ideal mixtures.

Another cautionary note: all of the previous thermodynamic arguments apply to equilibrium situations only, but most food systems are formulated and processed such that equilibrium is deliberately avoided, e.g., butter, ice cream, bread dough, mayonnaise. The same is true for most fabricated products, e.g., paper, metal alloys, ceramics, plastics.

3. Equilibrium or Kinetics?

Although thermodynamics predicts whether a physical or chemical process *can* occur, it does not predict whether such a process *will* occur within a measurable time period. For example, at 25°C, liquid water has a lower free energy than a mixture of gaseous oxygen and hydrogen, i.e., liquid water is the stable phase under such conditions, and the conversion of the gaseous mixture to liquid water should occur spontaneously. However, the gases do not react. They do so, explosively, when a small amount of manganese dioxide powder is added (catalyst). The system is thus seen to be under kinetic control, and its observed behavior is dictated by the reaction rate, although the reaction could not take place under any circumstances if the free energy condition was not satisfied.

A distinction therefore must be made between true equilibrium and a (kinetic) stationary state. In practice this can be done by subjecting a system to a perturbation, e.g., raising the temperature, followed by a return to the initial temperature. If the system returns to its previous state (viscosity, pH, turbidity, etc.), i.e., exhibits no hysteresis, it is in equilibrium. Only then can one be sure that vapor pressure is a measure of activity.[43] If it does not, but it exhibits hysteresis and settles to another time-independent state, then it was under kinetic control. Examples are provided by concentrated polymer solutions, such as those illustrated in Figure 5.[10]

It has been emphasized repeatedly in recent years that, where a system is under kinetic control, the term water activity is meaningless and should not be used.[2,15,16,30,43,69] The experimentally measured vapor pressure (or relative humidity, RH) in the headspace over a food product is actually an apparent, relative vapor pressure (RVP), which cannot then be related to Aw or any other equilibrium thermodynamic quantity. In practical situations, p/p° *may* still be a good measure of stability and safety, but this cannot be taken for granted, and extreme care must be taken to ensure that it is indeed the case. In practice, deviations from ideal behavior can be expected for $Aw < 0.995$, calling into question the validity of Equation 3, and the onset of nonequilibrium behavior can be expected at $p/p^\circ < 0.9$, making the uncritical application of thermodynamics dangerous. In the realm of IMFs ($0.65 < Aw < 0.95$),[43] safety and stability therefore depend almost completely on kinetic factors and not on a true Aw.

A prime example of the confusion between equilibrium and kinetics is provided by Labuza's well-known "food stability map"[70] shown in Figure 6, in which relative deterioration rates (kinetics) are plotted against alleged water activity (thermodynamics). Such a practice is not to be recommended. While it has been suggested that this generalized diagram can be used to define safety limits for the spoilage of foods, van den Berg[43] has described such usage as a misapplication of the water activity concept. In any case, there is no formal cause/effect relationship

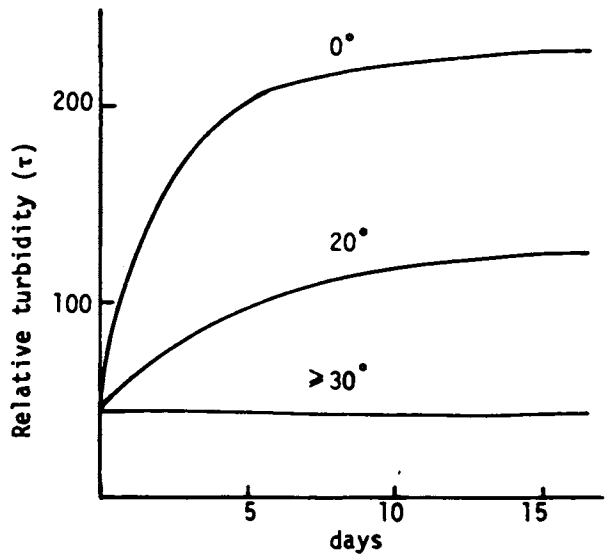

FIGURE 5. The increase in relative turbidity of an 8.5% aqueous solution of polyvinyl alcohol after rapid quenching from 90°C to the temperature indicated. (Reproduced with permission from Reference 10.)

between a reaction *rate* and Aw, which is an equilibrium thermodynamic function. In other words, y is *not* a function of x, as is implied. Note also that time dependence of a process has no place in equilibrium thermodynamics. No doubt some form of correlation can be described between a rate constant k and p/p°, but the generalized plot in Figure 6 is misleading,[43] and its misuse can be dangerous.[69] A comparison of maps drawn for different temperatures would probably show up its shortcomings, while a comparison of maps drawn for food systems composed of different solutes would most certainly do so.[2,15,16,30,43,69]

The map in Figure 6 can be useful generically, because it indicates qualitatively, for a given product, that at very low water content and measured RVP, lipid oxidation, and other free-radical reactions occur more rapidly than at somewhat higehr RVP, whereas in the limit of high RVP and moisture content, biological reactions occur with increasing rates. However, in order for Figure 6 to be universally applicable, the absolute values of RVP relevant to the quantitative spoilage behaviors of a product should be independent of the particular food system and its specific solutes composition. As is well known, this is emphatically not the case. For different food products composed of characteristic mixtures of different solutes, e.g., bread and pudding, at the same moisture content or the same measured RVP, the deterioration rate curves in Figure 6 would not be identical.

Van den Berg[43] has emphasized that the ef-

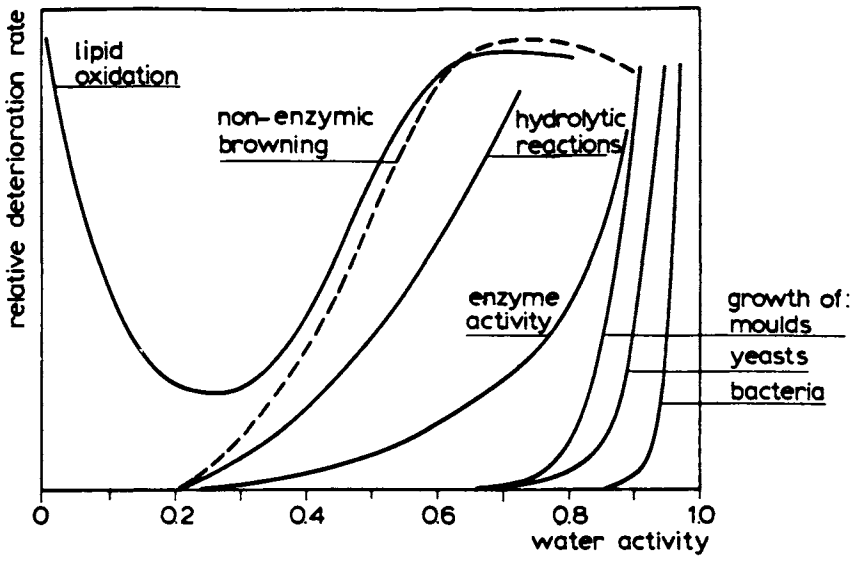

FIGURE 6. Generalized diagram of relative deterioration rates of food spoilage mechanisms as a function of water activity ("food stability map"). (Reproduced with permission from Reference 70.)

fect of water activity in foods depends on the composition of the solute(s). He has cited specific literature examples of both (a) different microbial reactions at identical Aw values adjusted with different solutes and (b) identical microbial reactions at different Aw values adjusted with different solutes. Other similar examples have been reported by Lang[71] and reviewed by Gould and Christian.[72] As a general rule, RVP increases with increasing solute molecular weight (MW), at the same solute concentration. Consequently, the effect of solute MW on microbiological stability is such that, at the same RVP, polymeric solutes produce more stable systems than do monomeric or oligomeric solutes.[16,71] Even though RVP is equal, the apparent "availability" of water is greater in the system containing the lower MW solute. Conversely, at the same moisture content, the lower MW solute system is more stable, apparently because its water "availability" is lower. Van den Berg[43] has concluded, in accord with Franks,[2] Gould,[11] and Gould and Christian,[72] that "apparently the microbial cell is not just a simple osmometer that stops working at a certain osmotic pressure." The term "water availability", although frequently used, is prone to misunderstanding, and its use should be discouraged, because it focuses unwarranted attention on the behavior of water in isolation. The actual basis for the concept of "water availability" concerns the nonequilibrium behavior, i.e., the kinetic nature, of a plasticizing diluent (e.g., a concentrated solute-water blend), in terms of its cooperative mobility and its mobilizing contribution to an included reporter (e.g., a microbial cell or amorphous food polymer in an aqueous sugar solution) compared with the corresponding plasticizing effectiveness of water alone. In a related vein, Mathlouthi et al.[73] have recently demonstrated that the mobilities of specific carbohydrate-water solutions (i.e., plasticizing solute-water diluents), rather than their Aw values, are the primary determinant of enzymatic activity (of lysozyme) and enzyme stability (of yeast alcohol dehydrogenase) in concentrated solutions of various small sugars and polyols at room temperature.

A more recent and graphic confirmation of these facts with respect to the rate of germination of mold spores has been reported by Slade and Levine.[14-16,30] Near room temperature, the initial germination of mold spores of *Aspergillus parasiticus* depends only on the availability of water, not on the presence of nutritents.[71] The experimental protocol, adapted from a microbiological assay used by Lang,[71] compared the inhibitory effects on conidia germination for a series of concentrated solutions of selected monomeric and polymeric glass-formers. The germination is essentially an all-or-nothing process, with the massive appearance of short hyphae surrounding the previously bare spores occurring within 1 d at 30°C in pure water or dilute solution (RVP $\simeq$ 1.0). As shown in Table 2,[16] the various glass-formers were assayed in pairs, deliberately matched as to the individual parameters of approximately equal RVP (at 30°C), solute concentration, MW, Tg′ and/or Wg′ (i.e., the particular Tg and Wg of the maximally freeze-concentrated solution[8,32,74]). Since true water activity is a colligative property of dilute solutions (i.e., it depends primarily on the number density of solute molecules),[2,43] solutes of equal MW, at the same concentration, should produce equal values of Aw. While this is generally true for dilute solutions, it is well known that concentrated solutions of, for example, different monosaccharide or disaccharide sugars, produce significantly different values of measured RVP at equal solute concentrations.[75,76] The relationship between experimental results for number of days required to germinate (as a relaxation time) and measured solution RVP was scrutinized. These results demonstrated conclusively that the observed rates of germination at 30°C showed no relationship with the measured RVPs. However, an approach based on mobility transformations to describe the kinetics of this mechanical relaxation process did facilitate interpretation of the germination data.[30] Rates of such a relaxation process reflect the kinetic nature of the plasticizing diluent (in this case, concentrated aqueous solutions), which depends on the cooperative translational mobility of the solute-water blend, rather than on "water availability" or "water activity" as reflected by measured apparent RVP. The results shown in Table 2 represented a graphic experimental demonstration of the failure of the Aw concept to account for the relative efficacy of different solute additives for microbial stabilization.

TABLE 2
Germination of Mold Spores of *Aspergillus Parasiticus* in Concentrated Solutions[16]

	Design parameters					Solution		Days required to germinate at 30°C
RVP[a] (30°C)	Tg′ (°K)	Wg′[b] (w% H_2O)	Tg (°K)	Tm (°K)	Tm/Tg	Conc. (w% H_2O)	Solute type	
Controls								
1.0						100	None	1
~1						99	Glucose (α-D)	1
~1						99	Fructose (β-D)	1
~1						99	PVP-40	1
~1						99	Glycerol	2
0.92	251.5	35	373	—		50	PVP-40	21
0.92	227.5	49.5	302	444.5	1.47	60	α-Methyl glucoside	1
0.83	231	49	373	397	1.06	50	Fructose	2
0.83	208	46	180	291	1.62	60	Glycerol	11
0.99	243.5	20	316	402	1.27	60	Maltose	2
0.97	241	36	325	465	1.43	60	Sucrose	4
0.95	250	31	349	406.5	1.16	50	Maltotriose	8
0.93	232	26	303	412.5	1.36	50	Mannose	4
0.95	250	31	349	406.5	1.16	50	Maltotriose	8
0.92	251.5	35	373	—		50	PVP-40	21
0.93	232	26	303	412.5	1.36	50	Mannose	4
0.87	231	49	373	397	1.06	54	Fructose	2
0.92	227.5	49.5	302	444.5	1.47	60	α-Methyl glucoside	1
0.87	231	49	373	397	1.06	54	Fructose	2
0.92	227.5	49.5	302	444.5	1.47	60	α-Methyl glucoside	1
0.70	231	49	373	397	1.06	30	Fructose	2
0.85	230	29	304	431	1.42	50	Glucose	6
0.83	231	49	373	397	1.06	50	Fructose	2
0.82	230.5	48	293	—		40	1/1 Fructose/ Glucose	5
0.98	247	36	339	—		50	PVP-10	11
0.98	231	49	373	397	1.06	60	Fructose	2
0.93	247	36	339	—		40	PVP-10	11
0.95	251.5	35	373	—		60	PVP-40	9
0.99	247	36	339	—		60	PVP-10	11
0.99	243.5	20	316	402	1.27	60	Maltose	2

[a] Relative vapor pressure measured after 7 d "equilibration" at 30°C.
[b] Wg′ expressed here in terms of w% water, for ease of comparison with solution concentration (also expressed in terms of w% water).

Despite the weight of such evidence, the misuse of Aw, a thermodynamic concept rigorously applicable only to dilute aqueous solutions at equilibrium, as a parameter to describe RVPs of concentrated aqueous systems of multiple, diverse solutes continues to be an everyday occurrence in the food industry. The real danger in this careless and oversimplified usage relates to government-defined and -imposed specifications for values of Aw (e.g., derived from Figure 6) required by law for microbiological safety and stability of IMF products for human consumption.[69] The potential for disaster inherent in naive compliance with such a rigid quantitative approach is frightening. The possibility that a community of food scientists could believe that specifying a maximum Aw value of 0.85 (or 0.75 or even 0.65) for a cheese cake filling can guarantee product safety, without any consideration of the nature of the mixture of water-compatible solids used to produce a particular Aw value, is both disheartening and potentially deadly.

Van den Berg[43] has remarked, with considerable understatement, that "it is not surprising therefore that in recent years, misconceptions have led to some difficulties in the preservation of intermediate moisture products." For example,[69] consider an intermediate-moisture pet food product that was originally formulated with a mixture of solutes (so-called "water binders") predominated by glucose and glycerol. This commercial product was empirically determined to be microbiologically safe and stable at an Aw of 0.92, which was thus incorporated as a product specification. Then, for the purpose of cost reduction, the glucose-glycerol combination was replaced by fructose and propylene glycol, but the Aw specification was not lowered in a corresponding and appropriate fashion,[30] but rather naively kept at 0.92. The financially disastrous result required a recall of millions of dollars worth of spoiled product. With knowledge of similar cases, van den Berg[43] concluded that "although Scott in his acclaimed papers was aware of the theoretical background of water activity, he did not distinguish clearly enough between product RVP and thermodynamic Aw." At least part of the subsequent blame for the current state of affairs must also rest with those who continue to make uncritical and indiscriminate use of Scott's work.

Take-home lesson: most physical and chemical processes that occur in intermediate moisture systems are under kinetic control (diffusion-limited), and product stability corresponds to a stationary state but not to equilibrium. Important practical implications of this statement are treated in later sections. Note: free radical-induced reactions may be an exception to the above rule. For now, suffice it to quote van den Berg's[43] conclusion regarding Figure 6: "it is more appropriate to make a clear distinction between the equilibrium nature of water activity and the kinetics of deterioration reactions . . . In practice, conclusions with regard to safe and economic specifications for dehydration and storage of a specific product should be drawn up only after careful consideration of the relevant water relations and conducting shelf-life studies . . . Because microorganisms respond differently to identical Aw levels set by different solutes, and because many foods are not in a state of equilibrium, as evidenced by hysteresis effects during humidification and drying, the use of water activity concepts cannot guarantee the accurate prediction of food shelf-life."

4. Water Activity and the Control of Microbiological Growth

As alluded to earlier, microbiological safety is the overriding consideration in food processing and storage. Products have to be seen to be safe for a period that extends beyond the stated shelf-life. Microbial and fungal growth must therefore be inhibited. Common techniques include sterilization (by heat or irradiation), pasteurization (extends shelf-life while maintaining quality), and moisture control. Like all other living organisms, microorganisms require water for their metabolism and growth. The cell is sensitive to osmotic pressure differences, as reflected in Aw. Conventional wisdom states that, for each cell type, there is a limiting Aw below which it cannot grow/metabolize. Usually the Aw values for optimal growth fall in the range (>0.99) where true equilibrium conditions exist, so that p/p° is probably a true description of Aw. This is no longer true for the limiting growth conditions (see Figure 7).[77] The absolute limit for microbial growth seems to be at RH = 60%, which is close to the value (55%) quoted for DNA denaturation. There is an upper growth limit for some organisms (e.g., halophilic bacteria, *Xeromyces*).

In their partly dehydrated states, cells stop growing and become metabolically inert. They sometimes survive in this state for long periods and may increase greatly in heat resistance, even by factors in excess of 1000-fold. They superficially resemble bacterial endospores, which are by far the most dormant and resistant forms of life on Earth.[72]

Many vegetative cells can respond to osmotic stress by the synthesis of cytoplasmic solutes (osmoregulation), i.e., they lower the internal "Aw", and this enables them to survive and grow. Osmoregulatory solutes include K^+, proline, betaines, glutamic acid, glucose, trehalose, sucrose, sorbitol, and glycerol.[72] They interfere minimally with the stabilities of intracellular enzymes at concentrations where most of the environmental solutes, especially NaCl, cause se-

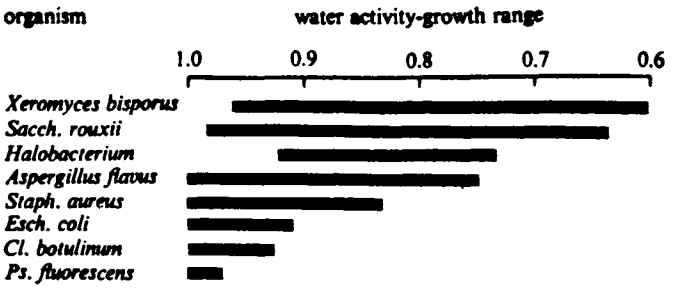

FIGURE 7. The water activity ranges for microbial growth of various microorganisms. (From Gould, G. W. and Measures, J. C., *Phil. Trans. R. Soc. London B.*, 278, 151, 1977. With permission.)

vere inhibition. They have high solubilities; they sometimes exist in concentrations >1 *M*. They have been termed "compatible solutes". Their synthesis requires energy and metabolic readjustments, as seen in the growth behavior of *B. subtilis* that has been subjected to a NaCl shock (see Figure 8).[77] Compatible solutes play a significant role in rendering overwintering insects resistant to freezing. The question is — why are they compatible?

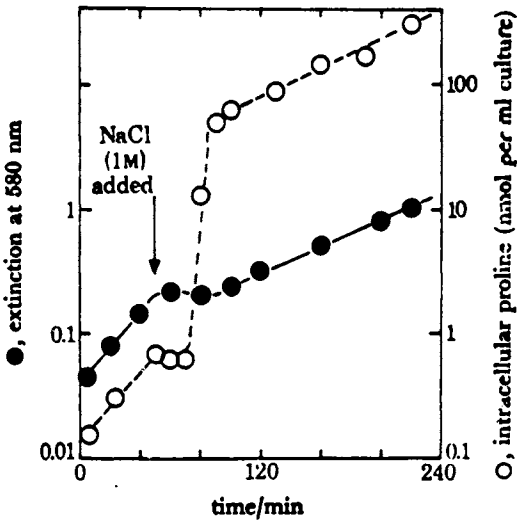

FIGURE 8. The growth behavior of *B. subtilis*, and its synthesis of proline, in response to a NaCl shock. (From Gould, G. W. and Measures, J. C., *Phil. Trans. R. Soc. London B.*, 278, 151, 1977. With permission.)

That Aw is not the only determinant of growth is demonstrated by culturing cells in different media at the same Aw. For example, as reviewed by van den Berg,[43] the limiting Aw values for some *Pseudomonas* species are 0.970 (in NaCl), 0.964 (in sucrose), and 0.945 (in glycerol). If a product was formulated to Aw = 0.970 with sucrose, it might not be safe. In any case, the measured RH is not necessarily related to Aw, i.e., what looks like osmotic equilibrium may be a steady state.

For any given solute, cell viability is usually correlated almost linearly with osmolality. The same holds for the effect of osmolality (Aw) on the stability of isolated enzymes, but notice, as shown in Figures 9[10] and 10,[10] the qualitatively different effects: sulfates stabilize most enzymes against heat denaturation, whereas CNS^-, NO_3^- or ClO_4^-, at the same measured Aw, destabilize enzymes almost to the same degree.

As mentioned earlier, there is no reason to believe that cells have evolved mechanisms capable of sensing Aw as such, i.e., they do not respond as simple osmometers.[11,72] Are there some other parameters that would form the basis of more rationally based criteria of cell activity as influenced by water and the aqueous environment? We do not know of any, but we can speculate that such criteria should include some factor related to environmental osmolality, but also[72]

1. Some measure of membrane permeability to the major solutes that are present
2. Some factor related to ionic vs. nonionic nature of the solutes (e.g., the salting-in vs. salting-out effect of salts, as illustrated in Figure 9, or nonelectrolytes, and the thermal stabilizing or destabilizing effect on en-

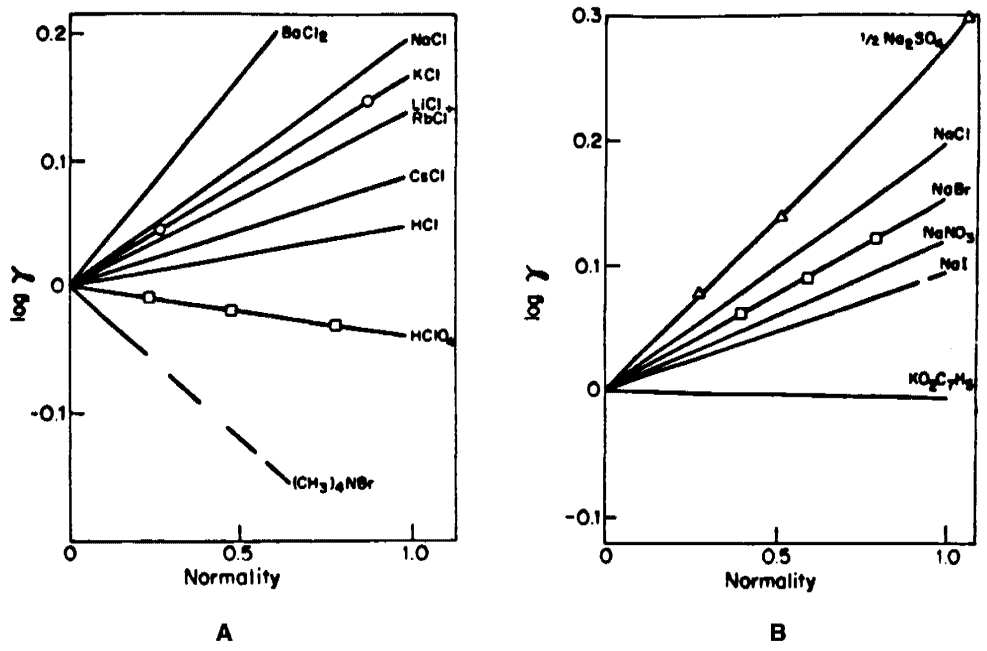

FIGURE 9. (A) Activity coefficients of ne benzene in aqueous chlorides, $HClO_4$ and $(CH_3)_4NBr$. (B) As in (A), but for Na^+-salts and K^+benzoate. (Reproduced with permission from Reference 10.)

zymes of nonionic hydroxy compounds, as shown in Figure 10)

3. Some factor related to the chemical (stereochemical) nature of the solutes (e.g., the marked differences in Aw between isomers at equal concentrations, as observed for ribose and xylose (see Figure 11))[10]
4. Some factor to take account of specific nutritional or toxic effects of the molecules that are present

So far, no synthesis of all these factors has been attempted.

Cautionary note — As described earlier, attempts to control the growth of food pathogens or other spoilage bacteria only by adjustment of RH can lead to disaster. Even chemically closely similar compounds (e.g., glucose and fructose) may have very different degrees of growth inhibition potential at the same measured RH, as they have likewise been shown by the results in Table 2 to have very different degrees of inhibition of mold spore germination.

Similar arguments apply to control by pH buffering. Isolated protein experiments show that the stability toward thermal denaturation is a function of pH, but the quantitative details of the function vary for different buffer systems. For example, denaturation temperature of ribonuclease at pH 2.1, I = 0.019:

Buffer	HCl–KCl	$H_2PO_4^-$–H_3PO_4	SO_4^{2-}–HSO_4^-
Temp. °C	29.9	32	43

The growth of cells in buffered systems may also depend on the nature of the buffer salts used. For instance, phosphates and acetates are used in the metabolism of *S. cerevisiae*, and do not act solely as pH controls. Citrate and phthalate ions are not metabolically active; they function as "normal" buffers. The growth behavior therefore depends not just on the pH but on the chemical nature of the buffer.

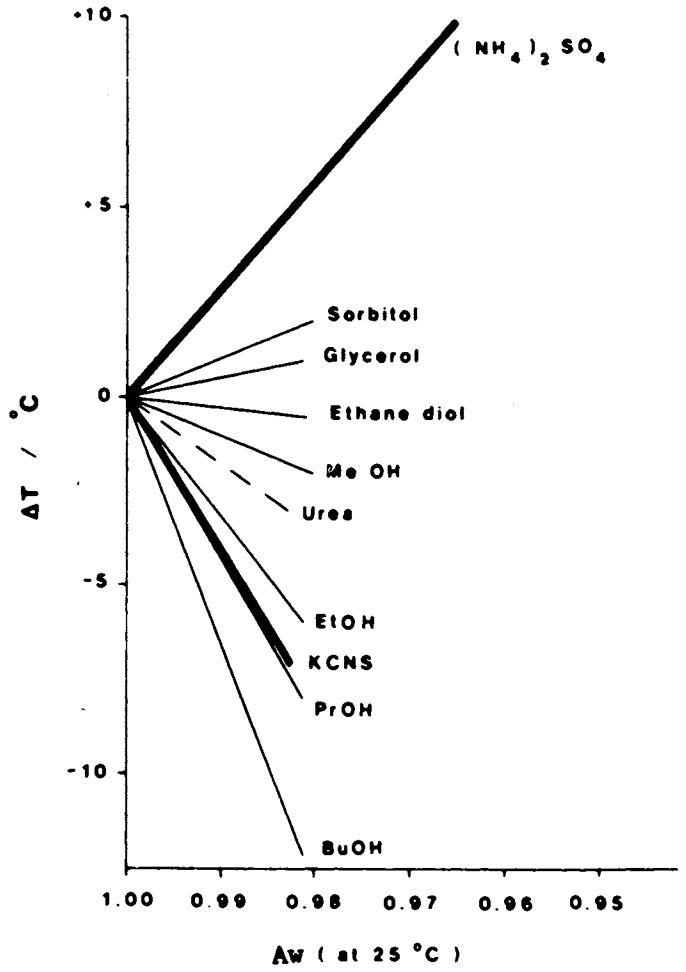

FIGURE 10. The effect of the osmolality (Aw) of various stabilizing or destabilizing solutes (mostly nonionic hydroxy compounds) on the thermal stability of ribonuclease enzyme at pH 7. (Reproduced with permission from Reference 10.)

Example: Growth of *S. aureus* at pH 5.4

	Generation time (h) at R.H. values:				
Acid	**0.99**	**0.95**	**0.93**	**0.91**	**0.89**
Citric	2.11	3.26	4.07	6.92	–
Phosphoric	0.84	1.36	3.85	–	–
HCl	0.49	1.66	2.36	7.83	–
Acetic	1.62	1.88	3.67	10.42	–

Conclusion: RH and pH are easy to measure, but they are only partially diagnostic of cell growth and metabolic rates.

5. Moisture Distribution in Heterogeneous Systems

All intermediate moisture systems are heterogeneous in chemical composition and/or physical structure. Most foods contain mixtures of proteins, carbohydrates, and lipids, each with a different affinity for water. Depending on such differences and also on diffusion rates within different substrates, water will become distributed non-uniformly in the product. This forms the basis of isopiestic vapor pressure measurements.

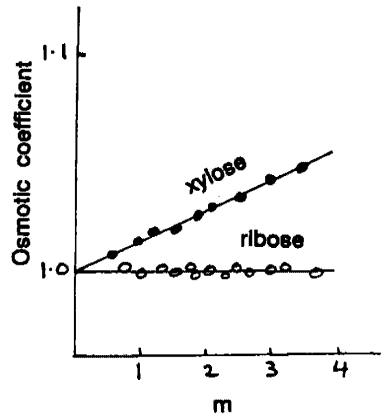

FIGURE 11. The marked difference in the variation of osmotic coefficient with solute molal concentration for the stereoisomers, ribose and xylose, at equal concentrations. (Reproduced with permission from Reference 10.)

It is commonly found that carbohydrates will dehydrate proteins, with the result that the carbohydrate component of a product may become susceptible to microbial growth, while the protein component is "safe".

Physical heterogeneity arises from the coexistence of several phases; commonly a crystalline phase can coexist with an amorphous solid phase (e.g., starch). In practice, the moisture content is calculated per gram solid. However, if the crystalline phase is anhydrous, the water is physically confined to the amorphous domains, and a more relevant estimate would be grams water per gram amorphous solid. When the crystalline phase is also hydrated (e.g., starch, gelatin), the moisture content may be non-uniformly distributed between the crystalline and amorphous domains, and separate estimates of grams water per gram crystalline solid and grams water per gram amorphous solid should be made. The ease of migration of water through a multiphase material depends on whether the amorphous component is in the glassy or rubbery (plastic) state and on the interfacial properties of the crystalline and amorphous domains. At $T < Tg$, diffusion-limited processes are inhibited during a realistic time period, so that water in the amorphous domains becomes essentially "unavailable" (i.e., immobilized) for typical deterioration reactions within practical food storage time periods.[8,14,16,43]

Physical heterogeneity and consequent unavailability of water can also arise from the existence of microscopic capillaries or pores in food systems such as biological tissues (with intact cell structure) and other porous materials (e.g., fabricated foods such as gels and emulsions). Pure water in capillaries of radius <1000 Å has a highly curved concave interface and consequently a lowered vapor pressure, depressed freezing point, and elevated boiling point relative to bulk water. The magnitude of the effect (on RVP, freezing point, and boiling point), which increases with decreasing capillary radius, can be calculated from Kelvin's equation.[78] Thus, in capillaries of 10 Å radius, even in the absence of dissolved solutes, water has a vapor pressure less than one third that of bulk water and a depressed freezing point of −15°C, so that such water can remain unfrozen indefinitely at freezer-storage temperatures above −15°C. In practice, water in capillaries <40 Å radius has been reported to be nonfreezing.[78]

No great reliance should be placed on moisture sorption isotherms, or on calculations based on such isotherms, for the following reasons. Both the Langmuir and BET equilibrium sorption theories are firmly based on a number of basic assumptions:[62,79]

1. The solid surface is inert and uniform; all sorption sites are equivalent.
2. The adsorbate does not penetrate the solid.
3. No interactions between sorbed molecules.
4. Sorption equilibrium is established such that the rates of adsorption and desorption are equal.
5. Only the first sorbed layer is affected by the solid substrate. Beyond that, multilayer sorption can be treated as condensation.

None of these assumptions holds good for food materials. The surfaces are not uniform; sorbed water molecules do interact, so that the probability of a site being occupied depends on whether neighboring sites are occupied; water penetrates and softens (plasticizes) the substrate,[15,25] thus affecting the nature of the surface (see Figure 12);[80] and equilibrium is *not* established,[15,26] as demonstrated by the inevitable sorption hysteresis[43,62] (see Figure 13).[43] Many workers have demonstrated that no sorption the-

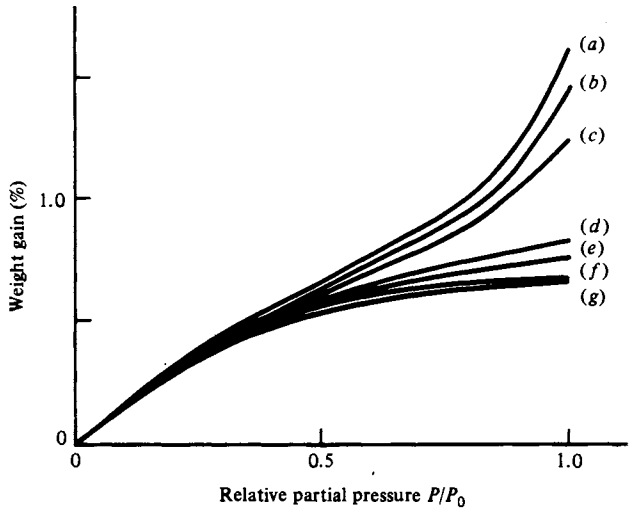

FIGURE 12. "Equilibrium" water vapor sorption isotherms of epoxy resin: (a) 25°C; (b) 35°C; (c) 75°C; (d) 100°C; (e) 125°C; (f) 150°C; (g) 175°C. (From Moy, P. and Karasz, F. E., *Water in Polymers,* Rowland, S. P., Ed., ACS Symp. Ser. 127, American Chemical Society, Washington, D.C., 1980, 505. With permission.)

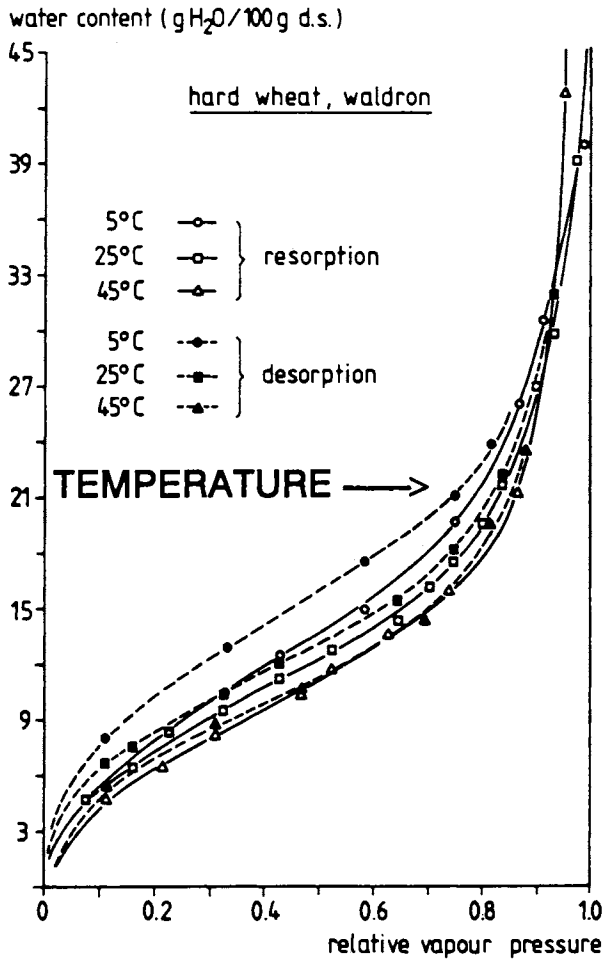

FIGURE 13. Hysteresis effect between desorption and resorption at three temperatures, as observed for milled hard wheat, type Waldron, origin U.S. (From van den Berg, C., *Concentration and Drying of Foods,* MacCarthy, D., Ed., Elsevier, London, 1986, 11. With permission.)

ory originally derived from equilibrium thermodynamics is capable of explaining this widely observed phenomenon of adsorption/desorption hysteresis which characterizes most "real world", non-equilibrium, sorbent-water systems. Despite this fact, the current literature still abounds with arguments over which is the best sorption theory (e.g., BET, GAB, etc.)[79] to apply to be *un*able to understand hysteresis.

The calculation of a notional monolayer coverage (e.g., BET) is meaningless under such conditions. As mentioned earlier, most free energy functions for aqueous solutions can be fitted by simple one- or two-parameter equations, but the assignment of physical meaning to the parameters is questionable. A correlation is no evidence for a cause/effect relationship. That is not to deny the practical usefulness of sorption isotherms; correlations may exist between isotherm shapes and shelf-lives. Thus, a particular isotherm may predict the storage life of tuna steaks and another the shelf-life of cheese crackers, but if the formulation of the cracker dough is altered, so will be the shape of the sorption isotherm. As a means of prediction from first principles, isotherms have very limited uses.

The fundamental problem with using moisture sorption isotherms to predict the shelf-lives of solid and semi-solid foods from their measured RVPs is that, due to the non-equilibrium nature of both aqueous food systems and sorption experiments,[14-16] the exact position and shape of an isotherm are sensitive to many factors, including[12,43]

1. Chemical composition, i.e., the specific combination of particular solutes and their MWs (e.g., sugars, polyols, polysaccharides, proteins) (see Figure 14)[81]
2. Temperature (see Figure 14), and its large effect on hysteresis (see Figure 13, where van den Berg[43] showed that (a) the extent

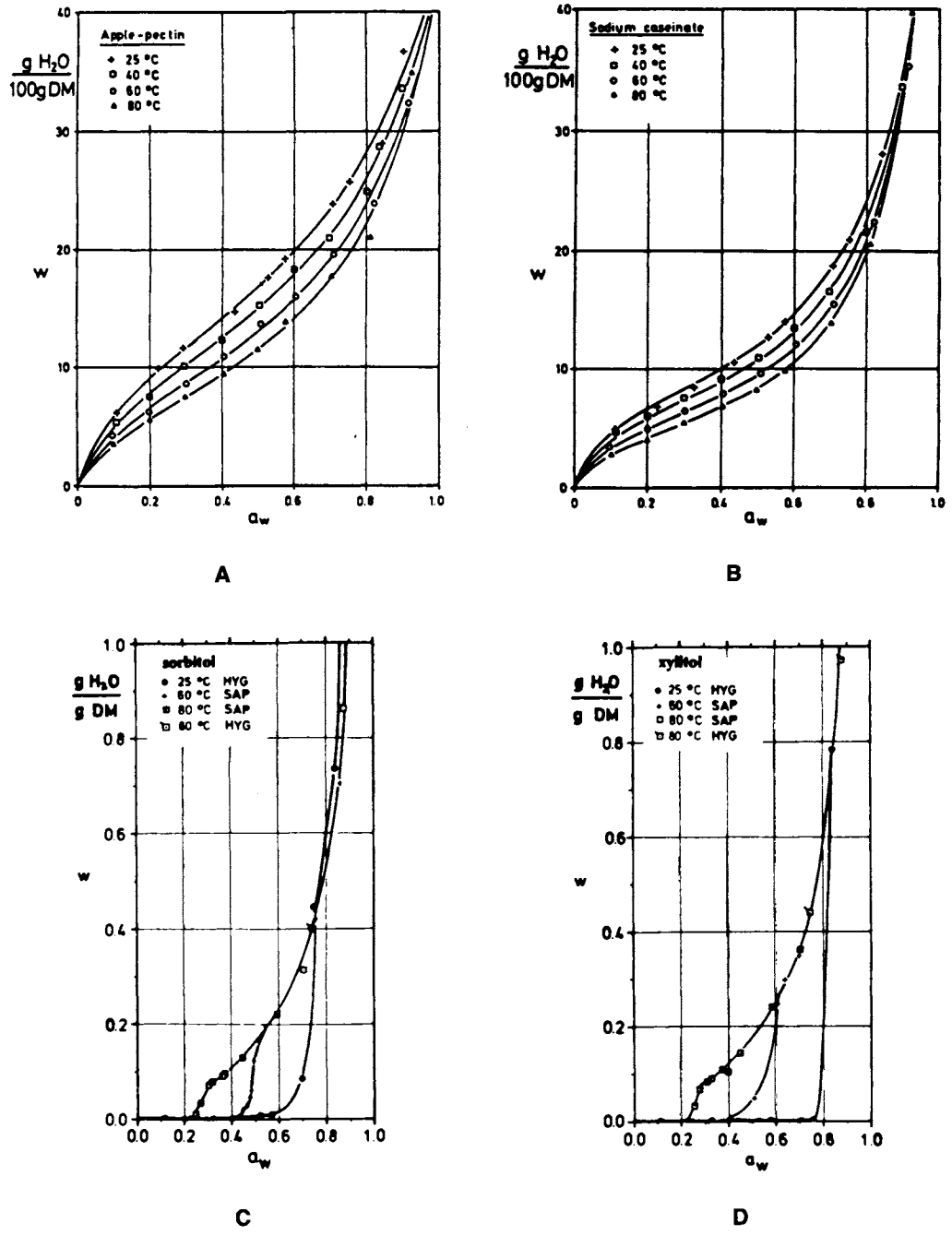

FIGURE 14. Sorption isotherms of (A) apple pectin and (B) sodium caseinate at 25, 40, 60, and 80°C. Adsorption isotherms of (C) sorbitol and (D) xylitol at 25, 60, and 80°C (HYG = Hygrostat; SAP = Sorption apparatus "rotasorp"). (From Weisser, H., *Properties of Water in Foods,* Simatos, D. and Multon, J. L., Eds., Martinus Nijhoff, Dordrecht, 1985, 95. With permission.)

of hysteresis between resorption and desorption isotherms measured at 5, 25, and 45°C for milled wheat increased with decreasing temperature, and (b) the effect of temperature was greater on the desorption isotherms than on the resorption isotherms)

3. Physical structure and state, i.e., amorphous or crystalline (see Figure 15A vs.

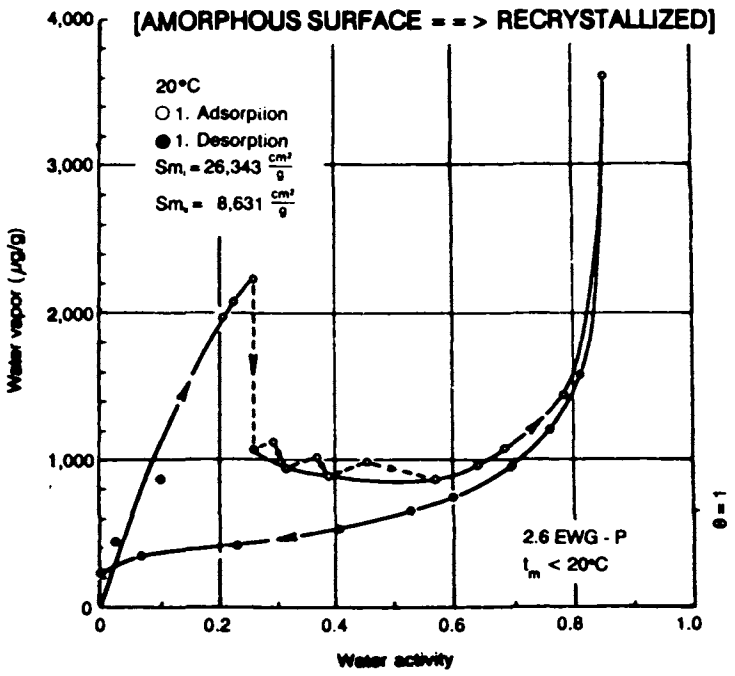

A

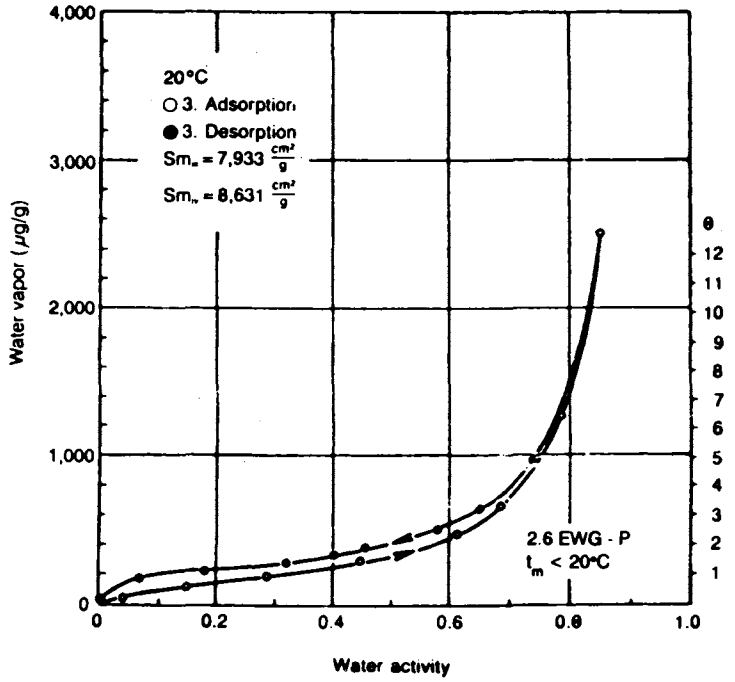

B

FIGURE 15. Sorption isotherms of (A) dry-milled sucrose and (B) crystalline sucrose, showing adsorption and desorption of water vapor. (From Niediek, E. A., *Food Technol.*, 42(11), 81, 1988. With permission.)

15B[82] for amorphous vs. crystalline sucrose), glassy or rubbery (see Figure 12, where the water-plasticized polymeric sorbent was still glassy up to 75°C, but had become rubbery by 100°C)[80]

4. Experimental history, i.e., previous desorption/resorption cycles (and resulting sample water content), and the hysteresis arising therefrom (see Figures 13 and 16A, where, in the latter, Bizot et al.[83] showed that, starting with fresh (wet) native potato starch, (a) there was a gradual closing of the hysteresis loop with repeated desorption/resorption cycles, and (b) the desorption curves were affected more than the resorption curves by the cycling history)
5. Sample history, i.e., origin and pretreatment (and resulting sample water content), and the hysteresis arising therefrom (see Figure 16B, where Bizot et al.[83] showed for a particular potato starch sample that (a) the extent of hysteresis depended on the pretreatment (native, dried vs. gelatinized, freeze-dried), and (b) the effect of pretreating the sample and thereby changing its microscopic structure was again greater on the desorption curve than on the resorption curve)
6. Isotherm measurement methodology

As a consequence of hysteresis, the RVP of a sample at a given moisture content differs between its adsorption and desorption isotherms. For equal RVP, there is greater apparent water "availability" (i.e., plasticizer mobility) in the system prepared by removing water, so the desorption system is less stable. Van den Berg[43] has pointed out that, in practice, factors 4 and 5 can have unknown and unpredictable effects on isotherms and their accuracy and reproducibility. For example, in Figure 16A, at a given moisture content, depending on whether the sample is being dried or remoistened and how many times it had occurred previously, there are six different choices of measured RVP or so-called "Aw" for this sample of native potato starch. Thus, van den Berg further cautions against using sorption isotherms measured by other workers when accurate isotherms are required, noting the wide scatter in literature values of isotherms for various food products, and emphasizes the limited value, except as a first estimate, of literature compilations of food isotherms.[43]

Examples from everyday experience serve to illustrate the consequences of sorption hysteresis due to sample history, as revealed in Figure 17. If we plot measured RVP in the headspace above the product vs. water content of the material (data from van den Berg)[43] for a series of common food systems that spans wide ranges of RVP and water content, the overall shape of the resulting curve resembles that of a typical sorption isotherm for a single food material. The most obvious departure from this overall behavior is the anomalous location of the data point for a raisin, which exhibits unexpectedly low RVP for such a moisture content. It is inferred that the anomalous behavior is due to desorption hysteresis, because the raisin is the only product in the series that is an IMF created by dehydration. It is interesting to note that the other two products that depart from the overall behavior exhibit the opposite anomaly. These two materials (French bread and Gouda cheese) are distinguished from others in the series by the fact that creation of these products, such that they have high quality, requires a deliberate thermosetting process.[25,26]

In the moisture management of IMF products, packaging is important. If dry air comes into contact with a product of high water content, then water evaporates from the surface. This sets up a concentration gradient, with the results that solutes migrate toward the interface together with the water. Also, solutes migrate away from the interface (which is a region of high concentration). The evaporation of water lowers the surface temperature of the solid, causing heat transfer between air and the solid, as well as inside the solid. If the air is not dry, then moisture might condense on the surface and migrate into the bulk, a well-known phenomenon. Lipid surface layers and membranes significantly retard such moisture redistribution processes.

Limited attempts have been made to map the sorption characteristics of lysozyme.[84] There is no reason why similar procedures cannot be applied more generally. The protein/enzyme complex was subjected to long-term desiccation at room temperature under vacuum. Water vapor

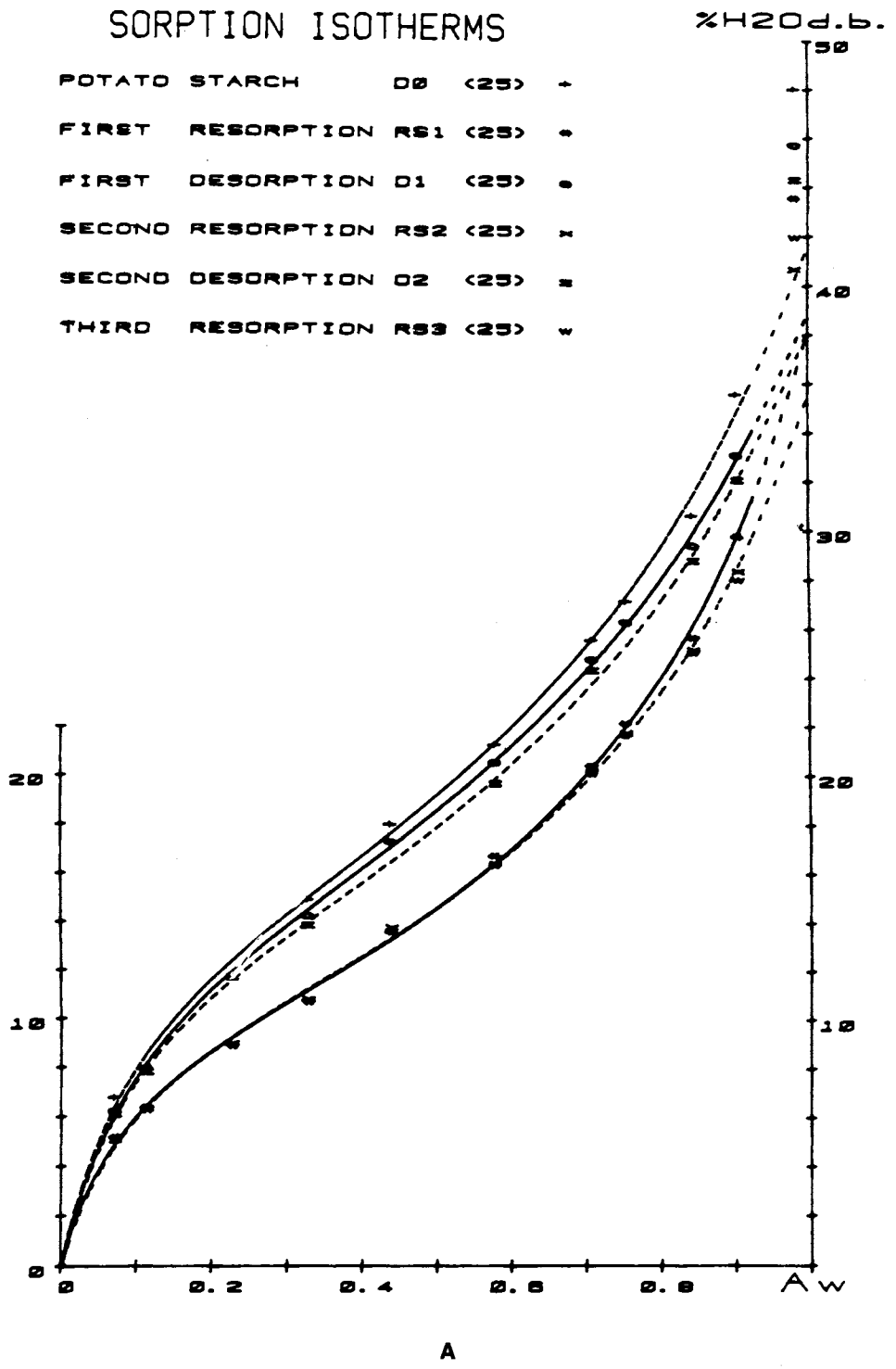

A

FIGURE 16. (A) Successive desorption-"resorption" cycles on fresh native potato starch (water content determination 1.5 h at 130°C; conditioning 8 d, reduced pressure, saturated salt solutions). (B) Comparison between sorption isotherms of potato starch: native (dotted lines) and 5% freeze-dried gel (full line). (From Bizot, H., Buleon, A., Mouhoud-Riou, N., and Multon, J. L., *Properties of Water in Foods,* Simatos, D. and Multon, J. L., Eds., Martinus Nijhoff, Dordrecht, 1985, 83. With permission.)

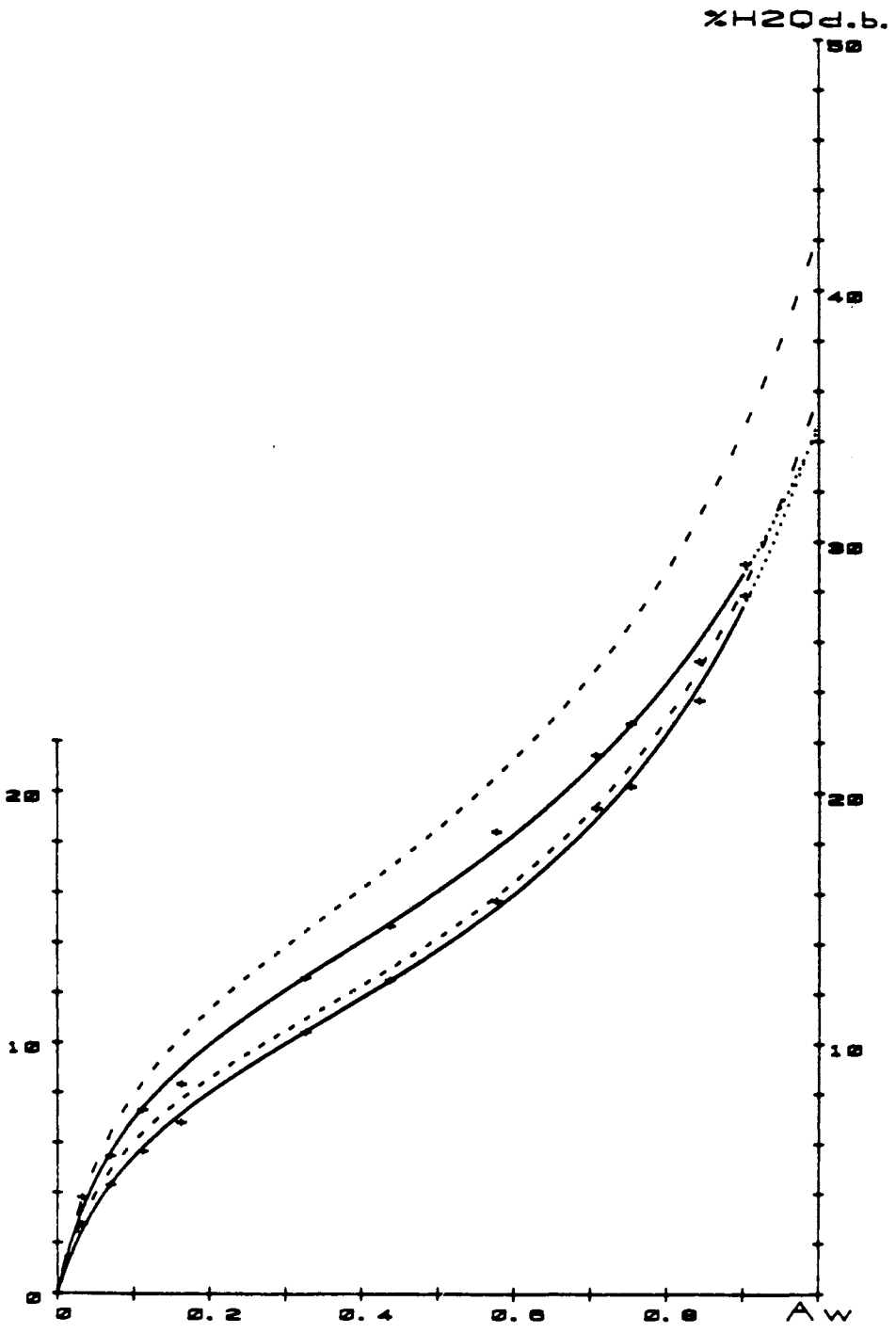

B

was then readmitted and the following properties were monitored:

1. Infrared amide bands (monitor peptide bonds)
2. Infrared COO^- bands (monitor acidic residues: glu, asp)
3. Infrared $-OD$ stretch (monitors perturbations of water molecules)

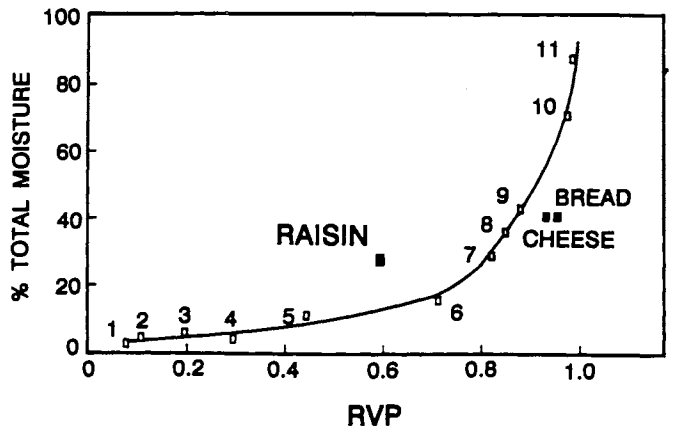

FIGURE 17. Plot of measured RVP at room temperature vs. water content for a series of common foods. Key to numbered data points: (1) crisp potato chips; (2) nonfat dry milk powder; (3) cookie; (4) boiled candy; (5) dry pasta; (6) wheat flour; (7) condensed milk; (8) marmalade; (9) sausage; (10) meat; (11) milk. (Data adapted from van den Berg, C., *Concentration and Drying of Foods,* MacCarthy, D., Ed., Elsevier Applied Science, London, 1986, 11.)

4. Specific heat (monitors internal degrees of freedom of macromolecule)
5. EPR (or NMR) rotational correlation time (estimate of freedom of rotational diffusion of macromolecule)
6. Enzyme activity

Changes and plateaus in the various properties as functions of moisture content indicate the order in which different atomic groupings become hydrated, as shown in the scheme in Figure 18.[85] Eventually enzyme activity is recovered (beginning at about 0.2 g water/g enzyme),[86] but full recovery only occurs at hydration levels of 9 grams water per gram enzyme. The moisture sorption isotherm for lysozyme is quite conventional in appearance[87] and does not (cannot) reveal any of the details shown in the scheme in Figure 18.

6. The Mythology of Bound Water

The food technology literature abounds in references to "bound" water (so do the literatures of other technological and biological disciplines). To be taken seriously, binding must be specified in terms of either position, energy, or lifetime. It must also be established that the binding is of an equilibrium type. The assignment of hydration numbers or hydration shells, obtained by fitting experimental data to a correlation equation, is not in itself proof of water binding, nor is the observation that a certain proportion of water in a complex amorphous material does not freeze within the time of the experiment. The notion that solid materials bind water (as manifested by measurements of so-called "water-binding capacity") can be of no help in the formulation of IMF products. The conclusive arguments debunking this popular myth and an alternative perspective based on the established role of water as a plasticizer of glass-forming materials are detailed in later sections.

III. AN ALTERNATIVE APPROACH TO MOISTURE MANAGEMENT IN FOOD SYSTEMS: THE FOOD POLYMER SCIENCE APPROACH

A. Key Elements of the Food Polymer Science Approach

Among a small but increasing number of food scientists, especially since 1980, there has been

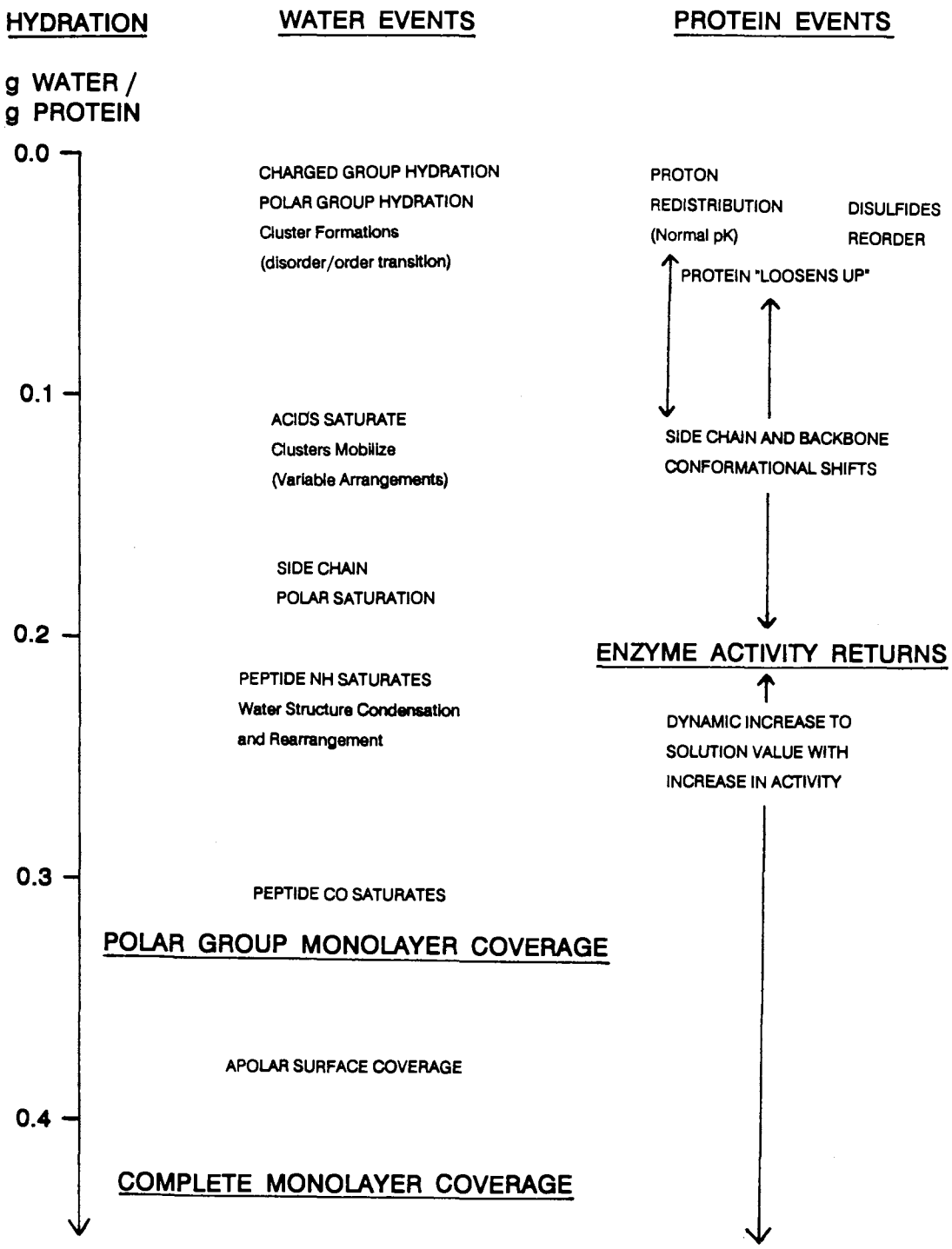

FIGURE 18. Scheme showing events postulated on sequential hydration of dry lysozyme. (From Franks, F., *Characterization of Proteins,* Franks, F., Ed., Humana Press, Clifton, NJ, 1988, 127. With permission.)

a growing awareness of the value of a polymer science approach to the study of food materials, products, and processes.[6-8,17-19,21,27,29-61,63-66,88-99] In this respect, food science has followed the compelling lead of the synthetic polymers field. As reviewed in detail in a number of recent publications,[15,16,20,22-26,28,34] the emerging research discipline of "food polymer science" empha-

sizes the fundamental and generic similarities between synthetic polymers and food molecules, and provides a new theoretical and experimental framework for the study of food systems that are kinetically constrained. On a theoretical basis of established structure-property relationships from the field of synthetic polymer science,[100-122] this innovative discipline has developed to unify structural aspects of foods, conceptualized as kinetically metastable, completely amorphous or partially crystalline, homologous polymer systems, with functional aspects, dependent upon mobility and conceptualized in terms of "water dynamics" and "glass dynamics".[15,16,20,22-26,28,34] These unified concepts have been used to explain and predict the functional properties of food materials during processing and product storage.[8,14,17-19,21,27,30-33,35-39] Key elements of this theoretical approach to investigations of food systems, with relevance to moisture management and water relationships, include recognition of[15,16,20,22-26,28,34-42]

1. The behavior of foods and food materials as classic polymer systems, and that the behavior is governed by dynamics rather than energetics
2. The importance of the characteristic temperature Tg, at which the glass-rubber transition occurs, as a physicochemical parameter that can determine processibility, product properties, quality, stability, and safety of food systems
3. The central role of water as a ubiquitous plasticizer of natural and fabricated amorphous food ingredients and products
4. The effect of water as a plasticizer on Tg and the resulting non-Arrhenius, diffusion-limited behavior of amorphous polymeric, oligomeric, and monomeric food materials in the rubbery liquid state at $T > Tg$
5. The significance of non-equilibrium glassy solid and rubbery liquid states (as opposed to equilibrium thermodynamic phases) in all "real world" food products and processes, and their effects on time-dependent structural and mechanical properties related to quality and storage stability.

In previous reports and reviews,[8,14-39] we have described how the recognition of these key elements of the food polymer science approach and their relevance to the behavior of a broad range of different types of foods (e.g., IMFs, low-moisture foods, frozen foods, starch-based foods, gelatin-, gluten-, and other protein-based foods) and corresponding aqueous model systems has increased markedly during this decade. We have illustrated the perspective afforded by using this conceptual framework and demonstrated the technological utility of this new approach to understand and explain complex behavior, design processes, and predict product quality, safety, and storage stability, based on fundamental structure-property relationships of food systems viewed as homologous families (i.e., monomers, oligomers, and high polymers) of partially crystalline glassy polymer systems plasticized by water. Referring to the food polymer science approach, John Blanshard (personal communication, 1987) has stated that "it is not often that a new concept casts fresh light across a whole area of research, but there is little doubt that the recognition of the importance of the transition from the glassy to the crystalline or rubbery state in food-stuffs, though well known in synthetic polymers, has opened up new and potentially very significant ways of thinking about food properties and stability." In a recent lecture on historical developments in industrial polysaccharides, James BeMiller has echoed Blanshard's words by remarking that a key point regarding the future of polysaccharide research and technology is "the potential, already partly realized, in applying ideas developed for synthetic polymers to polysaccharides; for example, the importance of the glassy state in many polysaccharide applications."[123]

In the rest of this article, we illustrate the theory and practice of food polymer science by highlighting selected aspects of experimental studies of both natural food materials and fabricated food ingredients and products, the results of which have been interpreted based on the theoretical physicochemical foundation provided by food polymer science. The studies have demonstrated the major opportunity offered by this food polymer science approach to expand not only our quantitative knowledge but also, of broader practical value, our qualitative understanding of moisture management and water re-

lationships in food products and processes well beyond the limited scope and shortcomings of the traditional Aw approach.

The technological importance of the glass transition in amorphous polymers and the characteristic temperature at which it occurs (Tg) is well known as a key aspect of synthetic polymer science.[107-109] Eisenberg[110] has stated that "the glass transition is perhaps the most important single parameter which one needs to know before one can decide on the application of the many non-crystalline (synthetic) polymers that are now available." Especially in the last several years, a growing number of food scientists have increasingly recognized the practical significance of the glass transition as a physicochemical event that can govern food processing, product properties, quality, safety, and stability.[4-8,12,14-66,74,82,88-99,124-126]

This recognition has gone hand-in-hand with an increasing awareness of the inherent non-equilibrium nature of all "real world" food products and processes, as exemplified by the category of IMFs, in which amorphous carbohydrates (polymeric and/or monomeric) and proteins are major functional components.[14,16] Other specific examples illustrative of food systems whose behavior is governed by dynamics far from equilibrium and of the practical problems of food science and technology posed by their non-equilibrium nature include graininess and iciness in ice cream, reduced survival of frozen enzymes and living cells, reduced activity and shelf-stability of freeze-dried proteins, lumping of dry powders, bloom on chocolate, recipe requirements for gelatin desserts, cooking of cereals and grains, expansion of bread during baking, collapse of cake during baking, cookie baking — effects of flour and sugar, and staling of baked products.[15] Thermal and thermomechanical analysis methods have been shown to be particularly well-suited to study such non-equilibrium systems, in order to define structure-activity relationships, e.g., of synthetic amorphous polymers, from measurements of their thermal and mechanical properties.[117] Differential scanning calorimetry (DSC) and dynamic mechanical analysis (DMA) have become established methods for characterizing the kinetic (i.e., time-dependent) transition from the glassy solid to the rubbery liquid state that occurs at Tg in completely amorphous and partially crystalline, synthetic and natural polymer systems,[127] including many food materials.[128] The focus of a polymer science approach to thermal analysis studies of structure-function relationships in food systems[8,14-39] emphasizes the insights gained by an appreciation of the fundamental similarities between synthetic amorphous polymers and glass-forming aqueous food materials with respect to their thermal, mechanical, and structural properties. Based on this approach, DSC results have been used to demonstrate that product quality and stability often depend on the maintenance of food systems in kinetically metastable, dynamically constrained, time-dependent glassy and/or rubbery states rather than equilibrium thermodynamic phases, and that these non-equilibrium physical states determine the time-dependent thermomechanical, rheological, and textural properties of food materials.[8,14-39]

Plasticization, and its modulating effect on the temperature location of the glass transition, is another key technological aspect of synthetic polymer science.[109] In that field, the classic definition of a plasticizer is "a material incorporated in a polymer to increase the polymer's workability, flexibility, or extensibility".[109] Characteristically, the Tg of an undiluted polymer is much higher than that of a typical low MW, glass-forming diluent. As the diluent concentration of a solution increases, Tg decreases monotonically, because the average MW of the homogeneous polymer-plasticizer mixture decreases, and its free volume increases.[107] A polymer science approach to the thermal analysis of food systems (both model and real) involves recognition of the critical role of water as an effective plasticizer of amorphous polymeric, oligomeric, and monomeric food materials.[4-8,14-66,74,88-94,98,124] Sears and Darby[109] have stated unequivocally that "water is the most ubiquitous plasticizer in our world." Karel[54] has noted that "water is the most important . . . plasticizer for hydrophilic food components." It has become well documented, in large part through DSC studies, that plasticization by water results in a depression of the Tg (and of the melt viscosity and elastic modulus) of completely amorphous and partially crystalline food ingredients, and that

this Tg depression may be advantageous or disadvantageous to product processing, functional properties, and storage stability. Recently, there has been expanding interest in the importance of the effect of water as a plasticizer of many different food materials and other biopolymers (see[15,25,26] and references therein), including starch, gluten,[99] starch hydrolysis products (SHPs),[59] low MW sugars[42,66,124] and polyhydric alcohols,[42,91] gelatin, collagen, elastin, lysozyme and other enzymes, and the semicrystalline cellulose and amorphous hemicelluloses and lignin components of wood.[129]

Atkins[90] has succinctly stated the important observation that "water acts as a plasticizer, dropping the Tg of most biological materials from about 200°C (for anhydrous polymers, e.g., starch, gluten, gelatin)[15] to about −10°C or so (under physiological conditions of water content), without which they would be glassy" (in their native, *in vivo* state). The latter Tg of about −10°C is in fact characteristic of high MW biopolymers at or above moisture contents near 30% corresponding to physiological conditions, as has been reported for many polymeric carbohydrates and proteins, including starch, gluten, gelatin,[15] hemicelluloses,[129] and elastin.[90] Elastin epitomizes a case where this subzero Tg is critical to healthy physiological function. Elastin exists as a completely amorphous, water-plasticized, covalently crosslinked (via disulfide bonds), network-forming polymer system whose viscoelastic properties have been likened to those of wheat gluten.[45,88] In its role as a major fibrous structural protein of skin, ligaments, and arteries, elastin exists *in vivo* as a rubbery liquid that demonstrates classic rubber-like elasticity[107] only as long as its Tg remains well below 0°C, due to a water content of 0.40 g/g protein. In contrast, in the pathologic state of arteriosclerosis ("hardening of the arteries"), elastin becomes a glassy solid at body temperature due to a decrease in water content to 0.17 g/g and a corresponding increase in Tg to 40°C (as shown by the so-called "glass curve" of Tg vs. moisture content in Figure 19A).[130,131] As with the case of lysozyme described earlier, the moisture sorption isotherm for dry elastin (see Figure 19B)[132] is also quite conventionally sigmoid-shaped in appearance and does not reveal the critical implications of the

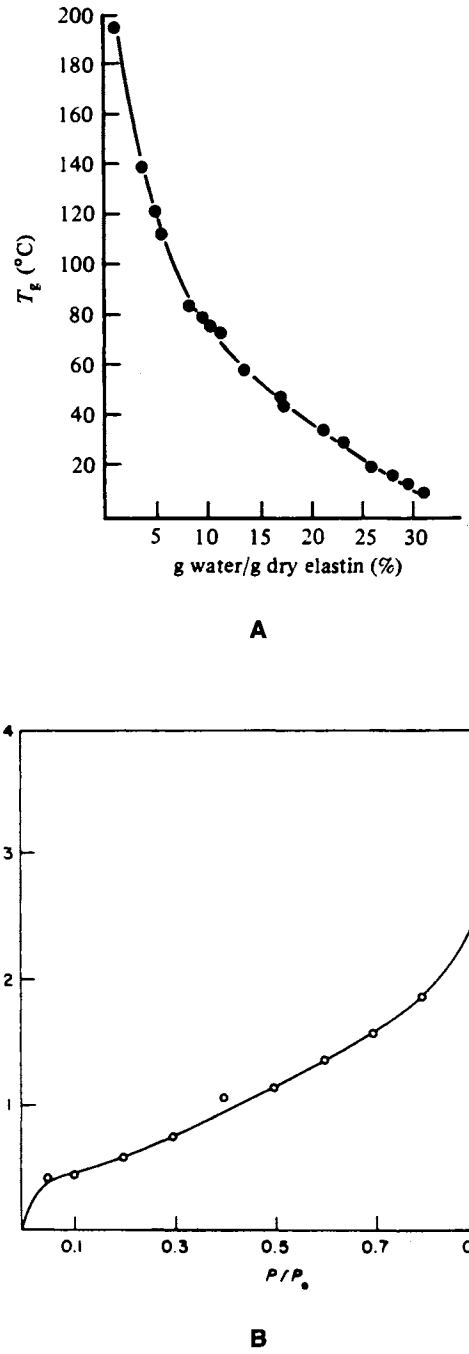

FIGURE 19. (A) Tg as a function of water content for elastin. (Reproduced with permission from Reference 130.) (B) Sorption isotherm for water in elastin at 25°C. (From Scandola, M., Ceccorulli, G., and Pizzoli, M., *Int. J. Biol. Macromol.*, 3, 147, 1981. With permission.)

structure-function relationship described earlier.

A unified conceptual approach to research on water relationships in food polymer systems, based on established principles translated from

synthetic polymer science, has enhanced our qualitative understanding of structure-function relationships in a wide variety of food ingredients and products.[8,14-39] Lillford et al.[45,97] have advocated a related "materials science approach" to studies of (1) the influence of water on the mechanical behavior of dough and batter before, during, and after baking, and (2) the mechanical properties of solid food foams as affected by "the plasticizing action of water". Similarly, in a recent review of structure-property relationships in starch, Zobel[61] has cited concepts used to characterize synthetic polymers and advocated this approach to provide increased understanding of the amorphous state and its role in determining physical properties of native and gelatinized starches. Others who have recently applied a synthetic polymers approach to characterize the glass transition, crystallization, melting, or annealing behavior of food polymers such as starch or gluten have included Blanshard,[47-49,88,94] Hoseney,[51-53,95,96] Ring,[59,92] Biliaderis,[46] and Fujio.[99] A central theme of our so-called "food polymer science" approach focuses on the effect of water as a plasticizer on the glass transition and resulting diffusion-limited behavior of water-soluble or water-miscible (collectively referred to as water-compatible) and water-sensitive amorphous materials or amorphous regions of partially crystalline materials.[15,25,26] Plasticization, on a molecular level, leads to increased intermolecular space or free volume, decreased local viscosity, and concomitant increased mobility.[107] Plasticization implies intimate mixing, such that a plasticizer is homogeneously blended in a polymer, or a polymer in a plasticizer. Note that a true solvent, capable of cooperative dissolution of the ordered crystalline state and having high thermodynamic compatibility and miscibility at all proportions, is always also a plasticizer, but a plasticizer is not always a solvent.[109] Water-compatible food polymers such as starch, gluten, and gelatin, for which water is an efficient plasticizer but not necessarily a good solvent, exhibit essentially the same physicochemical responses to plasticization by water as do many water-compatible synthetic polymers[111] and many readily soluble monomeric and oligomeric carbohydrates.[15] This fact demonstrates two underlying precepts of the food polymer science approach: (1) synthetic amorphous polymers and glass-forming aqueous food materials are fundamentally similar in behavior, and (2) food ingredients can be viewed generically as members of homologous families of completely amorphous or partially crystalline polymers, oligomers, and monomers, soluble in and/or plasticized by water. The series from glucose through malto-oligosaccharides to the amylose and amylopectin components of starch exemplifies such a homologous polymer family.

On a theoretical basis of established structure-property relationships for synthetic polymers, the functional properties of food materials during processing and product storage can be successfully explained and often predicted.[15,25,26] The discipline of food polymer science has developed to unify structural aspects of foods, conceptualized as completely amorphous or partially crystalline polymer systems (the latter typically based on the classic "fringed micelle" morphological model[100,103,113] shown in Figure 20),[24] with functional aspects, depending on mobility and conceptualized in terms of the integrated concepts of "water dynamics" and "glass dynamics". Through this unification, the appropriate kinetic description of the non-equilibrium thermomechanical behavior of food systems has been illustrated in the context of a "dynamics map", shown in Figure 21.[30] This map was derived from a generic solute-solvent state diagram,[74,133] in turn based originally on a more familiar equilibrium phase diagram of temperature vs. composition. The dynamics map, like the "supplemented state diagram",[133] is complicated by the attempt to represent aspects of both equilibrium and non-equilibrium thermodynamics in a single figure. The primary distinction at atmospheric pressure is that the equilibrium regions are completely described as shown in two dimensions of temperature and composition, with no time dependence, while the non-equilibrium regions emphatically require the third dimension of time, expressed as t/τ, where τ is a relaxation time. In this way, the time dependence of a dynamic process can be defined in terms of the relationship between the experimental time scale and the time frame of the relaxation process undergone by the system. The established principle of time-temperature superpositioning[134] has been extended to

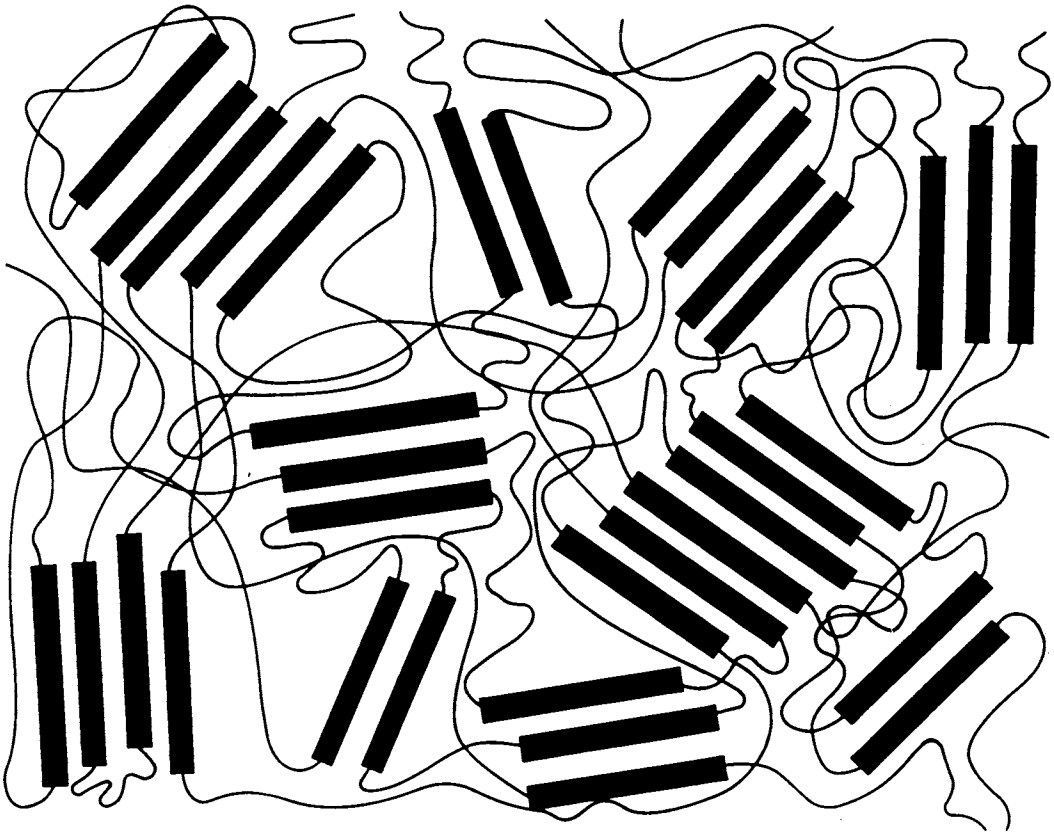

FIGURE 20. "Fringed micelle" model of the crystalline-amorphous structure of partially crystalline polymers. (From Slade, L. and Levine, H., *Advances in Meat Research*, Vol. 4, Collagen as a Food, Pearson, A. M., Dutson, T. R., and Bailey, A., Eds., AVI, Westport, 1987, 251. With permission.)

define "mobility transformations" in terms of the critical variables of time, temperature, and moisture content (with pressure as another variable of potential technological importance). The dynamics map has been used[30] to describe mobility transformations in water-compatible food polymer systems that exist in kinetically metastable glassy and rubbery states[15,25,26] always subject to conditionally beneficial or detrimental plasticization by water. For example, the kinetics of starch gelatinization have been explained in terms of mobility transformations by locating on the dynamics map the alternative pathways of complementary plasticization by heat and moisture.[22,23,26] The map domains of moisture content and temperature, traditionally described with only limited success using concepts such as Aw and "bound water" to interpret and explain sorption isotherms and sorption hysteresis, have been treated alternatively in terms of water dynamics.[15,16] As the name implies, water dynamics focuses on the mobility and eventual "availability" of the plasticizing diluent (be it water alone or an aqueous solution) and a theoretical approach to understanding how to control the mobility of the diluent in glass-forming food systems that would be inherently mobile, unstable, and reactive at temperatures above Tg and moisture contents above Wg. This concept has provided an innovative perspective on the moisture management and structural stabilization of IMF systems[16] and the cryostabilization of frozen, freezer-stored, and freeze-dried aqueous glass-forming food materials and products.[8,27,31-34,40-42]

Glass dynamics deals with the time- and temperature-dependence of relationships among composition, structure, thermomechanical properties, and functional behavior. As its name implies, glass dynamics focuses on (1) the glass-forming solids in an aqueous food system, (2)

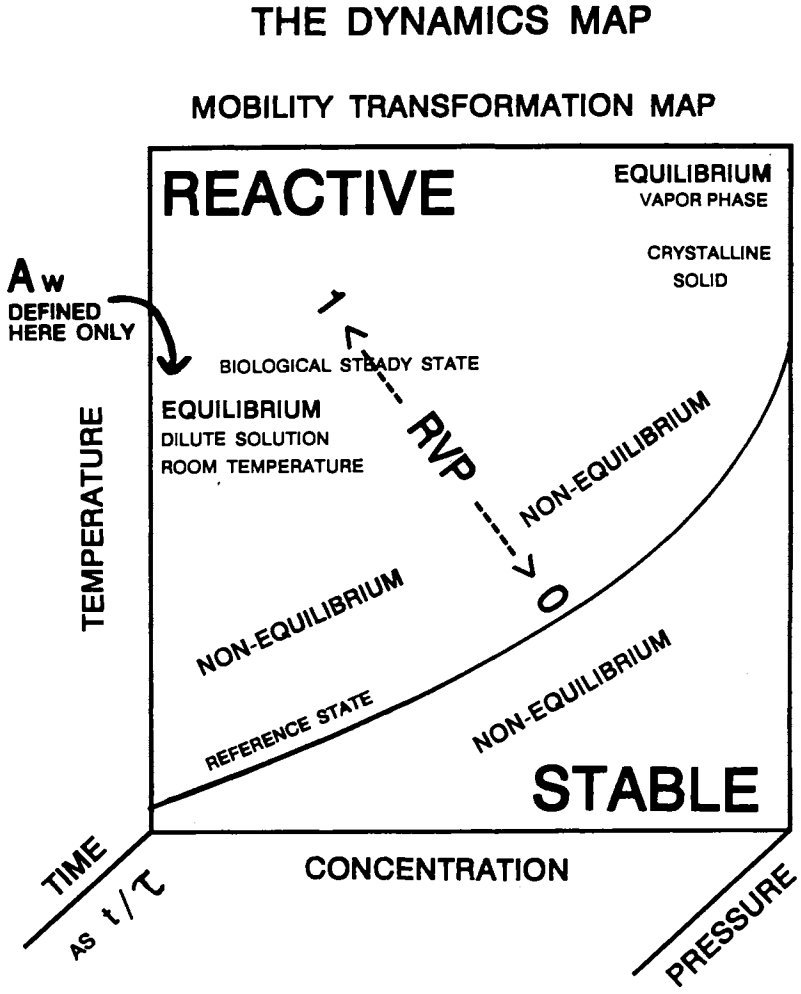

FIGURE 21. A four-dimensional "dynamics map", with axes of temperature, concentration, time, and pressure, which can be used to describe mobility transformations in non-equilibrium glassy and rubbery systems. (From Slade, L. and Levine, H., *Pure Appl. Chem.*, 60, 1841, 1988. With permission.)

the Tg of the resulting aqueous glass that can be produced by cooling to $T < Tg$, and (3) the effect of the glass transition and its Tg on processing and process control, via the relationships between Tg and the temperatures of the individual processing steps (which may be deliberately chosen to be first above and then below Tg). This concept emphasizes the operationally immobile, stable, and unreactive situation (actually one of kinetic metastability) that can obtain during product storage (of a practical duration) at temperatures below Tg and moisture contents below Wg. It has been used to describe a unifying concept for interpreting "collapse" phenomena, which govern, for example, the time-dependent caking of amorphous food powders during storage.[8,27] Collapse phenomena in completely amorphous or partially crystalline food systems[54,64,66,126,135-138] are diffusion-limited consequences of a material-specific structural and/or mechanical relaxation process.[8] The microscopic and macroscopic manifestations of these consequences occur in real time at a temperature about 20°C above that of an underlying molecular state transformation.[30,66] This transformation from kinetically metastable amorphous solid to unstable amorphous liquid occurs at Tg.[8] The critical effect of plasticization (leading to increased free volume and mobility in the dynamically constrained glass) by water on Tg is a key aspect of collapse and its mechanism.[27]

A general physicochemical mechanism for

collapse has been described,[8] based on occurrence of the material-specific structural transition at Tg, followed by viscous flow in the rubbery liquid state.[137] The mechanism was derived from Williams-Landel-Ferry (WLF) free volume theory for (synthetic) amorphous polymers.[101,107] It has been concluded that Tg is identical to the phenomenological transition temperatures observed for structural collapse (Tc) and recrystallization (Tr). The non-Arrhenius kinetics of collapse and/or recrystallization in the high viscosity (η) rubbery state are governed by the mobility of the water-plasticized polymer matrix.[8] These kinetics depend on the magnitude of $\Delta T = T - Tg$,[8,66] as defined by a temperature-dependent exponential relationship derived from WLF theory. Glass dynamics has proven a useful concept for elucidating the physicochemical mechanisms of structural/mechanical changes involved in various melting and (re)crystallization processes.[15] Such phenomena are observed in many partially crystalline food polymers and processing/storage situations, including, for example, the gelatinization and retrogradation of starches.[20] Glass dynamics has also been used to describe the viscoelastic behavior of amorphous polymeric network-forming proteins such as gluten and elastin.[25]

1. "Fringed Micelle" Structural Model

The "fringed micelle" model, shown in Figure 20, was originally developed to describe the morphology of partially crystalline synthetic polymers. It is particularly useful for conceptualizing a three-dimensional network composed of microcrystallites (with crystalline melting temperature, Tm) that crosslink amorphous regions (with glass transition temperature, Tg) of flexible-coil chain segments.[139] In pure homopolymers, for which Tg is always at a lower temperature than Tm,[106] the amorphous domains can exist in a glassy solid physical state at $T < Tg$ or in a rubbery liquid state at $Tg < T < Tm$.[15] The model is especially applicable to synthetic polymers that crystallize from an undercooled melt or concentrated solution to produce a metastable network of relatively low degree of crystallinity. Typically, such polymers contain small crystalline regions of only about 100 Å dimensions.[103] Thus, the model has also often been used to describe the partially crystalline structure of aqueous gels of biopolymers such as starch and gelatin,[17,18,61,65,103,139] in which the amorphous regions contain plasticizing water and the microcrystalline regions, which serve as physical junction zones, are crystalline hydrates. The model has also been used to conceptualize the partially crystalline morphology of frozen aqueous food polymer systems, in which case the ice crystals represent the "micelles" dispersed in a continuous amorphous matrix (the "fringe") of solute-unfrozen water (UFW).[15] An important feature of the model, as applied to high MW polymer systems such as starch (both native granular and gelatinized)[21] and gelatin, concerns the interconnections between crystalline and amorphous domains. A single long polymer chain can have helical (or other ordered) segments located within one or more microcrystallites that are covalently linked to flexible-coil segments in one or more amorphous regions.[139] Moreover, in the amorphous regions, chain segments may experience random intermolecular "entanglement couplings",[112] which are topological interactions rather than covalent or non-covalent chemical bonds.[140] Thus, in terms of their thermomechanical behavior in response to plasticization by water and/or heat, the crystalline and amorphous domains are neither independent of each other nor homogeneous.[106]

2. The Dynamics Map

The key to our new perspective on concentrated, water-plasticized food polymer systems relates to recognition of the fundamental importance of the dynamics map mentioned earlier. As shown in Figure 21, the major area of the map (i.e., the area surrounding the reference state in two dimensions and projecting into the third, time, dimension) represents a non-equilibrium situation corresponding to the temperature-composition region of most far-reaching technological consequence to aqueous food systems, including IMFs.[16] The critical feature in the use of this map is identification of the glass transition as the reference state, a conclusion[30] based on WLF

theory for glass-forming polymers. This line of demarcation (representing the glass curve of Tg vs. composition) serves as a basis for description of the non-equilibrium thermomechanical behavior of water-compatible polymeric materials in glassy and rubbery states, in response to changes in moisture content, temperature, and time.[15,30,40-42] Mobility is the transcendent principle underlying the definition of the glass transition as the appropriate reference state,[16] because mobility is the key to all transformations in time (or frequency), temperature, and composition between different relaxation states for a technologically practical system.[30] An interesting illustration of the practical relevance of mobility transformations to shelf-life problems in real food products is shown in Figure 22.[141] Marsh and Wagner[141] have described a "state of the art" computer model that can be used to predict the shelf-life of particular moisture-sensitive products, based on the moisture-barrier properties of a packaging material and the temperature/humidity conditions of a specific storage environment. As shown in Figure 22, shelf-life (i.e., time) increases with decreasing temperature and humidity conditions (e.g., Minneapolis in the winter) and decreases correspondingly with increasing temperature and humidity (e.g., Miami in the summer), such that shelf-life varies by a factor of 4 between the highest and lowest temperature/moisture combinations.

The interdependent concepts of water dynamics and glass dynamics embodied in the dynamics map have provided insights into the relevance of the glassy reference state to functional aspects of a variety of food systems.[15,30] For example, the kinetics of all constrained relaxation processes, such as translational and rotational diffusion, which are governed by the mobility of a water-plasticized polymer matrix in glass-forming systems, vary (from Arrhenius to WLF-type) between distinct temperature/structure domains, which are divided by this glass transition.[15,25,30] Thus, while familiar Arrhenius kinetics are ap-

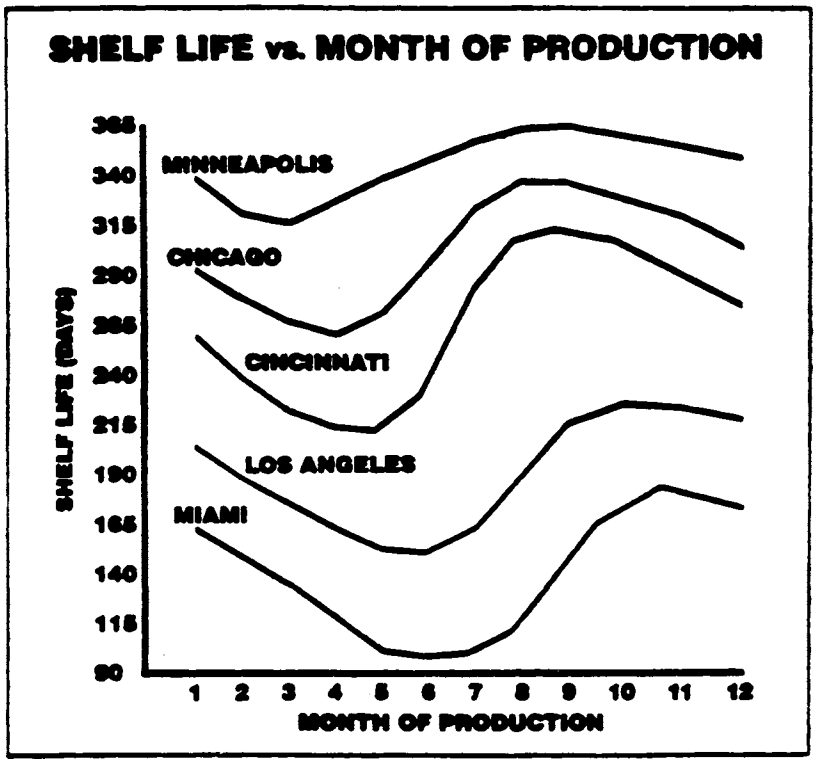

FIGURE 22. Plot of shelf life vs. month of production for a typical moisture-sensitive food product. (From Marsh, K. S. and Wagner, J., *Food Eng.*, 57(8), 58, 1985. With permission.)

plicable below Tg in the glassy solid state of very low mobility and very slow diffusion (the domain of glass dynamics, labeled STABLE in Figure 21), WLF kinetics[107] are applicable above Tg in the viscoelastic, rubbery liquid state of accelerating mobility and diffusion (the domain of water dynamics, labeled REACTIVE in Figure 21).[30] The WLF equation[101,107] defines the kinetics of molecular-level relaxation processes, which will occur in practical time frames only in the rubbery state above Tg, in terms of an exponential, but non-Arrhenius, function of ΔT above this boundary condition.[8,26,66] Of course, the highest mobility and most rapid diffusion occur in the region above a second set of reference lines, the equilibrium liquidus and solidus curves (shown and discussed later), which demark the upper boundary of the WLF region where Arrhenius kinetics again apply.[33] Within the WLF region, kinetics accelerate according to the WLF equation from the extremely steep temperature dependence of WLF kinetics just above Tg to the familiarly moderate temperature dependence of Arrhenius kinetics on approaching Tm.[30] The WLF equation describes the profound range of the kinetics between Tg and Tm, with correspondingly profound implications for process control, product quality, safety, and shelf-life. Sperling[114] has remarked that "for a generation of (synthetic) polymer scientists and rheologists, the WLF equation has provided a mainstay both in utility and theory." It should be noticed in Figure 21 that Aw would be correctly defined only in the region of the map corresponding to a dilute solution at equilibrium at room temperature. In contrast, the actual measured RVP of an IMF (non-equilibrium) system would approach zero in the limit of the glassy reference state at temperatures below Tg and moisture contents $<$ Wg, but would increase toward 1.0 with increasing temperature above Tg and increasing moisture content above Wg.

One particular location among the continuum of Tg values along the reference glass curve in Figure 21 results from the behavior of water as a crystallizing plasticizer and corresponds to an operationally invariant point (called Tg′) on a state diagram for any particular solute.[4-8,31-34,40-42,74] Tg′ represents the solute-specific subzero Tg of the maximally freeze-concentrated, amorphous solute/UFW matrix surrounding the ice crystals in a frozen solution. As illustrated in the idealized state diagram shown in Figure 23, the Tg′ point corresponds to, and is determined by, the point of intersection of the kinetically determined glass curve for homogeneous solute-water mixtures and the non-equilibrium extension of the equilibrium liquidus curve for the Tm of ice.[8,31-34] This solute-specific location defines the composition of the glass that contains the maximum practical amount of plasticizing moisture (called Wg′, expressed as g UFW/g solute or weight % (w%) water, or alternatively designated in terms of Cg′, expressed as w% solute)[8,15] and represents the transition from concentrated fluid to kinetically metastable, dynamically constrained solid which occurs on cooling to T $<$ Tg′.[16] In this homogeneous, freeze-concentrated solute-water glass, the water represented by Wg′ is not "bound" energetically but rather rendered unfreezable in a practical time frame due to the immobility imposed by the extremely high local viscosity of about 10^{12} Pa s at Tg′.[4-8,15,25,26,30-34,40-42] Marsh and Blanshard[94] have recently documented the technological importance of freeze-concentration and the practical implication of the description of water as a readily crystallizable plasticizer, characterized by a high value of Tm/Tg ratio $\simeq 2$.[30,89] A theoretical calculation[94] of the Tg of a typically dilute (i.e., 50%) wheat starch gel fell well below the measured value of about -5 to -7°C for Tg′,[17,20] because the theoretical calculation based on free volume theory did not account for the formation of ice and freeze-concentration that occurs below about -3°C. Recognition of the practical limitation of water as a plasticizer of water-compatible solutes, due to the phase separation of ice, reconciled the difference between theoretical and measured values of Tg.[94] Moreover, the theoretical calculations supported the measured value of $\simeq$27% water[17,20] for Wg′, the maximum practical water content of an aqueous wheat starch glass. The calculated water content of the wheat starch glass with Tg of about -7°C is $\simeq$28%.[94]

Within a homologous polymer family (e.g., from the glucose monomer through maltose, maltotriose, and higher malto-oligosaccharides to the amylose and amylopectin high polymers of starch), Tg′ increases in a characteristic fashion

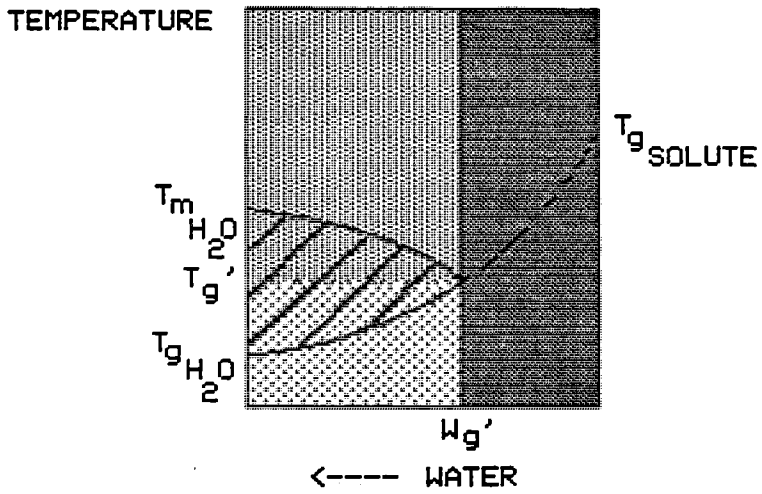

FIGURE 23. Idealized state diagram of temperature vs. w% water for an aqueous solution of a hypothetical, glass-forming, small carbohydrate (representing a model frozen food system), illustrating how the critical locations of Tg′ and Wg′ divide the diagram into three distinguishable structure-property domains.

with increasing solute MW.[8,27,31] This finding has been shown to be in full accord with the established and theoretically predictable variation of Tg with MW for homologous families of pure synthetic amorphous polymers,[107,113,114] described in the next section. The insights resulting from this finding have proven pivotal to the characterization of structure-function relationships in many different types of completely amorphous and partially crystalline food polymer systems.[8,14-39] It should be noted that Tg′ also corresponds to the subzero Tg mentioned by Atkins[90] as being characteristic of many water-plasticized, rubbery biopolymers *in vivo*.

3. The Effect of Molecular Weight on Tg

For pure synthetic polymers, in the absence of diluent, Tg is known to vary with MW in a characteristic and theoretically predictable fashion, which has a significant impact on resulting mechanical and rheological properties.[26,107] For a homologous series of amorphous linear polymers, Tg increases with increasing number-average MW ($\overline{M}n$), due to decreasing free volume contributed by chain ends, up to a plateau limit for the region of entanglement coupling in rubber-like viscoelastic random networks (typically at $\overline{M}n = 1.25 \times 10^3$ to 10^5 Da[112]), then levels off with further increases in $\overline{M}n$.[107,113] Below the entanglement $\overline{M}n$ limit, there is a theoretical linear relationship between increasing Tg and decreasing inverse $\overline{M}n$.[114] (For polymers with constant values of $\overline{M}n$, Tg increases with increasing weight-average MW ($\overline{M}w$), due to increasing local viscosity.[30] This contribution of local viscosity is reported to be especially important when comparing different MWs in the range of low MWs.[107])The difference in three-dimensional morphology and resultant mechanical and rheological properties between a collection of nonentangling, low MW polymer chains and a network of entangling, high MW, randomly coiled polymer chains can be imagined as analogous to the difference between masses of elbow macaroni and spaghetti.[26] For synthetic polymers, the $\overline{M}n$ at the boundary of the entanglement plateau often corresponds to about 600 backbone chain atoms.[114] Since there are typically about 20 to 50 backbone chain atoms in each polymer segmental unit involved in the cooperative translational motions at Tg,[102] entangling high polymers are those with at least about 12 to 30 segmental units per chain.[26] Figure 24[114] illustrates the characteristic dependence of Tg on $\overline{M}n$ (expressed in terms of the degree of polymerization, DP) for several homologous series of synthetic amorphous polymers. In this semi-log plot, the Tg values for each polymer reveal three distinguishable inter-

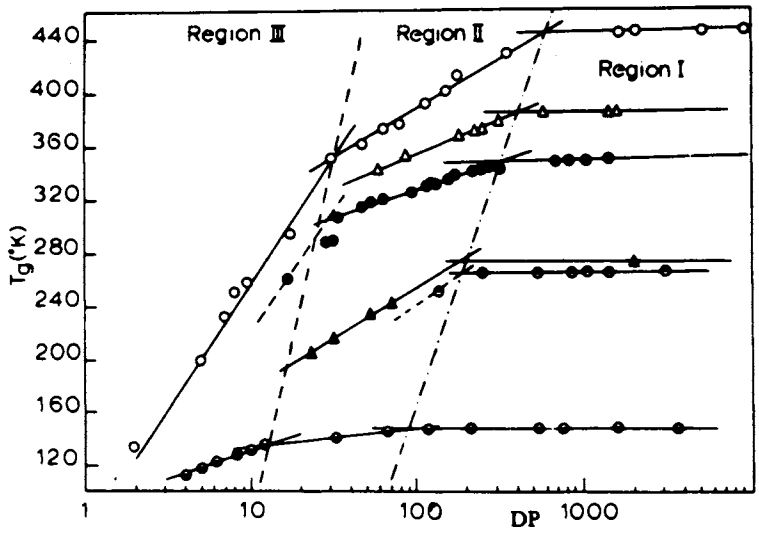

FIGURE 24. Plot of Tg as a function of log DP (degree of polymerization) (a measure of $\overline{Mn}$), for poly(alpha-methyl-styrene) (open circles); poly(methylmethacrylate) (open triangles); poly(vinyl chloride) (solid circles); isotactic polypropylene (solid triangles); atactic polypropylene (circles, top half solid); and poly(dimethylsiloxane) (circles, bottom half solid). (From Sperling, L. H., *Introduction to Physical Polymer Science*, Wiley-Interscience, New York, 1986. With permission.)

secting linear regions: (III) a steeply rising region for non-entangling small oligomers; (II) an intermediate region for non-entangling low polymers; and (I) the horizontal plateau region for entangling high polymers.[142] From extensive literature data for a variety of synthetic polymers, it has been concluded that this three-region behavior is a general feature of such Tg vs. log $\overline{Mn}$ plots, and demonstrated that the data in the non-entanglement regions II and III show the theoretically predicted linear relationship between Tg and inverse $\overline{Mn}$.[142]

4. Water Plasticization

Water acting as a plasticizer is well known to affect the Tg of completely amorphous polymers and both the Tg and Tm of partially crystalline polymers (see References 15, 25, 26 and references therein). Water is a "mobility enhancer", in that its low MW leads to a large increase in mobility, due to increased free volume and decreased local viscosity,[107] as moisture content is increased from that of a dry solute to a solution.[16,30] The direct plasticizing effect of increasing moisture content at constant temperature is equivalent to the effect of increasing temperature at constant moisture and leads to increased segmental mobility of chains in amorphous regions of glassy and partially crystalline polymers, allowing in turn a primary structural relaxation transition at decreased Tg.[108,109] State diagrams illustrating the extent of this Tg-depressing effect have been reported for a wide variety of synthetic and natural, water-compatible, glassy and partially crystalline polymers. In such diagrams[15,25,26] (e.g., see the one for elastin in Figure 19A), the smooth glass curve of Tg vs. composition shows the dramatic effect of water on Tg especially at low moisture contents (i.e., $\lesssim$10 weight % [w%] water). In this region, Tg generally decreases by about 5 to 10°C/w% water[15] (~12°C/w% for elastin), from the neighborhood of 200°C for the anhydrous polymer.[90] Another example is shown in Figure 25,[43] which depicts the amylopectin of freshly gelatinized starch as another typical water-compatible, completely amorphous polymer, which exhibits a Tg curve from about 125°C for pure anhydrous starch to about −135°C, the Tg of pure amorphous solid water,[143] passing through Tg′ at about −5°C (and Wg′ ≃ 27 w% water).[18]

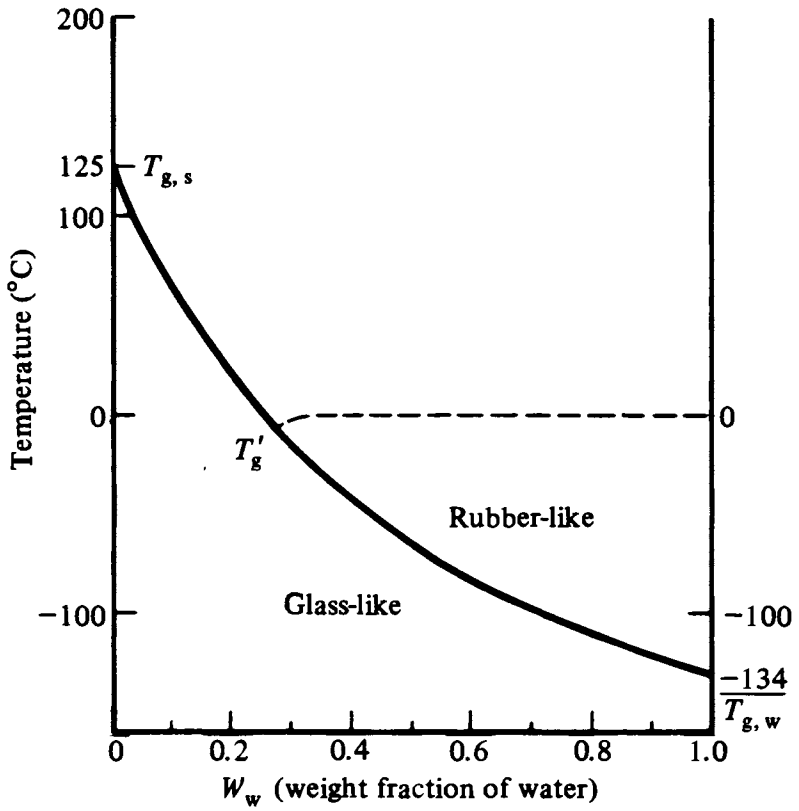

FIGURE 25. State diagram, showing the approximate Tg temperatures as a function of mass fraction, for a gelatinized starch-water system. (From van den Berg, C., *Concentration and Drying of Foods,* MacCarthy, D., Ed., Elsevier, London, 1986, 11. With permission.)

Figure 25 shows the Tg of starch decreasing by about 6°C/w% water for the first 10 w% moisture, in good agreement with another published glass curve for starch calculated from free volume theory.[49,94] Similarly, the glass curve for water-compatible, amorphous gluten[99] in Figure 26[51] shows a decrease in Tg from >160°C at ≤1 w% water to 15°C at 16 w% water, a depression of about 10°C/w% water in this moisture range. The plasticizing effect of water on gluten continues at higher moisture contents, until Tg falls to Tg′ ≃ −7.5°C and Wg reaches Wg′ ≃ 26 w% water ≃0.35 g UFW/g gluten.[25]

The plasticizing effect of water on the Tg of three other glass-forming food materials is illustrated and compared in the state diagrams shown in Figure 27.[91,129] Hemicellulose,[129] an amorphous component of wood, is another typical water-compatible biopolymer, with a dry Tg of about 200°C, which is dramatically depressed (by more than 15°C/w% water for the first 10% water) to a Tg around −10°C (i.e., Tg′) at about 30% moisture.[90] Hemicellulose, like starch, gluten, and elastin, exhibits the characteristic behavior common to all water-compatible, glass-forming solutes:[15] the practical limit to the extent of plasticization (i.e., depression of Tg by water) is determined by the phase separation of crystalline ice below 0°C, so that the minimum Tg achievable during slow cooling in a practical time frame is the solute-specific Tg′ (with the corresponding maximum content of plasticizing moisture, Wg′).[8,30-34] Accordingly, the glass curve shown for hemicellulose in Figure 27 is typical of the "practical glass curve for a water-compatible solute" that levels off at Tg′<0°C, rather than continuing along the monotonic descent of the "complete glass curve" to the Tg of water itself. In contrast to hemicellulose, lignin, the other major amorphous component of wood, typifies a high polymer that is only water-sensitive rather than water-compatible.[15] Its glass curve also starts at

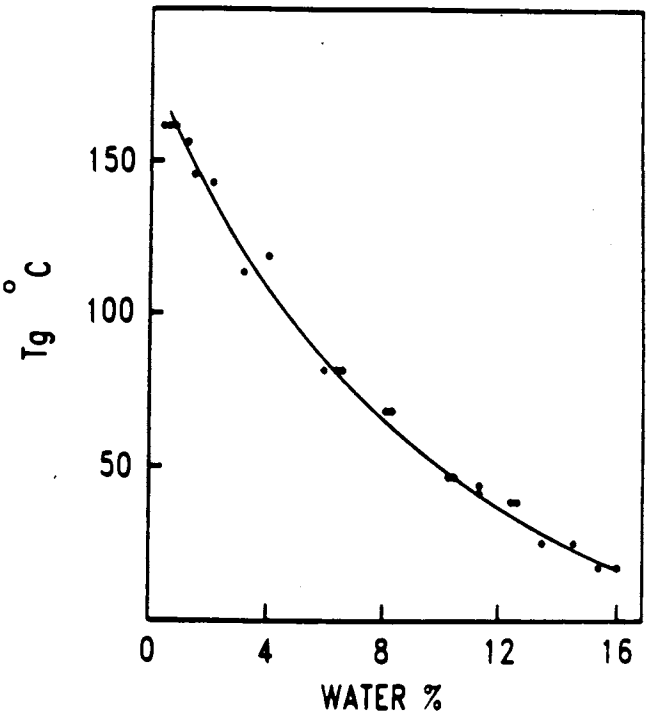

FIGURE 26. Change in Tg as a function of moisture for a hand-washed and lyophilized wheat gluten. (From Hoseney, R. C., Zeleznak, K., and Lai, C. S., *Cereal Chem.*, 63, 285, 1986. With permission.)

about 200°C for the dry solid and decreases by more than 10°C/w% water for the first 10% water. But the glass curve shown for lignin in Figure 27 is typical of the "practical glass curve for a water-sensitive solute"; it levels off at a lower moisture content and at a temperature well above 0°C. Lignin exhibits the characteristic behavior common to all water-sensitive, glass-forming solutes (e.g., synthetic high polymers that are relatively hydrophobic, such as polyethylene, poly[vinyl acetate], and nylons):[15] the practical limit to its extent of plasticization by water is determined by its much more limited water-solubility and thermodynamic compatibility, leading to the phase separation of liquid water (as clusters of water molecules) above 0°C, which would subsequently freeze on further cooling to 0°C.[15] Thus, the minimum Tg achievable during cooling of a lignin-water mixture is not Tg′, but some higher Tg>Tm of ice (about 50°C for lignin, as shown in Figure 27), because Tg cannot be depressed to Tg′ by clustered water in a separate (non-plasticizing) liquid phase.[15,30] In contrast to the two high MW biopolymers represented in Figure 27, sorbitol is a water-compatible, glass-forming, monomeric polyol. As shown in Figure 27, the glass curve for quench-cooled, completely amorphous sorbitol-water mixtures[91] begins at a much lower temperature (Tg = −2°C for anhydrous sorbitol),[28,91] because of the low MW of this solute, and shows an extent of plasticization of sorbitol at low moisture of about 3 to 4°C/w% water. The glass curve shown for sobitol in Figure 27 is the "complete glass curve" up to 50 w% water, as a result of quench-cooling to avoid phase separation of ice at water contents >Wg′, and would continue smoothly down to the Tg of pure amorphous water at about −135°C,[91] as do the "complete" glass curves of all water-compatible solutes, regardless of MW.[8,15,16] If these sorbitol-water mixtures had been cooled more slowly, so that ice formation and maximal freeze-concentration of the solute could have occurred during the experimental time frame, they would have been expected to manifest the "practical" glass curve for sorbitol, with

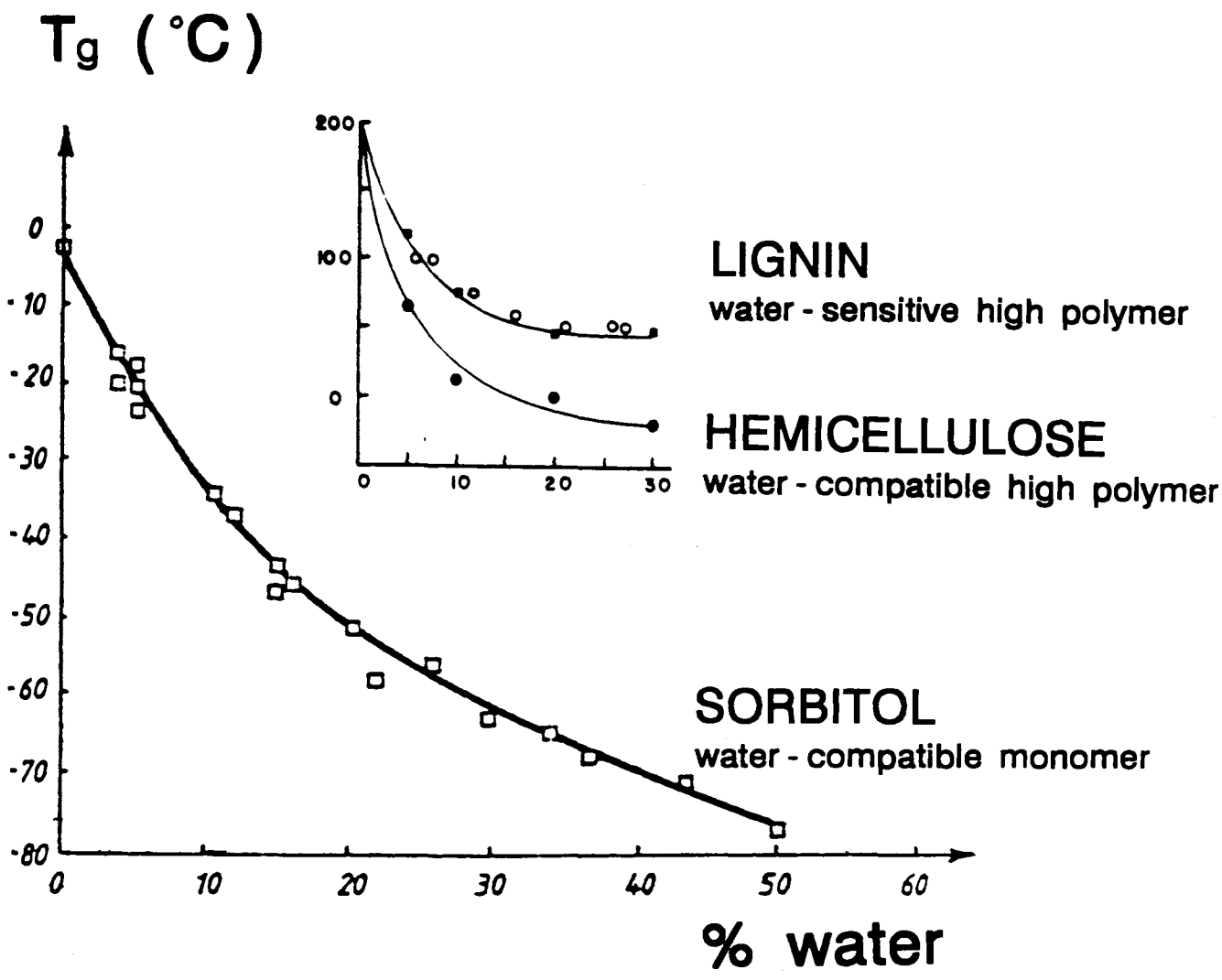

FIGURE 27. "Glass curves" of Tg as a function of weight percent water. The "complete" glass curve for sorbitol (adapted with permission from Reference 91) is shown up to 50 w% water. The "practical" glass curves for hemicellulose and lignin (adapted with permission from Reference 129) are shown up to 30 w% water.

invariant values of Tg = Tg′ ≃ −43.5°C and Wg = Wg′ ≃ 19 w% water ≃ 0.23 g UFW/g sorbitol.[27,33]

According to the prevailing view in the current synthetic polymer literature, the predominant contribution to the mechanism of plasticization of water-compatible glassy polymers by water at low moisture content derives from a free volume effect.[111,144,145] Free volume theory[107] provides the general concept that free volume is proportional to inverse $\overline{M}n$, so that the presence of a plasticizing diluent of low MW leads to increased free volume, allowing increased backbone chain segmental mobility. (Note that Sears and Darby[109] have stated that "free volume is considered thermodynamically as a solvent.") The increased mobility is manifested as a decreased Tg of the binary polymer-diluent glass.[94,109] For synthetic amorphous high polymers, it is well known that the ability of a diluent to depress Tg decreases with increasing diluent MW,[146] as predicted by free volume theory. These facts are illustrated in Figure 28,[107] which shows a series of glass curves for solutions of polystyrene with various compatible organic diluents that can be undercooled without crystallizing. These smooth curves illustrate the characteristic plasticizing effect of low MW, glass-forming diluents

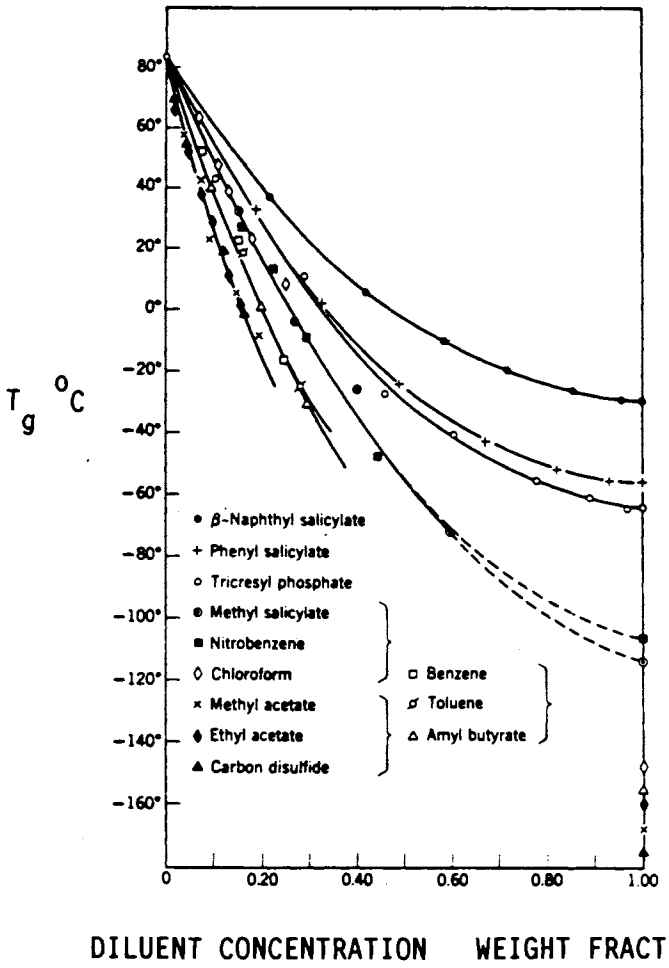

FIGURE 28. Glass transition temperatures of polystyrene solutions with various diluents of low molecular weight, plotted against weight fraction of diluent. (From Ferry, J. D., *Viscoelastic Properties of Polymers*, 3rd ed., John Wiley & Sons, New York, 1980. With permission.)

of low Tg on a typical polymer of higher Tg: Tg decreases monotonically with increasing concentration (weight fraction) of diluent, because the $\overline{M}w$ of the homogeneous polymer-plasticizer mixture decreases and its free volume increases.[114] Figure 28 also shows that, at a given weight fraction of diluent, Tg of the mixture increases with increasing MW of the diluent (generally over the entire set of diluents, but rigorously within a homologous series), because the Tg values of the neat diluents likewise generally increase with increasing MW and decreasing free volume.[114]

In contrast, the effect of synthetic polymer plasticization by a crystallizing diluent has been illustrated by Tg results for blends of poly(vinyl chloride) (PVC) with a terpolymeric organic plasticizer that is able to crystallize on undercooling, as shown in Figure 29.[147] In this interesting case of a polymer and plasticizer with more nearly equal MWs, while the diluent depresses the Tg of the polymer in the typical fashion, the polymer simultaneously depresses the crystallization temperature (Tcr) of the plasticizer. Thus, with increasing PVC concentration in the blend, Tcr of the plasticizer decreases as Tg of the blend increases. Upon cooling, crystallization of the plasticizer can no longer occur, within a realistic experimental time frame, in the region (on the state diagram in Figure 29) of temperature and

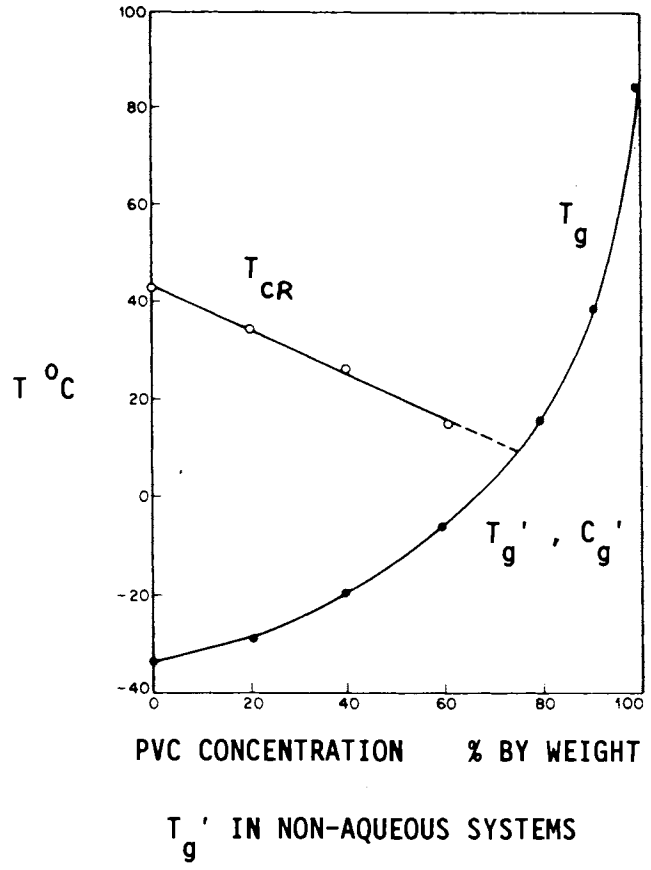

FIGURE 29. Crystallization and glass temperatures in terpolymeric plasticizer (TP)/polyvinyl chloride (PVC) blends as a function of PVC concentration. (From Bair, H. E., *Thermal Characterization of Polymeric Materials,* Turi, E. A., Ed., Academic Press, Orlando, 1981, 845. With permission.)

blend composition where the extrapolated crystallization curve intersects the glass curve at a particular point, which can be designated as Tg'.[30] Below a critical diluent concentration (i.e., the composition of the glass at Tg'), crystallization on cooling of the plasticizer, which would be readily crystallizable if pure, essentially ceases at an incomplete extent, due to the immobility imposed by the vitrification of the glass-forming plasticizer-polymer blend. Wunderlich[105] has described several other cases of the same type of behavior for binary mixtures of a synthetic amorphous polymer and its crystallizable monomer.[148] In each case, "the monomer liquidus curve was observed as usual. At its intersection with the Tg vs. concentration curve of the macromolecule, which shows a decreasing Tg with increasing amount of monomer (plasticization), the whole system becomes glassy without crystallization of the monomer. The polymer-rich side of the phase diagram remains thus a single-phase region throughout, while the monomer-rich samples change on cooling from a liquid solution to a two-phase system that consists of liquid solution and crystalline monomer at higher temperature, and changes at lower temperature to glassy solution and crystalline monomer."[105] The analogy between this behavior (as exemplified in Figure 29) of a non-aqueous high-polymer system, with its characteristic Tg' and corresponding composition Cg', and the general behavior of aqueous glass-forming systems of water-compatible solutes (discussed earlier and described with respect to the idealized state diagram in Figure 23) is important and fundamental to interpreting the non-equilibrium behavior of food polymer systems in the general context of the dynamics map and mobility transformations.[30]

Recent reports[111,144,145] have demonstrated that the effectiveness of water as a plasticizer of synthetic polymers[15] (by analogy with the effectiveness of typical low MW organic plasticizers, as shown in Figure 28) primarily reflects the low molar mass of water. These workers have discounted older concepts of specific interactions, such as disruptive water-polymer hydrogen bonding in polymer hydrogen-bonded networks, or plasticizing molecules becoming "firmly bound" to polar sites along a polymer chain, in explaining water's plasticizing ability. Although hydrogen bonding certainly affects solubility parameters and contributes to compatibility of polymer-water blends,[109] it has been convincingly shown that polymer flexibility does not depend on specific hydrogen bonding to backbone polar groups.[121] Rather, the relative size of the mobile segment of linear backbone,[114] and thus the relative $\overline{M}w$ of its blend with water, governs the magnitude of plasticization and so determines Tg.[121] To negate the older arguments for site-specific hydrogen bonding, NMR results have been cited that clearly indicate that water molecules in polymers with polar sites have a large degree of mobility.[144,145] As used in this context, mobility is defined in terms of translational and rotational degrees of freedom for molecular diffusion on a time scale of experimental measurements.[30] Franks[4-7,40-42,149,150] has advocated a similar view and presented similar evidence to try to dispel the popular[151] but outdated[57] myths about "bound" water and "water-binding capacity" in glass-forming food polymers or low MW materials. For example, as discussed later, proton NMR has been used to test the accessibility of water with reduced mobility in the crystalline regions of retrograded wheat starch gels.[152] Such gels are partially crystalline, with B-type hydrated crystalline regions in which water molecules constitute an integral structural part of the crystal unit cell.[153,154] NMR results have shown that all the water in such a starch gel can be freely exchanged with deuterium oxide.[152] Most recently, Ellis[111] has reported results of a comprehensive DSC study that show that several diverse synthetic "amorphous polyamides in pure and blended form exhibit a monotonic depression of Tg as a function of water content", and which "lend further credence to the simple and straightforward plasticizing action of water in polar polymers irrespective of their chemical and physical constitution." These results have helped to confirm the conclusions[15,25] that (1) the behavior of hydrophilic polymers with aqueous diluents is precisely the same as that of nonpolar synthetic polymers (e.g., polystyrene in Figure 28) with organic diluents, and (2) water-compatible food polymers such as starch, gelatin, elastin, and gluten, for which water is an efficient plasticizer but not necessarily a good solvent, exhibit the same physicochemical responses to plasticization as do many water-compatible synthetic polymers (e.g., poly[vinyl pyrrolidone] [PVP]).[15] A characteristic extent of plasticization at low moisture, typically in the range of about 5 to 10°C/w% water (as shown for starch in Figure 25 and gluten in Figure 26), but occasionally somewhat less than 5°C/w% (e.g., sorbitol in Figure 27) or as much as 20°C/w% (e.g., hemicellulose in Figure 27), has been shown to apply to a wide variety of water-compatible glassy and partially crystalline food monomers, oligomers, and high polymers.[15,25,26,66] As mentioned earlier, the excellent agreement between the measured value of Tg'[17,20] and the theoretical value recently calculated from free volume theory[49,94] for an aqueous wheat starch gel with $\gtrsim$27% moisture also lends further support to these conclusions.

In partially crystalline polymers, water plasticization occurs only in the amorphous regions.[62,145,155-157] In linear synthetic polymers with anhydrous crystalline regions and a relatively low capacity for water in the amorphous regions (e.g., nylons),[155] the % crystallinity affects Tg, such that increasing % crystallinity generally leads to increasing Tg.[145] This is due primarily to the stiffening or "antiplasticizing" effect of disperse microcrystalline crosslinks, which leads to decreased mobility of chain segments in the interconnected amorphous regions.[156] The same effect is produced by covalent crosslinks,[145] which, when produced by radiation, occur only in amorphous regions.[144] In polymers with anhydrous crystalline regions, only the amorphous regions are accessible to penetration and therefore plasticization by water.[144,145,157] Similar phenomena are observed in partially crystalline polymers with hydrated crystalline regions, such as gelatin and starch.[15,19,24] In native starches, hy-

drolysis by aqueous acid (''acid etching'') or enzymes, at T < Tm, can occur initially only in amorphous regions.[153] Similarly, acid etching of retrograded starch progresses in amorphous regions, leading to increased relative crystallinity (or even increased absolute crystallinity, by crystal growth) of the residue.[153] Dehumidification of granular starch proceeds most readily from initially mobile amorphous regions, leading to non-uniform moisture distribution.[62] In partially gelatinized starches, dyeability by a pigment increases with increasing amorphous content.[158] It should be noted, however, that plasticization of the amorphous regions (e.g., the backbone segments and branch points of amylopectin molecules) of native granular starches by sorbed water is neither instantaneous nor simultaneous with the initial swelling caused by water uptake. It has recently been demonstrated by Aguerre et al.[159] that ''the uptake of water takes place between the concentric layers'' of the granule, leading to ''interlamellar expansion of the starch granule structure.'' This sorbed water must subsequently diffuse from the interlamellar spaces to the amorphous regions of the granule before plasticization of the polymer molecules or chain segments in those amorphous regions can begin. The effective Tg that immediately precedes and thereby determines the temperature of gelatinization (Tgelat) in native starch depends on the extent and type (B vs. A vs. V polymorphs) of crystallinity in the granule (but not on amylose content) and on total moisture content and moisture distribution.[17-21] For normal and waxy (i.e., all amylopectin) starches, Tgelat increases with increasing % crystallinity,[160] an indirect effect due to the disproportionation of mobile short branches of amylopectin from amorphous regions to microcrystalline ''micelles'', thereby increasing the average MW and effective Tg of the residual amorphous constituents,[21] because these branches are unavailable to serve as ''internal'' plasticizers.[109] Two other related phenomena are observed as a result of the non-uniform moisture distribution in situations of overall low moisture content for polymers with hydrated crystalline regions:[15] (1) atypically high Tg/Tm (in K) ratios $\geqslant 0.80$ but, of course, <1.0,[89,105] in contrast to the characteristic range of 0.5 to 0.8 for many partially crystalline synthetic polymers,[102] and (2) a pronounced apparent depressing effect of water on Tm[93,161] as well as Tg, such that both Tg and Tm decrease with increasing moisture content.

To put this modern concept of water plasticization in a more familiar context of the older, more traditional literature on ''bound'' and ''unfreezable'' water and on water sorption by food polymers at low moisture (reviewed in detail elsewhere),[15,25] the earliest-sorbed water fraction is most strongly plasticizing, always said to be ''unfreezable'' in a practical time frame, and often referred to as ''bound''. The later-sorbed water fraction is said to be freezable, referred to as ''free'', ''mobile'', or ''loosely bound'', and is either weakly or non-plasticizing, depending on the degree of water compatibility of the specific polymer. As mentioned earlier, the degree of water compatibility relates to the ability of water to depress Tg to Tg′, and to the magnitude of Wg′.[15,16] Regardless of context, a key fact about the ''freezability'' of water relates to the homogeneous process for the prerequisite nucleation step of ice crystallization.[162] Even at temperatures as low as −40°C (the homogeneous nucleation temperature for ice in pure water),[4] a minimum on the order of 200 water molecules must associate within a domain of about 40 Å in order to form a critical nucleus that will grow spontaneously into an ice crystal.[4] Thus, within any food material at low moisture, clusters of water molecules of lower density than about 200 molecules/40 Å would certainly require temperatures below −40°C or heterogeneous catalysts for nucleation to occur.[33]

The solute-specific, invariant quantity of unfrozen water captured in the glass that forms at Tg′, defined as Wg′,[8] is traditionally referred to by many food scientists and technologists as one measure of ''bound'' water.[151] However, ''bound'' water, with respect to either frozen or room-temperature food systems, is a misnomer that has persisted for at least the last 30 years, despite constant debate[3,8,15,25,26,57,58,64] and evermore convincing arguments that the concepts of ''bound'' water, ''water binding'', and ''water-binding capacity'' of a solute are incorrect, inappropriate, and misleading rather than helpful.[4-7,40-42,149,150] The concept of ''bound'' water originated in large part from a fundamental misconception that discrete ''free'' and ''bound''

physical states of water in food materials (or "free", "loosely bound", and "tightly bound" states) could provide a valid representation of water molecules in a solution at ambient temperature.[34] Actually, at $T > Tg'$, water molecules in a solution exist within a single physical state (i.e., liquid) characterized not by any kind of static geometry but rather by a dynamic continuum of degrees of hindered instantaneous mobility.[25] In this liquid solution state, individual water molecules are only transitorally hydrogen-bonded to individual polar sites on the solute.[149,150]

As explained recently,[8,30-34] the solute-specific value of Wg' is the maximum amount of water that can exist with that solute in a spatially homogeneous, compatible blend that, in the rubbery state, exhibits long-range cooperative relaxation behavior described by WLF kinetics, but not long-range lattice order. Further dilution beyond Wg' results in loss of cooperative mobility and onset of short-range fluid mechanics, described by Arrhenius kinetics. Thus, expression of Wg' as a water/solute number ratio (i.e., a "notional hydration number")[149] actually represents the technologically practical maximum limit for the amount of water that can act as a plasticizer of a particular solute,[6,15] rather than the amount of water that is "bound" to, or whose dynamics are governed by, that solute. Part of the reason for the persistence of the concept of "bound" water in such concentrated solute systems, despite convincing evidence of its invalidity, relates to a conclusion inadvisedly extrapolated from findings for very dilute solutions. The addition of a few isolated solute molecules to pure water already causes a profound effect on the self-diffusion properties in the solution. The hindered diffusion of water molecules instantaneously in the vicinity of individual solute molecules is construed as the effect of "viscous drag"; these less-mobile water molecules are visualized to be "pulled along" with the solute during flow. But it has been demonstrated repeatedly[149,150] than the less-mobile water molecules are freely exchangeable with all of the water in the solution, leading to the inescapable consensus view that the water is not bound to the solute. On the other hand, in describing dilute solutions, no one has ever suggested that the solute molecules are "bound" to water molecules. When the situation is reversed, adding a few water molecules to an anhydrous solute profoundly changes the viscoelastic properties of the solute via water plasticization, which increases the free volume and decreases the local viscosity.[34] Why then, in light of this evidence of a dramatic *increase* in the mobility of the solute, have many found it so easy to jump to the conclusion that these water molecules must be "bound" to solute molecules?

It is only recently becoming more widely acknowledged and accepted[15,25,33,50,57,58] that the so-called "bound" water corresponding to Wg' is not energetically bound in any equilibrium thermodynamic sense. Rather, it is simply kinetically retarded, due to the extremely high local viscosity ($\sim 10^{12}$ Pa s) of the metastable glass at Tg', and thus dynamically constrained from the translational and rotational diffusion required for ice crystal growth.[4-8,30-34,40-42] The crucial finding that water is not "strongly bound" to polar groups on hydrophilic polymers has been demonstrated in an especially convincing fashion by the meticulous low-temperature DSC and ambient-temperature sorption studies of Pouchly and Biros[163-166] on the thermodynamic interaction of water with (and plasticizing effect on) hydrophilic synthetic polymers in glassy and rubbery states. This conclusion regarding the true nature of "bound" water does not mean that there are not solute-water hydrogen bonds in the glass at Tg', only that such hydrogen bonds are the normal consequence of dissolution of a solute in water rather than the cause of the kinetic retardation that renders this water "unfreezable" in real time.[34] The stabilizing free energy of such solute-water hydrogen bonds is no greater than for water-water hydrogen bonds in ice.[150,163-166] Analogously, for model solutions of small sugars at room temperature, results of NMR and dielectric relaxation measurements have shown that "the residence time of a given water molecule at a solvation site (i.e., a hydroxyl group on a sugar) is extremely short, <1 ns."[149,150] Furthermore, such results, from studies of synthetic polymers[145] and polymeric carbohydrate and protein gels[58,152] alike, have demonstrated conclusively that water molecules said to be "bound" to polar groups on such polymeric solutes are in fact highly mobile (especially compared to the mobility of water in ice)[167] and able to exchange

freely and rapidly, likewise on a NMR time scale, with other (so-called "free" or "bulk") water molecules and deuterium oxide. Other studies have concluded that "bound" water has thermally labile hydrogen bonds,[163-166] shows cooperative molecular mobility,[168] has a heat capacity approximately equal to that of liquid water rather than ice,[131,164,168] and has some capability to dissolve salts.[169]

It has been concluded recently that "in the past, too much emphasis has been given to water activity and "water binding"."[57] In fact, the typical observation of two relaxation peaks (ascribed, following traditional dogma, to "free" and "bound" water) for all biological tissues and solutions that have been examined in dielectric experiments[170] is entirely consistent with, and exactly analogous to, the behavior of synthetic polymers with their non-aqueous, non-hydrogen bonding organic plasticizers.[109] The traditional point of view on the "structuring" effect of solutes on water (and its association with the concept of water activity), which helped give rise to the myth of "bound" water, is rightfully being replaced[57] by a new perspective and emphasis on the mobilizing effect of water acting as a plasticizer on solutes, which has led to a deeper qualitative understanding of structure-function relationships in aqueous food polymer systems.[8,14-39] For example, Labuza, who in the past has been a very well known proponent of the concept of "bound" water,[151] now writes, in the context of the "water binding capacity (WBC)" of dietary fiber, that "in fact, current opinion on bound water (if there is such a thing) is that it is very different from what the expression commonly means . . . Product development scientists should take the WBC values that currently are being bandied about with a grain of salt."[171]

5. Williams-Landel-Ferry Theory and WLF Kinetics

As alluded to earlier, the glass transition in amorphous systems is a temperature-, time- (or frequency-), and composition-dependent, material-specific change in physical state, from a glassy mechanical solid (capable of supporting its own weight against flow due to the force of gravity) to a rubbery viscous fluid (capable of flow in real time).[107] In terms of thermodynamics, the glass transition is operationally defined as a second-order transition[114] and denoted by (a) a change in slope of the volume expansion (which is a first-order derivative of the free energy), (b) a discontinuity in the thermal expansion coefficient, and (c) a discontinuity in the heat capacity (which is a second-order derivative of the free energy).[119]

The glass transition is also operationally defined, based on mechanical properties, in terms of a mechanical relaxation process such as viscosity. Figure 30[15] (adapted from Reference 4) shows that, as the temperature is lowered from that of the low η liquid state above Tm, where familiar Arrhenius kinetics apply, through a temperature range from Tm to Tg, a completely different, very non-Arrhenius, non-linear form of the kinetics, with an extraordinarily large temperature dependence,[172] becomes operative.[173] Then, at a temperature where mobility becomes limiting, a state transition occurs, typically manifested as a three orders-of-magnitude change in viscosity, modulus, or mechanical relaxation rate.[110,114] At this glass transition temperature, the viscosity of a liquid is $\simeq 10^{12}$ Pa s (10^{13} Poise), and the calorimetrically determined (e.g., by DSC) structural relaxation time for such a liquid is about 200 s.[172,174] A "mechanical" glass tran-

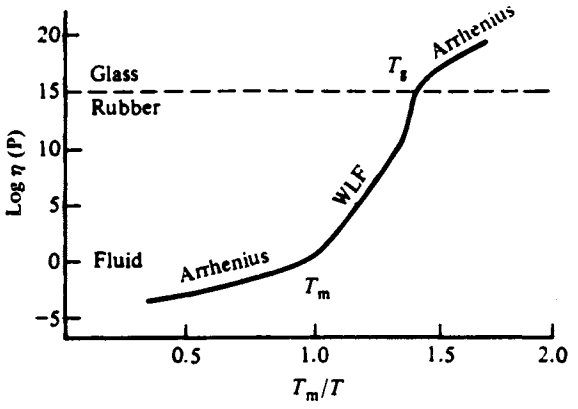

FIGURE 30. Viscosity as a function of reduced temperature (Tm/T) for glassy and partially crystalline polymers. (From Levine, H. and Slade, L., *Water Science Reviews,* Vol. 3, Franks, F., Ed., Cambridge University Press, Cambridge, 1988, 79. With permission.)

sition can be defined by combinations of temperature and deformation frequency for which sufficiently large numbers of mobile units (e.g., small molecules or backbone chain segments of a macromolecule) become cooperatively immobilized (in terms of large-scale rotational and translational motion) during a time comparable to the experimental period,[121,172,173,175] such that the material becomes a mechanical solid capable of supporting its own weight against flow. Arrhenius kinetics become operative once again in the glassy solid, but the rates of all diffusion-limited processes are much lower in this high η solid state than in the liquid state.[15] In fact, the difference in average relaxation times between the two Arrhenius regimes is typically more than 14 orders of magnitude.[30]

At temperatures above Tg, plasticization by water affects the viscoelastic, thermomechanical, electrical, guest/host diffusion, and gas permeability properties of completely amorphous and partially crystalline polymer systems to an extent mirrored in its effect on Tg.[15] In the rubbery range above Tg for completely amorphous polymers or between Tg and Tm for partially crystalline polymers (in either case, typically from Tg to about Tg + 100°C for well-behaved synthetic polymers),[30] the dependence of viscoelastic properties on temperature (i.e., the effect of increasing temperature on relative relaxation times) is successfully predicted[116] by the WLF equation, an empirical equation whose form was originally derived from the free volume interpretation of the glass transition.[101,107] The WLF equation can be written as[89,101]

$$\log_{10}\left(\frac{\eta}{\rho T}\Big/\frac{\eta g}{\rho g Tg}\right) = -\frac{C1(T-Tg)}{C2+(T-Tg)}$$

where η is the viscosity or other diffusion-limited relaxation process, ρ the density, and C1 and C2 are coefficients that describe the temperature dependence of the relaxation process at temperatures above the reference temperature, Tg. C1 is proportional to the inverse of the free volume of the system at Tg, while C2 is proportional to the ratio of free volume at Tg over the increase in free volume due to thermal expansion above Tg (i.e., ratio of free volume at Tg to the difference between the volumes of the rubbery liquid and glassy solid states, as a function of temperature above Tg).[107] C1 and C2 take on the values of "universal constants" (17.44 and 51.6, respectively, as extracted from experimental data on many synthetic amorphous polymers)[101] for well-behaved polymers.[30] The WLF equation describes the kinetic nature of the glass transition and has been shown to be applicable to any glass-forming polymer, oligomer, or monomer.[107] These particular values for the "universal constants" have also been shown to apply to molten glucose,[101] amorphous glucose-water mixtures,[176] amorphous sucrose and lactose powders at low moisture,[66] and concentrated solutions of mixed sugars,[89] as examples of relevance to foods.

The equation defines mobility in terms of the non-Arrhenius temperature dependence of the rate of any diffusion-limited relaxation process occurring at a temperature T compared to the rate of the relaxation at the reference temperature Tg, shown here in terms of log η related usefully to ΔT, where $\Delta T = T - Tg$. The WLF equation is valid in the temperature range of the rubbery or undercooled liquid state, where it is typically used to describe the time-/temperature-dependent behavior of polymers.[173] The equation is based on the assumptions that polymer free volume increases linearly with increasing temperature above Tg and that segmental or mobile unit viscosity, in turn, decreases rapidly with increasing free volume (as illustrated implicitly in Figure 30).[107] Thus, the greater the ΔT, the faster a system is able to move (due to increased free volume and decreased mobile unit viscosity), so the greater is the mobility, and the shorter is the relaxation time. In essence, the WLF equation and resulting master curve of log ($\eta/\eta g$) vs. $T - Tg$[89,101] represent a mobility transformation, described in terms of a time-temperature superposition.[30] Such WLF plots typically show a 5 orders-of-magnitude change in viscosity (or in the rates of other relaxation processes) over a 20°C interval near Tg,[6] which is characteristic of WLF behavior in the rubbery fluid range.[30] For example, as demonstrated by Soesanto and Williams,[89] the effects of temperature and concentration on the mobility of fluids above Tg can be combined to create a single master curve, which represents the WLF equation. The viscosity data shown in Figure 31[89] were obtained for highly concentrated (>90 w%)

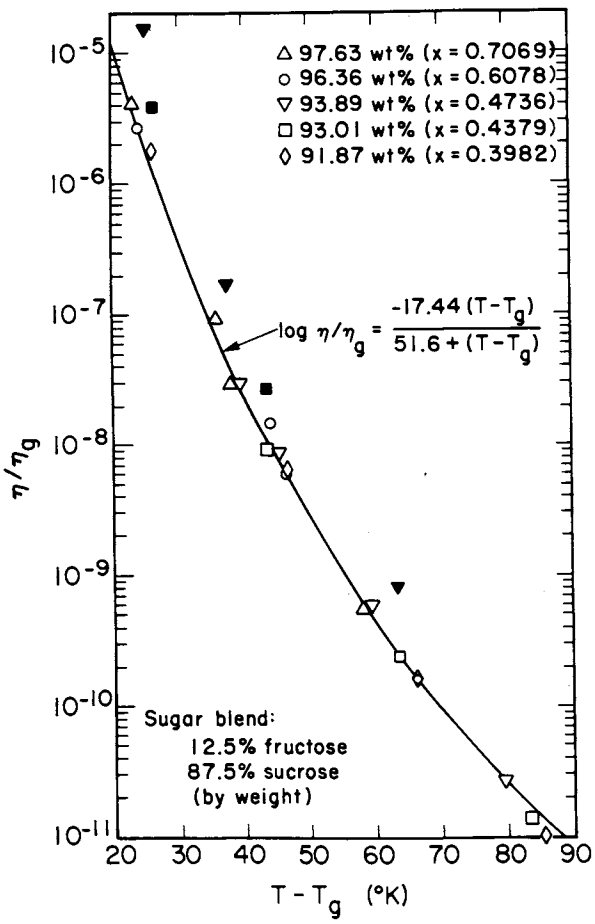

FIGURE 31. Temperature dependence of viscosity for aqueous solutions of a 12.5:87.5 (w/w) fructose:sucrose blend, illustrating the fit of the data to the curve of the WLF equation. (From Soesanto, T. and Williams, M. C., *J. Phys. Chem.*, 85, 3338, 1981.)

aqueous mixtures of fructose and sucrose. These results showed a five orders-of-magnitude change in the viscosity of concentrated sugar solutions, over a 20°C interval near Tg, a finding in excellent accord with the behavior predicted by the quantitative form of the WLF equation, with its "universally" applicable numerical values of the coefficients C1 = 17.44 and C2 = 51.6. These results constituted the first experimental demonstration that concentrated fructose and sucrose solutions obey the WLF equation quantitatively as well as synthetic high polymers. Similarly, it had been shown previously that a completely amorphous glucose melt, in the absence of diluent, has the same coeffients in the WLF equation, and thus also behaves like a typical well-behaved synthetic high polymer.[101,177]

In the context of the utility of the WLF equation, the underlying basis of the principle of time-temperature superpositioning is the equivalence between time (or frequency) and temperature as they affect the molecular relaxation processes that influence the viscoelastic behavior (i.e., the dual characteristics of viscous liquids and elastic solids) of polymeric materials and glass-forming small molecules.[107,134] This principle is illustrated in Figure 32,[26] which shows a master curve of the modulus as a function of temperature or frequency for a typical partially crystalline synthetic high polymer.[112] Figure 32 has been used to describe the viscoelastic behavior of such materials, as exemplified by a kinetically metastable gelatin gel in an undercooled liquid state, in the context of WLF theory.[178] At T > Tg, gelatin gels manifest a characteristic rubber-like elasticity,[179] due to the existence of a network of entangled, randomly coiled chains.[180] With increasing temperature, a gelatin gel traverses the five regions of viscoelastic behavior characteristic of synthetic, partially crystalline polymers,[180] as illustrated in Figure 32: (1) at T < Tg, vitrified glass; (2) at T = Tg, glass transition to leathery region, typically manifested as a three orders-of-magnitude decrease in modulus; (3,4) at Tg < T < Tm, rubbery plateau to rubbery flow; and (5) at T > Tm, viscous liquid flow. It is interesting to note that at Tg < T < Tm, a gelatin gel is freely permeable to the diffusion of dispersed dyes and molecules as large as hemoglobin;[25] only at T < Tg is such dye diffusion greatly inhibited.[181]

The WLF equation is not intended for use much below Tg (i.e., in the glassy solid state) or in the very low viscosity liquid state ($\eta < 10$ Pa s),[89] typically 100°C or more above Tg, where Arrhenius kinetics apply.[107,173,182] For partially crystalline polymers, the breadth of the temperature range of the rubbery domain of WLF behavior corresponds to the temperature interval between Tg and Tm,[104,107] as illustrated in Figure 30. Cheng[183] has noted that the size of this temperature interval between Tg and Tm may be as much as several hundred degrees for synthetic high polymers. An analysis of the variation of the size of this temperature interval with the Tm/Tg ratio of representational synthetic polymers and glass-forming, low MW carbohydrates has been reported recently.[30] This study compared

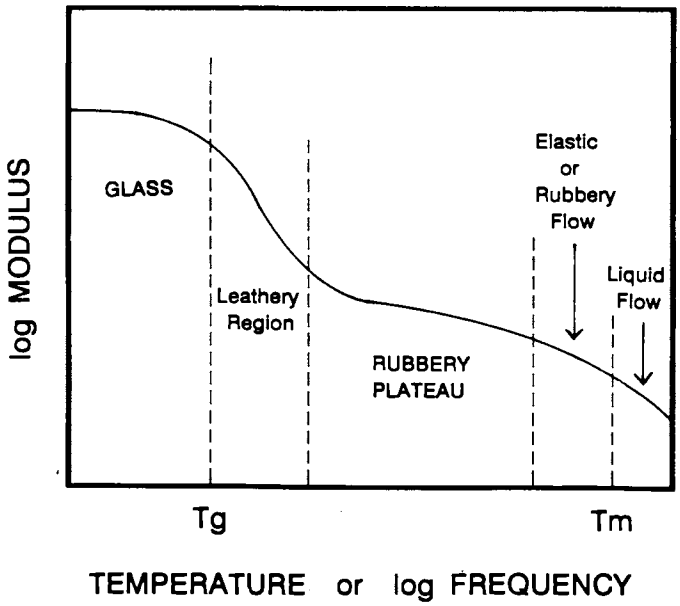

FIGURE 32. Master curve of the modulus as a function of temperature or frequency, illustrating the five regions of viscoelastic behavior characteristic of synthetic partially crystalline polymers. (From Levine, H. and Slade, L., *Dough Rheology and Baked Product Texture: Theory and Practice,* Faridi, H. and Faubion, J. M., Eds., Van Nostrand Reinhold/AVI, New York, 1989, 157. With permission.)

the WLF behavior of kinetically metastable carbohydrate-water systems to the corresponding knowledge base for synthetic high polymers. According to the conventional description, a typical well-behaved synthetic high polymer (e.g., a representational elastomer) would manifest its Tg around 200°K in the completely amorphous state, and its Tm around 300°K in the completely crystalline state,[105] so that the ratio of Tm for the pure crystalline material to Tg for the completely amorphous material is about 1.5 (or Tg/Tm about 0.67).[102] Such a polymer would also have a local viscosity of about 10^{12} Pa s and a free volume fraction of about 2.5% at Tg.[107] (This contribution of free volume to the discontinuity in heat capacity observed at Tg is illustrated in the plot of heat capacity vs. temperature for glassy, crystalline, and partially crystalline glassy materials, shown in Figure 33.) For this typical well-behaved polymer, WLF kinetics are considered to be operative in a temperature range about from Tg to 100°C above Tg.[101] It can be seen that this operational definition is related to the typical Tm/Tg ratio of 1.5, since in such a case the difference in temperature between Tg and Tm would be about 100°C. Figure 34A[30] illustrates the conventional description of the relaxation behavior of a typical well-behaved polymer (e.g., polyvinyl acetate[177,184]), which would obey the standard form of the WLF equation with the coefficients C1 = 17.44 and C2 = 51.6. In this plot of log a_T vs. ΔT, the relaxation rate progresses from WLF behavior very near Tg to Arrhenius behavior at about 100°C above Tg. Within this temperature range, where technological process control would be expected, relaxation rates for WLF behavior near Tg would change by a factor of 10 for every 3°C change in temperature. In contrast, for Arrhenius behavior with familiar $Q_{10} = 2$ kinetics above Tm, a factor of 10 change in relaxation rate would require a 33°C change in temperature.

Another class of amorphous polymers has been described[30] as typical but not well-behaved, in the sense that they are readily crystallizable.[102,105,107,118] Highly symmetrical polymers such as poly(vinylidene chloride) and poly(vinyl cyclohexane), which manifest crystalline melting

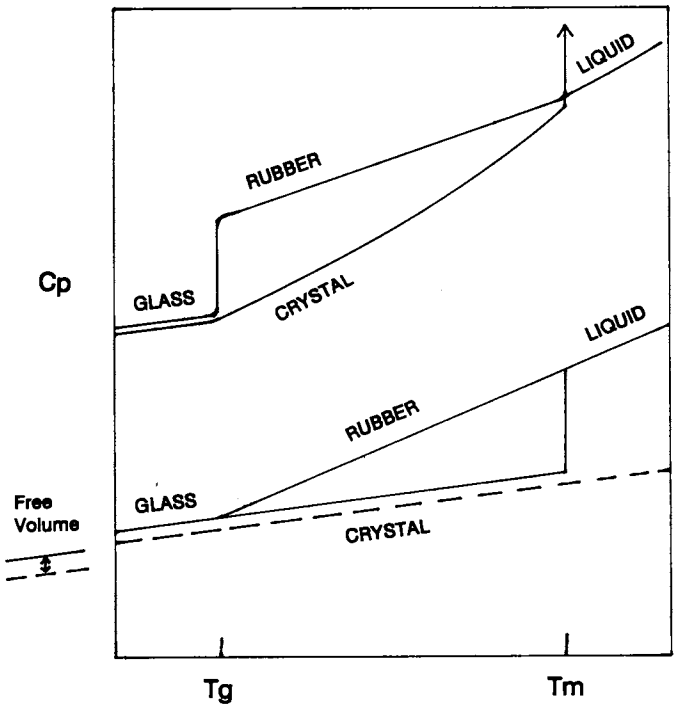

FIGURE 33. Plot of heat capacity as a function of temperature for glassy, crystalline, and partially crystalline glassy materials, illustrating the contribution of free volume to the discontinuity in heat capacity at Tg.

enthalpies of ≃170 J/g, fit this class. For such polymers, the ratio of Tm/Tg is frequently ⩾1.5, so the temperature range between Tg and Tm is ⩾100°C. Different WLF coefficients would be required to describe their relaxation profile, as illustrated by the plot in Figure 34B drawn for C1 = 20.4 and C2 = 154.8. For a representational case of Tg ≃ 200°K (with ηg ≳ 10^{12} Pa s, and free volume fraction ≃2.5%) and Tm/Tg ≃ 2 (Tg/Tm ≃ 0.5), Tm would be ≃400°K. Thus, there would be about a 200°C region in which relaxation rates would change from WLF behavior near Tg (in this case, by a factor of 10 for every 6°C) to Arrhenius behavior near Tm (by a factor of 10 for every 33°C). A notable example of a material with Tm/Tg ≃ 2 is water.[89]

A third class of polymers, often characterized by highly unsymmetrical structures, has been described[30] as atypical and poorly behaved, in that Tg is near Tm.[102,105] For such polymers, with Tm/Tg ≪ 1.5 (i.e., ≃1.25, or Tg/Tm ≃ 0.8), a quantitatively different form of the WLF equation would be required to describe their relaxation profile. In this case, as illustrated in Figure 34C, using C1 = 12.3 and C2 = 23.3, the intercept of log a_T was plotted as ≃ −3 for ΔT = 0 (i.e., at Tg), in contrast to Figures 34A and B, where log a_T was defined as 0 at Tg. For a representational polymer in this class, Tg ≃ 200°K (with ηg ≪ 10^{12} Pa s, and free volume fraction ⩾2.5%) and Tm ≃ 250°K. Thus, the temperature range in which WLF kinetics would be operative is much smaller than usual. Relaxation rates would change from WLF behavior near Tg (in this case, by a factor of 10 for every 1°C) to Arrhenius behavior above Tm (by a factor of 10 for every 33°C) over a region of only about 50°C. The synthetic polymer cited as the classic example of this behavior, which has been attributed to anomalously large free volume at Tg, is bisphenol polycarbonate, with Tm/Tg ≃ 1.18.[102] This category of behavior has also been reported[15,28] to be exemplified by food materials such as native starch and gelatin (due to non-uniform distribution of moisture in amorphous and crystalline regions of these high polymers at low moisture) and the

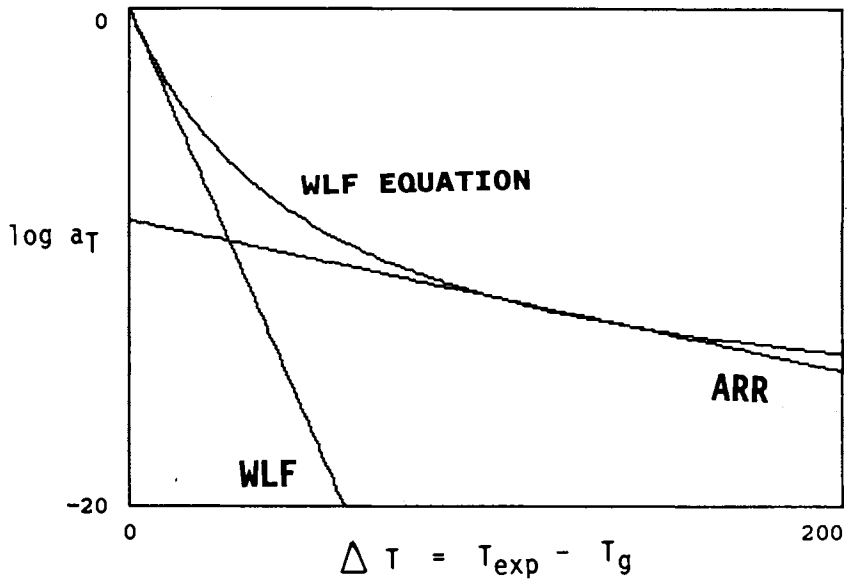

A

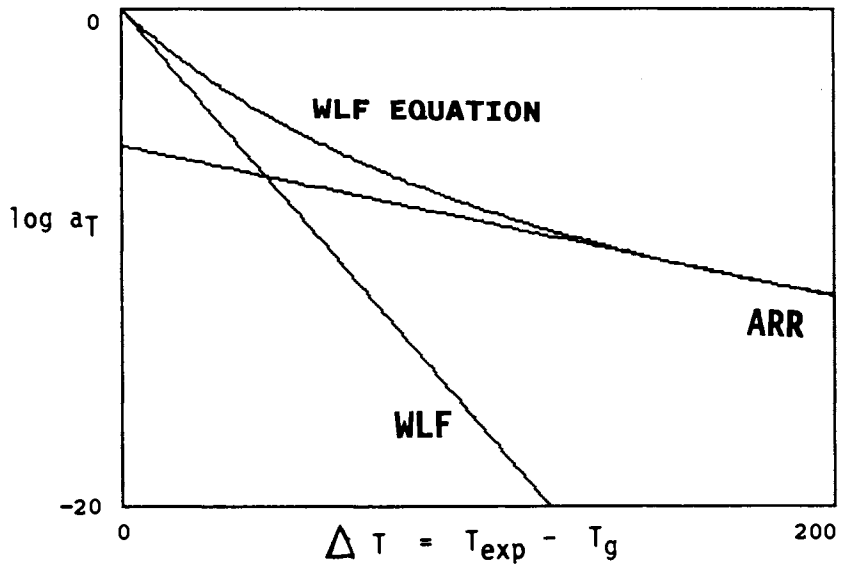

B

FIGURE 34. WLF plots of the time-temperature scaling parameter (WLF shift factor), a_T, as a function of the temperature differential above the reference state, Tg, with the limiting regions of low and high ΔT defined by the WLF and Arrhenius kinetic equations, respectively. The curves of the WLF equation (with coefficients C1 and C2 as noted) illustrate the temperature dependence of the relaxation rate behavior for hypothetical polymers with Tm/Tg ratios of: (A) 1.5 (C1 = 17.44, C2 = 51.6); (B) 2.0 (C1 = 20.4, C2 = 154.8); (C) 1.0 (C1 = 12.3, C2 = 23.3); (D) 2.0, 1.5, and 1.0. (From Slade, L. and Levine, H., *Pure Appl. Chem.*, 60, 1841, 1988. With permission.)

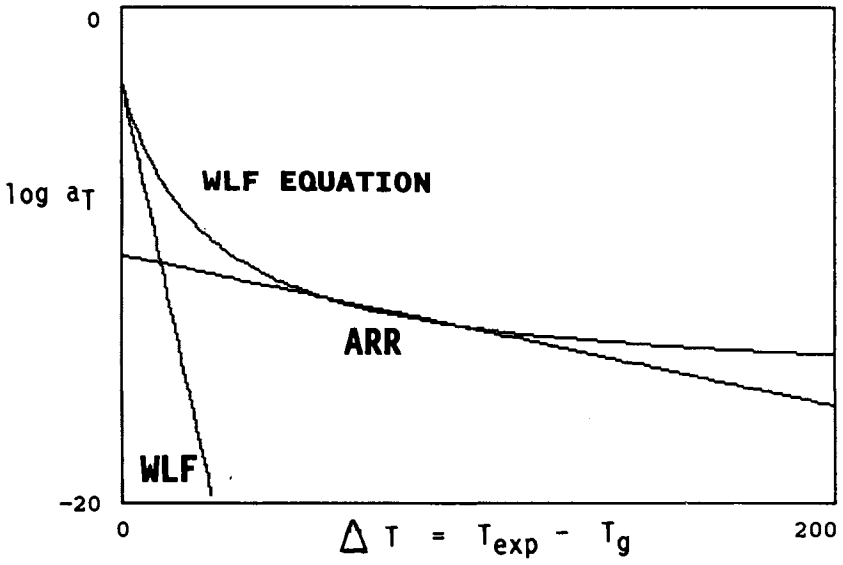

FIGURE 34C.

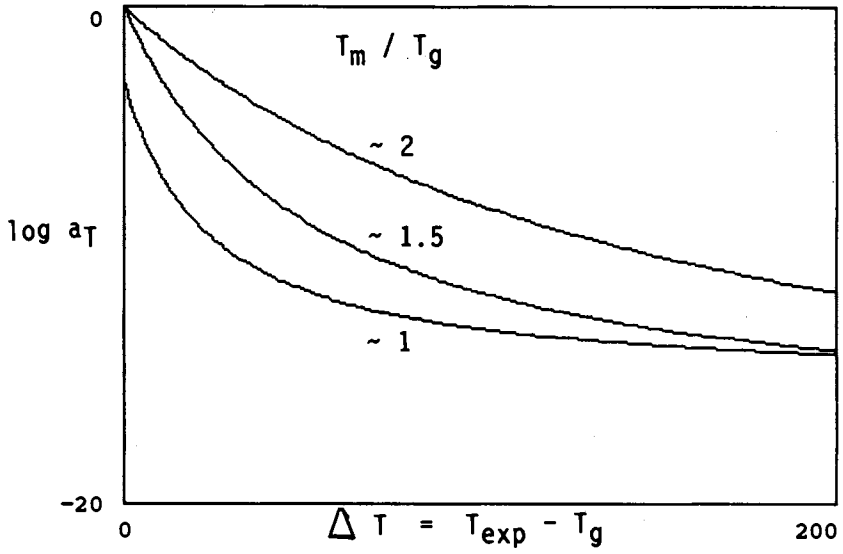

FIGURE 34D.

simple sugars fructose and galactose (due to anomalous translational free volume of these anhydrous monosaccharides).[30]

The three types of behavior exemplified in Figures 34A through C, in which the Tm/Tg ratio is either the typical value of 1.5, or much greater, or much less, have been compared in order to examine how the respective relaxation profiles change in the temperature interval between Tm and Tg for representational, diluent-free polymers with a common value of Tg.[30] As illustrated in Figure 34D, this analysis revealed the critical significance of the Tm/Tg ratio for any given polymer. For a common value of Tg, different values of Tm/Tg for different polymers (e.g., carbohydrates) can be used to compare relative mobilities at Tg and at $T \gg Tg$.[30] For different values of Tg, relative mobilities can be compared based on values of the difference, Tm − Tg, rather than the ratio, Tm/Tg.[30] In Figure 34D, the behavior of log a_T was compared for different values of Tm/Tg (i.e., about 2, 1.5, and the extreme

case of 1.0), to determine how mobility varies in the kinetically constrained regions of this mobility transformation map. At T ≫ Tg, the overall free volume for different polymers may be similar,[107] yet individual free volume requirements for equivalent mobility may differ significantly, as reflected in the Tm/Tg ratio. The anisotropy in either rotational mobility (which depends primarily upon free volume)[107] or translational mobility (which depends primarily upon local viscosity, as well as free volume)[107] may be the key determinant of a particular polymer's relaxation behavior. The glass transition is a cooperative transition[106,172,173,183] resulting from local cooperative constraints on mobility, and Tg represents a thermomechanical property controlled by the local small molecule or segmental, rather than macroscopic, environment of a polymer. On cooling a viscous fluid of relatively symmetrical mobile units with relatively isotropic mobility, translational motions would be expected to be "locked in" at a higher temperature before rotational motions, because of the slower structural relaxations associated with the larger scale translational diffusion.[185,186] In this case, cooperative constraints of local viscosity and free volume on translational diffusion determine the temperature at which the glass transition is manifested, as a dramatic increase in relaxation times compared to the experimental time frame. However, in the case of motional anisotropy, molecular asymmetry has a much greater effect on rotational than translational diffusion, so that rotational motions could be "locked in" before translational motions as the temperature is lowered.[187,188] As illuminated by Figure 34D, a very small ratio of Tm/Tg (i.e., close to 1.0) is accounted for by an anomalously large free volume requirement for rotational diffusion.[102] When the free volume requirement is so large, a glass transition (i.e., vitrification of the rubbery fluid) on cooling can actually occur even when the local viscosity of the system is relatively low. Thus, instead of the typical "firmness" for a glass ($\simeq 10^{12}$ Pa s), such a glass (e.g., of bisphenol polycarbonate, or anhydrous fructose or galactose) may manifest a $\eta g \ll 10^{12}$ Pa s.[15,16,89,172] In such a glass, the time constant for translational diffusion may be anomalously small, indicative of high translational mobility. In contrast, in the glass of a typical well-behaved polymer, the time constant for translational diffusion would be greater than that for rotational diffusion, so that an increase in local viscosity would be concomitant with a decrease in free volume.[186] The above analysis has pointed out the critical significance of anomalous values of Tm/Tg ratio (for the dry solute) close to 1.0 on the mobility, resultant relaxation behavior, and consequent technological process control for non-equilibrium food polymer systems (in the *presence* of water) in their supra-glassy fluid state above Tg,[30] in terms of the WLF kinetics of various translational diffusion-limited, mechanical/structural relaxation processes, such as gelatinization, annealing, and recrystallization of starch.[21]

An interesting comparison has been made between the characteristic WLF ranges discussed above: (1a) about 100°C or more above Tg for many typical, completely amorphous, synthetic polymers, and (1b) from <50°C to 200°C or more between Tg and Tm for different categories of partially crystalline synthetic polymers, and (2) the relative breadth of the temperature range for the WLF region relevant to frozen aqueous food systems, i.e., the magnitude of the rubbery domain between Tg′ and the Tm of ice.[34] As illustrated conceptually in Figure 35,[34] the rubbery domains between Tg and Tm (represented by the solid vertical bars) for pure water (about 135°C) and pure solute (e.g., about 140°C for sucrose)[28] are similar in breadth to the 100 to 200°C span of the WLF region between Tg and Tm for many synthetic polymers.[30,104] In contrast, the breadth of the temperature range between Tg′ and Te (the melting temperature for the eutectic mixture of crystalline solute and ice) in Figure 35 is much smaller. For example, as reported for the specific case of a frozen sucrose solution,[33] the magnitude of the WLF rubbery domain between Te (−14°C)[133] and Tg′ (−32°C)[29] is only 18°C. The significant implications of this fact to the texture and freezer-storage stability of frozen food products[33,34] is discussed later.

Description of the time-/temperature-dependent behavior of food systems by the WLF equation requires selection of the appropriate reference Tg for any particular glass-forming material (of a given MW and extent of plasticization),[89,101,176] be it Tg for a low-moisture system or Tg′ for a frozen system.[8,27,66] For a typical,

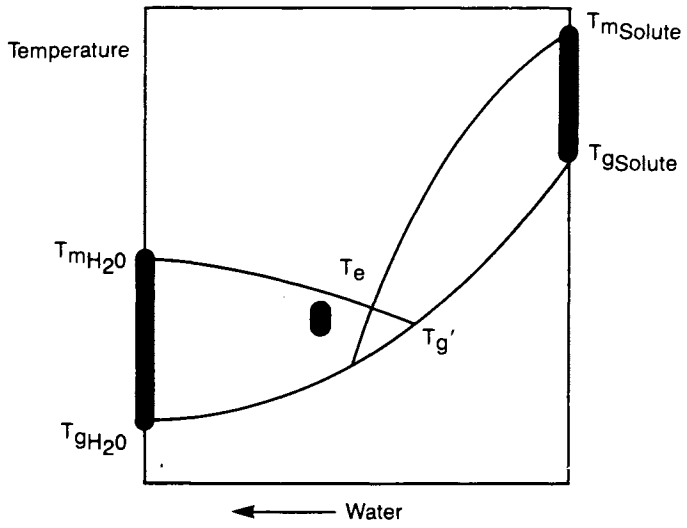

FIGURE 35. Idealized solute-water state diagram illustrating the relative magnitudes of $\Delta T = Tm - Tg$, the temperature range corresponding to the Williams-Landel-Ferry rubbery region, for pure solute, pure water, and the freeze-concentrated, amorphous solute-unfrozen water matrix which would exist at temperatures between the Tm of ice and Tg'. (From Levine, H. and Slade, L., *Thermal Analysis of Foods,* Ma, C.-Y. and Harwalker, V. R., Eds., Elsevier, London, 1990, 221. With permission.)

diluent-free polymer, Tg of the undercooled liquid is defined in terms of an iso-free volume state of limiting free volume[107] and also approximately as an iso-viscosity state somewhere in the range from 10^{10} to 10^{14} Pa s.[4,89,172,189] This iso-viscosity state refers to local, not macroscopic, viscosity. This fact constitutes a critical conceptual distinction,[30] as explained with respect to Figure 34D.

It is interesting to consider whether the WLF equation, which predicts the dependence of the viscoelastic properties of glass-forming polymers on temperature in terms of ΔT above Tg, could be transformed to an analogous empirical equation that predicts quantitatively the dependence of polymer properties on dilution by plasticizer in terms of ΔP (for plasticizer) away from the reference Tg of the undiluted glassy polymer. For example, one could examine the polystyrene plasticization data shown in Figure 28, and calculate the extent of depression of Tg as a function of diluent concentration for different plasticizers. If the experimental temperature is maintained constant, equivalent to the Tg of the undiluted polystyrene, then each extent of depression of Tg is equivalent to a ΔT. For the undiluted polymer, "ΔT above Tg" is achieved by raising the experimental temperature. For the diluted polymer, "ΔT above Tg" is achieved by keeping the experimental temperature constant and lowering the Tg of the system. One could plot these "ΔT" values, achieved by plasticization, in order to transform the graph of log a_T vs. ΔT in Figure 34A into a graph of log a_P vs. ΔP, by substituting the required amount of plasticizer for a given ΔT. Since the WLF equation for the effect of increased temperature on relative relaxation times is an empirical equation, it would be equally legitimate to obtain an equation for log a_P vs. ΔP.

The transformation from ΔT to ΔP would be strictly legitimate only for a system of a single monodisperse linear "polymer" (i.e., higher MW) and a single "plasticizer" (i.e., lower MW), and only if the free volume requirements for both translational and rotational mobility were the same for the "mobile segment" in the dry polymer, the diluted polymer system, and in the pure plasticizer. These conditions *might* be met in experiments in which the monomer, dimer, and low MW oligomers were used as the plasticizer series

for a particular linear polymer. Certainly, the conditions are not met when water is the plasticizer, not even for plasticization of small sugars, much less for starch (which is a mixture of branched and linear polymers with at least bimodal and broad MW distribution).

The most severe complication is that it would be essentially impossible in practice to verify experimentally the form of the WLF equation for log a_P vs. ΔP. Williams, Landel, and Ferry[101] were able to obtain sufficient data for so many polymers to be able to construct an empirical equation for log a_T vs. ΔT, because heat transfer is quite efficient in the solid state. It is experimentally feasible to raise the internal temperature of a sample with appropriate geometry from below Tg to well above Tg and expect that the temperature will be essentially uniform throughout the sample. Then a determination of viscosity, or self-diffusion coefficient for a reporter molecule, or other manifestation of mechanical relaxation will give usable data for construction of log a_T vs. ΔT above Tg. In contrast, mass transport is "infinitely" slow in the (glassy) solid state, and much slower in the leathery and rubbery states than can be accommodated in typical experimental time frames. Consequently, one would rarely be able to keep the experimental temperature constant and achieve ΔT values that represent uniform, steady-state moisture distribution for a sample at varying amounts of sample total moisture. For biological high polymers, the Tg of the undiluted polymer is usually so high as to cause degradation if this dry Tg is used as the experimental temperature. If one uses experimental temperatures below dry Tg and waits for plasticized Tg to drop to and below the experimental temperature, the experimental time scales will be unreasonable, and the instantaneous moisture gradients will allow incidental chemical and physical changes to occur in the system. For small sugars with lower dry Tg values, but that are readily crystallizable (a property usually related to a large temperature interval between Tm and Tg, such that the homogeneous nucleation temperature is well above Tg),[15] small extents of plasticization allow crystallization, and the bulk mechanical properties no longer reflect the effect of plasticizer on Tg. Possibly the best experimental system for direct construction of log a_P vs. ΔP (to allow comparison to the indirect method of transforming log a_T vs. ΔT, based on Tg vs. ΔP data) would be dry amorphous fructose glass plasticized by water. However, it is notoriously difficult to dry fructose syrups, and, in any event, the resulting equation could not be used to predict behavior for any other sugar.

Our feeling is that we must settle at present for a qualitative and indirect picture of log a_P vs. ΔP as a universal concept. For particular combinations of polymer and plasticizer, where the Tg vs. ΔP are known, one can substitute, for ΔT in the WLF equation, the plasticizer concentration that produces an extent of depression of dry Tg equivalent to ΔT.

WLF kinetics differ from Arrhenius kinetics in several important respects,[30,34] and we have emphasized the contrast because we believe that the qualitative differences are as influential as the quantitative differences in their impact on both experimental approach and technological significance.[39] A comparison between WLF and Arrhenius kinetics begins with the recognition that the temperature dependence of microscopic relaxation parameters (including the self-diffusion coefficient, viscosity, rotational and translational relaxation rates or times, and macroscopic processes that rely on them) changes monotonically from a steep dependence of log relaxation rate on temperature just above Tg to a shallow dependence above Tm, i.e., over a material-specific temperature range from Tg to far above Tg.[4,30,172,190] This realization manifests two underlying diagnostic characteristics that distinguish WLF from Arrhenius kinetics.[39] First, the coefficient of the temperature dependence (so-called "activation energy") is defined as a constant in the expression for Arrhenius kinetics, and a plot of log relaxation rate vs. 1/T is a straight line. But the coefficient itself is temperature dependent in the WLF expression; a plot of log relaxation rate vs. 1/T is characteristically curvilinear in the material-specific temperature range between Tg and Tm,[190] approaching linearity only below Tg or above Tm.[34] The absolute value of the derivative of log relaxation parameter vs. 1/T increases as Tg is approached from above, and decreases abruptly to an approximately constant value as the temperature falls below Tg, or decreases gently to an approximately constant value

as temperature is elevated above Tm and far above Tg, where the constant value corresponds to the Arrhenius coefficient (activation energy) that characterizes the particular system and relaxation process.[39] The shape of the derivative profile and the temperature range over which the derivative varies are material-specific properties: typically a range of $\gtrsim$100°C for materials with a ratio of Tm/Tg $\gtrsim$ 1.5, or a range of <100°C for materials with a ratio of Tm/Tg < 1.5.[30] Clearly, it is the fact that the derivative varies in a material-specific and temperature-dependent fashion, rather than the particular magnitude of the derivative, that constitutes the salient feature of WLF kinetics.[39] Second, there is no explicit reference temperature in the expression for Arrhenius kinetics, because in fact, the implicit reference temperature is taken generically to be 0 K, regardless of the distinctive thermomechanical properties of a system, and even though Arrhenius kinetics are applicable only below Tg and above Tm.[4,15,107] In contrast, the WLF expression benefits from an explicit material-specific reference temperature, which is the Tg of a component or compatible blend.[107] Therefore, it is critical to note that when the rate or time scale of a relaxation process can be shown to depend on a material-specific reference Tg, Arrhenius kinetics are not applicable to describe mobility transformations (time-temperature-moisture superpositions) for that process in the rubbery range from Tg to Tm, regardless of whether the average slope of the log k vs. 1/T curve can be empirically fitted by a Q_{10}=n rule and regardless of the particular magnitude of n.[39] In summary, in the temperature and composition domain sufficiently above Tg, where equilibrium and steady-state thermodynamics apply, the coefficient of the temperature dependence of log relaxation rate is defined by Arrhenius kinetics to be a constant and is observed to approximate a relatively small constant value over a typical experimental range of about 20°C.[39] In the increasingly non-equilibrium domain of temperature and composition approaching Tg from above, the coefficient of the temperature dependence of log relaxation rate on 1/T is not a constant and increases evermore rapidly over a range of 20°C.[30] Typically, Arrhenius rates for aqueous systems above Tm might increase fourfold over a temperature range of 20°C,[39] while WLF rates near Tg would increase by 4 or 5 orders of magnitude.[6,30,34] As an example illustrating the significance of the difference between WLF and Arrhenius kinetics, Chan et al.[176] have noted that the dielectric relaxation behavior of amorphous glucose plasticized by water is "remarkably similar" to that of synthetic amorphous polymers in glassy and rubbery states. They showed that the rates of this mechanical relaxation process, which depends on rotational rather than translational mobility, follow the WLF equation for water-plasticized glucose mixtures in their rubbery state above Tg, but follow the Arrhenius equation for glucose-water glasses below Tg.[176] Also noteworthy is Angell's[191] pertinent observation that the temperature dependence of the transport and relaxation properties of undercooled liquid water is strikingly non-Arrhenius in the temperature range from Tm to the homogeneous nucleation temperature at −40°C (corresponding to a portion of the WLF rubbery domain shown in Figure 35). This non-Arrhenius temperature dependence also typifies the case for many other viscous liquid systems that undergo restructuring processes that require the "cooperative involvement of other molecular motions".[172,191] Included in these other viscous liquid systems that exhibit non-Arrhenius behavior are concentrated aqueous solutions at subzero temperatures,[190] according to a suggestion by Hofer et al.[189]

The impact of WLF behavior on the kinetics of diffusion-limited relaxation processes in water-plasticized, rubbery food polymer systems has been conceptually illustrated by the idealized curve shown in Figure 36.[34] Relative relaxation rates, calculated from the WLF equation with its universal numerical constants, demonstrate the non-linear logarithmic relationship: for ΔT = 0, 3, 7, 11, and 21°C, corresponding relative rates would be 1, 10, 10^2, 10^3, and 10^5, respectively. These rates illustrate the 5 orders-of-magnitude change, over a 20°C interval above Tg, typically shown by WLF plots, as mentioned earlier with respect to Figure 31. They are dramatically different from the rates defined by the familiar Q_{10} = 2 rule of Arrhenius kinetics for dilute solutions. As pointed out with respect to Figure 34A, for Arrhenius behavior above Tm, a factor of 10 change in relaxation rate would require a 33°C

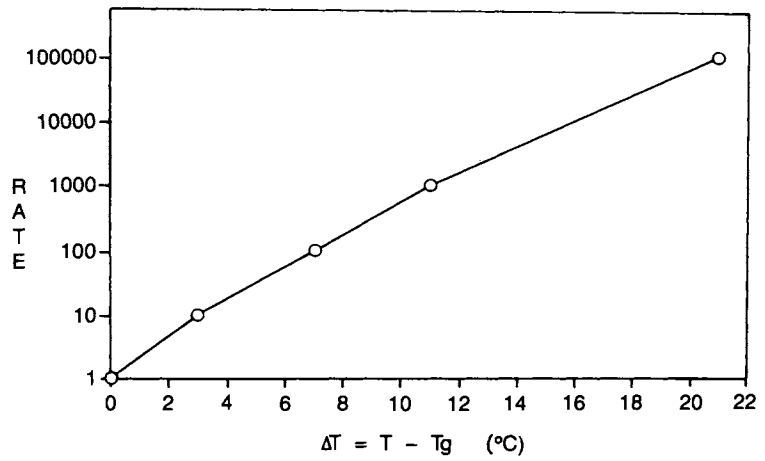

FIGURE 36. Variation of the rate of a diffusion-limited relaxation process against $\Delta T = T - Tg$, as defined by the Williams-Landel-Ferry equation with its "universal" numerical constants of C1 = 17.44 and C2 = 51.6. (From Levine, H. and Slade, L., *Thermal Analysis of Foods,* Ma, C.-Y., and Harwalker, V. R., Eds., Elsevier, London, 1990, 221. With permission.)

change in temperature, in comparison to a 3°C change for WLF behavior near Tg of a partially crystalline polymer of Tg/Tm = 0.67.[30]

Another general example of WLF-governed relaxation behavior concerns the kinetics of (re)crystallization.[15,25,26] (Re)crystallization is a diffusion-limited process[192] that, on a time scale of technological significance, can only occur within the WLF rubbery domain.[104] The propagation step in the recrystallization mechanism approaches a zero rate at T < Tg for an amorphous but crystallizable solute (either polymeric[104] or monomeric), initially quenched from the melt or liquid solution state to a kinetically metastable solid state. Due to immobility in the glass, migratory diffusion of either large main-chain segments or small molecules, required for crystal growth, would be inhibited over realistic times. However, the propagation rate increases exponentially with increasing ΔT above Tg (up to Tm),[94] due to the mobility allowed in the rubbery state. Thus, a recrystallization transition from unstable (i.e., undercooled) amorphous liquid to (partially) crystalline solid may occur at T > Tg,[44,55,193] with a rate defined by the WLF equation.[8] The facts that time-dependent recrystallization can only occur at temperatures above Tg and manifests kinetics defined by the WLF (rather than Arrhenius) equation[27] were recently confirmed in an experimental study of the recrystallization of amorphous, freeze-dried sugars (i.e., sucrose, lactose) by Roos and Karel.[66] Other specific examples of such a recrystallization process (i.e., a collapse phenomenon) include ice and solute (e.g., lactose in dairy products)[50] recrystallization in frozen aqueous systems at T > Tr ≡ Tg′.[8]

One of the most critical messages to be distilled at this point is that the structure-property relationships of water-compatible food polymer systems are dictated by a moisture-temperature-time superposition.[8,137,155] Referring to the idealized state diagram in Figure 23 (which reflects the "real world" cases illustrated in Figures 19A, 25, 26, and 27) as a conceptual mobility map (which represents an extension of the dynamics map in Figure 21), one sees that the Tg curve represents a boundary between non-equilibrium glassy and rubbery physical states in which various diffusion-limited processes (e.g., collapse phenomena involving mechanical and structural relaxations) either can (at T > Tg and W > Wg′, the high-moisture portion of the water dynamics domain corresponding to the upper-left part of Figure 23, or T > Tg and W < Wg′, the low-moisture portion of the water dynamics domain corresponding to the upper-right part of Figure 23) or cannot (at T < Tg, in the domain of glass dynamics corresponding to the bottom part of Figure 23) occur over realistic times.[8,15,40,41] The

WLF equation defines the kinetics of molecular-level relaxation processes, which will occur in practical time frames only in the rubbery state above Tg, in terms of an exponential, but non-Arrhenius, function of ΔT above this boundary condition.[8]

Further discussion of (1) Tg′ as the appropriate reference temperature for WLF kinetics in high-moisture food systems at temperatures above Tg′ and (2) Wg′ as the maximum *practical* amount of plasticizing water in such systems with water contents > Wg′ is detailed in a later Section IV.D.

6. Crystallization/Gelation Mechanism

A classic description of crystallization as a three-step mechanism has been widely used for partially crystalline synthetic polymers crystallized, from the melt or concentrated solution, by undercooling from T > Tm to Tg < T < Tm.[104,139] The mechanism is conceptually compatible with the "fringed micelle" model.[194] It involves the following sequential steps, which apply universally to all crystallizable substances, regardless of MW:[104] (1) nucleation (homogeneous) — formation of critical nuclei, (2) propagation — growth of crystals from nuclei by intermolecular association, and (3) maturation — crystal perfection (by annealing of metastable microcrystallites) and/or continued slow growth (via "Ostwald ripening"). Within this universal description, flexible macromolecules are distinguished from small molecules by the possibility of nucleation by intramolecular initiation of ordered (e.g., helical) chain segments and propagation by association of chain segments for the high polymers.[104]

The thermoreversible gelation, from concentrated solution, of a number of crystallizable synthetic homopolymers and copolymers has been reported to occur by this crystallization mechanism.[146,194-196] In contrast, a different gelation mechanism, not involving crystallization and concomitant thermoreversibility, pertains to polymers in solution that remain completely amorphous in the gel state.[25] Such high polymers are distinguished from oligomers by their capacity for intermolecular entanglement coupling, resulting in the formation of rubberlike viscoelastic random networks (called gels, in accord with Flory's[197] nomenclature for disordered three-dimensional networks formed by physical aggregation) above a critical polymer concentration.[107] It has been demonstrated for many synthetic linear high polymers that the mechanism of gelation from concentrated solution can be distinguished by a simple dilution test.[198] Gelation due to entanglement in a completely amorphous polymer-diluent network can be reversed by dilution, whereas a thermoreversible, partially crystalline, polymer-diluent network gel cannot be dispersed by dilution.[15] Examples of food polymers that can form such amorphous entanglement gels include gluten in unoriented wheat flour dough, sodium caseinate in imitation mozzarella cheese, and casein in real cheese.[25] As summarized by Mitchell,[140] "entanglement coupling is seen in most high MW polymer systems. Entanglements (in completely amorphous gels) behave as crosslinks with short lifetimes. They are believed to be topological in origin rather than involving chemical bonds." Importantly, hydrogen bonding need not be invoked to explain the viscoelastic behavior of completely amorphous gels formed from solutions of entangling polysaccharides or proteins.[25]

The gelation-via-crystallization process (described as a nucleation-limited growth process[195]) produces a metastable three-dimensional network[196] crosslinked by "fringed micellar"[194] or chain-folded lamellar[195] microcrystalline junction zones composed of intermolecularly associated helical chain segments.[146] Such partially crystalline gel networks may also contain random interchain entanglements in their amorphous regions.[195] The non-equilibrium nature of the process is manifested by "well-known aging phenomena"[194] (i.e., maturation),[15] attributed to time-dependent crystallization processes that occur subsequent to initial gelation. The thermoreversibility of such gels is explained in terms of a crystallization (on undercooling) ↔ melting (on heating to T > Tm) process.[195] Only recently has it been recognized that for synthetic polymer-organic diluent systems (e.g., polystyrene-toluene), such gels are not glasses[199] ("gelation is not the glass transition of highly plasticized polymer"[194]) but partially crystalline rubbers,[146]

in which the mobility of the diluent (in terms of rotational and translational motion) is not significantly restricted by the gel structure.[199] Similarly, for starch and gelatin gels, water as the diluent is highly mobile, and amounts > Wg′ freeze readily at subzero temperatures.[26] The temperature of gelation (Tgel) is above Tg,[199] in the rubbery fluid range up to about 100°C above Tg. Tgel is related to the flow relaxation temperature, Tfr, observed in flow relaxation of rigid amorphous entangled polymers[146] and to Tm observed in melts of partially crystalline polymers.[194] The basis for the MW-dependence of Tgel has been identified[146] as an iso-viscous state (which may include the existence of interchain entanglements) of $\eta gel/\eta g = 10^5/10^{12} = 1/10^7$, where ηg at Tg $\simeq 10^{12}$ Pa s.

The distinction among these transition temperatures becomes especially important for elucidating how the morphology and structure of food polymer systems relate to their thermal and mechanical behavior.[25] This distinction is a particularly important consideration when experimental methods involve very different time frames (e.g., mechanical measurements during compression tests or over prolonged storage; thermal analysis at scanning rates varying over 4 orders of magnitude; relaxation times from experiments at acoustic, microwave, or NMR frequencies)[200-204] and sample preparation histories (i.e., temperature, concentration, time).[25] In the case of morphologically homogeneous, molecular amorphous solids, Tg corresponds to the limiting relaxation temperature for mobile polymer backbone-chain segments. In the case of morphologically heterogeneous, supra-molecular networks, the effective network Tg corresponds to the Tfr transition above Tg for flow relaxation[146] of the network. For example, the ratio of Tfr/Tg varies with MW from 1.02 to 1.20 for polystyrene above its entanglement MW.[205] Tfr defines an iso-viscous state of 10^5 Pa s for entanglement networks (corresponding to Tgel for partially crystalline networks).[146] Tgel of a partially crystalline network would always be observed at or above Tfr (≡ network Tg) of an entanglement network; both transitions occur above Tg, with an analogous influence of MW and plasticizing water.[25] As an example, the effective network Tg responsible for mechanical firmness of freshly baked bread would be near room temperature for low extents of network formation, well above room temperature for mature networks, and equivalent to Tgel near 60°C for staled bread, even though the underlying Tg for segmental motion, responsible for the predominant second-order thermal transition, remains below 0°C at Tg′.[25]

Curiously, it has been well-established for a much longer time[195] that the same three-step polymer crystallization mechanism describes the gelation mechanism for the classic gelling system, gelatin-water.[105,139] The fact that the resulting partially crystalline gels[206] can be modeled by the "fringed micelle" structure is also widely recognized.[17,24,104,139] However, while the same facts are true with respect to the aqueous gelation of starch (i.e., retrogradation, a thermoreversible gelation-via-crystallization process that follows gelatinization and "pasting" of partially crystalline native granular starch-water mixtures),[207] and despite the established importance of gelatinization to the rheological properties of bread doughs during baking[208,209] and of retrogradation to the time-dependent texture of fresh-baked vs. aged breads,[210] recognition of starch (or pure amylose or amylopectin) retrogradation as a thermoreversible polymer crystallization process has been much more recent and less widespread.[45-47,61,63,65,92,211-221] Blanshard[49,94] has recently applied synthetic polymer crystallization theory to investigate the kinetics of starch recrystallization and thereby gain insight into the time-dependent textural changes (i.e., staling due to firming) occurring in baked products such as bread. Similarly, Zeleznak and Hoseney[95] have applied principles of polymer crystallization to the interpretation of results on annealing of retrograded starch during aging of bread stored at superambient temperatures. Many of the persuasive early insights in this area have resulted from the food polymer science approach to structure-property relationships in starch of Slade and her various co-workers.[17-23,26,30,35,46]

Slade et al.[17-23,26,30,35,46] have used DSC results to demonstrate that native granular starches, both normal and waxy, exhibit non-equilibrium melting,[105] annealing, and recrystallization behavior characteristic of a kinetically metastable, water-plasticized, partially crystalline polymer system with a small extent of crystal-

linity. This group has stressed the significance of the conclusion, in which others have concurred,[47-49,60,61,63,65,93,222-225] that gelatinization is a non-equilibrium polymer melting process. Gelatinization actually represents a continuum of relaxation processes (underlying a structural collapse)[207] that occurs (at T > Tg) during heating of starch in the presence of plasticizing water and in which crystallite melting is indirectly controlled by the dynamically constrained, continuous amorphous surroundings.[21] That is, melting of microcrystallites, which are hydrated clusters of amylopectin branches,[153,154] is controlled by prerequisite plasticization ("softening" above Tg) of flexibly coiled, possibly entangled chain segments in the interconnected amorphous regions of the native granule, for which the local structure is conceptualized according to the "fringed micelle" model.[20] Such non-equilibrium melting in metastable, partially crystalline polymer network systems, in which the crystalline and amorphous phases are neither independent of each other nor homogeneous, is an established concept for synthetic polymers.[105,183] In fact, Wunderlich[106] and Cheng[183] have both stressed the point that the melting of partially crystalline synthetic polymers is *never* an equilibrium process. Slade et al. have suggested,[17-23,26,35,46] and others have agreed,[60,65,221,224,225] that previous attempts (e.g., References 161, 226, 227) to use the Flory-Huggins thermodynamic treatment to interpret the effect of water content on the Tm observed during gelatinization of native starch have failed to provide a mechanistic model, because Flory-Huggins theory[100] only applies to melting of polymers in the presence of diluent under the conditions of the equilibrium portion of the solidus curve. In this context, it is interesting to note Cheng's[183] recent observation that multicomponent systems of solid polymers (especially those containing copolymers, such as a mixture of native normal starch [amylose + amylopectin] and water, where amylopectin can be considered a block copolymer[21,105]) "are even more beset by non-equilibrium problems (than are single-polymer systems). Only in the amorphous state above the glass transition can one expect (sluggish) equilibration."

An interesting and graphic illustration of the concept of non-equilibrium melting in partially crystalline synthetic polymer systems has been presented by Wunderlich[105] and is detailed here in generic terms to help the reader better understand the applicability of this concept to the gelatinization of native granular starch. Wunderlich described the case of a synthetic block copolymer produced from comonomers A and B. Monomer A was readily crystallizable and capable of producing a high MW, crystalline homopolymer of relatively low "equilibrium" Tm. In contrast, monomer B was not crystallizable and produced a completely amorphous, high MW homopolymer with a Tg much higher than the "equilibrium" Tm of homopolymer A. When a minor amount of A and a major amount of B were copolymerized to produce a linear block polymer (with runs of repeat A covalently backbone-bonded to runs of repeat B to yield a molecular structure of the type –BBBBB–AAAA–BBBBBBB–AAA–BBBBBB–), the resulting product could be made partially crystalline by crystallization from solution. Because the A and B domains were covalently linked, macroscopic phase separation upon crystallization of A was prevented, and microcrystalline "micelles" of A blocks remained dispersed in a three-dimensional amorphous network of B block "fringes". When the melting behavior of this block copolymer was analyzed by DSC, the melting transition of the crystalline A domains was observed at a temperature *above* the Tg of the amorphous B domains. The A domains were kinetically constrained against melting (by dissociation and concomitant volume expansion)[105] at their "equilibrium" Tm by the surrounding continuous glassy matrix of B. The A domains were only free to melt (at a non-equilibrium Tm $\gg$ "equilibrium" Tm) *after* the B domains transformed from glassy solid to rubbery liquid at their Tg. Another interesting example of similar non-equilibrium melting behavior is solution-crystallized poly(phenylene oxide).[228]

The fact that water plasticization occurs only in the amorphous regions of partially crystalline, water-compatible polymers is critical to the explanation of how these metastable amorphous regions control the non-equilibrium melting behavior of the crystalline regions. The concept of non-equilibrium melting established for synthetic partially crystalline polymers has been applied to

biopolymer systems such as native starch, in order to describe the mechanical relaxation process[17-23,26,30] that occurs as a consequence of a dynamic heat/moisture/time treatment.[229,230] The existence of contiguous microcrystalline and amorphous regions (e.g., in native starch, the crystallizable short branches and backbone segments with their branch points, respectively, of amylopectin molecules) covalently linked through individual polymer chains creates a "fringed micelle" network. Relative dehydration of the amorphous regions to an initial low overall moisture content leads to the kinetically stable condition in which the effective Tg is higher than the "equilibrium" Tm of the hydrated crystalline regions. Consequently, the effective Tm[21] is elevated and observed only after softening of the amorphous regions at Tg. Added water acts directly to plasticize the continuous glassy regions, leading to the kinetically metastable condition in which their effective Tg is depressed. Thus, the "fringe" becomes an unstable rubber at $T > Tg$, allowing sufficient mobility and swelling by thermal expansion and water uptake for the interconnected microcrystallites, embedded in the "fringed micelle" network, to melt (by dissociation, with concomitant volume expansion)[105] on heating to a less kinetically constrained Tm only slightly above the depressed Tg. For such a melting process, use of the Flory-Huggins thermodynamic treatment to interpret the effect of water content on Tm has no theoretical basis,[106,161,231] because, while water as a plasticizer does affect directly the Tg and indirectly the Tm of polymers such as starch, the effect on Tm is not the direct effect experienced in equilibrium melting (i.e., dissolution) along the solidus curve. In contrast to the case of native starch, in which initial "as is" moisture is limiting, in an excess-moisture situation such as a retrograded wheat starch gel with $\gtrsim$27 w% water (Wg′), in which the amorphous matrix would be fully plasticized and ambient temperature would be above Tg (i.e., $Tg' \simeq -5°C$), the fully hydrated and matured crystalline junctions would show the actual, lower (and closer to "equilibrium") Tm of $\simeq$60°C for retrograded B-type starch.[17-23,26] (Note the analogy between the above description of non-equilibrium melting in native granular starch and the case described previously of non-equilibrium melting in a synthetic, partially crystalline block copolymer. In this context, it is interesting that Wunderlich[105] defines branched polymers as a special case of copolymers, using the example of a synthetic polymer with crystallizable branches.)

Retrogradation has been described[17,18,20-23,26] as a non-equilibrium (i.e., time/temperature/moisture-dependent) polymer recrystallization process in completely amorphous (in the case of waxy starches) starch-water melts. In normal starches, retrogradation has been recently confirmed to involve both fast crystallization of amylose and slow recrystallization of amylopectin.[63,92,215,218-221] Amylopectin recrystallization has been described[17,18,20-23,26] as a nucleation-limited growth process that occurs, at $T > Tg$, in the mobile, viscoelastic, "fringed micelle" gel network plasticized by water, and which is thermally reversible at $T > Tm$. This description has also been confirmed recently, for both amylopectin[92,215] and amylose.[211-214,220] The aging effects typically observed in starch gels and baked bread have been attributed (as in synthetic polymer-organic diluent gels) to time-dependent crystallization processes (i.e., maturation), primarily involving amylopectin, which occur subsequent to initial gelation.[63,65,92,94,219,221,225] With respect to these effects, Slade[18] has reported that "analysis of results (of measurements of extent of recrystallization vs. time after gelatinization) by the classic Avrami equation may provide a convenient means to represent empirical data from retrogradation experiments,[63,94,183,219,232] but some published theoretical interpretations[233] have been misleading." Complications, due to the non-equilibrium nature of starch recrystallization via the three-step mechanism, limit the theoretical utility of the Avrami parameters, which were originally derived to describe crystallization under conditions far above the glass curve[26] and where details about nucleation events and constant linear growth rates were readily measurable.[104] Others have agreed with this conclusion[63,211] and pointed out that such an Avrami analysis allows no insight regarding crystal morphology[219] and provides no clear mechanistic information.[49,183] Furthermore, the Avrami theory gives no indication of the temperature dependence of the crystallization rate.[63,94]

It should be recalled that the same three-step crystallization mechanism also applies to low MW compounds,[4,104] such as concentrated aqueous solutions and melts of low MW carbohydrates,[16,30] and to recrystallization processes in frozen systems of water-compatible food materials.[15,27,32]

7. Polymer Crystallization Kinetics Theory

The classic theory of crystallization kinetics, applied to synthetic partially crystalline polymers,[104] is illustrated in Figure 37[26] (adapted from References 104, 139, 192). This theory has also been shown to describe the kinetics of starch retrogradation[17,18,20,49,94,95] and gelatin gelation.[17,24,139,195,234] Figure 37 shows the dependence of crystallization rate on temperature within the range Tg < T < Tm, and emphasizes the fact that gelation-via-crystallization can only occur in the rubbery (undercooled liquid) state, between the temperature limits defined by Tg and Tm.[15,94] These limits, for gels recrystallized from high MW gelatin solutions of concentrations up to about 65 w% gelatin (i.e., W > Wg′ ≃ 35 w% water), are about −12°C (= Tg′) and 37°C, respectively, while for B-type starch (or purified amylopectin) gels recrystallized from homogeneous and completely amorphous gelatinized sols or pastes containing ≳27 w% water (= Wg′), they are about −5°C (= Tg′) and 60°C, respectively.[17,18] In gelatinized potato starch:water mixtures (1:1 w/w), retrogradation has been demonstrated at single storage temperatures between 5 and 50°C.[235] In retrograding potato and wheat starch gels, low-temperature storage (at 5 and 4°C, respectively) results in recrystallization to lower-Tm, less symmetrically perfect polymorphs than those produced by storage at room temperature.[232,235] Conversely, a higher crystallization temperature generally favors formation of the higher-Tm, more stable A-type, rather than B-type, starch polymorph.[236,237] For amylopectins from waxy maize and other botanical sources, thermoreversible gelation-via-crystallization from concentrated (>10 w% solute) aqueous solution has been observed after long-term storage at 1 to 5°C.[92,216,218] In baked bread, low (4°C), intermediate (25°C), and high (40°C)-temperature storage results in starch recrystallization manifested by corresponding lower, intermediate, and higher-Tm staling endotherms.[95] In a 50% wheat starch gel, the extent of crystallization increases with decreasing storage temperature in the range 2 to 37°C (i.e., displays a negative temperature dependence), and the rate of recrystallization to the B-form is more rapid at 2 than at 37°C.[94] In contrast to the familiar Tm of about 60°C for thermoreversible B-type amylopectin gels with excess moisture stored at room temperature (and for stale bread),[20] the corresponding Tm for thermoreversible V-type amylose gels is well above 100°C,[35,92] owing in part to the much higher $\overline{DP}w$ of the amylose chain segments (i.e., $\overline{DP}w$ ≃ 50 vs. ≃15 for amylopectin)[92] comprising the microcrystalline junction zones. Analogously, the familiar Tm well above 100°C for various V-type lipid-amylose crystalline complexes[35] is much higher than the corresponding Tm of about 70°C reported for a lipid-amylopectin crystalline complex.[20] These findings are fully consistent with the established relationship between increasing chain length (and MW) and increasing Tm within

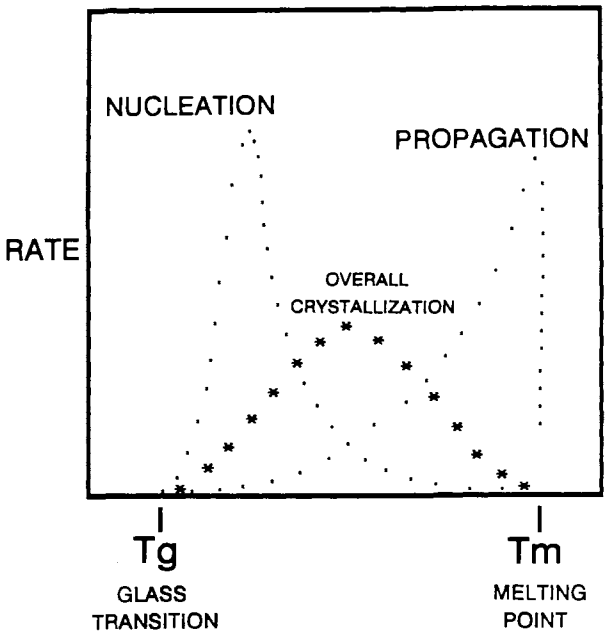

FIGURE 37. Crystallization kinetics of partially crystalline polymers, expressed in terms of crystallization rate as a function of temperature. (Reproduced with permission from Reference 26.)

homologous families of partially crystalline synthetic polymers.[105,113]

As illustrated by Figure 37 and the above results on the temperature dependence of starch recrystallization, the rate of crystallization would be practically negligible at $T < Tg$, because nucleation is a liquid-state phenomenon (i.e., in part, a transport process through a viscous medium)[49,94] that requires translational and orientational mobility, and such mobility is virtually disallowed (over realistic times) in a mechanical solid of $\eta \gtrsim 10^{12}$ Pa s.[4] The temperature of homogeneous nucleation (Th) can be estimated from the ratio of Th/Tm (K),[30] which is typically near 0.8 for partially crystalline synthetic polymers as well as small molecules, with a reported range of 0.78 to 0.85.[104,115] The rate of propagation goes essentially to zero below Tg, because propagation is a diffusion-limited process[192] for which practical rates also require the liquid state. At $T > Tm$, the rate of overall crystallization also goes to zero, because, intuitively, one realizes that crystals can neither nucleate nor propagate at any temperature at which they would be melted instantaneously.

Figure 37 illustrates the complex temperature dependence of the overall crystallization rate and of the rates of the separate mechanistic steps of nucleation and propagation. According to classic nucleation theory, the nucleation rate is zero at Tm and increases rapidly with decreasing temperature (and increasing extent of undercooling (Tm − T)) over a relatively narrow temperature interval, which for undiluted synthetic polymers begins at an undercooling of 30 to 100°C.[104] Within this temperature region, the nucleation rate shows a large negative temperature coefficient.[94,139] At still lower temperatures (and greater extents of undercooling), where nucleation relies on transport and depends on local viscosity, the nucleation rate decreases with decreasing temperature and increasing local viscosity, to a near-zero rate at Tg.[94,104] In contrast, the propagation rate increases rapidly with increasing temperature, from a near-zero rate at Tg, and shows a large positive temperature coefficient over nearly the entire rubbery range, until it drops precipitously to a zero rate at Tm.[94,104,139] The fact that the nucleation and propagation rates show temperature coefficients of opposite sign in the temperature region of intermediate undercooling has been explained[94] by pointing out that "when the temperature has been lowered sufficiently to allow the formation of (critical) nuclei (whose size decreases with decreasing temperature),[4,49] the (local) viscosity is already so high that it prevents growth of crystalline material."[192] The maturation rate for non-equilibrium crystallization processes, like the propagation rate, increases with increasing temperature, up to the maximum Tm of the most mature crystals.[15,18]

As shown by the symmetrical curve in Figure 37, the overall crystallization rate (i.e., the resultant rate of both the nucleation and propagation processes), at a single holding temperature, reaches a maximum at a temperature about midway between Tg and Tm, and approaches zero at Tg and Tm.[17,18,49,94,104,139] Identification of the location of the temperature of maximum crystallization rate has been described[104] in terms of a universal empirical relationship (based on two underlying concepts) for the crystallization kinetics of synthetic high polymers. The first concept identifies a model polymer (e.g., a readily crystallizable elastomer with Tg = 200 K and Tm = 400 K) as one for which the temperature dependence of polymer melt viscosity is described by WLF kinetics.[104] (The same concept has been shown to be applicable to describe the non-equilibrium thermomechanical relaxation behavior of "typical" and "atypical" food carbohydrates in aqueous glassy and rubbery states.)[30] The second concept empirically defines a reduced temperature, based on Tg and Tm for typical polymers, as $(T - Tg + 50\ K)/(Tm - Tg + 50\ K)$.[104] (An analogous reduced temperature scale, based on Tg′ and Tm, has been shown to describe the rotational mobility [i.e., dielectric relaxation behavior] of concentrated aqueous sugar solutions in the supraglassy fluid state.)[30] For all synthetic high polymers analyzed, the temperature position of the maximum crystallization rate, on a universal master curve like the one shown in Figure 37, occurs at about 0.6 of the reduced temperature scale.[104] Low MW synthetic compounds have been fitted to a similar curve, but with a different position for the maximum crystallization rate, at about 0.8 of the reduced temperature scale.[104] Based on this empirical relationship for synthetic high polymers,

the calculated single holding temperature for maximum crystallization rate would be about 300 K for the model elastomer (in fact, exactly midway between Tg and Tm), −3°C for a gelatin gel with ≳35 w% water (a temperature made inaccessible without detriment to product quality due to unavoidable ice formation), 14°C for a typical B-type starch (or amylopectin) gel with ≳27 w% water, and 70°C for a V-type amylose gel (based on Tm = 153°C[92]).[26] It has been noted[26] that the calculated value of about 14°C for B-type starch is similar to (1) the empirically determined subambient temperature for the maximum rate of starch recrystallization and concomitant crumb firming during aging, reported in an excellent study of the kinetics of bread staling by Guilbot and Godon,[238] but not previously explained on the basis of the polymer crystallization kinetics theory described above, and (2) the temperature of about 5°C recently calculated from Lauritzen-Hoffman polymer crystallization kinetics theory by Marsh and Blanshard[94] for a 50% wheat starch gel. The fact that these subambient temperatures are much closer to the operative Tg (i.e., Tg′) than to Tm,[26] unlike the situation depicted by the symmetrical shape of the crystallization rate curve in Figure 37 that typifies the behavior of many synthetic polymers, clearly indicates that the crystallization process for B-type starch (or pure amylopectin) is strongly nucleation-limited.[18,20,94]

In contrast to the maximum crystallization rate achievable at a single temperature, Ferry[239] showed for gelatin that the rate of gelation can be further increased, while the phenomenon of steadily increasing gel maturation over extended storage time can be eliminated, by a two-step temperature-cycling gelation protocol that capitalizes on the crystallization kinetics defined in Figure 37. He showed that a short period for fast nucleation at 0°C (a temperature above Tg′ and near the peak of the nucleation rate curve), followed by another short period for fast crystal growth at a temperature just below Tm, produced a gelatin gel of maximum and unchanging gel strength in the shortest possible overall time. Recently, Slade has shown that a similar temperature-cycling protocol can be used to maximize the rate of starch recrystallization in freshly gelatinized starch-water mixtures with at least 27 w% water,[18,20] resulting in a patented process for the accelerated staling of starch-based food products.[36] Zeleznak and Hoseney[95] subsequently adopted this protocol in their study of the temperature dependence of bread staling.

IV. THE FOOD POLYMER SCIENCE DATA BANK AND ITS PHYSICOCHEMICAL FOUNDATION

As emphasized by the discussion in Section II, for pragmatical time scales and conditions (temperature, concentration, pressure), where "real-world" food systems are usually far from equilibrium, familiar treatments (e.g., water activity and moisture sorption isotherms) based on the equilibrium thermodynamics of very dilute solutions fail.[30] This is not too surprising, since limiting partial molar properties reflect the independent behavior of solute in the limit of infinite dilution where free volume is maximum at a given temperature, while Tg′-Wg′ properties reflect the cooperative behavior of plasticizer blends composed of concentrated solute-water mixtures at the limiting minimum value of free volume to observe relaxation within experimental time scales. As suggested by the information reviewed in Section III, successful treatments require a new approach to emphasize the kinetic description, relate time-temperature-concentration-pressure through underlying mobility transformations, and establish reference conditions of temperature and concentration (characteristic for each solute).[30] In this section covering the food polymer science data bank and its physicochemical foundation, it is demonstrated (and then corroborated in Section V) that small carbohydrate-water systems, with well-characterized structure and MW above and below the limit for entanglement coupling, provide a unique framework for the investigation of non-equilibrium behavior:[30] definition of conditions for its empirical demonstration, examination of materials properties that allow its description and control, identification of appropriate experimental approaches, and exploration of theoretical interpretations. This framework has been applied to the other major categories of food materials included in the data bank.

The food polymer science data bank has been established from measured thermal properties of hundreds of individual food materials, including (a) small carbohydrates — sugars, polyhydric alcohols, and glycoside derivatives; (b) carbohydrate oligomers and high polymers — starches and SHPs; (c) high MW, non-starch polysaccharides; (d) amino acids; (e) proteins; (f) organic acids; (g) biological tissues — fruits and vegetables; and (h) a wide variety of other food ingredients and products.[8,14-39] The data bank consists of the following reference parameters, measured for each individual solute by DSC (see methods described elsewhere):[8,27,28,34] (1) Tg′, the particular subzero Tg of the maximally freeze-concentrated glass that is formed on slow cooling of a 20 w% aqueous solution of the non-crystallizing solute to T < Tg′; (2) Wg′, the corresponding water content of the maximally freeze-concentrated glass that is formed on slow cooling of a 20 w% aqueous solution of the non-crystallizing solute to T < Tg′, representing the amount of water rendered "unfreezable" on a practical time scale (expressed as g UFW/g solute) by immobilization with the solute in this dynamically constrained, kinetically metastable amorphous solid of extremely high local viscosity; (3) Tm of the anhydrous crystalline solute; and (4) Tg of the completely amorphous, anhydrous solute, resulting from vitrification via quench-cooling after melting of the crystalline solute.

A. Monomeric, Oligomeric, and Polymeric Carbohydrates

The 84 small carbohydrates listed in Table 3[6-8,27-31,40-42] are polyhydroxy compounds (PHCs) of known, monodisperse (i.e., $\overline{M}w/\overline{M}n = 1$) MWs. These PHCs represent a comprehensive but non-homologous series of mono-, di-, and small oligosaccharides and their derivatives, including many common sugars, polyols, and glycosides, covering a MW range of 62 to 1153 Da. The 91 SHPs listed in Table 4[8,32,34] are monomeric, oligomeric, and high-polymeric carbohydrates, representing a homologous family of glucose polymers. These SHPs represent a spectrum of commercial products (including modified starches, dextrins, maltodextrins, corn syrup solids, and corn syrups), with polydisperse MWs (i.e., $\overline{M}w/\overline{M}n \gg 1$), covering a very broad range of dextrose equivalent (DE, where DE = 100/($\overline{M}n$/180.2)) values from 0.3 to 100.

1. Tg′ Database

Figure 38[8] shows typical low-temperature DSC thermograms for 20 w% solutions of (a) glucose and (b) a 10 DE maltodextrin (Star Dri 10). In each, the heat flow curve begins at the top (endothermic down), and the analog derivative trace (endothermic up and zeroed to the temperature axis) at the bottom. For both thermograms, instrumental amplification and sensitivity settings were identical, and sample weights comparable. It is evident that the direct analog derivative feature of the DSC (DuPont Model 990) greatly facilitates deconvolution of sequential thermal transitions, assignment of precise transition temperatures (to ±0.5°C for Tg′ values of duplicate samples), and thus overall interpretation of thermal behavior, especially for such frozen aqueous solutions exemplified by Figure 38A. We commented in 1986[8] on the surprising absence of previous reports of the use of derivative thermograms, in the many earlier DSC studies of such systems with water content >Wg′ (see Franks[4] for an extensive bibliography), to sort out the small endothermic and exothermic changes in heat flow that typically occur below 0°C. Most modern commercial DSC instruments provide a derivative feature, but its use for increased interpretative capability still appears to remain much neglected in the thermal analysis of foods in general, and frozen aqueous food systems in particular.[34,189]

Despite the handicap of such instrumental limitations in the past, the theoretical basis for the thermal properties of aqueous solutions at subzero temperatures has come to be increasingly understood.[4-6,74,133,240-242] As shown in Figure 38A, after rapid cooling (about 50°C/min) of the glucose solution from room temperature to < −80°C, slow heating (5°C/min) reveals a minor Tg at −61.5°C, followed by an exothermic devitrification (a crystallization of some of the previously UFW) at Td = −47.5°C, followed by another (major) Tg, namely, Tg′, at −43°C, and finally

TABLE 3
Tg', Wg', Dry Tg, Dry Tm, and Tm/Tg Ratio for Sugars and Polyols[27,28]

Polyhydroxy compound	MW	Tg' °C	Wg' (g UFW/g)	Dry Tg °C	Dry Tm °C	Tm/Tg °K
Ethylene glycol	62.1	−85	1.90			
Propylene glycol	76.1	−67.5	1.28			
1,3-Butanediol	90.1	−63.5	1.41			
Glycerol	92.1	−65	0.85	−93	18	1.62
Erythrose	120.1	−50	1.39			
Threose	120.1	−45.5				
Erythritol	122.1	−53.5	(Eutectic)			
Thyminose (deoxyribose)	134.1	−52	1.32			
Ribulose	150.1	−50				
Xylose	150.1	−48	0.45	9.5	153	1.51
Arabinose	150.1	−47.5	1.23			
Lyxose	150.1	−47.5		8	115	1.38
Ribose	150.1	−47	0.49	−10	87	1.37
Arabitol	152.1	−47	0.89			
Ribitol	152.1	−47	0.82			
Xylitol	152.1	−46.5	0.75	−18.5	94	1.44
Methyl riboside	164.2	−53	0.96			
Methyl xyloside	164.2	−49	1.01			
Quinovose (deoxyglucose)	164.2	−43.5	1.11			
Fucose (deoxygalactose)	164.2	−43	1.11			
Rhamnose (deoxymannose)	164.2	−43	0.90			
Talose	180.2	−44		11.5	140	1.45
Idose	180.2	−44				
Psicose	180.2	−44				
Altrose	180.2	−43.5		10.5	107	1.34
Glucose	180.2	−43	0.41	31	158	1.42
Gulose	180.2	−42.5				
Fructose	180.2	−42	0.96	100	124	1.06
Galactose	180.2	−41.5	0.77	110	170	1.16
Allose	180.2	−41.5	0.56			
Sorbose	180.2	−41	0.45			
Mannose	180.2	−41	0.35	30	139.5	1.36
Tagatose	180.2	−40.5	1.33			
Inositol	180.2	−35.5	0.30			
Mannitol	182.2	−40	(Eutectic)			
Galactitol	182.2	−39	(Eutectic)			
Sorbitol	182.2	−43.5	0.23	−2	111	1.42
2-*O*-methyl fructoside	194.2	−51.5	1.61			
β-1-*O*-methyl glucoside	194.2	−47	1.29			
3-*O*-methyl glucoside	194.2	−45.5	1.34			
6-*O*-methyl galactoside	194.2	−45.5	0.98			
α-1-*O*-methyl glucoside	194.2	−44.5	1.32			
1-*O*-methyl galactoside	194.2	−44.5	0.86			

TABLE 3 (continued)
Tg′, Wg′, Dry Tg, Dry Tm, and Tm/Tg Ratio for Sugars and Polyols[27,28]

Polyhydroxy compound	MW	Tg′ °C	Wg′ (g UFW/g)	Dry Tg °C	Dry Tm °C	Tm/Tg °K
1-*O*-methyl mannoside	194.2	−43.5	1.43			
1-*O*-ethyl glucoside	208.2	−46.5	1.35			
2-*O*-ethyl fructoside	208.2	−46.5	1.15			
1-*O*-ethyl galactoside	208.2	−45	1.26			
1-*O*-ethyl mannoside	208.2	−43.5	1.21			
Glucoheptose	210.2	−37.5				
Mannoheptulose	210.2	−36.5				
Glucoheptulose	210.2	−36.5	0.77			
Perseitol (mannoheptitol)	212.2	−32.5	(Eutectic)			
1-*O*-propyl glucoside	222.2	−43	1.22			
1-*O*-propyl galactoside	222.2	−42	1.05			
1-*O*-propyl mannoside	222.2	−40.5	0.95			
2,3,4,6-*O*-methyl glucoside	236.2	−45.5	1.41			
Isomaltulose (palatinose)	342.3	−35.5				
Nigerose	342.3	−35.5				
Cellobiulose	342.3	−32.5				
Isomaltose	342.3	−32.5	0.70			
Sucrose	342.3	−32	0.56	52	192	1.43
Gentiobiose	342.3	−31.5	0.26			
Laminaribiose	342.3	−31.5				
Turanose	342.3	−31	0.64	52	177	1.38
Mannobiose	342.3	−30.5	0.91	90	205	1.32
Melibiose	342.3	−30.5				
Lactulose	342.3	−30	0.72			
Maltose	342.3	−29.5	0.25	43	129	1.27
Maltulose	342.3	−29.5				
Trehalose	342.3	−29.5	0.20	79	203	1.35
Cellobiose	342.3	−29		77	249	1.49
Lactose	342.3	−28	0.69			
Maltitol	344.3	−34.5	0.59			
Isomaltotriose	504.5	−30.5	0.50			
Panose	504.5	−28	0.59			
Raffinose	504.5	−26.5	0.70			
Maltotriose	504.5	−23.5	0.45	76	133.5	1.16
Nystose	666.6	−26.5		77	—	
Stachyose	666.6	−23.5	1.12			
Maltotetraose	666.6	−19.5	0.55	111.5	—	
Maltopentaose	828.9	−16.5	0.47	125	—	
α-Cyclodextrin	972.9	−9				
Maltohexaose	990.9	−14.5	0.50	134	—	
Maltoheptaose	1153.0	−13.5	0.27	138.5	—	

the melting of ice, beginning at $T > Tg'$ and ending at Tm. In Figure 38B, the maltodextrin solution thermogram shows only an obvious Tg′ at −10°C, followed by Tm. These assignments of characteristic transitions (i.e., the sequence $Tg < Td < Tg' < Tm$) and temperatures have been

TABLE 4
Tg′ Values for Commercial SHPs[8]

SHP	Manufacturer	Starch source	DE	Tg′, °C	Gelling
AB 7436	Anheuser Busch	Waxy maize	0.5	−4	
AmioGum 23	Amaizo		1	−4	
47TT110	Staley	Potato	0.6	−4.5	
Paselli SA-2	AVEBE (1984)	Potato (Ap)	2	−4.5	Yes
Stadex 9	Staley	Dent corn	3.4	−4.5	Yes
Paselli SA-2	AVEBE (1987)	Potato	2	−5	
78NN128	Staley	Potato	0.6	−5	Yes
78NN122	Staley	Potato	2	−5	Yes
V-O Starch	National	Waxy maize		−5.5	Yes
N-Oil	National	Tapioca		−5.5	Yes
ARD 2326	Amaizo	Dent corn	0.4	−5.5	Yes
Paselli SA-2	AVEBE (1986)	Potato (Ap)	2	−5.5	Yes
Glucidex 2B	Roquette	Waxy maize	2	−5.5	
ARD 2308	Amaizo	Dent corn	0.3	−6	Yes
AB 7435	Anheuser Busch	Waxy/dent blend	0.5	−6	
Star Dri 1	Staley (1984)	Dent corn	1	−6	Yes
Crystal Gum	National	Tapioca	5	−6	Yes
Maltrin M050	GPC	Dent corn	6	−6	Yes
Star Dri 1	Staley (1986)	Waxy maize	1	−6.5	Yes
Paselli MD-6	AVEBE	Potato	6	−6.5	Yes
Dextrin 11	Staley	Tapioca	1	−7.5	Yes
MD-6-12	V-Labs		2.8	−7.5	
Capsul	National (1987)	Waxy maize	5	−7.5	
Stadex 27	Staley	Dent corn	10	−7.5	No
MD-6-40	V-Labs		0.7	−8	
Star Dri 5	Staley (1984)	Dent corn	5	−8	No
Star Dri 5	Staley (1986)	Waxy maize	5.5	−8	No
Paselli MD-10	AVEBE	Potato	10	−8	No
Paselli SA-6	AVEBE	Potato (Ap)	6	−8.5	No
α-Cyclodextrin	Pfanstiehl			−9	
Capsul	National (1982)	Waxy maize	5	−9	
Lodex Light V	Amaizo	Waxy maize	7	−9	
Paselli SA-10	AVEBE	Potato (Ap)	10	−9.5	No
Morrex 1910	CPC	Dent corn	10	−9.5	
Star Dri 10	Staley (1984)	Dent corn	10	−10	No
Maltrin M040	GPC	Dent corn	5	−10.5	
Frodex 5	Amaizo	Waxy maize	5	−11	
Star Dri 10	Staley (1986)	Waxy maize	10.5	−11	No
Lodex 10	Amaizo (1986)	Waxy maize	11	−11.5	No
Lodex Light X	Amaizo	Waxy maize	12	−11.5	
Morrex 1918	CPC	Waxy maize	10	−11.5	
Mira-Cap	Staley	Waxy maize		−11.5	
Maltrin M100	GPC	Dent corn	10	−11.5	No
Lodex 5	Amaizo	Waxy maize	7	−12	No
Maltrin M500	GPC	Dent corn	10	−12.5	
Lodex 10	Amaizo (1982)	Waxy maize	12	−12.5	No
Star Dri 15	Staley (1986)	Waxy maize	15.5	−12.5	No
MD-6	V-Labs			−12.5	
Maltrin M150	GPC	Dent corn	15	−13.5	No
Maltoheptaose	Sigma		15.6	−13.5	
MD-6-1	V-Labs		20.5	−13.5	
Star Dri 20	Staley (1986)	Waxy maize	21.5	−13.5	No

TABLE 4 (continued)
Tg′ Values for Commercial SHPs[8]

SHP	Manufacturer	Starch source	DE	Tg′, °C	Gelling
Maltodextrin Syrup	GPC	Dent corn	17.5	−14	No
Frodex 15	Amaizo	Waxy maize	18	−14	
Maltohexaose	Sigma		18.2	−14.5	
Frodex 10	Amaizo	Waxy maize	10	−15.5	
Lodex 15	Amaizo	Waxy maize	18	−15.5	No
Maltohexaose	V-Labs		18.2	−15.5	
Maltrin M200	GPC	Dent corn	20	−15.5	
Maltopentaose	Sigma		21.7	−16.5	
Staley 200	Staley (1987)	Corn	26	−17	
Maltrin M250	GPC (1987)	Dent corn	25	−17	
Maltrin M250	GPC (1982)	Dent corn	25	−17.5	
N-Lok	National	Blend		−17.5	
Staley 200	Staley	Corn	26	−19.5	
Maltotetraose	Sigma		27	−19.5	
Frodex 24	Amaizo (1987)	Waxy maize	28	−19.5	
Frodex 24	Amaizo (1982)	Waxy maize	28	−20.5	
Frodex 36	Amaizo	Waxy maize	36	−21.5	
DriSweet 36	Hubinger	Corn	36	−22	
Maltrin M365	GPC	Dent corn	36	−22.5	
Staley 300	Staley	Corn	35	−23.5	
Globe 1052	CPC	Corn	37	−23.5	
Maltotriose	V-Labs		35.7	−23.5	
Frodex 42	Amaizo (1982)	Waxy maize	42	−25.5	
Frodex 42	Amaizo (1987)	Waxy maize	42	−25.5	
Neto 7300	Staley (1987)	Corn	42	−25.5	
Staley 1300	Staley (1987)	Corn	43	−26	
Neto 7300	Staley (1982)	Corn	42	−26.5	
Globe 1132	CPC	Corn	43	−27.5	
Staley 1300	Staley (1982)	Corn	43	−27.5	
Neto 7350	Staley	Corn	50	−27.5	
Maltose	Sigma		52.6	−29.5	
Globe 1232	CPC	Corn	54.5	−30.5	
Staley 2300	Staley	Corn	54	−31	
Sweetose 4400	Staley	Corn	64	−33.5	
Sweetose 4300	Staley	Corn	64	−34	
Globe 1642	CPC	Corn	63	−35	
Globe 1632	CPC	Corn	64	−35	
Royal 2626	CPC	Corn	95	−42	
Glucose	Sigma	Corn	100	−43	

reconciled definitively with actual state diagrams previously reported for various solutes, including small sugars and water-soluble polymers.[4,32,33,242]

It has been demonstrated[8,33] that the thermogram for the glucose solution in Figure 38A represents a characteristic example, if somewhat trivial case,[30] of the unusual phenomenon of multiple values of Tg in glass-forming systems, which is a subject of increasing current interest in the cryotechnology field.[8,27,31-34,175,243-248] Due to incomplete phase separation[175,243-246] in an incompletely frozen aqueous solution, two distinguishable, dynamically constrained glasses, with local domains of sufficient dimension and cooperativity to allow ready detection, may coexist.[30,246] One is a "bulk" glass with the same spatial homogeneity and solute concentration as the original dilute solution and a corresponding low value of

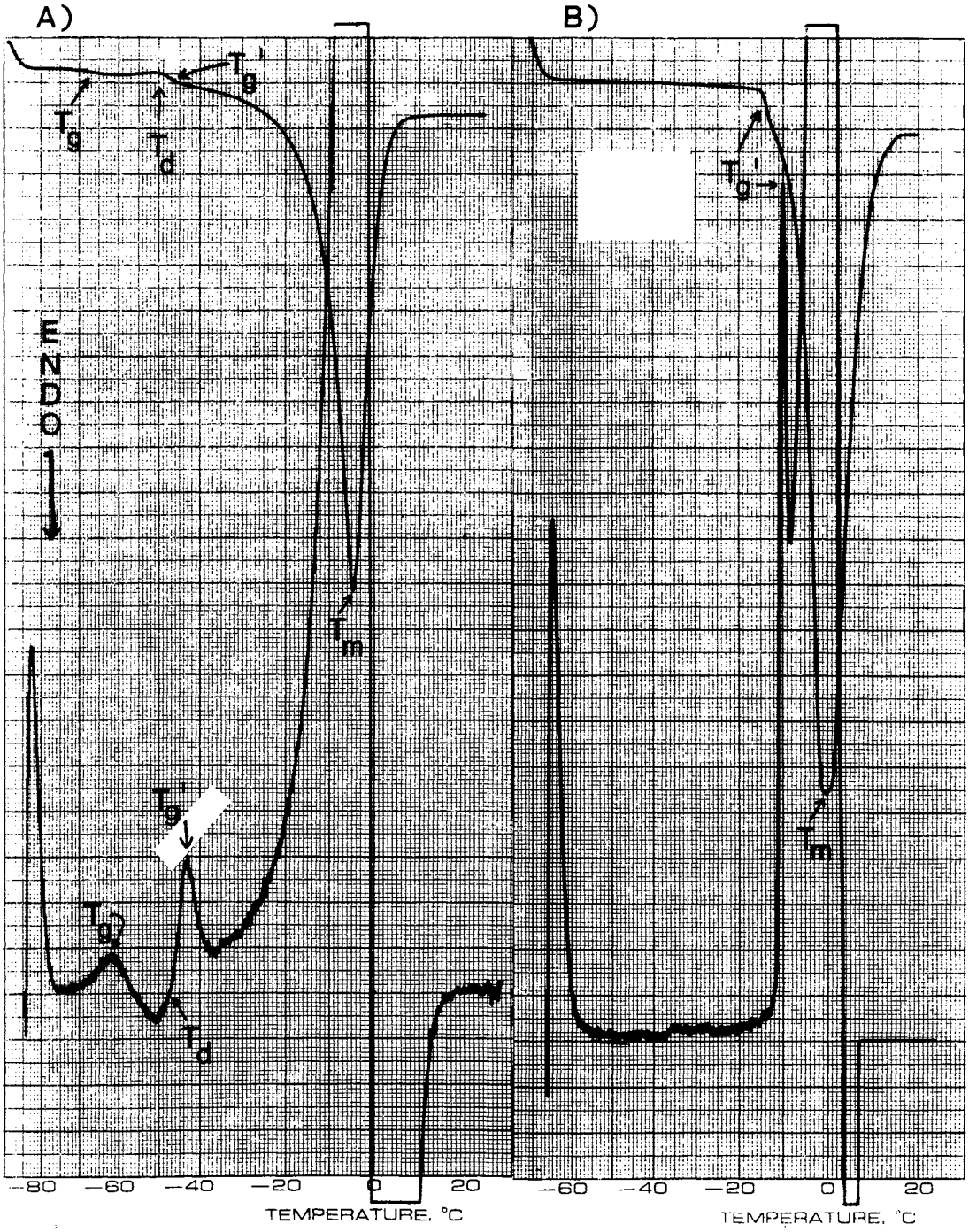

FIGURE 38. DuPont 990 DSC thermograms for 20 w% solutions of (a) glucose, and (b) Star Dri 10 (10 DE) maltodextrin. In each, the heat flow curve begins at the top (endothermic down), and the analog derivative trace (endothermic up and zeroed to the temperature axis) at the bottom. (From Levine, H. and Slade, L., *Carbohydr. Polym.*, 6, 213, 1986. With permission.)

Tg. The other, surrounding the ice crystals, is the freeze-concentrated glass with a higher value of Tg that is Tg′.[8,27,31-34] The lower limiting value of Tg for the dilute bulk glass is Tg of pure amorphous water itself, and the upper limiting value of Tg′ for the freeze-concentrated glass is Tm of pure crystalline water.[33] The observation of such a Tg + Tg′ doublet depends on sample

moisture content, cooling/heating history, and pressure history,[30,246] and represents an example of the difficulty that can be encountered in deconvoluting the non-equilibrium effects of sample history,[249,250] and the resulting potential for misinterpretation that can arise when experiments on frozen aqueous systems are not designed from a knowledge of the operative reference state.[243-245] It should be noted that other cases of multiple-Tg phenomena that have been reported are readily distinguishable from the Tg + Tg′ doublet behavior of incompletely frozen aqueous solutions. One type of general behavior (i.e., not restricted to low-temperature aqueous systems), representing another trivial case, involves simple molecular incompatibility in a two-component system, where, due to a lack of spatial homogeneity on a dimensional scale $\gtrsim$100 Å,[106] two separate glasses with different values of Tg may coexist. A non-trivial case of multiple values of Tg can result from a liquid-liquid phase separation (which can be pressure-induced or -facilitated in some instances,[247] but in others can occur at atmospheric pressure),[248] leading to spatial inhomogeneity in aqueous solutions of, for example, lithium chloride and tetraalkylammonium halides at low temperatures. Another non-trivial case can result from the formation of specific stoichiometric complexes in aqueous solutions of, for example, glycerol, DMSO, and lithium chloride[247] where each complex would exhibit its own discrete Tm (or eutectic melting temperature) and Tg′.

The idealized state diagram shown in Figure 39,[33] modified from MacKenzie and Rasmussen,[242] exemplifies those previously reported and reveals the various distinctive cooling/heating paths that can be followed by solutions of monomeric (glucose) vs. polymeric (maltodextrin) solutes. In the case of glucose, partial vitrification of the original solution can occur, as illustrated by Figure 38A, when the selected cooling rate is high relative to the rate of freezing out of ice.[5] Yet, in the case of maltodextrin, that same cooling rate would be low relative to the rate of freezing, and less vitrification is observed,[8] as shown in Figure 38B. This result is perhaps surprising, since relative rates of diffusion processes might have been expected to be more retarded in the maltodextrin solution of greater $\overline{M}w$ than in the glucose solution.[30,32] In fact, the relative rate of ice *growth* is greater in glucose solution than in maltodextrin solution.[32] However, in this example, the rate-limiting event that determines whether freezing or vitrification will predominate is the prerequisite nucleation step for the freezing process.[33] An empirical examination of available data[8,30-34] shows that efficient retardation of ice crystal growth is provided by solutes for which Tg′ of the freeze-concentrated glass is high, while enhanced potential for partial vitrification is provided by solutes for which the value of Wg′ is high, most typically concomitant with a low value of Tg′.[32] This empirical observation serves as the basis for two operational definitions of a "good" aqueous-glass former:[33,251] (1) a solute that enhances the vitrification of water as a solute-water glass over the energetically favored phase separation of ice, and (2) a solute that provides an aqueous glass with a high value of Wg′. As can be deduced from the relative sizes of the ice peaks for the samples of identical concentration and comparable weight in Figure 38A and 38B, Wg′ for the glucose-water glass is greater than Wg′ for this 10 DE maltodextrin-water glass,[8] so that glucose is a better aqueous-glass former than this maltodextrin by both criteria. The greater effect of glucose than 10 DE maltodextrin on ice nucleation cannot be attributed simply to a greater colligative depression of the homogeneous nucleation temperature by the smaller MW solute compared to the larger solute at the same w% concentration.[30,33] PVP, with $\overline{M}n$ more than 10 times greater than that of a 10 DE maltodextrin, is a good aqueous-glass former,[135] like glucose. Indeed, values of Wg′ for aqueous glasses of PVPs are greater than Wg′ of the aqueous glucose glass,[27] an anomaly inconsistent with the expected observation that the values of Tg′ for PVP glasses are greater than that of the glucose glass.[8] The location of Wg′ and Tg′ on the dynamics map for a particular solute determines the overall shape of the aqueous glass curve for that solute, such that higher values of either parameter result in a steeper rise in Tg with increase in w% solute at low solute concentrations.[16,30] The number of critical nuclei formed in a volume of solution at a given temperature within a given time interval depends both on the local viscosity of the solution and the temperature-dependence of the number

of water molecules required to constitute a critical nucleus through density fluctuations of pure water molecules.[5,40-42] Higher values of Wg′ suggest that lower nucleation temperatures would be required to create a critical nucleus, due to the smaller local dimensions available for unperturbed density fluctuations of pure water. Higher values of Wg′ or Tg′ suggest that the local viscosity of the solution would become limiting near temperatures that would effect nucleation of pure water. The value of Wg′ relates to both of the factors that determine the kinetics of ice nucleation in solution and, thus, to the ability of a solute to enhance partial vitrification at a selected cooling rate.[33]

However, as demonstrated by the DSC thermograms in Figure 38, in either general case, and regardless of initial cooling rate, rewarming from T < Tg′ forces the system through a solute-specific glass transition at Tg′.[8] As illustrated in the state diagram in Figure 39, the Tg′-Cg′ point represents a "universal crossroads" on this map, in that all cooling/heating paths eventually lead to this point.[33] As shown by one of the idealized paths in Figure 39, slow cooling of a stereotypical sugar solution from room temperature (point X) to a temperature corresponding to point Y can follow the path XVSUWY, which passes through the Tg′-Cg′ point, W. In the absence of undercooling (e.g., upon deliberate nucleation), freezing (ice formation) begins at point V (on the equilibrium liquidus curve, at a subzero temperature determined by the MW and concentration of the particular solute, via colligative freezing point depression) and ends at point W (on the non-equilibrium extension of the liquidus curve). Due to vitrification of the Tg′-Cg′ glass at point W, some of the water in the original solution (i.e., an amount defined as Wg′) is left unfrozen in the time frame of the experiment. This UFW is not "bound" to the solute nor "unfreezable" on thermodynamic grounds, but simply experiences retarded mobility in the Tg′-Cg′ glass. The extremely high local viscosity of this kinetically-metastable, dynamically constrained glass prevents diffusion of a sufficient number of water molecules to the surface of the ice lattice to allow measurement of its growth in real time.[4-8,40-42] As exemplified by the thermogram for the maltodextrin solution in Figure 38B, rewarming from point Y to point X can follow the reversible path YWUSVX, passing back through the Tg′-Cg′ point at W.[33]

In contrast to the slow-cooling path XVSUWY in Figure 39, quench-cooling can follow the direct path from point X to point Z, whereby vitrification can occur at T = Tg, the temperature corresponding to point A, *without* any freezing of ice or consequent change in the initial solution concentration.[242] However, unlike path XVSUWY, path XZ is not realistically reversible in the context of practical warming rates.[251] Upon slow, continuous rewarming from point Z to point X, the glass (of composition Cg-Wg rather than Cg′-Wg′) softens as the system passes through the Tg at point A, and then devitrifies at the Td at point D.[242] Devitrification leads to disproportionation, which results in the freezing of pure ice (point E) and revitrification via freeze-concentration of the non-ice matrix to Cg′ (point F) during *warming*.[242] Further warming above Td causes the glass (of composition Cg′-Wg′ rather than Cg-Wg) to pass through the Tg′-Cg′ point at W (where ice melting begins), after which the solution proceeds along the liquidus curve to point V (where ice melting ends at Tm), and then back to point X. The rewarming path ZADFWUSVX[33] is exemplified by the thermogram for the glucose solution in Figure 38A.

Mention can be made here about the possible consequences of an annealing treatment,[163,164,246,252,253] whereby the rewarming process just described is interrupted by an isothermal holding step carried out at different points along the path ZADFWUSV. As described for metastable, partially crystalline synthetic polymer systems,[104] annealing is a kinetic (i.e., time-dependent), transport-controlled process of crystal growth and/or perfection that occurs at Ta, a temperature above Tg but below Tm, typically = 0.75 to 0.88 Tm (K),[102] for "well-behaved" polymer systems[30] with characteristic Tg/Tm ratios of 0.5 to 0.8 (K).[102,105] In this metastable rubbery domain defined by WLF theory, within the temperature range between Tg and Tm, annealing is a diffusion-limited, non-equilibrium, structural relaxation process (another collapse phenomenon) for which the rate is governed by WLF, rather than Arrhenius, kinetics.[15,21] Specifically with respect to the behavior of frozen aqueous

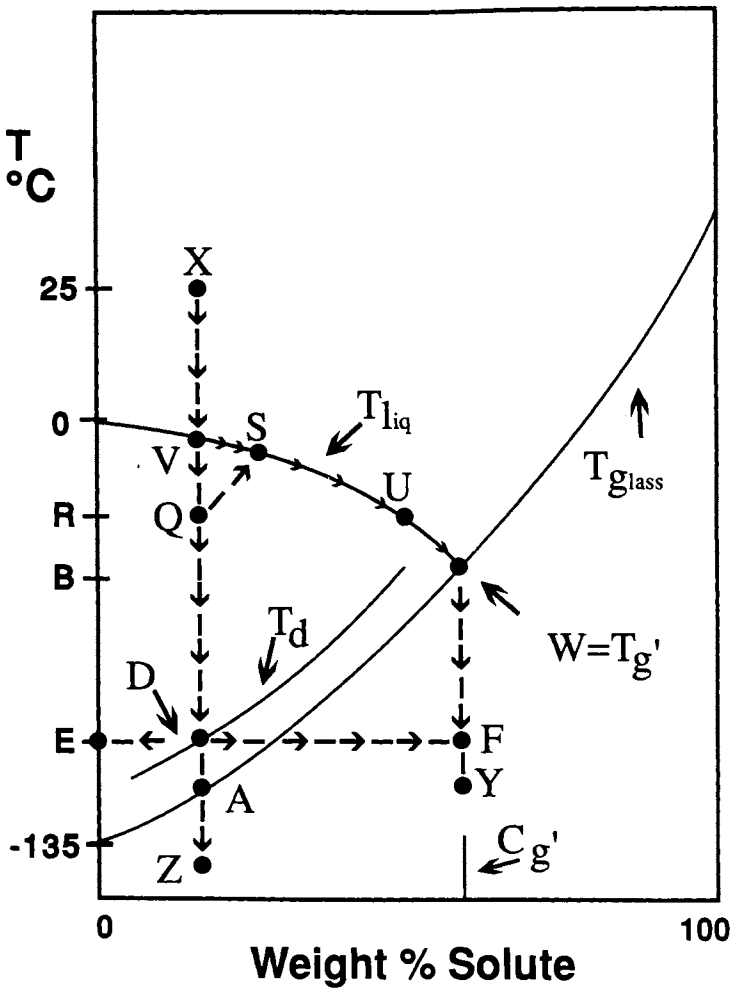

FIGURE 39. Idealized state diagram of temperature vs. weight percent solute for an aqueous solution of a hypothetical small carbohydrate (representing a model frozen food system), illustrating various cooling/heating paths and associated thermal transitions measurable by low-temperature differential scanning calorimetry (e.g., as shown by the thermograms in Figure 38). See text for explanation of symbols. (From Levine, H. and Slade, L., *Comments Agric. Food Chem.*, 1, 315, 1989. With permission.)

model solutions described by Figure 39, recognition of the time- and temperature-dependence of annealing is key to understanding the possible consequences potentially observable in a thermogram during rewarming after an annealing treatment performed at Ta < Tm of ice.[33] In all cases, the time required to achieve a measurable and comparable (in a reasonable and similar experimental time frame) extent of annealing is shortest at Ta just below Tm (greatest ΔT above Tg) and longest at Ta just above Tg (smallest ΔT).[21] For a solution initially quench-cooled from room temperature to T < Tg as described in Figure 39, the discussion[33] of the consequences of annealing can be complicated by the possible coexistence of two glasses with different glass transition temperatures (Tg and Tg′),[30] either or both of which could govern a subsequent annealing treatment. Annealing by an isothermal holding step at Tg < Ta < Td < Tg′ < Tm would be predicted to occur quite slowly, because of the still very high local viscosity of the amorphous matrix at Ta just above Tg. Unless the experimental holding time were quite long, the

subsequent thermogram (during warming from $T < Tg$, after recooling from Ta) might well be indistinguishable in appearance from the one in Figure 38A. Moreover, if both the Tg and Tg′ glasses were present after initial quench-cooling, the slow annealing at $Tg < Ta < Td < Tg'$ just described would only occur locally, rather than spacially homogeneously throughout the frozen sample. In contrast, annealing by isothermal holding at $Tg < Td < Tg' < Ta < Tm$ would be a much faster and more spacially homogeneous process. After a sufficiently long experimental holding time for complete annealing, the subsequent thermogram (during warming from $T < Tg$ of the original sample, after recooling from $Ta > Tg'$) would be predicted to show no detectable lower-temperature Tg or exothermic Td, only a Tg′ and Tm (i.e., have the qualitative appearance of Figure 38B). In the intermediate case of annealing by isothermal holding at $Tg < Td < Ta < Tg' < Tm$, some of the consequences of partial annealing could be seen after a reasonable holding time at Ta just below Tg′. The subsequent thermogram (during warming from $T < Tg$, after recooling from Ta) might still show a remnant of the lower-temperature Tg, but an undetectably small Td, in addition to Tg′ and Tm. In fact, thermograms similar to that just described have been reported for solutions of sugars and other solutes[252,253] after an annealing treatment at Ta ≡ the so-called "antemelting" transition temperature (Tam, discussed later) just below Tg′. In the above discussion,[33] the different annealing times have been, of necessity, described only in relative qualitative terms, because experimental results of previously published studies are insufficient to allow quantitative generalizations. Quantitative times corresponding to the different annealing scenarios described above would have to be determined experimentally on a system-specific basis, i.e., for each particular solute, solute concentration, range of absolute temperatures, and cooling/warming rate protocol.[443]

The third cooling path illustrated in Figure 39, XQSUWY, is the one most relevant to the practical cooling and warming rates involved in commercial frozen food processes.[33] Cooling of a solution from point X can proceed beyond point V (on the liquidus curve) to point Q, because the system can undercool to some significant extent before heterogeneous nucleation occurs and freezing begins.[4] Upon freezing at point Q, disproportionation occurs, resulting in the formation of pure ice (point R) and freeze-concentration of the solution to point S.[4] The temperature at point S is above that at point Q due to the heat liberated by the freezing of ice.[4] The freeze-concentrated matrix at point S concentrates further to point U, because more ice forms as the temperature of the system relaxes to that at point U. Upon further cooling beyond point U, ice formation and freeze-concentration continue as the system proceeds along the liquidus curve to point W. Vitrification of the Tg′-Cg′ glass occurs at point W, and further cooling of this glass can continue to point Y without additional ice formation in real time. Rewarming of the kinetically metastable glass from point Y to point X follows the path YWUSVX, which passes through the Tg′-Cg′ point at W. The above descriptions of the various cooling/warming paths illustrated in Figure 39 demonstrate the critical fact that, regardless of cooling/warming rates (within practical limits), every aqueous system of initial concentration $\leq Cg'$, cooled to $T \leq Tg'$, must pass through its own characteristic and operationally invariant Tg′-Cg′ point.[33] If, in commercial practice, a food product is not cooled to $T \leq Tg'$ after freezing, but rather is maintained within the temperature range between points V and W, that system would track back and forth along the liquidus curve as Tf fluctuates during storage.

The technological significance of Tg′ to the storage stability of frozen food systems, implicit in the preceding description of Figure 39, is discussed in Section IV.C. Suffice it to say for now that Tg′ (of the freeze-concentrated solution), rather than Tg (of the original solution), is the *only* glass transition temperature relevant to freezer-storage stability at a given freezer temperature Tf,[33] because almost all "frozen" products contain at least some ice. Consistent with the description of the cooling path XVQSUWY, most commercial food-freezing processes, regardless of cooling rate, induce ice formation beginning at point Q (via heterogeneous nucleation after some extent of undercooling). Since the temperature at point Q (generally in the neighborhood of $-20°C$[40,41]) is well above that at point A, the lower Tg, that of the glass with the original

solute(s) concentration in a typical high-moisture product, is never attained and therefore has no practical relevance.[33] Once ice formation occurs in a frozen product, the predominant system-specific Tg′ becomes the one and only glass transition temperature that controls the product's behavior during freezer storage at any Tf below Tm and either above or below Tg′.[33]

In many earlier DSC studies,[125,133,252-255] performed without benefit of derivative thermograms, a pair of transitions (each said to be independent of initial concentration), called "antemelting" (am) and "incipient melting" (im), were reported in place of a single Tg′. Even though the underlying physicochemical nature of the antemelting transition has never been explained,[256] this interpretation is still advocated by some workers.[57,257] In fact, for many different solutes, reported values of Tam and Tim[241,258,259] bracket that of Tg′. This led to the alternative interpretation[8] that Tam and Tim actually represent the temperatures of onset and completion of the single thermal relaxation event (a glass transition) that must occur at Tg′, as defined by the state diagram in Figure 39. A similar lack of consensus among workers in this field persists with respect to the Tg < Td < Tg′ sequence of transitions (Figure 38A) that is universally characteristic of frozen solutions of non-crystallizing solutes rewarmed after cooling to T < Tg.[32] Instead, some have referred to "anomalous double glass transitions"[243-245] or "the phenomenon of vitreous polymorphs"[246] exhibited by aqueous solutions of, e.g., propylene glycol and glycerol. Far from anomalously, for each solute, the higher Tg of the doublet coincides with Tg′.[32] Similarly, Tr, corresponding to the onset temperature for opacity during warming of completely vitrified aqueous solutions, and known to be independent of initial concentration, is still a topic of current interest and discussion as to its origin,[260,261] but is not yet widely recognized as simply coinciding with Tg′ for low MW, non-crystallizing carbohydrate solutes[32] and non-crystallizing water-compatible polymers, e.g., PVP.[8]

In comparison to commercial SHPs, such as the 10 DE maltodextrin in Figure 38B, a starch itself has a Tg′ value of about −5°C,[17,18] as illustrated by the low-temperature DSC thermogram in Figure 40B.[21] A freshly gelatinized (but not hydrolyzed) sample of native granular wheat starch, at uniformly distributed 55 w% total moisture, showed a prominent and reversible glass transition for the fully plasticized, completely amorphous starch polymers at −5°C, immediately preceding the Tm of ice. This Tg is the Tg′ for gelatinized wheat starch in excess moisture, where the latter condition is defined by Wg′ ≃ 27 w% water (i.e., about 0.37 g UFW/g starch),[17,18] as illustrated by the state diagram in Figure 25. For the same instrumental sensitivity settings, Tg′ was not detectable in Figure 40A, because the cooperative, controlling majority of the amorphous regions of partially crystalline native starch prior to gelatinization show a much higher Tg indicative of a much lower local effective moisture content.[20]

For various PHC and SHP solutes listed in Tables 3 and 4, the experimentally measured Tg′ value falls between those reported for Tam and Tim,[241,259] and within a few degrees of values reported for Tr and Tc (see References 8 and 27 and references therein). Reid[262] has recently reported a Tg′ value for glycerol similar to ours. Also in apparent agreement with one of our measured Tg′ values, i.e., of −85°C for ethylene glycol, Hallbrucker and Mayer[263] have observed an endothermic peak at −86°C, following devitrification above Tg ≃ −128°C, in DSC rewarming scans of "hyperquenched" aqueous glasses of 47 and 50 w% ethylene glycol. They have noted the good correspondence between their peak at −86°C and the weak endothermic peak observed on rewarming slow-cooled ethylene glycol-water solution glasses in DTA experiments by Luyet and Rasmussen,[241,259] which these latter workers named the putative "antemelting" transition, purported to take place at the ice-solution interface.

In Table 3, Tg′ values for this non-homologous collection of low MW, monodisperse sugars, polyols, and glycosides range from −85°C for ethylene glycol (MW 62) to −13.5°C for maltoheptaose (MW 1153). These results, plotted in Figure 41,[27] showed a monotonic relationship between increasing Tg′ and MW, which yielded a fair linear correlation (r = −0.934) between Tg′ and 1/MW, as shown in the inset of Figure 41. The major source of scatter in this plot was the group of glycosides with chemically

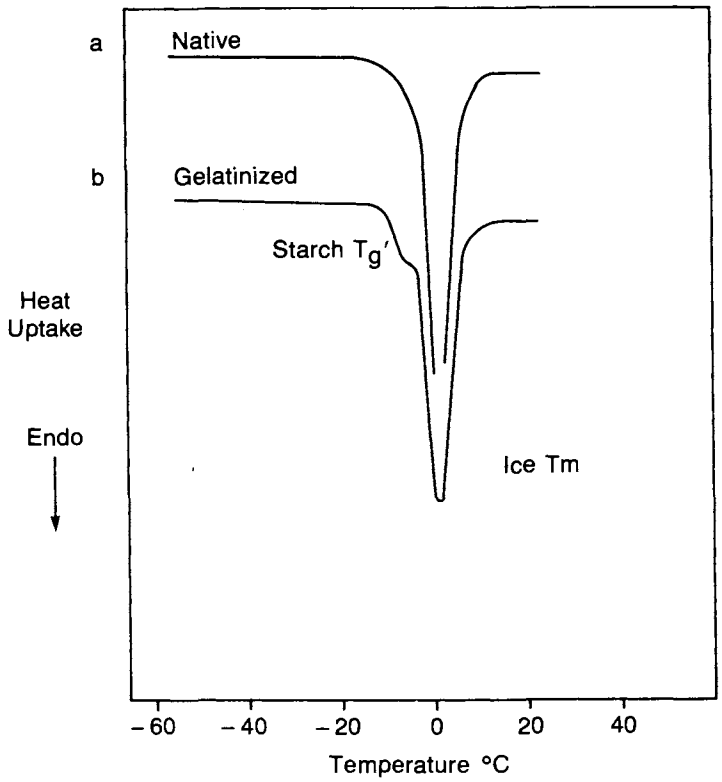

FIGURE 40. DuPont 990 DSC heat flow curves of wheat starch:water mixtures (45:55 w/w): (a) native granular; (b) immediate rescan after gelatinization of sample in (a), which reveals a prominent Tg′ at −5°C, preceding the Tm of ice. (From Slade, L. and Levine, H., *Carbohydr. Polym.*, 8, 183, 1988. With permission.)

diverse substituent groups. In contrast, the corresponding results for glucose and malto-oligosaccharides of DP 2-7 (excerpted from Table 3 and shown in Figure 42[15]) demonstrated a better linear correlation, with r = −0.99 for a plot of Tg′ vs. 1/MW, shown in the inset of Figure 42. This linear dependence[106] of the Tg′ results for the malto-oligosaccharides in aqueous solution exemplified the theoretical glass-forming behavior (i.e., diluent-free Tg vs. 1/MW) characteristic of a homologous family of non-entangling, linear, monodisperse oligomers.[107,113] In contrast, for a polydisperse mixture of solutes, such as a commercial SHP,[264] the observed Tg′ actually represents a weight-average contribution from the solute.[6,30,40-42] Thus, an initial comparison of Tg′ results for the heterogeneous SHPs in Table 4 and monodisperse PHCs in Table 3 showed that glucose is representative of other monosaccharides, while maltoheptaose is comparable to 15 to 20 DE maltodextrins ($\overline{M}n \simeq 900$ to 1200).[31]

For the SHPs in Table 4, a homologous series of glucose oligomers and polymers, Tg′ values range from −43°C for glucose (the monomer itself, of DE = 100) to −4°C for a 0.5 DE maltodextrin. A plot of Tg′ vs. DE (shown in Figure 43[8,32,34]) revealed a linear correlation between increasing Tg′ and decreasing DE (r = −0.98) for all SHPs with manufacturer-specified DE values.[8] Since DE is inversely proportional to $\overline{DP}n$ and $\overline{M}n$ for SHPs,[264] these results demonstrated that Tg′ increases with increasing solute $\overline{M}n$ (from $\overline{M}n$ = 180 for glucose to 36000 for 0.5 DE maltodextrin).[8] Such a linear correlation between Tg and $1/\overline{M}n$ is the general rule for any homologous family of pure, glass-forming polymers.[113] The equation of the regression line is DE = −2.2(Tg′, °C) − 12.8, and the plot of Tg′ vs. DE in Figure 43 has proven useful as a calibration curve for interpolating DE values of new or "unknown" SHPs.[27]

Results for polymeric SHPs have demon-

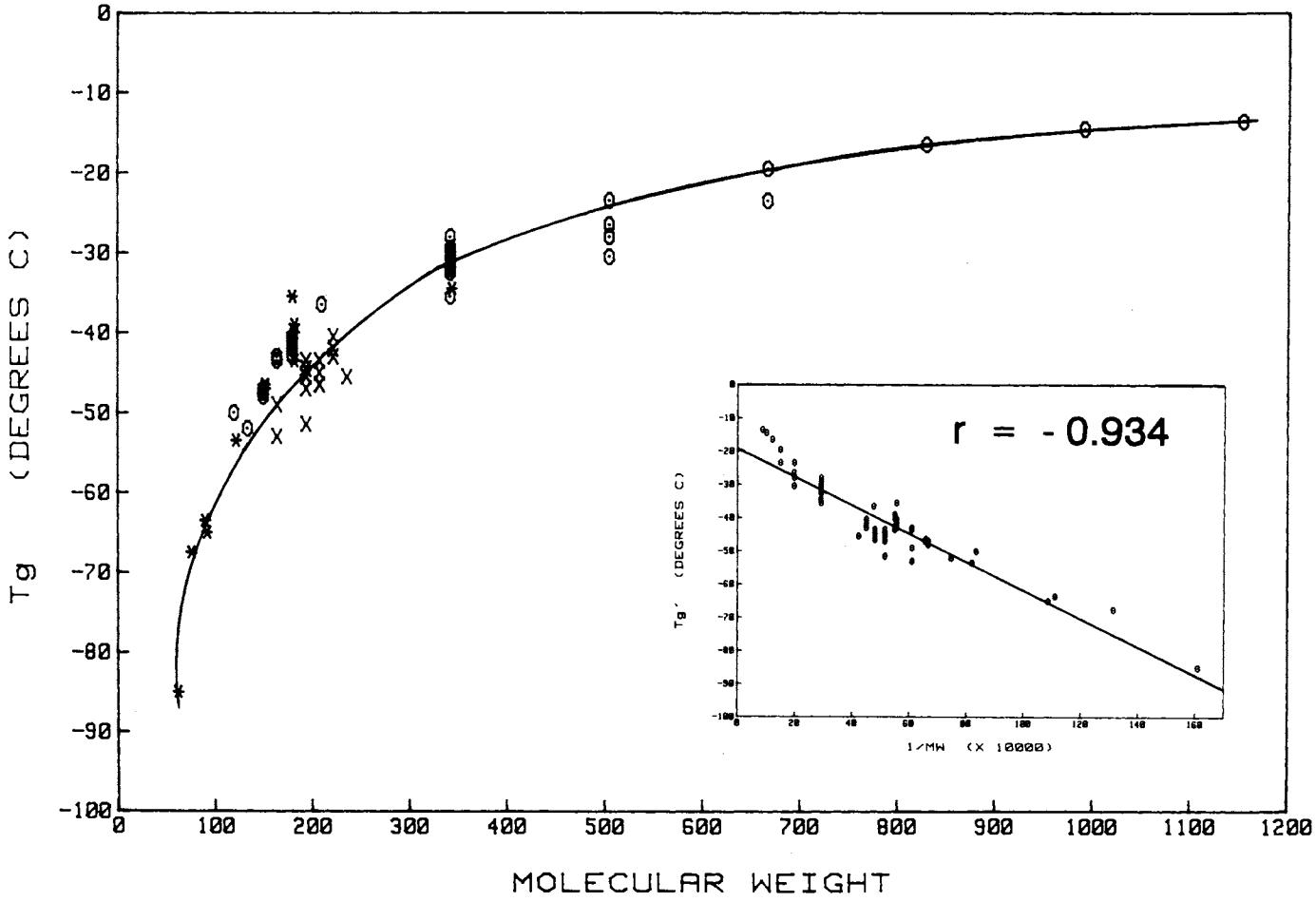

FIGURE 41. Variation of the glass transition temperature, Tg′, for maximally frozen 20 w% solutions against MW for the sugars (o), glycosides (x), and polyols (⋆) in Table 3. (Inset: plot of Tg′ vs. 1/MW ($\times 10^4$), illustrating the theoretically predicted linear dependence.) (From Levine, H. and Slade, L., *Food Structure — Its Creation and Evaluation,* Mitchell, J. R. and Blanshard, J. M. V., Eds., Butterworths, London, 1988, 149. With permission.)

strated that Tg′ depends rigorously on linear, weight-average DP ($\overline{DP}w$) for highly polydisperse solutes, so that linear polymer chains (e.g., amylose) give rise to a higher Tg′ than branched chains (e.g., amylopectin, with multiple chain ends[47]) of equal MW.[8,27] Due to the variable polydispersity and solids composition of commercial SHPs,[264,265] the range of Tg′ values for SHPs of the same specified DE can be quite broad. This behavior was shown by several pairs of SHPs in Table 4. For each pair, of the same DE and manufacturer, the hydrolysate from waxy starch (all amylopectin) had a lower Tg′ than the corresponding one from normal starch (containing amylose). This behavior was also exemplified by the Tg′ data for 13 10 DE maltodextrins in Table 4, for which Tg′ ranged from −7.5°C for a normal starch product to −15.5°C for a product derived from waxy starch, a ΔTg′ of 8°C. Such a ΔTg′ is greater than that between maltose (DP 2) and maltotriose (DP 3).[32] Further evidence was gleaned from Tg′ data for some glucose oligomers in Table 3. Comparisons of the significant Tg′ differences among maltose (1−>4-linked dimer), gentiobiose (1−>6-linked), and isomaltose (1−>6-linked), and among maltotriose (1−>4-linked trimer), panose (1−>4, 1−>6-linked), and isomaltotriose (1−>6, 1−>6-linked) have suggested that 1−>4-linked (linear amylose-like) glucose oligomers manifest greater "effective" linear chain lengths in solution (and, consequently, larger hydrodynamic volumes) than oligomers of the same MW that contain 1−>6 (branched amylopectin-like) links.[28] These re-

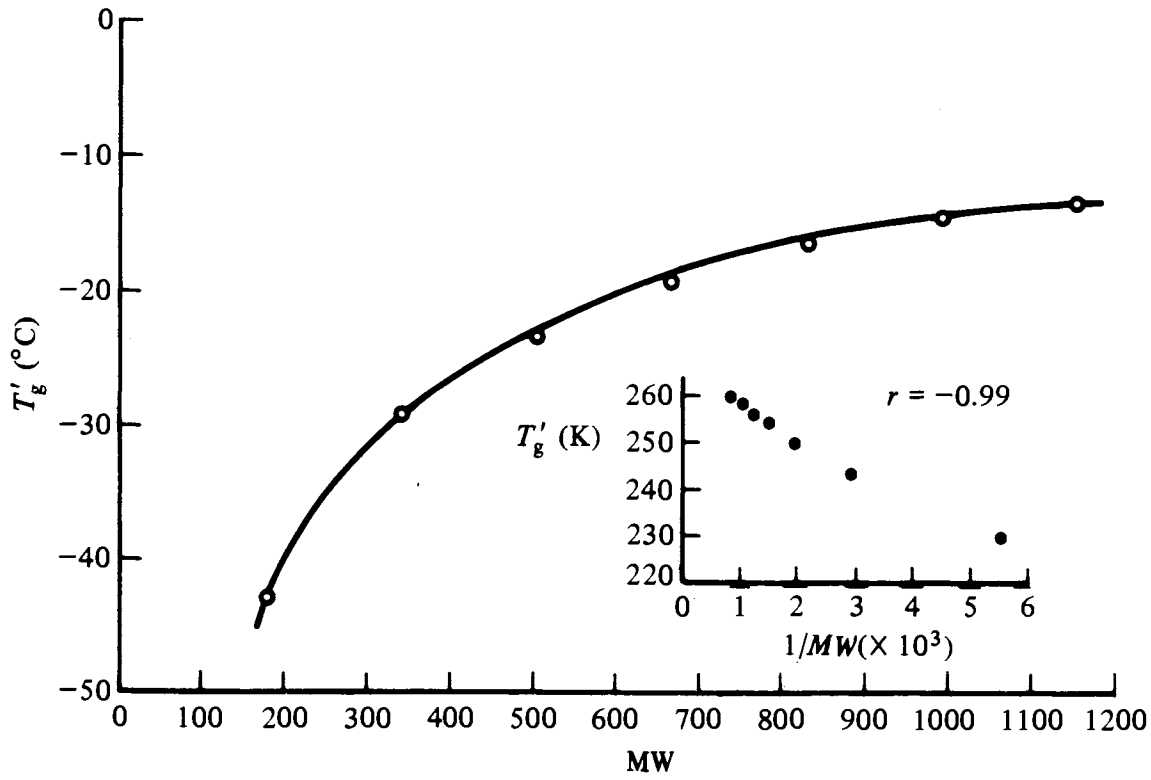

FIGURE 42. Variation of the glass transition temperature, Tg′, for maximally frozen 20 w% solutions against MW for the homologous series of malto-oligosaccharides from glucose through maltoheptaose in Table 3. (Inset: plot of Tg′ vs. 1/MW [× 1000] of solute, illustrating the theoretically predicted linear dependence.) (From Levine, H. and Slade, L., *Water Science Reviews,* Vol. 3, Franks, F., Ed., Cambridge University Press, Cambridge, 1988, 79. With permission.)

sults have also been used to illustrate the sensitivity of the Tg′ parameter to molecular configuration, in terms of linear chain length, as influenced by the nature of the glycosidic linkages in various non-homologous saccharide oligomers (not limited to glucose units) and the resultant effect on solution conformation.[31] Further evidence can be seen in Table 3, where, for sugars of equal MW (e.g., 164), ΔTg′ is as large as 10°C, a spread even larger than for the 10 DE maltodextrins.[32] Another interesting comparison is that between Tg′ values for the linear and cyclic α-(1−>4)-linked glucose hexamers, maltohexaose (−14.5°C) and α-cyclodextrin (−9°C). In this case, the higher Tg′ of the cyclic oligomer has led to a suggestion[15] that the ring of α-cyclodextrin apparently has a much larger hydrodynamic volume (due to its relative rigidity) than does the linear chain of maltohexaose, which is relatively flexible and apparently can assume a more compact conformation in aqueous solution.

The above comparisons have been discussed in the past to emphasize the subtleties of structure-property analyses of SHPs and PHCs by DSC.[34] The unavoidable conclusion, concerning the choice of a suitable carbohydrate ingredient for a specific product application, is that one SHP (or PHC) is not necessarily interchangeable with another of the same nominal DE (or MW). Characterization of fundamental structure-property relationships, in terms of Tg′, has been strongly advised before selection of such ingredients for fabricated foods.[8,27]

The Tg′ results for the commercial SHPs in Table 4 have demonstrated exactly the same characteristic Tg vs. $\overline{Mn}$ behavior as described earlier for synthetic amorphous polymers. Tg′ values for this series of SHPs (of polydisperse MWs, in the range from 180 for glucose to about 60,000 for a 360-DP polymer) have demonstrated their classic behavior as a homologous family of amorphous glucose oligomers and polymers.[8,27] The

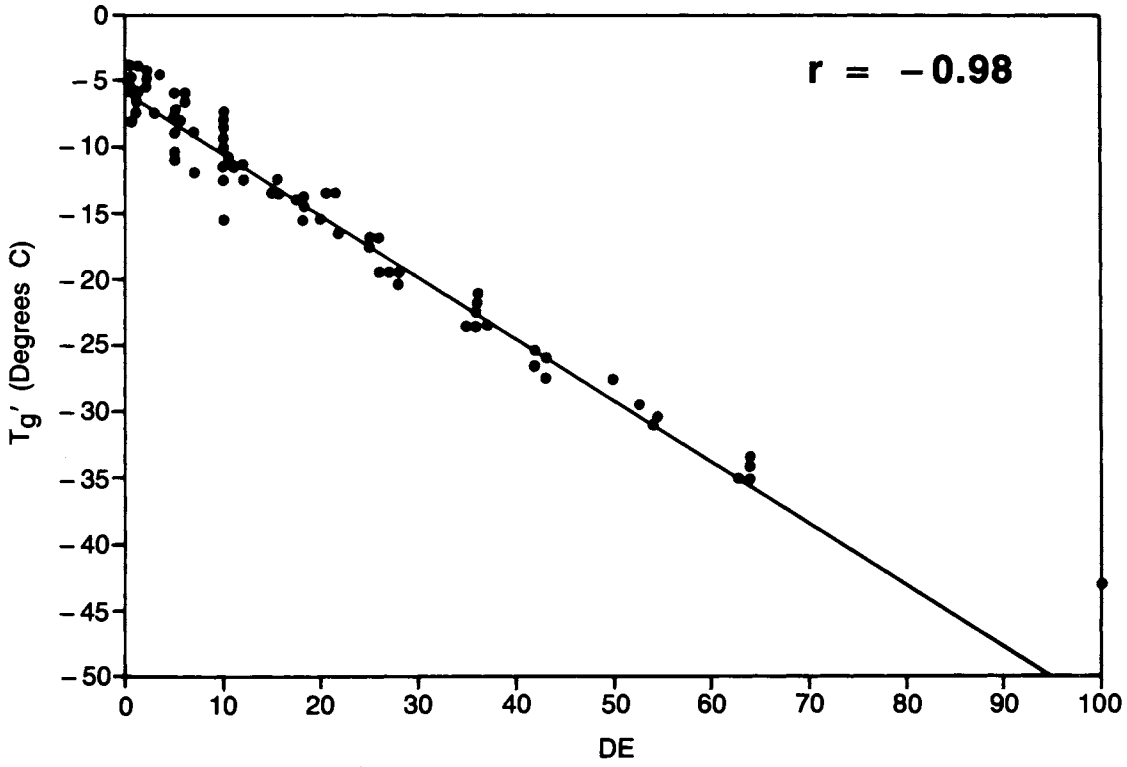

FIGURE 43. Variation of the glass transition temperature, Tg′, for maximally frozen 20 w% solutions against DE value for the commercial SHPs in Table 4. (Adapted from References 8, 32, and 34.)

plot of Tg′ vs. solute $\overline{M}n$ in Figure 44[8,32,34] clearly exhibits the same three-region behavior as shown in Figure 24:[26] (I) the plateau region indicative of the capability for entanglement coupling by high polymeric SHPs of DE $\leq$ 6 and Tg′ $\geq$ −8°C; (II) the intermediate region of non-entangling low polymeric SHPs of 6 < DE < 20; and (III) the steeply rising region of non-entangling, small SHP oligomers of DE > 20. The plot of Tg′ vs. $1/\overline{M}n$ in the inset of Figure 40, with a linear correlation coefficient r = −0.98, demonstrates the theoretically predicted linear relationship for all the SHPs in regions II and III, with DE values >6. The plateau region evident in Figure 44 has identified a lower limit of $\overline{M}n \simeq 3000$ ($\overline{DP}n \simeq 18$) for entanglement leading to viscoelastic network formation[100,197] by such polymeric SHPs in the freeze-concentrated glass formed at Tg′ and Cg′. This $\overline{M}n$ is within the typical range of 1250 to 19000 for minimum entanglement MWs of many pure synthetic amorphous linear high polymers.[112] The corresponding $\overline{DP}n$ of about 18 is within the range of 12 to 30 segmental units in an entangling high polymer chain, thus suggesting that the glucose repeat in the glucan chain (with a total of 23 atoms/hexose ring) may represent the mobile backbone unit involved in cooperative solute motions at Tg′.[26] The entanglement capability has been suggested to correlate well with various functional attributes (see the labels on the plateau region in Figure 44) of low DE SHPs, including a predicted[8] and subsequently demonstrated[27] ability (see the right-hand column in Table 4) to form thermoreversible, partially crystalline gels from aqueous solution.[211,266-275] It has been suggested[15] that SHP gelation occurs by a mechanism involving crystallization-plus-entanglement in concentrated solutions undercooled to T < Tm, as described in Section III.A.6.

In contrast to the commercial SHPs, the series of quasi-homologous, monodisperse PHCs in Table 3, including the homologous set of maltooligosaccharides up to DP 7, has been found to manifest Tg′ values that fall below the Tg′ limit defined by SHPs for entanglement and the onset

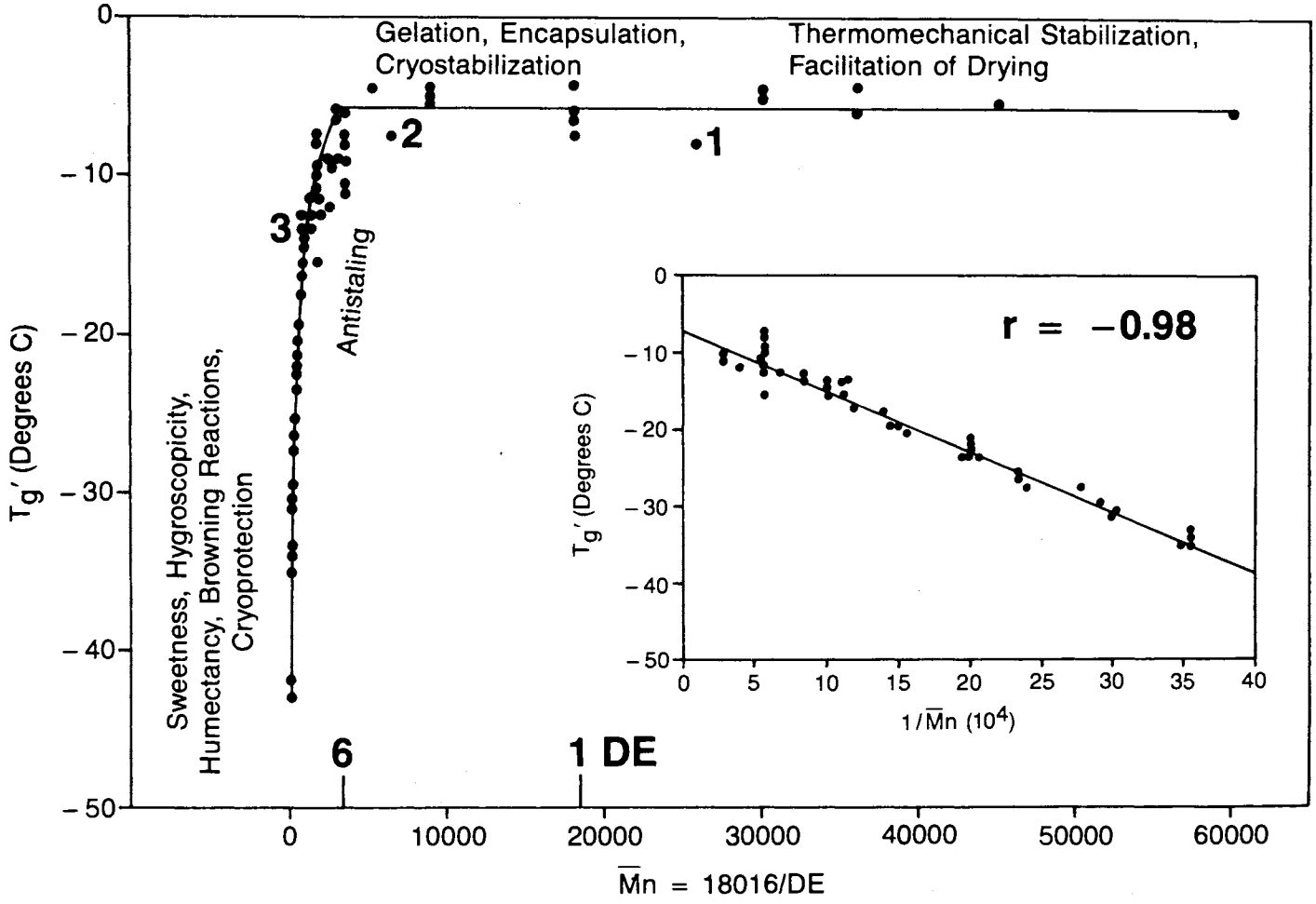

FIGURE 44. Variation of the glass transition temperature, Tg′, for maximally frozen 20 w% solutions against $\overline{Mn}$ (expressed as a function of DE) for the commercial SHPs in Table 4. DE values are indicated by numbers marked above x-axis. Areas of specific functional attributes, corresponding to three regions of the diagram, are labeled. (Inset: plot of Tg′ vs. 1/$\overline{Mn}$ [× 10000] for SHPs with $\overline{Mn}$ values below entanglement limit, illustrating the theoretically predicted linear dependence.) (From Levine, H. and Slade, L., *Carbohydr. Polym.*, 6, 213, 1986. With permission.)

of viscoelastic rheological properties and to be incapable of gelling from solution.[27,31] The plot of Tg′ vs. MW in Figure 41, drawn conventionally as a smooth curve through all the points,[113] can easily be visualized to represent two intersecting linear regions (III for MW <300 and II for 300 < MW <1200).[26] From the fair linearity of the Tg′ vs. 1/MW plot for all the data in the inset of Figure 41 (and from the better linearity of the corresponding plot for the series of maltooligosaccharides), it has been concluded that these diverse low MW sugars, polyols, and glycosides show no evidence of entanglement in the freeze-concentrated glass at Tg′. For these PHCs, none larger than a heptamer of MW 1153, the main plot in Figure 41 shows that region I, representing the entanglement plateau where Tg remains constant with increasing MW, has not been reached, in accord with the MW (and corresponding DP) range cited as the lower limit for polymer entanglement.

Tg′, as a physicochemically invariant but kinetically determined and structure-dependent thermal property of glass-forming solutions at subzero temperatures, has thus been used to interpret the thermomechanical behavior of carbohydrate-water systems in non-equilibrium glassy and rubbery states and to explain previously observed but poorly understood aspects of resulting functional behavior in various food ap-

plications.[8,27-34,40-42] It has been demonstrated that insights into structure-function relationships can be gleaned by treating Figure 44 as a predictive map, as indicated by the labeled regions of functional behavior for SHPs.[8,27] Some of the functional attributes of polymeric SHPs that fall on the entanglement plateau have been previously reported,[136] but not quantitatively explained from the theoretical basis of the entanglement capability revealed by DSC studies of Tg′.[8] For example, low DE maltodextrins and other high MW polymeric solutes are well known as drying aids for processes such as freeze-, spray-, and drum-drying.[137,138,254,276] Such polymeric stabilizers raise the observed Tc at a given moisture content, relative to the drying temperature, through their simultaneous effects of increasing the composite Tg′ and reducing the unfrozen water fraction (Wg′) of a system of low MW solids (with respect to freeze-drying)[40,41] or increasing the RVP (for all drying processes).[27] This stabilization of the glassy state facilitates drying without collapse or "melt-back".[28,40-42] By reducing the inherent hygroscopicity of a mixture of amorphous solids being dried, stabilizers such as proteins and polymeric carbohydrates can decrease the propensity of a system to collapse (from the rubbery state) due to plasticization by water.[15] These attributes are illustrated by recent findings on the freeze-drying behavior of beef extract with added dextrin[276] and of horseradish roots.[126] Figure 44 also suggested that maltodextrins to be used for encapsulation of volatile flavor and aroma compounds by freeze-drying (an application requiring superior barrier properties, i.e., relative impermeability to gases and vapors[55]) should be capable of entanglement and network formation ($Tg' \geq -8°C$). It had been reported[136-138] that effectiveness of encapsulation increases with increasing Tc, which increases with increasing $\overline{DP}n$ within a series of SHPs, but "a quantitative relationship between Tc and MW had not been established"[136] previously.

Figure 44 has been used as a guide to choose individual SHPs or mixtures of SHPs and PHCs that provide a particular target value of Tg′ in order to achieve desired complex functional behavior for specific food products.[8,27,31-34] Especially for applications involving such mixtures, data for the PHCs in Figure 41 have been used in combination with Figure 44,[37,38] since the leftmost portion of Figure 41 pertaining to low MW sugars and polyols corresponds to the sweetness/hygroscopicity/humectancy/browning/cryoprotection region of Figure 44. It was postulated that addition of a glass-forming sugar to an encapsulating maltodextrin would promote limited collapse and densification of the entangled network around an absorbed species, but would also decrease the ease of freeze-drying.[8] This postulate appeared consistent with reported results of improved encapsulation of volatiles in dense, amorphous matrices composed of a majority of maltodextrin (4 to 20 DE) plus a minority of mono- or disaccharide glass-former.[277,278]

2. Wg′ Database

As alluded to earlier, the thermograms in Figure 38 have also been used to illustrate some salient facts about Wg′.[8,27,30-34] Wg′ can be estimated from the measured area (enthalpy) under the ice-melting endotherm of the thermogram. By calibration with pure water, this measurement yields the weight of ice in a maximally frozen sample. The difference between the weight of ice and the known weight of total water in an initial solution is the weight of UFW in the glass at Tg′, per unit weight of solute. For a homologous series of 13 corn syrup solids (included among the SHPs listed in Table 4), a plot (not shown here) of Tg′ vs. the corresponding measured value of Wg′ demonstrated that Wg′ decreases with increasing Tg′, with $r = -0.91$.[8] For a larger, but less homologous, group of sugar syrup solids, another plot (not shown here) of Tg′ vs. Wg′ revealed the same trend of decreasing Tg′ (from $-19.5°C$ for a sample of 26 DE corn syrup solids to $-43°C$ for a high-fructose corn syrup (HFCS) 90) with increasing Wg′ (from 0.52 to 1.01 g UFW/g, respectively), with $r = -0.89$.[32] These results showed that as the solute $\overline{M}w$ increases, the fraction of total water unfrozen in the glass at Tg′ decreases and the extent of freeze-concentration increases. This fact is also illustrated by the thermograms in Figure 38. For comparable amounts of total water, the area under the ice-melting peak for the glucose solution is much smaller (i.e., Wg′ much larger) than that for the maltodextrin solution. Again in the context of the

idealized state diagram in Figure 39, these results, and many other experimental Wg′ (and Tg′) values for monomeric and polymeric carbohydrates, have been used to illustrate the general rule:[8,27,30-34] as $\overline{M}w$ of a solute (or mixture of homologous solutes) in an aqueous system increases, the Tg′-Cg′ point moves up the temperature axis toward 0°C and to the right along the composition axis toward 100 w% solute. As discussed in Section IV.C, the critical importance of this fact to the successful "cryostabilization" of frozen, freezer-stored, and freeze-dried foods has been described in the context of the functional behavior of food polymers vis-a-vis Tg′, especially with respect to the capability of inhibiting collapse processes in frozen and freeze-dried foods by formulating a fabricated product with polymeric "cryostabilizers" in order to elevate Tg′ relative to Tf.[8,27,30-34,40,41]

For the PHCs in Table 3, measured Wg′ values range from 1.90 g UFW/g for ethylene glycol to 0.20 to 0.30 g UFW/g for several sugars and polyols, including maltoheptaose. In contrast to the above-described results for a homologous set of glucose monomer and oligomer blends, the Tg′ vs. Wg′ results shown plotted in Figure 45[27] for the diverse PHCs yielded a r value of only −0.64. Thus, when Franks[6] noted that, among the (non-homologous) sugars and polyols most widely used as "water binders" in fabricated foods, "the amount of unfreezable water does not show a simple dependence on MW of the solute", he sounded a necessary caution. In fact, a plot of Wg′ vs. 1/MW for the substances in Table 3 showed an even poorer correlation, with r = 0.47.[27] The obvious conclusion was reached that the plot in Figure 45 could not be used as shown for predictive purposes, so the safest approach would be to rely on measured Wg′ values for each potential ingredient. However, the situation is not as nebulous as suggested by Figure 45. When some of the same data were replotted such that compounds were grouped by chemical class into specific homologous series (i.e., polyols, glucose-only solutes, and fructose- or galactose-containing saccharides), better linear correlations became evident.[15] These plots (shown in Figure 46[15]) illustrated the same linear dependence of Tg′ on the composition of the glass at Tg′ (i.e., as the amount of unfrozen, plasticizing water in the glass decreases, Tg′ increases) as did the data for the series of corn syrup solids. Still, Franks' suggestion[27] that future investigations of the non-equilibrium Tm and viscosity as functions of solute concentration, and the anomalous curvature of the liquidus as a function of solute structure, would be particularly worthwhile, for the most part continues to await experimentation, although Pegg and Arnaud have recently published "equilibrium" liquidus curves for glycerol and propylene glycol, compiled from experimentally measured freezing points for solute concentrations up to 60 w%.[279]

Because the effect of MW on Tg′ and Wg′ has been found to be such a critical aspect of the interpretive and predictive value of the food polymer science data bank,[8,14-39] this effect has been analyzed in detail.[30] As mentioned earlier, for pure synthetic polymers, in the absence of diluent, Tg varies with MW in the characteristic manner illustrated in Figure 24. For a homologous series of amorphous linear polymers, Tg increases with increasing MW, up to the limit of the entanglement plateau, then levels off with further increases in MW. The glass at Tg′ is not that of the pure, undiluted polymer, and so there is no theoretical basis for assuming that this Tg of the freeze-concentrated glass should depend on MW of the dry polymer. However, if the relative shapes of the polymer-diluent glass curves are similar within a polymer series, increases in MW lead to proportional increases in both Tg and Tg′.[30] Thus, as shown in Figures 41 and 44 for two extensive series of carbohydrates, the linear relationship between Tg and inverse MW of the solute does apply to the characteristic Tg′ of the solute-UFW glass. For the homologous series of commercial, polydisperse glucose oligomers and high polymers derived from starch, with $\overline{M}n$ values from 180 for glucose itself to about 60,000 for a 360 $\overline{DP}n$ polymer, Tg′ increased with decreasing inverse $\overline{M}n$ (with a linear correlation coefficient r = −0.98), up to a plateau limit for entanglement at $\overline{DP}n \simeq 18$ and $\overline{M}n \simeq 3000$. For the non-homologous series of small, monodisperse PHCs with known MWs in the range 62 to 1153, including many different sugars, polyols, and glycoside derivatives, Tg′

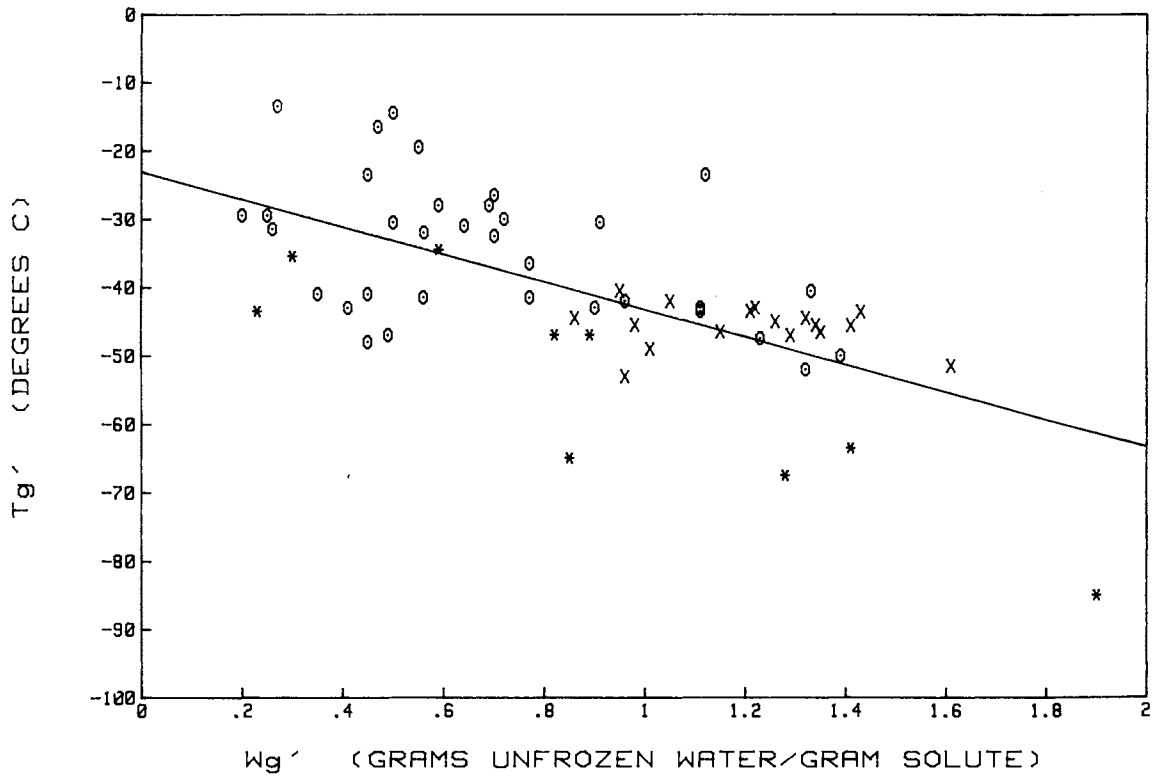

FIGURE 45. Variation of the glass transition temperature, Tg', for maximally frozen 20 w% solutions against Wg', the composition of the glass at Tg', in g unfrozen water/g solute, for the sugars (o), glycosides (x), and polyols (*) in Table 3. (From Levine, H. and Slade, L., *Food Structure — Its Creation and Evaluation,* Mitchell, J. R. and Blanshard, J. M. V., Eds., Butterworths, London, 1988, 149. With permission.)

also increased linearly with decreasing inverse MW ($r = -0.934$), but the entanglement plateau was not reached.

For these small PHCs of known MW (see Table 3), the actual $\overline{M}w$ and $\overline{M}n$ of the homogeneous solute-water mixture in the glass at Tg' were calculated from the corresponding Wg' values in Table 2 (converted from g UFW/g solute to w% water).[30] The results were plotted as Tg' vs. $1/\overline{M}n$ and Tg' vs. $1/\overline{M}w$ in Figures 47A and 47B,[30] respectively. Figure 47A shows the poor linear correlation ($r = -0.71$) with $\overline{M}n$, which might be expected, because while Tg does vary with free volume of the solution, free volume is most effective as a determinant of Tg when it varies with $1/\overline{M}n$ of the *solute*, due to the effect of the number of its molecular chain ends.[107] In contrast, Figure 47B shows the much better linear correlation ($r = -0.95$) of Tg' with $\overline{M}w$ of the aqueous PHC glass, a result that also supported a conclusion that Tg' and Wg' are not independent parameters of the mobility transformation.[30] Within the larger series of non-homologous PHCs in Table 3, the single homologous family of glucose and its linear malto-oligomers up to DP 7 showed (Figure 42 inset) an excellent linear correlation ($r = -0.99$) between Tg' and inverse MW of the dry sugar. Again, the relationship between Tg' and the actual $\overline{M}w$ and $\overline{M}n$ of the aqueous glass was examined by comparing plots of Tg' vs. $1/\overline{M}n$ (Figure 47C) and Tg' vs. $1/\overline{M}w$ (Figure 47D).[30] These results showed even more clearly than those in Figures 47A and B that there is no correlation between Tg' and $\overline{M}n$ ($r = -0.20$), but a very good correlation ($r = -0.985$) between Tg' and $\overline{M}w$.

The importance of this finding relates to the concept of the glass transition as an iso-relaxation state.[30,107] The molecular Tg is not related to *macroscopic* viscosity, and the origin of the temperature location of the molecular glass transition is not based on an iso-macroscopic viscosity state.[107]

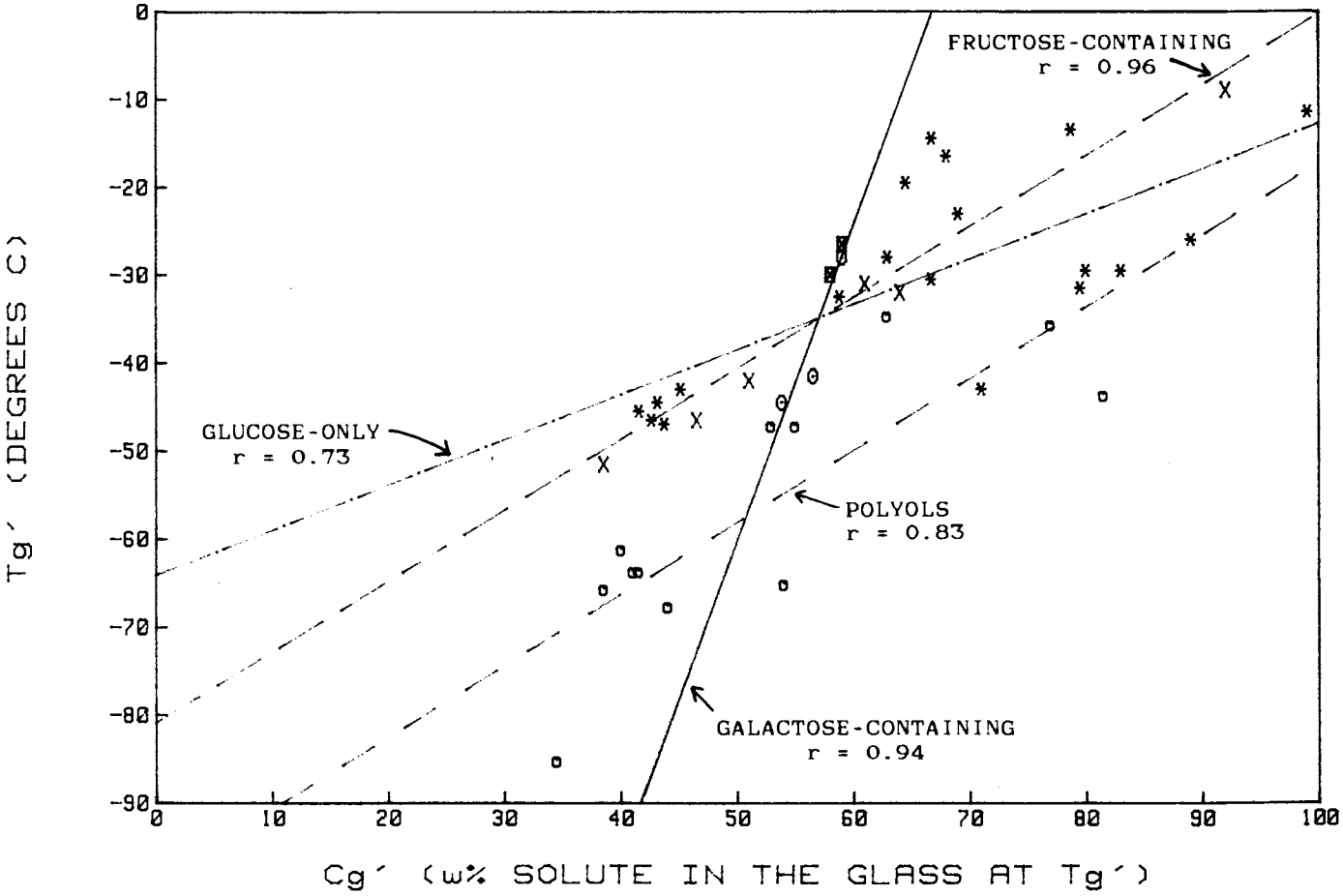

FIGURE 46. Variation of the glass transition temperature, Tg', for maximally frozen 20 w% solutions against Cg', the composition of the glass at Tg', in weight percent solute, for homologous series of polyhydric alcohols (o), glucose-only solutes (⋆), fructose- (x), and galactose-containing saccharides (O) in Table 3. (From Levine, H. and Slade, L., *Water Science Reviews,* Vol. 3, Franks, F., Ed., Cambridge University Press, Cambridge, 1988, 79. With permission.)

Moreover, the location of Tg is not based simply on either an iso-free volume or an iso-local viscosity state alone.[107] For MWs below the entanglement limit (e.g., ≈3000 for α-1 − >4 glucan oligomers), the temperature location of the molecular glass transition depends on the instantaneous average relaxation time compared to the experimental time frame. The operational relaxation time is an instantaneous property, because it depends on the instantaneous values of free volume and local viscosity. Free volume is associated with inverse $\overline{M}n$, rotational relaxation times, high average MWs, and low values of Tm/Tg ratio. Local viscosity is associated with $\overline{M}w$, translational relaxation times, low average MWs (e.g., small PHCs), and high values of Tm/Tg ratio.[30] (In contrast to the molecular glass transition, for MWs above the entanglement limit, the network Tg does involve macroscopic viscosity.[107]) The insight derived from these results led to the new suggestion[30] that different portions of the glass curve must be controlled by different parameters that determine molecular-level mobility, i.e., Tg is controlled by free volume (a function of inverse $\overline{M}n$) rather than local viscosity at higher values of average MW (i.e., higher solute concentrations in the glass, Cg), but by local viscosity (a function of $\overline{M}w$) rather than free volume at lower values of average MW (i.e., higher water concentrations in the glass, Wg).

The value of Tg' appears to reflect the hydrodynamic volume, in the glass, of the mobile "cluster entity"[89] represented by a solute molecule and its complement of unfrozen water mol-

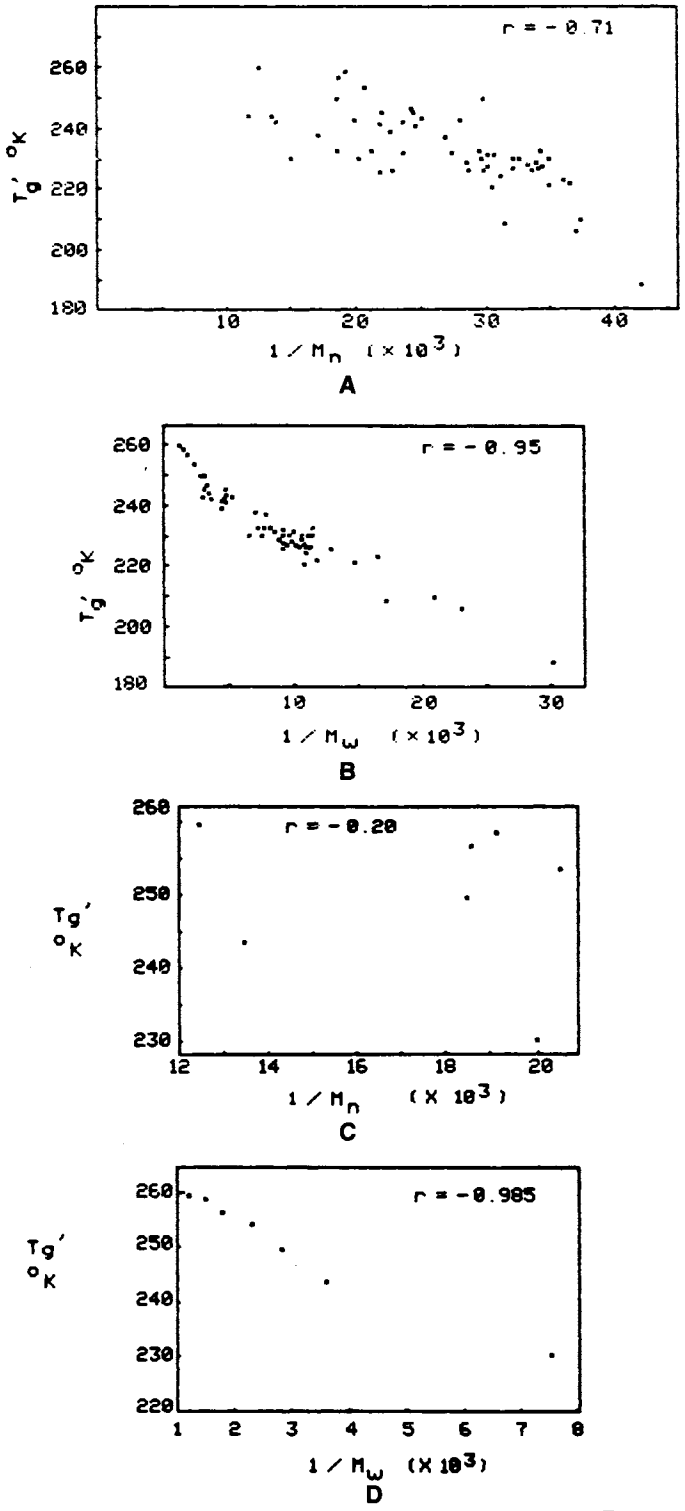

FIGURE 47. The variation of Tg′ with (A) inverse $\overline{Mn}$ and (B) inverse $\overline{Mw}$ calculated from Wg′ for the small carbohydrates listed in Table 3, and with (C) inverse $\overline{Mn}$ and (D) inverse $\overline{Mw}$ calculated from Wg′ for the homologous series of malto-oligosaccharides, from glucose through maltoheptaose, listed in Table 3. (From Slade, L. and Levine, H., *Pure Appl. Chem.*, 60, 1841, 1988. With permission.)

ecules, rather than a property of the isolated solute.[30] We have considered the question of whether it would be preferable to correlate Tg′ with partial molar volume (V°) rather than MW of dry solute,[31] since V°, like intrinsic viscosity, gives an indication of the effective solute size in solution. Just as free volume is related to inverse MW of monodisperse solutes (or inverse $\overline{M}n$ for polydisperse solutes) in the limit of zero dilution,[107] free volume should be related to inverse V° for comparison of conformational homologs of different MW in the limit of infinite dilution. But, of course, it is for comparison of different conformers of the same MW that we look for an advantage in the use of V° to replace MW. Unfortunately, while MW values are exact, an approach based on V° is not straightforward.[31]

Despite a relative wealth of V° data,[280] differences in the values for isomeric sugars are sufficiently small to discourage their use to interpret the influence of conformation on hydration[281] and may lie within the range of values reported by different research groups for a single sugar, in part due to differences in anomeric ratios.[282] If this complication is removed by comparison of methyl pyranosides, larger values of V° are observed for conformers with equatorial rather than axial OCH_3 substituents.[282] Similarly, for comparison of conformers at C4, contributions to apparent molar volumes are said to be greater for equatorial than for axial hydroxyls.[283] Yet, the general observation, for PHCs compared to their apolar structural analogs, is that hydroxyl groups are effectively invisible to limiting density measurements.[281,282] The greater contribution of certain equatorial hydroxyl groups to V° is attributed to greater spatial and orientational compatibility with the preexisting liquid water structure,[282] i.e., greater effective "specific hydration". Data for a few of the same sugars show that intrinsic viscosity increases with both contributions (MW and "specific hydration") to increasing V°.[284] We might expect, from this slim evidence, that both contributions to increased V° would also lead to increased Tg′.[31] However, there still remain the questions of temperature and concentration dependence of apparent molar volumes of PHCs.

Systematic extrapolation of V° data to subzero temperatures of interest for correlation with Tg′ is hindered by the paucity of data for mean limiting apparent molar expansibilities. Based on two relevant cases for which data are available,[282] such extrapolations would magnify differences in behavior predicted from measurements made near room temperature. The concentration dependence of apparent molar volumes is more questionable. As mentioned earlier, one of the most important, but often overlooked, aspects of the glass transition is its cooperative nature.[106] Upon slow cooling, the glass at Tg′, with solute-specific composition Wg′, represents the greatest dilution that retains this maximally cooperative behavior.[30] Cooperativity is maximum at the glass transition (where arrestation of large-scale molecular mobility occurs without change in structure), but decreases with increasing temperature or dilution above Tg (where retardation of mobility occurs and shows a WLF-type temperature dependence).[106,107] Of the two extremes, behavior in the limit of zero dilution is less remote from that of the cooperative system than is behavior in the limit of infinite dilution.[31] Apparent molar volumes of PHCs in aqueous solution have been shown to be characteristically (in contrast to apolar solutes) independent of concentration,[282] yet reported differences between apparent molar volumes for 3 and 10 w% solutions of a single sugar approach the greatest differences seen between equatorial vs. axial conformers at a single concentration.[283] There exists the possibility that a decrease in apparent molar volume upon extrapolation toward Tg′ and an increase upon extrapolation toward Cg′ might counterbalance.[31] Despite these issues, the subject is of sufficient interest to merit further exploration.

Wg′ results for the series of monomeric alkyl glycosides in Table 3 have been described[27,34] in terms of a possible relationship between the glycoside structure (e.g., position and size of the hydrophobic aglycone, which is absent in the parent sugar) and its function reflected by Wg′. Wg′ values for all methyl, ethyl, and propyl derivatives are much larger than those for the corresponding parent monosaccharides. However, Wg′ values appear consistently to be maximized for methyl or ethyl derivatives, and somewhat lower for the *n*-propyl derivatives. (In a related vein, Fahy et al.[251] have recently reported that methylation significantly enhances the glass-

forming tendency [i.e., potential for complete vitrification] of concentrated aqueous solutions of various polyols and other biological cryoprotectants.) It has been suggested that increasing hydrophobicity (of the aglycone) leads to both decreasing Wg′ and the demonstrated tendency toward increasing insolubility of propyl and larger glycosides in water.[27] The combined effects of several related mechanistic contributions almost obscure the underlying basis for this behavior. The predominant role of the methyl group provides the clue to the overall mechanism,[34] i.e., the phenomenon of "internal plasticization", by which the desired properties of depressed Tg and increased free volume and segmental mobility are achieved by incorporating them into the polymer itself, rather than by addition of exogenous plasticizer.[109] Internal plasticization to increase mobility of the polymer backbone can be achieved by branching. Additional free volume is provided by the motion of side chains, with greater contributions from chain ends associated with shorter side chains.[109] The traditional example of internal plasticization by side chains from synthetic polymer science, the poly(*n*-alkyl methacrylates),[109] mirrors the behavior of the alkyl glycosides of Table 3.[34] A monotonic depression of Tg is observed with increasing alkyl chain length, but the methyl group is most effective, and longer chains are progressively less effective. For the alkyl glycosides, internal plasticization is observed both directly, as depression of Tg′, and indirectly, as increase in Wg′. Although internal plasticization, by covalent attachment of the plasticizer to the polymer, serves to increase efficiency by retarding loss of plasticizer upon crystallization, long alkyl side chains eventually associate as seen for propyl side chains in the alkyl glycosides and for longer alkanes in high polymers.[105]

It has been demonstrated[34] that Wg′ values determined by the DSC method mentioned above are generally in good agreement with literature ranges for the so-called "water binding capacity (WBC)" values (determined by various methods other than DSC) of many different food ingredients, even though the spread of reported values for individual materials has often been considerable.[25,57] The latter fact is not surprising in view of experimental difficulties imposed by the kinetic constraints of the water-immobilization process and the wide variation in time frames (differing by orders of magnitude) for measurements of such relaxation processes.[167] Not surprising either is the consequent lack of reproducibility in, as well as frequent disagreement among, many types of "WBC" measurements,[34] including DSC. The dependence of the value of Wg′ on the specific time frame of the DSC measurement has been illustrated by a study of hydrated lysozyme glasses recently reported by Wolanczyk and Baust.[285] These workers have noted that the measured amount of unfrozen water decreases with increasing sub-ambient hold time (from 0 min to 24 h between cooling and subsequent rewarming) and decreasing sub-ambient hold temperature (from -50 to -150°C).

Ordinarily, one does not claim an accuracy of better than about 10% for DSC measurements of Wg′,[34] although some exceptionally precise studies have been reported.[163-166] Franks[149] has presented a comparison of experimental data from DSC, NMR, and dielectric relaxation measurements on concentrated solutions of several common small sugars, which summarizes the state of affairs. DSC results for unfrozen water at Tg′, expressed as a "notional hydration number" (explained earlier), were 3.7 for glucose and xylose, 3.5 for mannose, and 5.0 for maltose, with standard deviations of 12 to 20%. These "hydration numbers" were in surprisingly good agreement with NMR and dielectric relaxation results of 3.7 for glucose, 3.9 for mannose, and 5.0 for maltose. In comparison to the above DSC results, the Wg′ values shown in Table 3 correspond to calculated values of 4.1 for glucose, 3.7 for xylose, 3.5 for mannose, and 4.8 for maltose, in all cases within 11%[34] of the values reported by Franks.[149]

The method we advocate for determining Wg′,[8,27] i.e., from DSC measurements on a single maximally freeze-concentrated aqueous solution of 20 w% initial solute concentration, is not the only DSC method one can use to determine this technologically important quantity. Other workers[253,257,286,287] have recommended an "extrapolation method" for estimation of the limiting UFW content of a solute. In that method, a series of solutions covering a wide range of solute concentrations is analyzed, and the measured ice-melting peak areas (which decrease with

increasing solute concentration) are extrapolated to the solute concentration corresponding to zero peak area, i.e., the concentration that would allow no ice to form on slow cooling or rewarming, because all the water present in the solution would be "unfreezable" in the experimental time frame. In comparing results from the method we favor with those from the extrapolation method, and using sucrose as a common example, the following points are noteworthy. While we have reported a Cg′ value for sucrose of 64.1 w%,[27] as measured for a 20 w% sucrose solution (with a Tg′ of −32°C), Izzard et al.[287] have more recently reported Cg′ values for 2.6, 10.7, 20.2, 40.0, 60.1, and 65.8 w% (i.e., C > Ce) sucrose solutions of 35.1, 61.9, 63.9 (very close to our value), 71.7, 75.8, and 77.7 w% sucrose, respectively. Izzard et al.[287] have extrapolated their data to a limiting Cg′ value of ~80 w% sucrose (and a corresponding Tg′ value of ~ −35°C), which they claim to be the *correct* Cg′ for sucrose, while they claim that our value (which is 20% different from theirs) "is clearly incorrect". After considering the discussion below, the reader will have to decide if there is such a thing as a "right" or "wrong" answer for Cg′, as Izzard et al.[287] claim.

Obviously, the extrapolation method is much more time-consuming than the one-solution, constant-concentration method, and this aspect represents a practical disadvantage. Moreover, the 20 w% solute concentration that we use in determining Wg′ (and Tg′) for PHCs has greater technological relevance to, for example, the total saccharides content in many frozen desserts and related products than do other much higher or much lower solute concentrations. In rationalizing its disadvantages, advocates of the extrapolation method have, as mentioned above, claimed it to be more accurate than alternative one-point measurements of Wg′.[257,287] However, it has been recently pointed out,[39] and illustrated with the particular case of the galactose-water system reported by Blond,[257] that the extrapolation method is *invalidated* in every case in which solute or hydrate crystallization during the DSC measurements (which would be favored by higher solute concentrations and might or might not be revealed by separate or multimodal melting peaks during warming) cannot be ruled out explicitly. In other words, whenever one cannot be certain that the so-called "ice-melting" peak represents only the melting of crystalline ice and not crystalline solute (i.e., eutectic melting) or crystalline hydrate, the potential accuracy of the extrapolation method is obviated.

The foundation for understanding the behavior of the galactose-water system, and others like it that are subject to solute or hydrate crystallization, has been provided by Forsyth and MacFarlane:[260] "The phase behaviour of a number of solutions of possible interest in cryopreservation as a function of solute concentration has been investigated by thermal analysis techniques with three regions being identifiable[288]

1. Solutions of low solute concentration (e.g., 20 w%, for most small PHCs) that supercool below their equilibrium melting temperature but eventually freeze on sufficient cooling
2. Intermediate concentration regions where the solution will vitrify (i.e., become glassy) on rapid cooling; however, on rewarming devitrification (i.e., crystallization) will take place at some temperature Td
3. High solute concentration where the sample becomes vitreous on cooling and does not easily crystallize ice on warming, but may crystallize a hydrate"

In this context of the distinctive behavior observed for the three regions of concentration identified by the investigations of Angell and coworkers,[260,288] the extrapolation method for the estimation of UFW content (by extrapolation to zero of the measured total heat of melting of unidentified species after cooling and rewarming of solutions with a wide range of initial concentrations, spanning the three behavioral regions) is *invalidated in principle* (regardless of whether the melting enthalpy of crystalline solute or hydrate can be deconvoluted from the overall heat of melting). For each of the three kinetically distinctive regions of concentration, pertinent cooling and heating rates would have to be used, corresponding to the critically different time scales of the relaxation behavior in the three concentration regimes. This is *not* routinely done by practitioners of the extrapolation

method.[253,257,286,287] In accordance with the concentration regimes defined by Angell and coworkers,[260,288] initial concentrations of galactose below 50 w% represent region (1), and their time scale for crystallization of ice would be shorter than the times involved in a typical experimental DSC procedure (e.g., cooling and heating at 10°C/min).[257] Initial concentrations of galactose between 50 and 65 w% fall in region (2), and their time scale for crystallization of ice would coincide with the typical experimental time scale. Initial concentrations above 65 w% fall in region (3), and their time scale for nucleation and crystallization of ice would be much *longer* than the typical experimental time scale. Even after depression of the operative solute concentration to <50 w%, due to previous crystallization of beta-galactose or monohydrate, the homogeneous ice nucleation curve would approach the galactose-water glass curve, and ice nucleation would be avoided (as is concluded from the experimental observation[257] that no ice melts during rewarming), as predicted by Angell et al.[288] In summary, solutions of region (1) analyzed at subzero temperatures approach equilibrium behavior sufficiently to be sometimes mistaken[257] for "equilibrium states". Solutions of region (2) are sufficiently far from equilibrium to be recognized as such.[257] Solutions of region (3) are so far from equilibrium[172] that their non-equilibrium status is not evident. Systems in this deceptive status, which appears to be a "steady state", because relaxation times greatly exceed typical experimental time scales,[172] are often mistaken for "equilibrium states". One consequence of the complexity of this situation and the kinetic constraints imposed on it is the obviation of the utility and validity of the extrapolation method of determining Wg′, especially when that method is routinely practiced using constant cooling and heating rates for DSC analysis of all solution concentrations.[253,257,286,287]

In contrast to the invalidity of the extrapolation method of determining Wg′, particularly with respect to crystallizable solutes such as galactose, glucose, and sucrose, ambiguity can be minimized through the use of the one-point method of determining Wg′ for the construction of glass curves.[32] By the selection of (1) solutes that avoid solute, eutectic, or hydrate crystallization; (2) an initial solute concentration in region (1) for characterization of aqueous glasses; and (3) diluent-free solute to characterize glasses with concentration greater than Cg′, reliable values of Wg′ and corresponding glass curves can be determined.[30,39] Poly(vinyl pyrrolidone) is justly popular as a model solute for aqueous-glass systems.[4,32,242] Selection of 20 w% solute as the standard initial solution concentration ensures reproducible freeze-concentration to the technologically relevant composition at Tg′-Cg′,[32] especially for solutes such as galactose, glucose, sucrose, and fructose, which would be much more prone to solute crystallization (e.g., eutectic formation) or hydrate crystallization from much more concentrated solutions.[4]

As another part of an experimental approach to understanding "water dynamics" in intermediate-moisture carbohydrate systems, the basis for a relationship between Wg′ and apparent RVP has been investigated.[15,16] RVP (rather than "Aw") is generally assumed to be an indicator of "free water" content in such intermediate-moisture systems at room temperature,[75,76] while Wg′ (rather than "WBC") is properly described as a measure of their unfrozen water content. Both parameters represent behavioral (functional) manifestations of the constrained mobility of water in aqueous carbohydrate glasses and supra-glassy fluids.[30] The study involved a quasi-homologous series of sugar syrup solids from commercial high-fructose corn, ordinary corn, sucrose, and invert syrups, all of which are commonly used ingredients in IMF products. This was the same series mentioned earlier, which showed a linear correlation ($r = -0.89$) between decreasing Tg′ and increasing Wg′. RVP was measured for a series of solutions with 67.2 w% solids content after 9 d "equilibration" at 30°C and plotted against Wg′ for maximally frozen 20 w% solutions of the same solids. The plot (shown in Figure 48[16]), with RVP values in the range 0.78 to 0.98 and Wg′ values in the range 0.52 to 1.01 g UFW/g solute (corresponding Tg′ values in the range −19.5 to −43°C), produced a linear correlation coefficient $r = -0.71$ for the relationship between decreasing content of UFW in the glass at Tg′ and increasing RVP in the corresponding supra-glassy solution some 50 to 70°C above the Tg′ reference state. The scatter

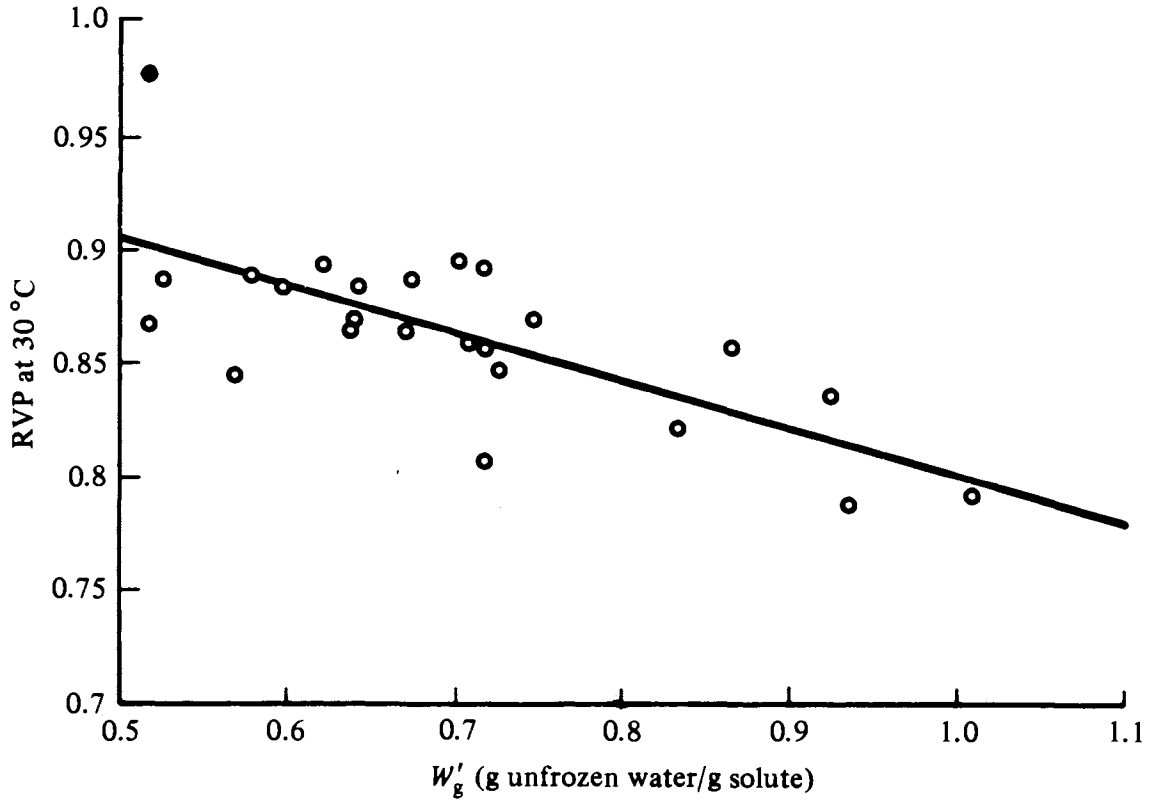

FIGURE 48. Variation of relative vapor pressure (measured for 67.2 w% solutions of various corn, sucrose, and invert syrup solids, after 9 d at 30°C) against Wg′, the composition of the glass at Tg′, in g unfrozen water/g solute, for maximally frozen 20 w% solutions of the same syrup solids. (From Slade, L. and Levine, H., *Food Structure — Its Creation and Evaluation,* Mitchell, J. R. and Blanshard, J. M. V., Eds., Butterworths, London, 1988, 115. With permission.)

in the data prohibited further insight into the question of water mobility in such systems. This was not unexpected, since many of the samples represented heterogeneous, polydisperse mixtures of polymeric carbohydrate solutes of unknown $\overline{M}w$ and MW distribution. While this study would be worth repeating with a homologous series of small monodisperse PHCs, the mold spore germination study described in Section II.A.3 was concluded to be a more definitive and revealing experimental approach to the issue of system mobility (especially at low moisture contents, i.e., W < 30 w% water, exemplifying a situation of W $\lesssim$ Wg for typical glass-forming PHCs) and eventual water "availability" (especially at high moisture contents, i.e., W $\gtrsim$ 70 w% water, exemplifying a situation of W $\gg$ Wg, likewise for typical glass-forming PHCs).[30]

3. Dry Tg, Dry Tm, and Tm/Tg Ratio

As explained earlier, if the relative shapes of the polymer-diluent glass curves are similar within a polymer series, increases in MW (of the diluent-free polymer) lead to proportional increases in both Tg and Tg′.[30] This fact has been demonstrated recently by the aqueous glass curves for maltose, maltotriose, and maltohexaose published by Orford et al.,[59] coupled with the Tg′-Wg′ values for these oligosaccharides from Table 3, as illustrated in Figure 49. Prior to this confirmation, it had been assumed that a plot of Tg vs. MW for dry PHCs or SHPs would reflect the same fundamental behavior as that of Tg′ vs. solute MW shown in Figures 41, 42, and 44.[28] Earlier evidence supporting this assumption had been provided by To and Flink,[136] who reported

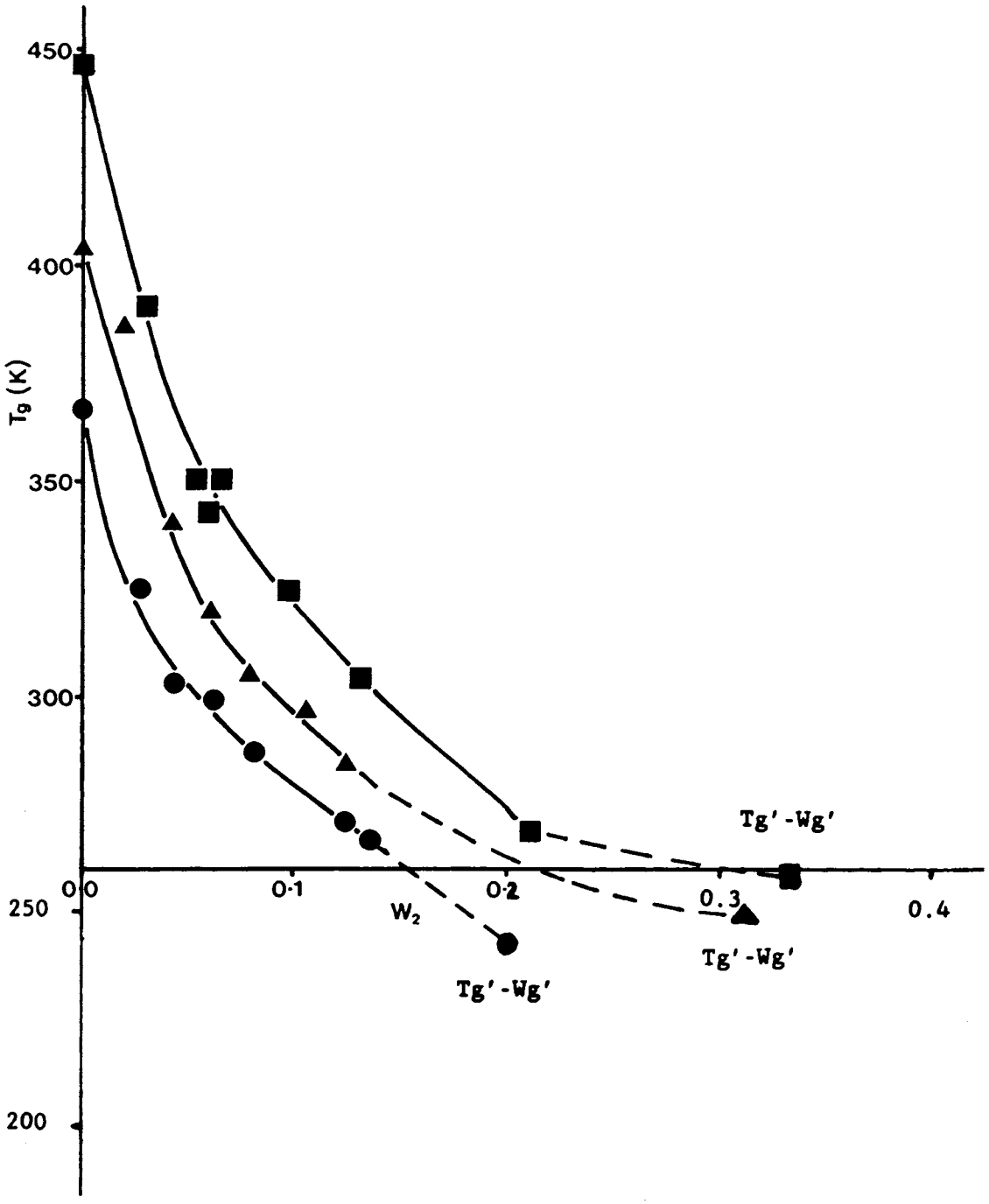

FIGURE 49. Graph of glass transition temperature (Tg) vs. mass fraction (w_2) of water for maltose (solid circles); maltotriose (solid triangles); and maltohexaose (solid squares). Reproduced, with permission, from Reference 59. The solid-line curves from Reference 59 are extrapolated (dashed lines) to the appropriate Tg'-Wg' points (from Table 3) for these saccharides.

a plot of Tc vs. DP for a series of low-moisture, fractionated SHP oligomers of $2 \leq DP \leq 16$ (i.e., non-entangling),[8] similar in shape to the plot of Tg' vs. MW for the non-entangling PHCs in Figure 41. It had been pointed out that Tc for low-moisture SHPs, which increases monotonically with increasing DP, represents a good quantitative approximation of dry Tg.[8] The basic as-

sumption was verified for the homologous series of glucose and its pure malto-oligomers of DP 2 to 7 in Table 3, as illustrated in Figure 50.[28] The plot of Tg vs. MW in Figure 50A showed that dry Tg increases monotonically with increasing MW of the monodisperse sugar, from Tg = 31°C for glucose (in good agreement with several other published values,[59,89,176] as shown in Table 5) to Tg = 138.5°C for maltoheptaose.[28] The plot in Figure 50A showed the same qualitative curvature (and absence of an entanglement plateau) as the corresponding Tg′ plot in Figure 42, and the plot of dry Tg vs. 1/MW in Figure 50B showed the same linearity and r value as the corresponding Tg′ plot in the inset of Figure 42. (The results shown in Figure 50A were subsequently corroborated by Orford et al.,[59] who recently reported a similar curve of dry Tg vs. DP for glucose and its malto-oligomers of DP 2 to 6.) Further verification of the assumption was demonstrated by a plot (shown in Figure 51[28]) of Tg vs. w% composition for a series of spray-dried, low-moisture powders (about 2 w% water) prepared from solution blends of commercial SHPs, Lodex 10 and Maltrin M365. This plot showed that Tg increases from 58°C for Maltrin M365 (36 DE, Tg′ = −22.5°C) to 121°C for Lodex 10 (11 DE, Tg′ = −11.5°C) for these SHPs at about 2 w% moisture. Here again, the characteristic monotonic increase of Tg with $\overline{M}w$ (≡ increasing composition as w% Lodex 10) and curvature expected and theoretically predicted for homologous (mixtures of) oligomers with $\overline{M}w$ values below the entanglement plateau limit were evident.

The glass curves (solid lines)[59] in Figure 49 for the three malto-oligosaccharides at low moistures (i.e., W < Wg′) are also noteworthy for their similarity to the glass curves shown earlier for starch (Figure 25), hemicellulose, sorbitol (Figure 27), elastin (Figure 19A), and gluten (Figure 26). At moisture contents ≤10 w%, maltose, maltotriose, and maltohexaose manifest extents of plasticization of about 9, 11, and 12.5°C/w% water, respectively,[59] values typical of many other water-compatible food oligomers and high polymers.[15,42,66] We have added the dashed portions to the solid lines in Figure 49 to show that the measured glass curves of Orford et al.[59] can be extrapolated, as expected, to the corresponding measured Tg′-Wg′ points (Table 3) on these state diagrams, at least in the cases of maltose and maltotriose. At moisture contents >Wg′, the Tg curves (for quench-cooled solute-water blends) would be expected to continue to extrapolate smoothly, but with more gradual curvature, to the Tg at about −135°C for pure amorphous solid water.

As mentioned earlier, beneath the generic approximation of $\eta g \simeq 10^{12}$ Pa s at Tg cited for many glass-forming synthetic polymers,[106,107] there are underlying distinguishing features, so that the glass transition is not rigorously a *universal* iso-viscosity state.[30,107] Were it so, in order for the glass transition to be both an iso-viscosity state and, as defined by the WLF equation, an iso-free volume state, all glass-forming liquids would have the same local viscosity at any given ΔT above Tg, to the extent that the WLF coefficients C1 and C2 are "universal" values.[107] The absolute viscosity of a glass at its Tg depends on the nature of the particular solute (e.g., its Tm/Tg ratio)[30] and plasticizer in question, and is thought to vary within the range 10^{10} to 10^{14} Pa s.[30,89,172,289] However, despite these qualifications, the concept that the glass curve of Tg vs. w% composition, for a particular solute-diluent system, reflects an iso-viscosity state for that system remains a valid and useful approximation.[189] Accordingly, all points along the glass curve (i.e., all compositionally dependent Tg values) for a given solute-diluent system represent glasses of approximately the same local viscosity at their Tg. Thus, for a particular glass-forming carbohydrate solute (of MW below the entanglement limit), the viscosity at Tg of the dry glass and at Tg′ of the maximally freeze-concentrated aqueous glass are approximately the same.[40-42] This point represents an important conceptualization related to food quality and safety. For example, for glucose and the malto-oligosaccharides through DP 7 shown in Figures 42 and 50, the corresponding glasses existing at the dry Tg and at Tg′-Wg′, although separated by temperature differentials of from 74°C for glucose to 152°C for maltoheptaose, have approximately the same viscosities. While this situation is also subject to qualification by the earlier-mentioned (1) fact that the temperature location of Tg is not based solely on either an iso-viscosity or iso-free volume state alone;[107] (2) suggestion that

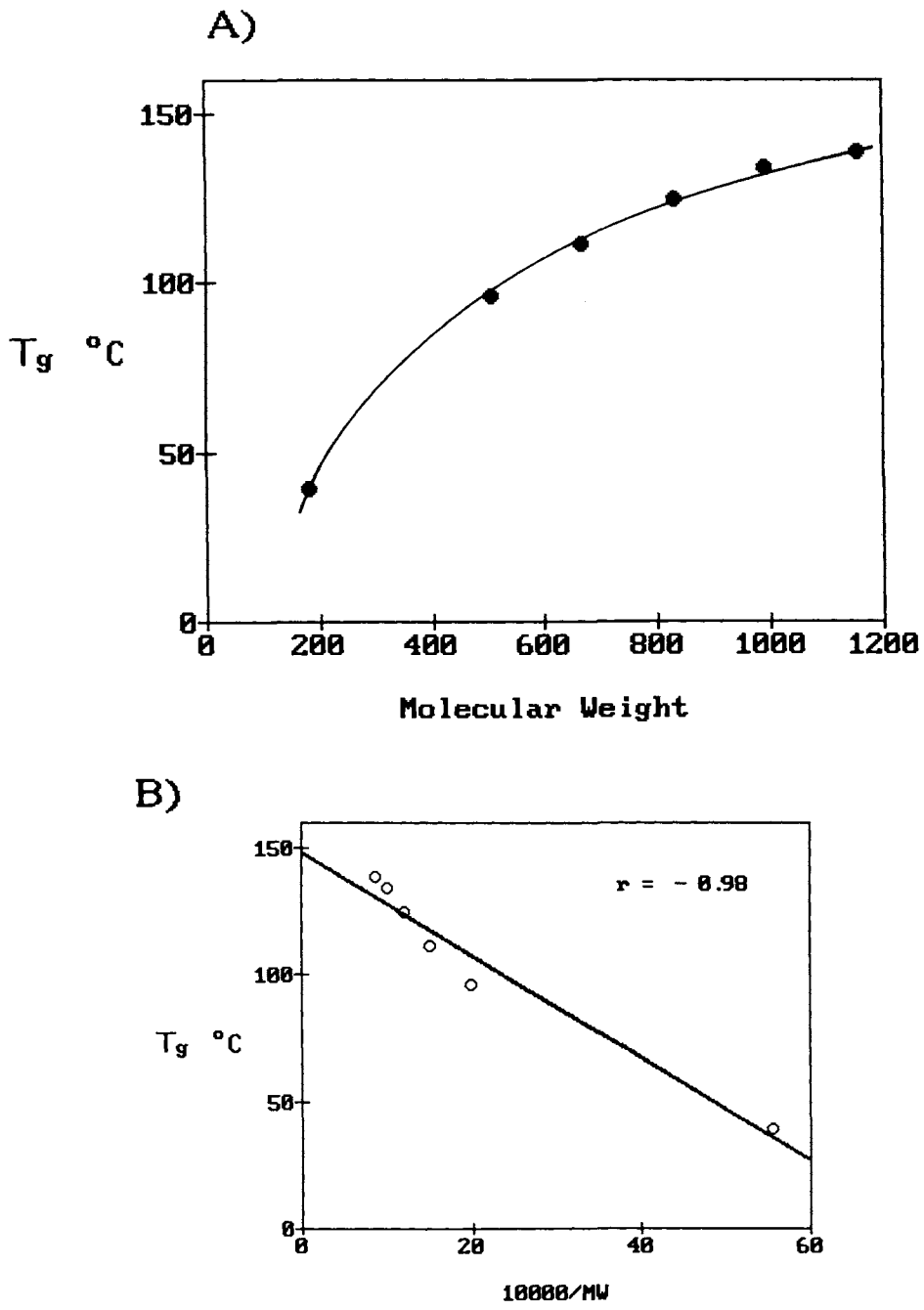

FIGURE 50. Variation of the glass transition temperature (Tg of dry powders) against (A) MW and (B) 10000/MW, for the homologous series of malto-oligosaccharides from glucose through maltoheptaose in Table 3. (From Levine, H. and Slade, L., *Water and Food Quality,* Hardman, T. M., Ed., Elsevier, London, 1989, 71. With permission.)

different portions of the glass curve are controlled by different mobility-determining parameters, i.e., free volume at lower moisture contents in the glass, but local viscosity at higher moisture contents in the glass;[30] and (3) realization that the best description of the glass transition is its definition as an iso-relaxation-time state,[30] the significance of the qualitative conceptual picture is not negated. The glass curve of approximately equivalent local viscosity still represents the

TABLE 5
Tg Values from DSC of Dry Sugars and Sugar Mixtures

Sugar	Tg, °K
Fructose	286,[a] 373[b] and 284[b]
Glucose	312,[a] 304,[b] 302,[c] 310,[d] 303,[e] 302[f]
Sucrose	330,[a] 325,[b] 340[c]
Fructose:glucose (1:1 w/w)	294,[a] 293[b]
Fructose:sucrose (1:7 w/w)	326,[a] 331[c]

[a] Value measured at 10°K/min heating rate.[124]
[b] Value measured at 10°K/min heating rate.[30]
[c] Value calculated or assumed, rather than measured.[89]
[d] Value measured at 10°K/min heating rate.[59]
[e] Value extrapolated to 0°K/min heating rate.[59]
[f] Value measured at 5°K/min heating rate.[176]

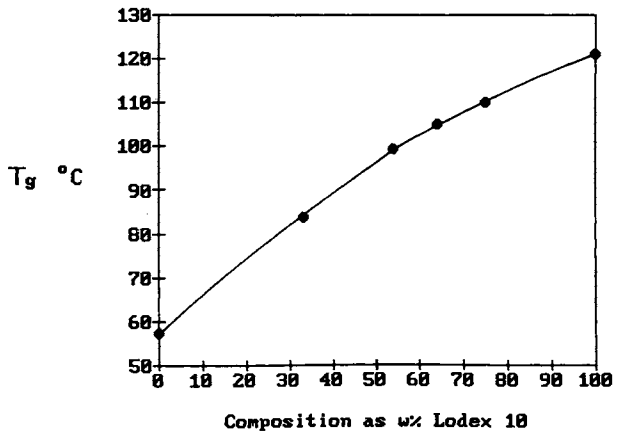

FIGURE 51. Variation of the glass transition temperature, Tg, against weight percent composition for spray-dried, low-moisture powders prepared from aqueous solution blends of Lodex 10 and Maltrin M365 SHPs. (From Levine, H. and Slade, L., *Water and Food Quality,* Hardman, T. M., Ed., Elsevier, London, 1989, 71. With permission.)

line of demarcation between long-term stability (at $\eta \geq \eta g$) and gradual deterioration (at $\eta < \eta g$),[8,40-42] whether one is talking about the shelf-life of a dry glucose candy glass (of Tg = 31°C) stored at ambient temperature or of a glucose-sweetened ice cream (of Tg′ = −43°C) stored in a freezer.

A compilation of measured values of dry Tg and dry Tm, and calculated Tm/Tg ratios, for various sugars and polyols is shown in Table 3.[28,30] Dry Tg values range from −93°C for glycerol (MW 92) to 138.5°C for maltoheptaose (MW 1153), and generally show the expected relationship of increasing Tg with increasing MW of the diluent-free PHC, but with several striking exceptions. Moreover, for a given MW, the spread of dry Tg values for different isomeric PHCs is large; in fact, many times larger than the corresponding spread of Tg′ values. For example: (1) among several pentoses and pentitols (MW ≃ 150), dry Tg values range from −18.5°C for xylitol to 9.5°C for xylose; (2) among several hexoses and hexitols (MW≃180), dry Tg values range from −2°C for sorbitol to 31°C for glucose (the anomalously high Tg values for anhydrous fructose and galactose are discussed in detail below); and (3) among several disaccharides (MW 342), dry Tg values range from 43°C for maltose to 90°C for mannobiose.

In Table 3, the calculated values of Tm/Tg (°K) ratio range from 1.62 to 1.06, with most values in the range 1.32 to 1.44. Of these sugars and polyols, fructose shows the most extremely anomalous Tm/Tg ratio of 1.06.[15,16] This value is much lower even than the lowest Tm/Tg ratio reported for a synthetic high polymer, i.e., 1.18 for bisphenol polycarbonate.[102] Levine and Slade[15] had reported previously that fructose's Tm/Tg ratio of 1.06 derives from the observation of *two* widely separated glass transition temperatures (see Table 5) in a quench-cooled, completely amorphous melt of pure crystalline β-D-fructose. The lower Tg appears at a lower temperature (11°C[30] or 13°C[124]) than the single values of Tg (around 30°C) of other common monosaccharides of the same MW, such as glucose and mannose. However, the much higher Tg is readily detectable at 100°C, a temperature only 24°C below the measured Tm of β-D-fructose. Another monosaccharide, galactose, shows analogous anomalous behavior, with a lower Tg similar to that of glucose and mannose, but a second, much higher Tg similar to the higher Tg of fructose.[28] The observed change in heat capacity at the higher Tg of fructose is smaller in magnitude than at the lower Tg, which may reflect either a smaller actual difference in heat capacity of the fructose population that vitrifies at the higher Tg than of the

second, structurally different fructose population that vitrifies at the lower Tg, or that the population of fructose molecules that vitrifies at the higher Tg of the conformationally heterogeneous melt is smaller, while the second population that vitrifies at the lower Tg is larger.[30] However, for reasons explained later, which are based on an interpretation of experimental results (including those in Table 2) involving several aspects of the anomalous behavior of fructose in non-equilibrium aqueous systems and processes, Slade and Levine have hypothesized that the higher Tg of dry fructose (and of galactose as well) is the critical one that defines the Tm/Tg ratio and controls the consequent mobility of plasticizing solute-water blends in their glassy and supra-glassy states.[15,16,30]

With respect to the unusual phenomenon of two values of Tg exhibited by quenched melts of fructose or galactose, Finegold et al.,[124] in their recent study of glass/rubber transitions and heat capacities of dry binary sugar blends, have reported similar anomalous behavior for the same two monosaccharides, and their contrast to well-behaved glucose and mannose. They have confirmed the existence of the higher-temperature "relaxation process" and that its amplitude (for fructose) is only 25% of that at the lower-temperature Tg.[124] While Finegold et al.[124] have remarked that "the actual physical origin of two distinct relaxation processes in an ostensibly one-component system is obscure", they have pointed out that both fructose and galactose are subject to complex mutarotation and have granted the possibility (suggested by Slade and Levine[30]) "that a quenched melt might exhibit microheterogeneity, with the appearance of two or more structural relaxations. This hypothesis is supported by the observation that annealing eventually removes the high-temperature relaxation process and increases the amplitude of the (low-temperature) relaxation."[124] Finegold et al. have also confirmed the earlier finding[15] that, in a two-component glass with another small sugar (in their case, sucrose or glucose[124]), the higher Tg of fructose is no longer detectable, as shown in Table 5 for a 1:1 (w/w) glucose:fructose glass (Tg = 20°C[30] or 21°C[124]) and a 1:7 (w:w) fructose:sucrose mixture.[89] This change in the thermomechanical behavior of fructose, to become more like glucose in the 1:1 mixture in the absence of diluent, is also manifested in the relative microbiological stability of concentrated solutions of glucose, fructose, and the 1:1 mixture, as will be discussed further with respect to Table 2.

In a possibly related vein discussed further below, it is interesting to note that Hallbrucker and Mayer[263] have also suggested the possibility of local microstructure in a heterogeneous molten fluid or glass of a one-component glass-forming system, in their discussion of the differences in thermal relaxation behavior between "hyperquenched" (i.e., cooling rate $>10^5$ °C/s) vs. slow-cooled glasses of aqueous or diluent-free PHC systems. They mentioned that the development of heterogeneous microstructure (i.e., local regions of different constitution and "activation energies") in a melt could contribute to the non-Arrhenius behavior of viscosity and flow processes in the temperature region above Tg. They have suggested "that hyperquenching produces a glass differing in local microstructure and (the temperature dependence of its) relaxation behavior from a slow-cooled glass," due to a corresponding difference in the temperature (relative to the Tg measured during subsequent rewarming) at which the molten fluid is immobilized to a glassy solid during cooling and thus at which the temperature dependence of relaxation processes switches from non-Arrhenius back to Arrhenius behavior.[263] Also pertinent to this line of discussion are recent remarks of Green and Angell,[290] who noted "that constant-composition samples (of molten glucose monohydrate) did yield variable Tg values depending on heat treatment. This reminds us that there is a structural variable for the solution (the anomer ratio), the time scale of which is much longer than the viscoelastic relaxation time and that may, therefore, be able to influence glass properties in new ways — all of which adds strength to Franks' recent call[281] (echoed by Slade and Levine[30]) for a renewed physicochemical interest in saccharide solutions."

Among a number of different cases of multiple values of Tg observed in amorphous and partially crystalline systems,[26,33] fructose may represent the interesting situation where two conformationally different populations of the same

chemical species manifest different free volume and local viscosity requirements for mobility.[30] Such a situation would arise if one of the conformational populations in a heterogeneous melt exhibited anisotropic rotational and translational mobilities, while the second population exhibited isotropic motion. For motional anisotropy, the free volume requirements for rotational mobility become much more stringent than those for translation,[187,188] and rotational relaxation would become limiting at a higher temperature than translational relaxation, as described with respect to Figure 34D for polymers with anomalously low values of Tm/Tg. For isotropic motion, the larger scale, slower translational relaxations become limiting at a higher temperature than rotational relaxations,[186,187] as described with respect to Figure 34D for polymers with typical and high values of Tm/Tg. For both anisotropic and isotropic motion, the temperature at which translational relaxations become limiting would be nearly the same. Thus, relaxation times for a conformational population with anisotropic motion would become limiting at a higher temperature, manifested as a higher Tg, than relaxation times for a second population with isotropic motion, manifested as a lower Tg.[30] A documented case, which might provide an explanation for the appearance of two conformationally different populations in a heterogeneous melt from a single crystalline conformation of a single chemical species, involves xylose, which has been shown to undergo rapid anomerization during melting.[291]

During the time between heating α-D-xylose to a temperature only slightly above Tm, to avoid decomposition, and quench-cooling the resulting melt to a glass in a conventional DSC experiment, a mixed population of anomers is able to form in the melt and be captured in the glass.[291] Thus, the initial crystal contains only the alpha anomer, while the final glass contains a simple anomeric mixture of α- and β-xylose,[124] and the particular conformer distribution in the glass depends on the experimental variables of temperature, pressure, and concentration. The fact that only a single value of Tg is observed for the xylose melt,[28,124] which is known to be conformationally heterogeneous, indicates either that all of the conformers are chemically and mechanically compatible so that a single glass vitrifies, or that all of the glasses that vitrify have the same free volume and local viscosity requirements for mobility and so the same value of Tg.[30] If other small PHCs, such as fructose and galactose, behave like xylose with respect to anomerization during the melting process, then depending on the specific Tm, the time the melt is held above Tm, and the quenching rate, they may also be capable of forming heterogeneous melts with conformationally different populations.[30] Then the fact that two values of Tg are observed would indicate that the two populations are not chemically and mechanically compatible and that they exhibit different free volume and local viscosity requirements for mobility. Finegold et al.[124] have reported another observation about the higher Tg of fructose that could support such speculation about the possibility of anomerization in a fructose melt. They noted that, after repeated heating and recooling of the initial fructose melt, the magnitude of the observed change in heat capacity at the higher Tg diminished and ultimately became undetectable, leaving only the lower Tg (representing the glass of the more stable anomer?[30]). This observation of changes in the sizes of the two populations upon repeated heating suggested that the difference in magnitude of the observed heat capacity for the two glasses after the initial fructose melt was due to different sizes of the two populations rather than different actual changes in heat capacities.[30]

There appear to be a number of analogies between aspects of (1) the double-glass-forming behavior of fructose and galactose and (2) the differences in thermal behavior, thermodynamic, and kinetic properties between ordinary slow-cooled vs. hyperquenched, diluent-free glasses of small PHCs such as ethylene glycol[263] and propylene glycol.[174] These analogies lead us to speculate about a common thread, as yet unidentified, in the two phenomena. Johari et al.[174] have suggested that "the temperature range over which the liquid-to-glass transition occurs on hyperquenching is wider than the range over which the transition occurs on normal cooling." In a corresponding fashion for each type of glass (and for glasses in general), "the temperature range of the glass transition is much less during the heating of a glass to liquid than it is during the cooling of a liquid to glass".[174] A hyperquenched

glass has a "fictive temperature" much higher than the normal Tg of a slow-cooled glass (of $\eta = 10^{12}$ Pa s) of the same material, i.e., hyperquenching immobilizes the liquid during quenching at higher temperatures than slow cooling.[174,263] Consequently, the kinetic and thermodynamic properties of a hyperquenched glass differ from those of a glass obtained by slow cooling.[174,263] For example, on subsequent rewarming, the Tg of a hyperquenched glass is observed at a higher temperature than the Tg of a corresponding slow-cooled glass.[174,263] (The Tg *observed* during heating [e.g., at 10°C/min] as a consequence of a particular previous sample history is a value of Tg somewhere below the fictive temperature [i.e., the fictively high Tg observed during fast cooling] and above the practical lower limiting Tg [i.e., the limiting value observed with ever slower cooling rates].[174]) As a consequence of higher fictive temperature, hyperquenching produces "a less dense glass (i.e., of lower viscosity) of a structure with a higher enthalpy and entropy, but with a much narrower distribution of structural relaxation times," the latter because the requirement for molecular cooperativity is gradually removed as the average intermolecular distance increases.[174] (It should be noted that the dependence of density on cooling rate is a general characteristic of glasses.[172]) As a consequence of lower density and viscosity in a hyperquenched glass at Tg, during rewarming of such a glass to temperatures above Tg, its constituent molecules exhibit greater rotational and translational mobility for diffusion-limited structural relaxation processes such as crystallization in the rubbery fluid.[263] For the same reasons, hyperquenched glasses show greater extents of structural collapse and resulting gradual viscous flow and concomitant densification (also referred to as sintering during heating) at temperatures 4 to 5°C above Tg than do slow-cooled glasses.[174] In contrast to the behavior of hyperquenched glasses at $T >$ Tg, during *sub*-Tg "aging" (referred to by Johari et al. as "annealing", but distinguished from the conventional definition of annealing at $Tg < Ta < Tm$[104]) of hyperquenched glasses, a spontaneous but slow structural relaxation, to a denser structure of lower fictive temperature and higher viscosity (more similar to the structure, viscosity, and fictive temperature of a slow-cooled glass), has been observed to begin at a temperature $\simeq$0.73 Tg (K).[174] (By analogy, relative to the higher Tg of fructose at 100°C, the temperature at which such sub-Tg aging would begin would be 0°C.) It has been suggested that hyperquenched and slow-cooled samples of the same PHC glass-former, after sufficient aging at a temperature very close to Tg, would reach an identical structural state and show indistinguishable DSC scans.[174] However, "for the same temperature and time of (aging), spontaneous structural relaxation in hyperquenched glasses at $T < Tg$ is much slower than in ordinary glasses".[174]

We infer from the above comparison of the properties and behavior of hyperquenched vs. slow-cooled glasses of the polyols, ethylene glycol and propylene glycol, that the higher-Tg glass of fructose (and galactose) appears to manifest certain characteristics of a hyperquenched glass, while in contrast, the lower-Tg glass of fructose (and galactose) manifests the expected characteristics of a slow-cooled glass. The parallels, even though not all-inclusive, are provocative. But how and why a single cooling rate of 50°C/min, applied to a molten fluid of diluent-free fructose or galactose, could cause the formation of two distinct glasses, with properties analogous to those produced (in separate experiments) in polyol systems by two drastically different experimental cooling rates, are unknown and especially mystifying in light of the fact that our same experimental protocol has produced a single glass with a single Tg for every other small PHC that we have examined, including glucose, mannose, xylose, etc.[30] Likewise, in the studies of hyperquenched vs. slow-cooled polyol glasses, only a single Tg was observed in all cases upon rewarming of the glass following vitrification during cooling of the liquid, regardless of the cooling rate.[174,263] We can only speculate about the possibility of a different relationship between cooling rate and the kinetics of mutarotation for (what could be)[30] the two distinguishable populations of structural entities existing, at least initially, in a cooled melt of fructose or galactose.

The fundamental issue regarding the anomalous thermomechanical properties of fructose (vs. e.g., glucose) in foods[16,30] is still open to debate. As mentioned earlier, Slade and Levine[30] have stressed the evidently controlling influence of the

higher Tg of dry fructose, and resultant anomalously low Tm/Tg ratio, on the mobility-related kinetic behavior of fructose-water systems. In apparent contradiction, Finegold et al.[124] have suggested "that the low temperature relaxation is significant in determining the thermomechanical behavior of (this dry) sugar", both alone and in dry binary blends with other sugars. They have presented experimental glass curves (shown in Figure 52[124]) in which dry Tg was found to vary smoothly with composition for binary blends of fructose + glucose and fructose + sucrose, and which extrapolate smoothly to the lower Tg at 13°C for fructose. By analogy with the thermomechanical properties of synthetic high polymers, they have noted that, "in fructose-glucose blends, fructose takes on the role of plasticizer, since it depresses the Tg of glucose. An effect of MW on Tg can be seen (in Figure 52) from a comparison of sucrose with an equimolar mixture of glucose and fructose."[124] They have also pointed out that the lower dry Tg values of fructose and galactose would result in more typical Tm/Tg ratios around 1.4, more in line with the values for other well-behaved hexoses.[124] As discussed later, reconciliation of these two apparently divergent points of view is suggested to depend in part on the critical conceptual distinction between the non-equilibrium properties of diluent-free vs. water-containing glasses and rubbers. Because fructose is such a technologically important sugar, its glass-forming behavior in aqueous food systems and the thermomechanical ramifications thereof are a subject worthy and in need of further study by physical chemists.

The results for Tm/Tg ratio in Table 3 showed that fructose has the lowest value, based on selection of the higher Tg value as the one of overriding thermomechanical importance,[30] while galactose (along with maltotriose) has the next-lowest. Thus, this dry fructose glass would be predicted to have the highest requirement for free volume in the glass at (the higher) Tg, and conversely the lowest local viscosity ($\lesssim 10^{10}$ Pa s).[30]

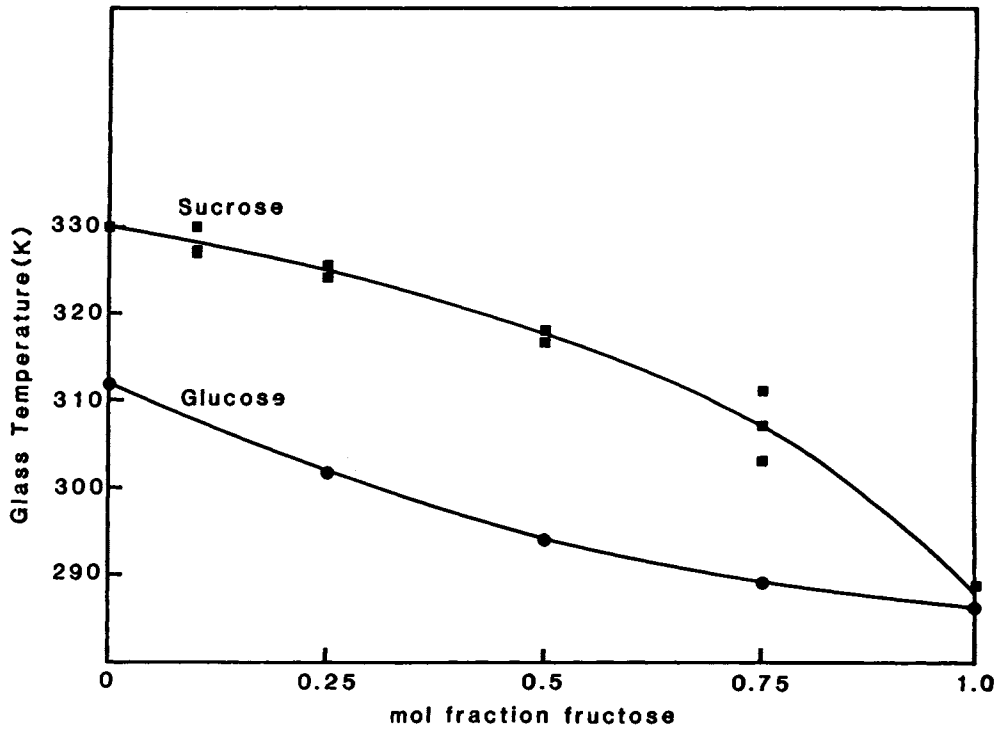

FIGURE 52. Glass/rubber transition temperature Tg vs. mol fraction of fructose for mixtures of fructose + glucose (circles) and fructose + sucrose (squares). The curve for the fructose-sucrose blends is a best-fit parabola. (From Finegold, L., Franks, F., and Hatley, R. H. M., *J. Chem. Soc. Faraday Trans. I.*, 85, 2945, 1989. With permission.)

Indeed, the Tg results of Finegold et al.[124] in Figure 52 can be interpreted as supporting this prediction. Because of its lower MW and concomitant higher free volume, fructose would be expected to take on the role of plasticizer and thus lower the Tg of sucrose in a dry binary blend. However, their finding[124] that fructose plasticizes glucose in a dry binary glass of these two monosaccharides (of the same MW) suggests that fructose manifests a higher free volume and lower local viscosity than glucose in the binary glass at its Tg. Such a situation would be consistent with a lower (rather than equal) Tm/Tg ratio for fructose in comparison to glucose. At the other end of the scale, glycerol, with the highest Tm/Tg ratio, would have the lowest requirement for free volume, but the highest viscosity ($\simeq 10^{14}$ Pa s) in its diluent-free glass at Tg. Consequently, at their respective values of Tg, a glycerol glass would be predicted to be significantly firmer (and thus less mobile and so more "stable" with respect to diffusion-limited relaxation processes) than a fructose glass.[30] This prediction awaits testing, with respect to both their diluent-free and Tg′-Wg′ glasses.

Experimental mobility transformation data for an extensive list of small carbohydrates, including most of the sugars, polyols, and glycoside derivatives in Table 3, are compiled in Table 6.[30] For each monodisperse PHC, Table 6 lists the measured Tg′ value for the maximally freeze-concentrated solute-UFW glass, which represents the reference state for the analysis that follows. This table also includes the corresponding Wg′ value (w% UFW), calculated $\overline{M}w$ and $\overline{M}n$ for the solute-water mixture in the glass at Tg′, the corresponding $\overline{M}w/\overline{M}n$ ratio, and the Tm/Tg ratios of some of the dry PHCs, from Table 3. The samples are ranked in Table 6 according to increasing value of $\overline{M}w$. Two other versions of this table, with samples ranked by increasing $\overline{M}n$ or increasing $\overline{M}w/\overline{M}n$ ratio, are not shown but will be alluded to, and so are left to the reader to construct.

If Table 6 had been ranked according to solute MW, all of the hexose monosaccharides would have appeared together, as they do in Table 3. But when such common sugars as fructose and glucose are ranked, not according to solute MW, but rather based on the Tg′-Wg′ reference state, they are widely separated on the list. The ranking according to increasing $\overline{M}n$ reflects decreasing requirement of free volume for mobility near Tg′ for PHCs with the same value of Tg′.[30] Thus, the free volume required for limiting mobility of fructose-water and captured in the fructose-water glass ($\overline{M}n$ = 33.3) is much greater than that for glucose-water ($\overline{M}n$ = 49.8). (Since the fructose-water glass at Tg′ has much greater free volume than the corresponding glucose-water glass, does the same relationship hold true for the corresponding dry glasses at Tg, as would be predicted from the much lower Tm/Tg ratio for fructose than for glucose?) It has been concluded that the composition and physicochemical properties of this glass at Tg′, which represents the crucial reference condition for technological applications involving any of the common functional properties of a small carbohydrate in water-containing food systems, cannot be predicted based on the MW of the dry solute.[30] The ranking according to increasing $\overline{M}w$ in Table 6 reflects increasing local viscosity in the glass at Tg′, for PHCs with the same values of Tg′ and $\overline{M}n$. Careful examination of the order of the PHCs in this table, compared to the different orders resulting from rankings by $\overline{M}n$ and $\overline{M}w/\overline{M}n$, has revealed that the order changes dramatically, depending on whether these small carbohydrates are ranked according to free volume, local viscosity, or the ratio of local viscosity/free volume.[30] Significantly, while ethylene glycol appears at the top of all three listings, trehalose appears at the bottom of the listing by $\overline{M}n$ (85.5), reflecting lowest free volume requirement for mobility near Tg′ compared to the other disaccharides in the list, while maltoheptaose appears at the bottom of Table 6 ($\overline{M}w$ = 911.7), reflecting very high local viscosity of the glass at Tg′, but next to last (preceding maltohexaose) in the order of increasing $\overline{M}w/\overline{M}n$ ratio (11.39). So again, it has been concluded that one cannot predict, based on MW of the dry solute, even for the homologous series of glucose oligomers from the dimer to the heptamer, where such small carbohydrates would rank in terms of the free volume and local viscosity requirements for mobility near the solute-water glass at Tg′-Wg′.[30]

TABLE 6
Mobility Transformation Data for Small Carbohydrate Aqueous Glasses[30]

Polyhydroxy compound	MW	Tg′ °K	Wg′ w%	$\bar{M}w$	$\bar{M}n$	$\bar{M}w/\bar{M}n$	Tm/Tg
Ethylene glycol	62.1	188.0	65.5	33.2	23.8	1.39	
Propylene glycol	76.1	205.5	56.1	43.5	27.1	1.61	
1,3-Butanediol	90.1	209.5	58.5	47.9	26.9	1.78	
Glycerol	92.1	208.0	45.9	58.1	31.9	1.82	1.62
Erythrose	120.1	223.0	58.2	60.7	27.9	2.17	
Deoxyribose	134.1	221.0	56.9	68.0	28.7	2.37	
Arabinose	150.1	225.5	55.2	77.2	29.7	2.60	
2-*O*-methyl fructoside	194.2	221.5	61.7	85.5	27.6	3.10	
Deoxyglucose	164.2	229.5	52.6	87.3	31.1	2.80	
Deoxygalactose	164.2	230.0	52.6	87.3	31.1	2.80	
Tagatose	180.2	232.5	57.1	87.6	29.3	2.99	
Arabitol	152.1	226.0	47.1	89.0	33.7	2.64	
1-*O*-methyl mannoside	194.2	229.5	58.8	90.5	28.7	3.15	
Methyl xyloside	164.2	224.0	50.2	90.7	32.3	2.81	
Ribitol	152.1	226.0	45.1	91.7	34.9	2.63	
Methyl riboside	164.2	220.0	49.0	92.6	33.0	2.81	
3-*O*-methyl glucoside	194.2	227.5	57.3	93.3	29.4	3.17	
α-1-*O*-methyl glucoside	194.2	228.5	56.9	93.9	29.6	3.18	
Xylitol	152.1	226.5	42.9	94.6	36.3	2.61	1.44
β-1-*O*-methyl glucoside	194.2	226.0	56.3	94.9	29.8	3.18	
Deoxymannose	164.2	230.0	47.4	94.9	33.9	2.80	
1-*O*-ethyl glucoside	208.2	226.5	57.4	98.9	29.4	3.36	
Fructose	180.2	231.0	49.0	100.8	33.3	3.03	1.06
1-*O*-ethyl galactoside	208.2	228.0	55.8	102.2	30.2	3.38	
Glucose:Fructose 1:1	180.2	230.5	48.0	102.3	33.7	3.04	
1-*O*-ethyl mannoside	208.2	229.5	54.8	104.1	30.7	3.39	
2-*O*-ethyl fructoside	208.2	226.5	53.5	106.5	31.3	3.40	
Ribose	150.1	226.0	32.9	106.7	44.0	2.43	1.37
α-1-*O*-methyl glucoside	194.2	227.5	49.5	106.9	33.2	3.22	1.47
6-*O*-methyl galactoside	194.2	227.5	49.5	107.0	33.2	3.22	
2,3,4,6-*O*-methyl glucoside	236.2	227.5	58.5	108.5	29.2	3.72	
Xylose	150.1	225.0	31.0	109.1	45.8	2.38	1.51
Galactose	180.2	231.5	43.5	109.6	36.6	2.99	1.16
1-*O*-propyl glucoside	222.2	230.0	55.0	110.0	30.7	3.58	
1-*O*-methyl galactoside	194.2	228.5	46.2	112.7	35.1	3.21	
1-*O*-propyl galactoside	222.2	231.0	51.2	117.6	32.6	3.60	
Allose	180.2	231.5	35.9	122.0	42.6	2.87	
1-*O*-propyl mannoside	222.2	232.5	48.7	122.7	34.0	3.60	
Glucoheptulose	210.2	236.5	43.5	126.6	37.2	3.40	
Sorbose	180.2	232.0	31.0	129.9	47.5	2.74	
Glucose	180.2	230.0	29.1	133.0	49.8	2.67	1.42
Mannose	180.2	232.0	25.9	138.1	54.0	2.56	1.36
Inositol	180.2	237.5	23.1	142.8	58.5	2.44	
Sorbitol	182.2	229.5	18.7	151.5	67.3	2.25	1.42
Mannobiose	342.3	242.5	47.6	187.8	35.7	5.26	1.32
Lactulose	342.3	243.0	41.9	206.5	40.1	5.15	
Isomaltose	342.3	240.5	41.2	208.8	40.7	5.13	
Lactose	342.3	245.0	40.8	209.9	41.0	5.12	
Turanose	342.3	242.0	39.0	215.7	42.6	5.06	1.38
Maltitol	344.3	238.5	37.1	223.2	44.6	5.01	
Sucrose	342.3	241.0	35.9	225.9	45.8	4.93	1.43
Gentiobiose	342.3	241.5	20.6	275.4	72.6	3.80	
Maltose	342.3	243.5	20.0	277.4	74.4	3.73	1.27

TABLE 6 (continued)
Mobility Transformation Data for Small Carbohydrate Aqueous Glasses[30]

Polyhydroxy compound	MW	Tg′ °K	Wg′ w%	$\overline{M}w$	$\overline{M}n$	$\overline{M}w/\overline{M}n$	Tm/Tg
Trehalose	342.3	243.5	16.7	288.2	85.5	3.37	1.35
Raffinose	504.5	246.5	41.2	304.2	41.6	7.31	
Stachyose	666.6	249.5	52.8	323.9	33.3	9.74	
Panose	504.5	245.0	37.1	324.0	45.7	7.08	
Isomaltotriose	504.5	242.5	33.3	342.3	50.4	6.79	
Maltotriose	504.5	249.5	31.0	353.5	53.7	6.58	1.16
Maltotetraose	666.6	253.5	35.5	436.5	48.4	9.03	
Maltopentaose	828.9	256.5	32.0	569.6	53.8	10.59	
Maltohexaose	990.9	258.5	33.3	666.6	52.1	12.79	
Maltoheptaose	1153.0	259.5	21.3	911.7	80.0	11.39	

Note: The samples are ranked according to increasing values of $\overline{M}w$.

B. State Diagrams

State diagrams and their physicochemical basis represent a central element of the food polymer science data bank. Having already described several state diagrams for water-compatible polymeric, oligomeric, and monomeric food materials, in the context of the effect of water as a plasticizer, let us review further what has been gleaned from such state diagrams, viewed as mobility transformation maps for solute-water systems.

Figure 53[30] shows experimental data for the glass curves of the small PHCs, glucose, fructose, and sucrose, and a 40,000 MW PVP (PVP-40).[15] This mobility transformation map for these common sugars and PVP was constructed from measured values of (a) dry Tg and (b) Tg′ and Cg′, coupled with (c) Tg of pure amorphous solid water, (d) Tm of pure ice, and (e) the equilibrium[133] and non-equilibrium portions of the liquidus curve. Figure 53 demonstrates that the maximum practical (i.e., spacially homogeneous) dilution of each amorphous solute corresponds to a particular glass in each continuum of glassy compositions. As described earlier, alternative paths, such as drying by evaporation or freeze-concentration,[4,27] lead to the same operationally invariant w% composition (Cg′), with its characteristic Tg′.[30] The elevation of Tg, due to increased solute concentration, dramatically affects the shape of the non-equilibrium, very non-ideal portion of the liquidus curve. In other words, the extreme departure from the equilibrium liquidus curve for each of these solutes is related to the shape of the corresponding glass curve.[30] The locus of Tg′ on the transformation map depends on both the free volume and local viscosity, and therefore on the inverse $\overline{M}n$ and inverse $\overline{M}w$, respectively,[107] of the dynamically constrained, kinetically metastable solution.[30] Thus, it has been suggested that the anomalous shape of the extrapolated liquidus curve is a consequence of the system's approach to the immobile, glassy domain, rather than the cause of the particular location of the glass at Tg′.[30,33,34] The anomalous shape of the liquidus, which has been described elsewhere,[6] reflects the non-equilibrium melting behavior of the ice and the improbably low values of apparent RVP of the solution that result from the constrained approach to the glassy domain, which represents the limiting range of relaxation rates compared to the time frame of observation.[30] Equally anomalous values have been observed for the RVPs of aqueous supra-glassy solutions of PHCs at ambient temperature,[15,16] as described later with regard to Table 2. In both of these situations, the apparent RVPs are often inappropriately referred to as Aws, even though they are clearly non-equilibrium values, controlled by, rather than controlling, the long relaxation times of the solute-water system.[30]

It should be noticed that the three-point glass curves in Figure 53 are all characteristically smoothly and continuously curved over the entire

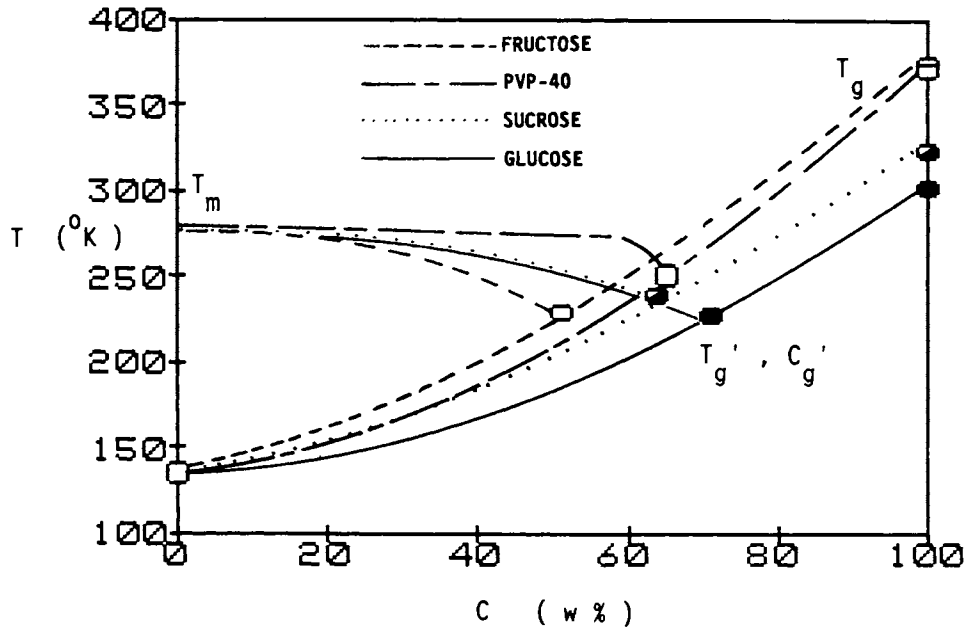

FIGURE 53. Solute-water state diagrams of temperature vs. concentration for fructose, glucose, sucrose, and PVP-40, which illustrate the effect of water plasticization on the experimentally measured glass curves, and the location of the invariant point of intersection of the glass curve and the non-equilibrium portion of the liquidus curve at Tg′ and Cg′, for each solute. (From Slade, L. and Levine, H., *Pure Appl. Chem.*, 60, 1841, 1988. With permission.)

range of solute-diluent w% compositions, as were the glass curves shown earlier in Figures 25, 28, and 29. Obviously, the shapes of these glass curves are determined by the particular locations of the Tg′-Cg′ and dry Tg points for each solute.[16] The glass curve for fructose-water is smoothly curved, only because it was drawn using the higher of the two dry Tg values (i.e., 100°C) for fructose.[15] If the lower dry Tg value of 11°C had been chosen instead, the resulting glass curve for fructose-water would not have been smooth. Rather, it would have a break (or cusp)[292] in it at Tg′-Cg′, such that the portion from Tg of water to Tg′-Cg′ would have a different curvature than the other portion from Tg′-Cg′ to the lower dry Tg. While unusually shaped glass curves, which exhibit a cusp in Tg as a function of composition (i.e., the Tg-composition variation is not monotonic), have been reported in the synthetic amorphous polymer literature for both miscible polymer-polymer and miscible polymer-diluent blends, such a cusp is generally manifested *only* when Tg is plotted vs. volume (rather than weight) fraction, and then *only* when one of the blend components is a high polymer with MW above the entanglement limit.[292] We know of only one report of such a cusp in a glass curve of Tg vs. w% composition (in that case, actually attributed to partial phase separation [i.e., immiscibility] in polymer-diluent mixtures),[293] but none of a cusp in any glass curve for a miscible solute-diluent blend (such as fructose-water) in which the solute MW is well below the entanglement limit. Other cases of maxima or minima in Tg-composition plots are ordinarily attributed to specific associations or complex formation occurring at stoichiometric compositions.[189] Thus, the smooth glass curve for fructose-water in Figure 53 represents supporting evidence for the choice of the higher dry Tg of fructose as the one which, in conjunction with the agreed location of Tg′ (and its corresponding Cg′-Wg′ composition),[6,7,14,27] determines the thermomechanical properties and thereby controls the mobility-related kinetic behavior of fructose-water systems in non-equilibrium glassy, rubbery, and supra-glassy states.[15,16,28,30]

It should be mentioned in passing that Hofer et al.[189] have recently reported an anomalous *depression* of the Tg of water (located at -135 ± 2°C) by the addition of quite small amounts of good aqueous-glass-forming solutes such as LiCl or ethylene glycol. Their Tg measurements of hyperquenched glasses of dilute binary aqueous solutions showed that the initial addition of ethylene glycol lowers the Tg of glassy water from -137°C to a minimum of -144°C for a solute concentration of <6.5 w% (*not* due to stoichiometric complex formation), after which Tg increases with increasing solute concentration (in the typical fashion for a solute of higher MW and diluent-free Tg than water), connecting with the glass curve for the "glass-forming composition region of concentrated solutions".[189] These new and surprising experimental results for Tg in the very low solute concentration region of the glass curve (previously inaccessible to complete vitrification at practical quench-cooling rates), even if substantiated by subsequent studies of other solutes by other investigators, have no bearing on the theoretical basis or experimental implications of the major portion of the solute-water glass curve, corresponding to the temperature-composition region of the dynamics map of greatest practical and technological relevance to food science.

We use weight fraction (w% concentration) for the abscissa of the dynamics map, rather than mole fraction as traditionally practiced for phase diagrams, for several reasons, of which the key supporting one was illustrated earlier by the results in Figure 47. As shown most definitively in Figures 47C and D, Tg′, the single most important point on a state diagram for any water-compatible solute, is determined by the $\overline{M}w$, rather than the $\overline{M}n$, of the solute-UFW composition in the maximally freeze-concentrated glass at Tg′-Wg′. Additional reasons include

1. To predict the composite Tg of compatible blends from the Tg values of individual components.[8] The Tg values of individual components already account for the occupied and free volume contributions to the limiting temperature for mechanical relaxations. Blending of components is then on a weight-fraction basis to determine the resulting local viscosity when volumes are added in different ratios.[30]
2. To allow the construction of state diagrams for materials with unknown MWs and linear DPs but known values of Tg.[15] Moreover, Tg and Wg are determined *not* by molecular volumes but by the volumes (sum of occupied + free) of mobile segments of polymer backbone or mobile units of the cooperative supra-glassy fluid, where the size of the mobile unit is roughly estimated from the total change in specific heat at Tg as a multiple of 11.3 J/K gmole of mobile unit.[106]
3. In a glass-forming mixture (e.g., a solute-plasticizer blend), before free volume becomes limiting, one can predict viscosity and mechanical relaxation times, based on the additivity of molar volumes. But once free volume becomes limiting (e.g., by increasing the solute concentration), cooperative motion of the supra-glassy fluid sets in, and τ is no longer predicted by molar volumes, but rather by the weight-average composition of the blend.[30] For two glass-forming mixtures of the same $\overline{M}n$ at the same temperature, the one with the larger $\overline{M}w$ will have greater η and greater τ.[107]

The latter reason why we plot mobility maps, such as those in Figure 53, in terms of weight fraction, rather than volume fraction, of solute is illustrated in Figures 54 through 56. In Figure 54, the plot of viscosity vs. w% solute data for sucrose and metrizamide[294] shows a comparison between a poor (metrizamide) and a good (sucrose) aqueous glass-former, both of which are hydrogen-bonding solutes. At a single temperature of 10°C, as the solute concentration of the poor glass-former increases, the average molar volume of the solution increases, and so the viscosity of the solution increases correspondingly, as predictable based on the additivity of molar volumes. But for the good aqueous glass-former, there is a concentration (between about 30 and 40 w% solute) above which the solution viscosity can no longer be predicted from the additivity of molar volumes, and above which one sees a dramatic influence of the limitation in free volume on the viscosity of such rubbery liquids.[30] This

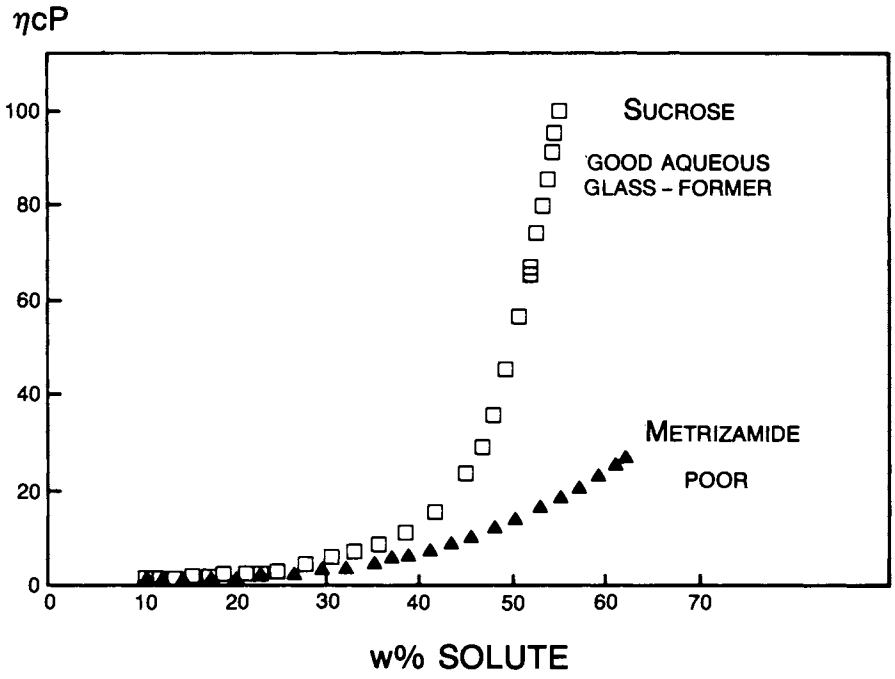

FIGURE 54. Plot of viscosity as a function of weight percent solute for aqueous solutions of two hydrogen-bonding solutes, sucrose and metrizamide, at 10°C. (From Cooper, T. G., *The Tools of Biochemistry,* Wiley-Interscience, New York, 1977. With permission.)

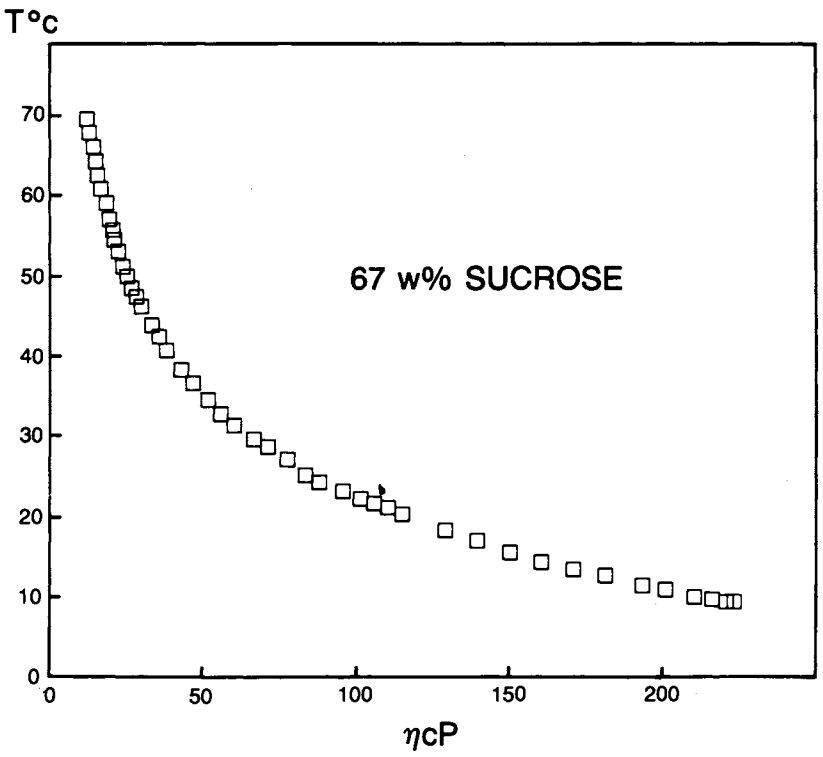

FIGURE 55. Plot of temperature vs. viscosity for a 67 wt% solution of sucrose in water. (Adapted from Parker, K. J., *Glucose Syrups and Related Carbohydrates,* Birch, G. G., Green, L. F., Coulson, C. B., Eds., Elsevier, Amsterdam, 1970, 58.)

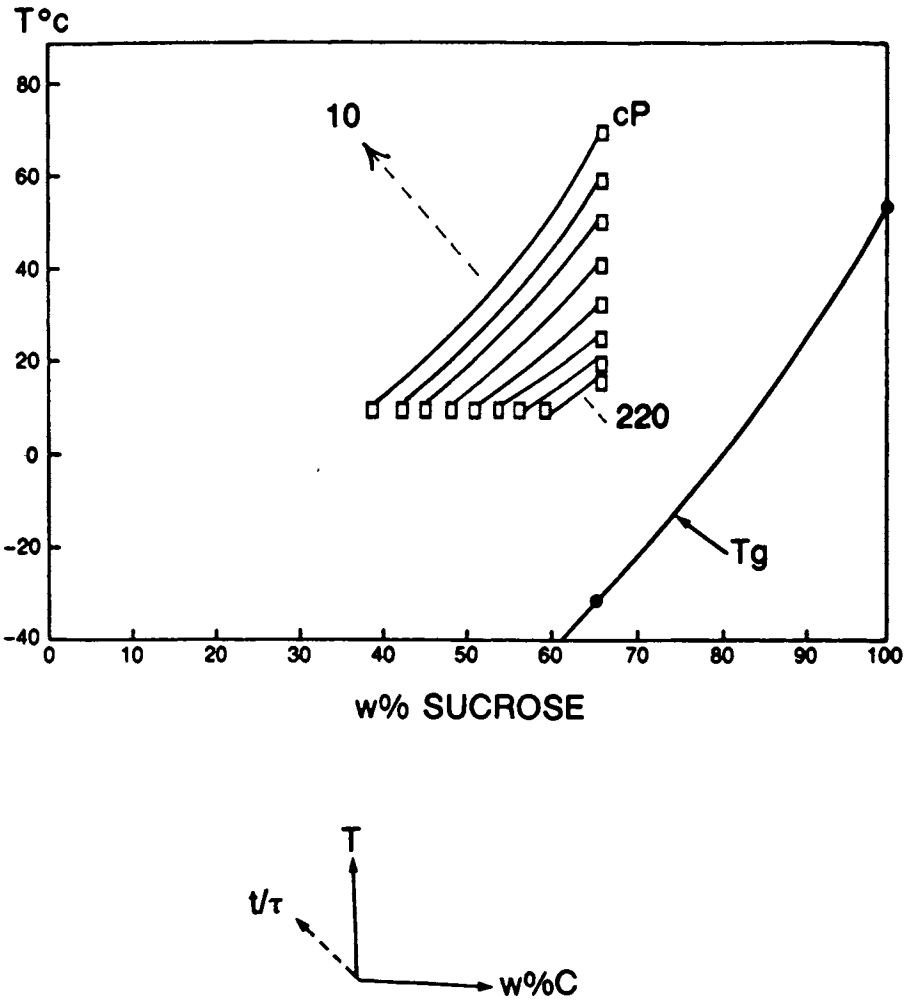

FIGURE 56. A two-dimensional mobility map for sucrose-water, plotted as temperature vs. weight percent sucrose, showing the relative locations of a series of iso-viscosity contours (constructed from the sucrose viscosity data in Figures 54 and 55) and a portion of the "complete" glass curve for sucrose-water.

behavior of the good glass-former reflects the cooperative nature of the glass transition.[106] While the experimental temperature of 10°C is well above the applicable Tg (i.e., Tg′ = −32°C) for such sucrose solutions, the limitations of free volume on mobility have been shown to be manifested even 100°C above the glass transition.[30,107] Thus, this cooperative behavior profoundly affects the observed time scales for mechanical relaxation processes such as viscosity in rubbery sucrose solutions. Figure 54 shows viscosity as a function of solute concentration for a single temperature. But we can also examine the effect of temperature on solution viscosity for a single sucrose concentration (67 w%),[295] as shown in Figure 55. As the temperature decreases from 70 to 10°C, viscosity increases dramatically. If we combine the sucrose data in Figures 54 and 55, by taking combinations of concentration and temperature that give the same solution viscosity, we can in fact build some iso-viscosity contours on the mobility map for sucrose, as shown in Figure 56. For example, combinations of 10°C and 38 w% sucrose and 70°C and 67 w% sucrose give exactly the same viscosity. Figure 56 demonstrates that relaxation times decrease dramatically with increasing ΔT or ΔW above the glass curve for sucrose-water solutions.[16] Thus, Figure 56 is actually a three-dimensional mobility map of content of water (acting as a

plasticizer), temperature (acting as a placticizer), and the experimental time scale (which for these viscosity experiments is constant) compared to the relaxation time (which decreases with decreasing w% solute concentration). This map, plotted as a function of weight fraction of solute, describes the time-dependence of the viscosity behavior of such rubbery or supra-glassy sucrose solutions.

Figure 57[30] illustrates the effects of a small PHC solute on the non-equilibrium thermodynamic properties of partially crystalline water, and focuses on glucose as an example of a typical, well-behaved, water-compatible polymer with a Tm/Tg ratio of 1.42. This dynamics map shows the effect of glucose addition on the Tg of water (in terms of measured values of Tg of the spacially homogeneous, aqueous glass), the Tm of phase-separated ice, and the Th of undercooled solutions.[4] Glucose elevates the Tg of water, through Tg′, up to the Tg of dry amorphous glucose, by its direct effect on the free volume and local viscosity of the resulting sugar-water solution.[107] At concentrations approaching infinite dilution, glucose affects the shape of the liquidus curve by colligative depression of the equilibrium Tm, and also depresses the non-equilibrium Th[296] of ice. However, at finite glucose concentrations in the range of technological importance, there is a non-colligative, very non-equilibrium effect of the solute on Tm, and a similarly anomalous effect on Th.[30] The changes in Tm and Th are empirically related by the ratio $\Delta Th/\Delta Tm \simeq 2$. Thus, at practicable concentrations of glucose, effective values of vapor pressure, osmotic pressure, Tm, Th, and crystal growth rate are all *instantaneous* values, determined by the effective relaxation time of the supra-glassy solution.[30] The dotted portion of the Th curve extrapolated below the Tg curve was included in Figure 57 to allude to the fact that, because this region of the dynamics map corresponds to a kinetically metastable domain in which homogeneous nucleation of ice is prohibited on a practical time scale,[288] such instantaneous values may persist for centuries (e.g., as demonstrated by the crystal growth rates of ice in undercooled PHC-UFW glass[7]). Indeed, the very enormity of the time-dependence beguiles with the appearance of equilibrium (e.g., as illustrated by the kinetics of water ad/absorption via diffusion in amorphous solids[297] or the water desorption "equilibration" of partially crystalline, rubbery substrates[83]).[30]

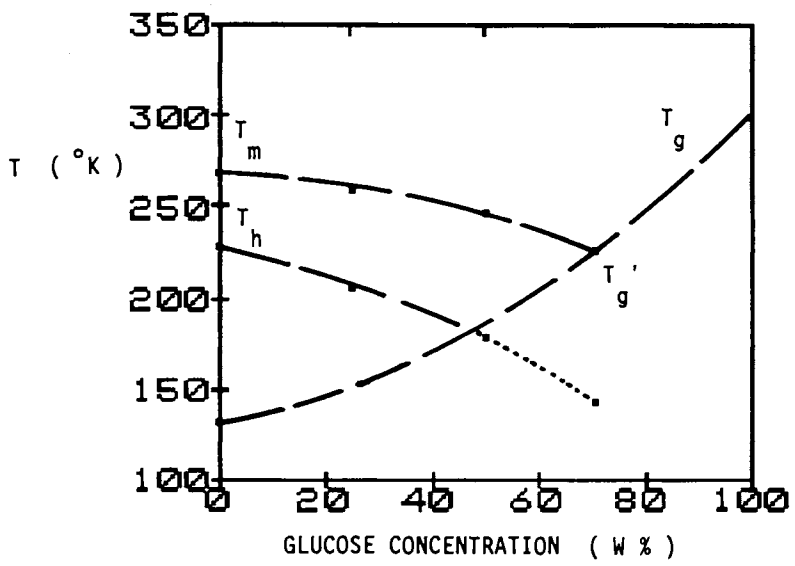

FIGURE 57. Glucose-water state diagram, which illustrates the relationship between the locations on this mobility transformation map of the curves for the glass transition temperature, Tg, the melting temperature, Tm, and the homogeneous nucleation temperature, Th. (From Slade, L. and Levine, H., *Pure Appl. Chem.*, 60, 1841, 1988. With permission.)

Figure 58[30] illustrates the effects of pressure, in the absence of solute, on the same non-equilibrium thermodynamic properties of partially crystalline water described in Figure 57, i.e., the Tg of pure amorphous solid water, the Tm of pure crystalline solid ice, and the Th of undercooled liquid water.[4,191] Increasing pressure elevates the Tg of numerous chemically and thermomechanically diverse polymers by about 20 ± 5°C per kbar (100 MPa).[107,120] The curve of predicted Tg values in Figure 58 was calculated on the basis of this same behavior for glassy water, which would show conventional volume expansion upon softening. Increasing pressure also depresses the Tm and Th of ice (the latter from −40°C at atmospheric pressure to a lower limit of −92°C at 2 kbar), an effect related to water's anomalous volume decrease upon melting.[4,191] The changes in Tm and Th produced by increasing pressure are empirically related by the ratio $\Delta Th/\Delta Tm \simeq 2$,[6] curiously analogous to the effect of solute cited above.[30] Thus, Figure 58 demonstrates that as Tg increases, both Tm and Th decrease anomalously.[30] It should be recalled that a 20°C change in Tg caused by a pressure change of 1 kbar would be comparable to a 5 orders-of-magnitude change in mechanical relaxation rates near Tg.[30]

The effects of a small PHC solute have been compared to the effects of pressure on the same non-equilibrium thermodynamic properties of partially crystalline water, by combining the results in Figures 57 and 58.[30] As illustrated in Figure 59,[30] the concentration and pressure scales were overlaid on this mobility transformation map so that one could compare the Tg of glucose-water glasses, the Tm of phase-separated ice in glucose solutions, and the Th of undercooled glucose solutions, all at atmospheric pressure, to the corresponding values of the predicted Tg of amorphous solid water alone, the Tm of pure crystalline ice, and the Th of undercooled liquid water, all up to 2 kbar. Figure 59 shows that glucose, representing a well-behaved molecular glass-former, at concentrations up to ≃25 w% in the glass, mimics high pressure in its effects on the thermomechanical behavior of water.[30] Both an increase in solute concentration and an increase in pressure result in an elevation of Tg and a concomitant depression of both the non-equilibrium Tm and Th (related by the same ratio $\Delta Th/\Delta Tm \simeq 2$).[30] By avoiding the eutectic be-

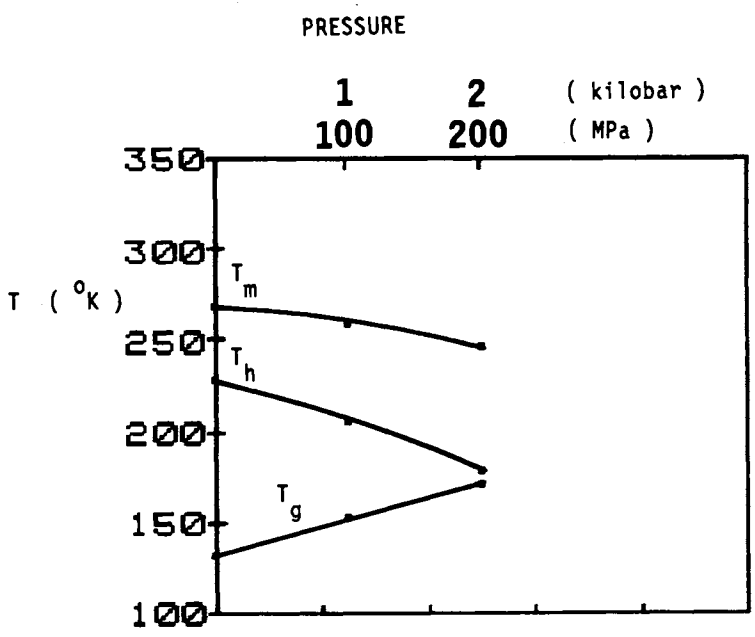

FIGURE 58. State diagram of temperature vs. pressure for pure water, which illustrates the effect of increasing pressure on the Tm, Th, and Tg curves. (From Slade, L. and Levine, H., *Pure Appl. Chem.*, 60, 1841, 1988. With permission.)

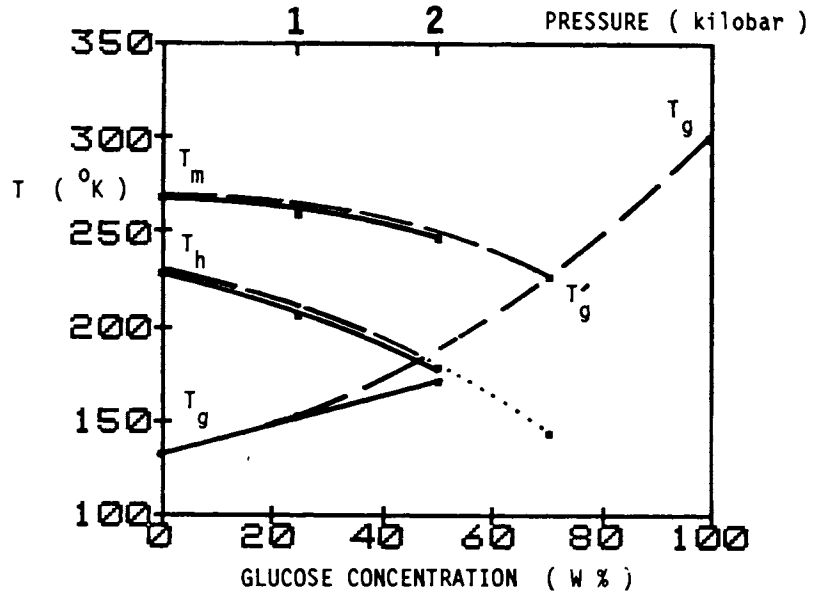

FIGURE 59. A superposition of the state diagrams in Figures 57 and 58, which illustrates the comparison between the effects of added glucose solute and increasing pressure on the non-equilibrium thermodynamic properties of water, in terms of its Tm, Th, and Tg. (From Slade, L. and Levine, H., *Pure Appl. Chem.*, 60, 1841, 1988. With permission.)

havior (i.e., ice I plus ice III) observed at pressures above 2 kbar for water alone[6,191] and instead allowing complete vitrification, higher solution concentrations of glucose ($\gtrsim$70 w%) have an even more drastic effect than pressure on the shapes of the non-equilibrium liquidus and Th curves.[30] So, while high pressure alone is not efficient for the prevention of ice formation, glucose solutions at high concentration,[241] or solutions of other even more ready aqueous-glass formers such as LiCl at much lower concentration ($\simeq$10 w%),[247,288] can be completely vitrified by cooling at atmospheric pressure. The additive effects of pressure and small PHC solute would allow complete vitrification at intermediate solution concentrations.[30] This has been demonstrated by Fahy et al.,[298] with respect to the concentration of a cryoprotectant solution required to achieve complete vitrification on cooling, in the context of vitrification as an approach to the cryopreservation of biological materials. They reported that, for concentrated solutions of a cryoprotectant such as propylene glycol, "high pressures lower Th and elevate Tg, thus shifting the point of intersection to a lower concentration of cryoprotectant".[298] Recent follow-up work by Forsyth and MacFarlane[299] has expanded the examination of the combined effects of solute concentration and pressure (up to 2 kbar) on Th and Tm of aqueous solutions of cryoprotectants such as propylene glycol. Their results showed that the Th-depressing effect of solute (e.g., 20 w% propylene glycol) at the highest pressures, over and above the Th-depressing effect of pressure in the absence of solute, is somewhat less than that predicted by the empirical ratio of $\Delta Th/\Delta Tm \simeq 2$, due to the relatively greater depressing effect of pressure on Tm than on Th of the solutions.[299]

It is worth pointing out that Figure 59 demonstrates that increased pressure serves as an "antiplasticizer", just as solute does, to elevate the Tg of water. However, the antiplasticizing effect of increased pressure is limited by the eutectic behavior of water (to form ice I plus ice III) above 2 kbar, whereas the antiplasticizing effect of solute is unlimited, if solute crystallization is avoided.

Taken together, the results in Figures 53 and 57 through 59 have been used to summarize the effects of water on thermomechanical behavior

of common sugars and the effects of pressure and common sugars on the non-equilibrium thermodynamics of partially crystalline water and aqueous solutions.[30] The aqueous glass curves in Figure 53 have been compared,[30] with emphasis on the recent finding of the striking difference in location on the mobility map of the curves for the two monosaccharides, fructose and glucose.[14] This comparison has shown that the glass curve for sucrose, at <50 w% solute, is located closer to that of fructose than glucose, but at >50 w% solute, sucrose is closer to glucose than fructose. In contrast, PVP-40, at <50 w% solute, is closer to glucose than fructose, but at >50 w% solute, PVP-40 is closer to fructose than glucose. As mentioned earlier, the insight derived from these results has led to the new suggestion that different portions of the glass curve must be controlled by different parameters that determine molecular-level mobility, i.e., Tg is controlled by free volume (a function of inverse $\overline{M}n$) rather than local viscosity at higher values of average MW (i.e., higher solute concentrations in the glass, Cg), but by local viscosity (a function of $\overline{M}w$) rather than free volume at lower values of average MW (i.e., higher water concentrations in the glass, Wg).[30]

The origin of the empirical ratio $\Delta Th/\Delta Tm \simeq 2$[4,6] had been previously obscured by the expectation that the liquidus curve must be colligatively controlled, while the Th curve is in part diffusion-controlled. The results in Figures 53 and 57 through 59 illustrated the parallel dynamic control over the non-equilibrium regions of both the liquidus and nucleation curves.[30] Figure 53 also points out that, at solute concentrations >20 w%, fructose and glucose (of equal MW) solutions have very different Tm, as well as Tg, profiles. So at these PHC concentrations (which are technologically the most important), the Tm curve is certainly not an equilibrium liquidus, but rather a non-equilibrium melting profile, which is affected by the underlying glass behavior.[30] Once again, the explanation for this behavior derives from the WLF kinetics governing the rubbery domain near Tg, where a 20°C temperature interval is equivalent to a range of 5 orders-of-magnitude in relaxation rates. Hence, within practical time frames, the immobility imposed by the glassy domain can have an all-or-nothing effect on homogeneous nucleation and crystal growth.[15,16,104,288]

As mentioned earlier, the effect on water of glucose concentrations up to 25 w% mimics the effect of pressure up to 100 MPa, and is nearly equivalent up to 50 w% glucose and 200 MPa pressure. However, while still higher pressure leads to nucleation of ice II or growth of ice III,[4] glucose concentrations >50 w% lead to continued elevation of Tg and so steadily increasing inhibition of all diffusion-limited processes, including nucleation and crystal growth of ice.[15,16] As a consequence, the lower limit of Th, to which pure water under high pressure can be undercooled without freezing, is −92°C.[4,191] In contrast, a glucose solution, of $C > Cg' \simeq 70$ w%, can be undercooled without limit, and complete vitrification will prevent ice formation in practical time frames.[241] In fact, Franks has calculated that the linear growth rate of ice, in an undercooled aqueous glass of typical viscosity of about 10^{13} Pa s at Tg, would be about 10,000 years per cm.[7] It should also be noted that, as a consequence of the differences between the map locations of the glass curves for fructose and glucose, the effect of fructose on the behavior of water is very different from the effect of pressure.[30] Even at concentrations as low as 20 w%, fructose causes a much greater elevation of the Tg of water and, concomitantly, a greater departure from the equilibrium liquidus curve.

As shown earlier by the results for PHCs in Figure 47, there is no correlation between Tg′ and $\overline{M}n$ of a given solute-UFW mixture, but a very good correlation between Tg′ and $\overline{M}w$. The significance of this finding has been related to the concept of the glass transition as an iso-relaxation state.[30,107] In order to explore the origin of this concept, the glass curves for the four solutes in Figure 53 were compared on the basis of a common value of Tg, and on the basis of a particular, distinctive Tg, as illustrated in Table 7.[30] For convenience, −32°C (the Tg′ of sucrose) was used as a common Tg, equivalent to drawing a horizontal line at Tg = −32°C so that it intersects the glass curves of Figure 53, as shown in Figure 60. The values of Tg′, as operationally invariant properties of the individual solutes, were used as a particular Tg. Then for each solute, the values of Wg or Wg′ corre-

TABLE 7
The Glass Transition as an Iso-Relaxation State. Relaxation Parameters are Compared on the Basis of a Common Value of Tg (−32°C) or Particular Values of Tg (Individual Values of Tg′)[30]

	Based on common Tg = −32°C						Based on particular Tg = Tg′			
Solute	Mw	$\overline{M}n$	$\overline{M}w$	$\overline{M}w/\overline{M}n$	Tg − Tg′ °C	Wg − Wg′ %	$\overline{M}n'$	$\overline{M}w'$	$\overline{M}w'/\overline{M}n'$	% Δ
Fructose	180	36	107	3.01	10	−4	33	101	3.03	<1
PVP-40	40000	46	24407	529	−10	4	51	26006	506	~4
Sucrose	342	46	226	4.93	0	0	46	226	4.93	
Glucose	180	55	140	2.52	11	−4	50	133	2.67	~6

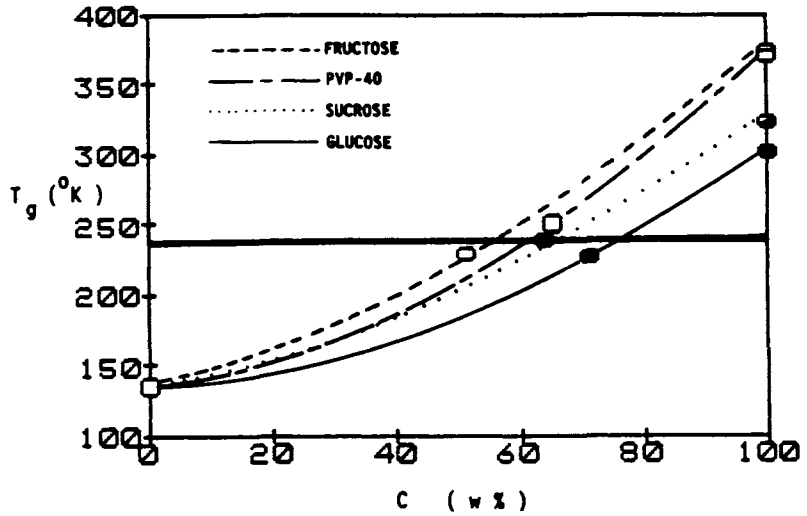

FIGURE 60. The solute-water state diagrams of temperature vs. concentration for fructose, glucose, sucrose, and PVP-40 from Figure 53 (without the liquidus curves), which illustrate the effect of water plasticization on the experimentally measured glass curves, and the location of the invariant point of intersection of the glass curve and the non-equilibrium portion of the liquidus curve at Tg′ and Cg′, for each solute. The horizontal solid line at −32°C intersects the four glass curves at the Tg′ of sucrose.

sponding to the selected values of Tg were used to calculate $\overline{M}n$ and $\overline{M}w$, which govern the relative relaxation behavior. The results in Table 7 showed that, for the glasses that would exist at −32°C, those of sucrose and PVP-40 (solutes very different in MW) would have about the same free volume (as indicated by equivalent $\overline{M}n$ values), but very different local viscosities (as indicated by the corresponding $\overline{M}w$ values). As a general rule, when two polymeric glasses that have the same $\overline{M}n$ but different $\overline{M}w$ are compared at the same temperature in the absence of diluent, local viscosity increases with increasing polydispersity index, $\overline{M}w/\overline{M}n$.[107] Importantly, for polymer-plasticizer blends such as PHC-water solutions, both the Wg composition of the aqueous glass and MW of the dry solute contribute to the shape of the glass curve, the value of the ratio $\overline{M}w/\overline{M}n$, and the associated relaxation behavior.[30] Thus, the aqueous PVP-40 glass, with a much higher $\overline{M}w/\overline{M}n$ ratio, would have a higher local viscosity than the comparable sucrose glass. The results in Table 7 illustrated the point emphasized earlier that the absolute viscosity of the glass at its Tg depends on the nature of the solute and can vary within the range 10^{10} to 10^{14} Pa s. However, despite such a range of absolute viscosities at Tg, the respective ranges of relative relaxation rates that would result at T>Tg can all be described by a master curve based on the

WLF equation with appropriate respective values of the WLF coefficients.[107] The aqueous-glass formers in Table 7 were also compared at their individual Tg′ temperatures and characteristic Wg′ compositions.[30] These results showed, for example, that while the corresponding $\overline{M}n'$ values for PVP-40 and glucose are similar, indicative of similar free volumes, their $\overline{M}w'$ values are very different. Again, this indicated that the aqueous PVP-40 glass at its Tg′ has a much higher local viscosity, and so much longer relaxation times, than the aqueous glucose glass at its Tg′. This comparison shed light on the underlying mechanism for the greater microbiological stability provided by polymers and proteins than by small PHCs in concentrated solutions with equivalent RVPs, which has been observed empirically, and ascribed to a hypothetical ability of polymers to "bind" water more tightly (so-called "polymer water") than can small PHCs (so-called "solute water").[71] The actual mechanism plays an important role in the mold spore germination experiment mentioned earlier and discussed further later with respect to Table 2. Overall, the results in Table 7 demonstrated that the ratio of $\overline{M}w/\overline{M}n$ provides a better prediction of the shape of the glass curve as an iso-state, which requires a description of both the temperature and the moisture content at which relaxation times become limiting, than does MW or $\overline{M}n$ or $\overline{M}w$ alone.[30]

(Further comment on the concept of "polymer water" vs. "solute water" is in order. It has been suggested[30] that this distinction between solutes and polymers, and between their corresponding "states" [i.e., extents of mobility] of water, with respect to the water sorption behavior of such substrates, is artificial, meaningless, and misleading. This speculative concept of "polymer water" vs. "solute water", advocated by Steinberg and co-workers,[71] is completely untested and unproven to date. It has been suggested[15] that the actual basis for a proper distinction among different solid substrates, during non-equilibrium water sorption, lies in the structural state [i.e., completely crystalline, partially crystalline, or completely amorphous] of a given substrate at a given sorption temperature. The "acid test" would be to compare the water sorption behavior at 25°C of two water-compatible substrates, a completely amorphous, high MW polymer [e.g., water-sensitive polyvinyl acetate] and a completely amorphous, low MW solute [e.g., water-soluble maltose], of the same structural and physical [i.e., solid or liquid] states at low moisture contents. PVAc and maltose happen to have essentially the same Tg values of 39°C at 0 w% moisture and about 19°C at 4 w% moisture. Because amorphous maltose and PVAc share essentially the same Tg vs. w% water "glass curve" at these low moisture contents, they would be predicted to show indistinguishable sorption behavior, as solid or rubbery liquid substrates, in the 0 to 4 w% moisture range at 25°C.)

The Tg′-Cg′ point represents the end of ice formation in real time on cooling to $T < Tg'$, and conversely, the beginning of ice melting and concomitant melt-dilution (i.e., the opposite of freeze-concentration) of the solute in the aqueous rubber on heating to $T > Tg'$.[33] For very dilute solutions, the shape of the equilibrium liquidus curve is defined energetically, based on colligative freezing point depression by solute. At solute concentrations near and above the eutectic composition, melting of the metastable solution is described by a non-equilibrium extension of the equilibrium liquidus curve.[4,34] This has been illustrated by the actual state diagram for sucrose-water shown in Figure 61,[33] which was compiled from several sources, including Figure 53.[15,27-30,50,133,300] As mentioned above, the shape of the non-equilibrium extension of the liquidus curve is kinetically determined by the underlying glass curve,[34] as illustrated by the portion of the liquidus curve in Figure 61 between the points Te-Ce and Tg′-Cg′, where Ce is the composition of the eutectic mixture of pure crystalline ice plus pure crystalline solute.[33] Thus, for a typical solute that does not readily undergo eutectic crystallization on cooling (e.g., sucrose), Tg′ does not represent the incidental intersection of an independently existing equilibrium liquidus curve with the glass curve, but rather corresponds to the circumstantial intersection of the non-equilibrium extension of the liquidus curve and the underlying supersaturated glass curve that determined its shape.[30]

The state diagram for sucrose in Figure 61 has provided several noteworthy revelations concerning the relative locations of the glass, soli-

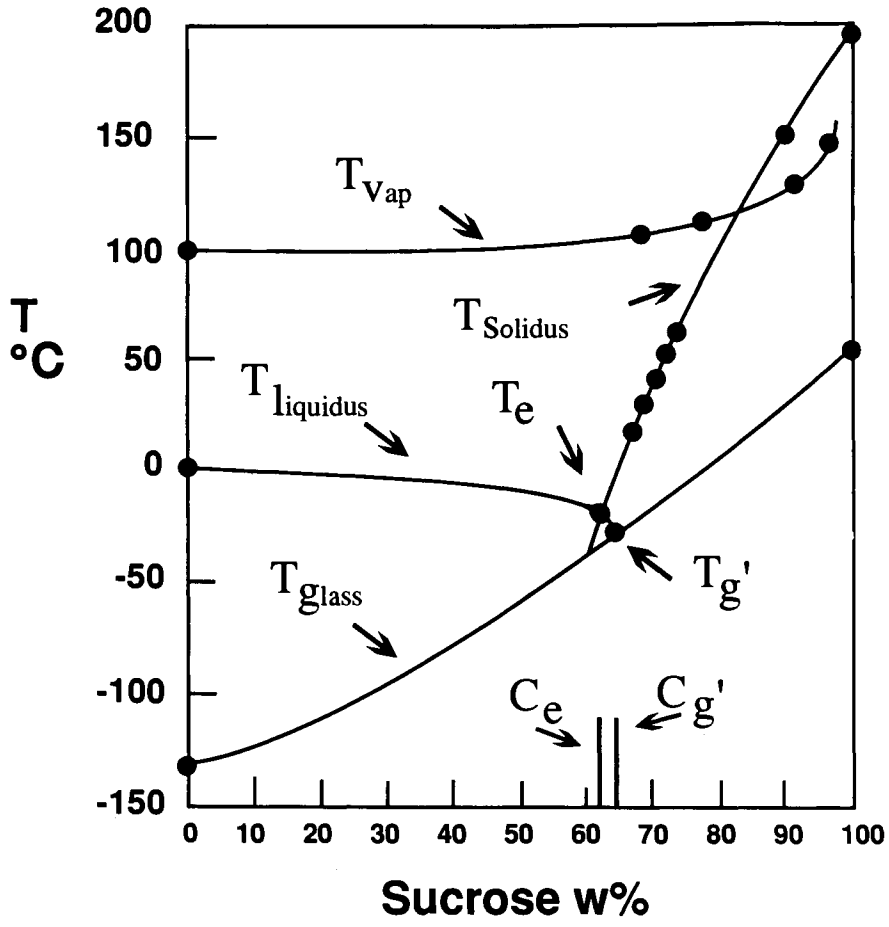

FIGURE 61. Solid-liquid state diagram for the sucrose-water system, illustrating the locations of the glass, solidus, and liquidus curves, and the points Tg′ and Te (eutectic melting temperature), corresponding, respectively, to the intersection of the liquidus (non-equilibrium extension) and glass curves and the intersection of the liquidus and solidus curves. The curve for the vaporization temperature of water as a function of sucrose concentration is also included. (From Levine, H. and Slade, L., *Comments Agric. Food Chem.*, 1, 315, 1989. With permission.)

dus, and liquidus curves.[33] Just as the liquidus curve describes the melting of crystalline solvent, in this case ice, the solidus curve describes the melting of crystalline solute. The melting process is called dilution when crystalline solvent melts in the presence of solution or dissolution when crystalline solute melts in the presence of its saturated solution. The solidus curve for the melting of crystalline sucrose decreases from Tm = 192°C for dry sucrose,[28,30] through several points for saturated sucrose solutions at different temperatures,[300] to Te = −14°C at Ce = 62.3 w% sucrose.[133] The glass curve decreases from Tg = 52°C for dry amorphous sucrose,[28,30,50] through Tg′ = −32°C at Cg′ = 64 w% sucrose,[29] to Tg = −135°C for pure amorphous solid water. The point Te-Ce is located at the intersection of the equilibrium solidus and equilibrium liquidus curves, while the point Tg′-Cg′ is located at the intersection of the non-equilibrium liquidus and glass curves. As mentioned earlier with respect to Figure 35, the temperature interval ΔT = Te-Tg′ between Te (as a particular value of Tm of ice) and Tg′ would correspond to an atypically small WLF rubbery domain of 18°C (relative to the typical Tm − Tg range of about 100°C for many diluent-free, synthetic amorphous polymers[30,107]) over which the microscopic viscosity of the sucrose-water solution would be estimated to decrease by about 13 orders of mag-

nitude from the characteristic ηg at Tg'.[30,89,107] (This value of $\Delta\eta$ was estimated as follows:[33] (1) at Tg'-Cg', $\eta g \simeq 10^{13}$ Pa s,[89] (2) at 20°C, $\eta \simeq 0.1$ Pa s for 62.3 w% sucrose,[300] and (3) at Te-Ce, $\eta e \simeq 1$ Pa s, based on an assumption of Arrhenius behavior between −14 and 20°C [i.e., at $T > Tm$, $Q_{10} = 2 \Rightarrow$ a factor of 10 change for a ΔT of 33°C].)[30] Consequently, the rates of deteriorative changes that depend on constrained diffusion in a frozen aqueous system of pure sucrose would be predicted correspondingly to *increase* by about 13 orders of magnitude vs. the rates at Tg',[33] with profound implications for the storage stability and kinetics of collapse processes in frozen food systems (e.g., ice cream and other frozen desserts and novelties) for which a freeze-concentrated sucrose solution could serve as a limiting model.[32,34] It has been noted that the 13 orders of magnitude predicted from the WLF equation[101] for the decrease in microscopic viscosity and concomitant increase in diffusion-limited relaxation rate over a rubbery domain with a temperature span from Tg' to Tg' + 18°C are based only on the effect of increasing temperature above the Tg' reference state, and not on any effect of dilution due to the melting of ice, which would begin on heating to $T > Tg'$, on the solute concentration in the rubbery fluid.[33] Such an effect of melt-dilution would obviously cause a further decrease in viscosity over and above the WLF-governed behavior. The resultant effect on diffusion-limited reaction rate (e.g., enzyme-substrate interactions)[8] would not be so obvious. The rate could increase *or* decrease, depending on whether or not the solute being diluted is a participant in the reaction.[33] The sucrose-water system shown in Figure 61 is remarkable with respect to the minimal effect of melt-dilution on heating from Tg' to Te. The sucrose concentration only decreases by 1.7 w%, from Cg' = 64 w% to Ce = 62.3 w%, over a temperature range of 18°C, due to the near-vertical path (compared to the path of colligative freezing point depression in the equilibrium portion) of the extremely non-equilibrium extension of the liquidus curve at $C > Ce$.[33] Despite this fact, the above discussion is not meant to negate the importance of melt-dilution (stressed by Simatos et al.[98]) as temperature is increased above Tg'. Analogous to experience in drier systems at $T > Tg'$ and $W < Wg'$,[28] either addition of water (ΔW) or increase in temperature (ΔT) above the glass curve accomplishes decreased relaxation times. However, water-rich systems differ from drier systems in that water is equivalently as effective as temperature as a plasticizer for drier systems at $C > Cg'$, but the practical limit of efficacy of water as a plasticizer is exceeded at $C < Cg'$.[26,30]

PVP is a completely water-miscible, non-crystallizable, synthetic, flexible-coil polymer that represents a much-studied model for amorphous polymeric food materials.[4] The state diagram for PVP-water (PVPs of $\overline{Mn} = 10^4$, 4.4×10^4, and 7×10^5) in Figure 62,[15] compiled from several sources,[4,8,74,133,242,301] is the most complete one presently available for this polymer.[27] We include it here, because this figure exemplifies in a single diagram a number of the points illustrated by the other state diagrams described earlier. For example, as shown in Figure 62, PVP exhibits a smooth Tg curve from about 100°C for dry PVP-44 to −135°C for amorphous solid water. As with the various other water-compatible materials described earlier, the plasticizing effect of water on the Tg of PVP is most dramatic at low moisture contents, such that for PVP-44, Tg decreases by about 6°C/w% water for the first 10 w%. Figure 62 also illustrates that the phenomenological threshold temperatures for different collapse processes all correspond to the particular Tg' (or other Tg relevant to the situation in question), which is a function of the MW and concentration of the solute.[8,27] Thus, for PVP-44, $Tg' \simeq Tr \simeq Tc \simeq -21.5$°C and $Cg' \simeq 65$ w% PVP ($Wg' \simeq 0.54$ g UFW/g PVP),[4,8,133,242] while for PVP-700, $Tg \simeq Tc \simeq T$ sticky point $\simeq 120$°C at about 5 w% residual moisture.[27] The equivalent of Tr for ice or solute recrystallization, Tc for collapse, and the concentration-invariant Tg' for an ice-containing system has explained[8] why Tr and Tc are always observed to be concentration-independent for any initial solute concentration lower than Cg',[4,260] as illustrated in Figure 62. Figure 62 also illustrates the effect of increasing solute MW on dry Tg (which increases in the order PVP-10 < PVP-44 < PVP-700) and on Tg' and Cg'. As mentioned earlier, with increasing solute

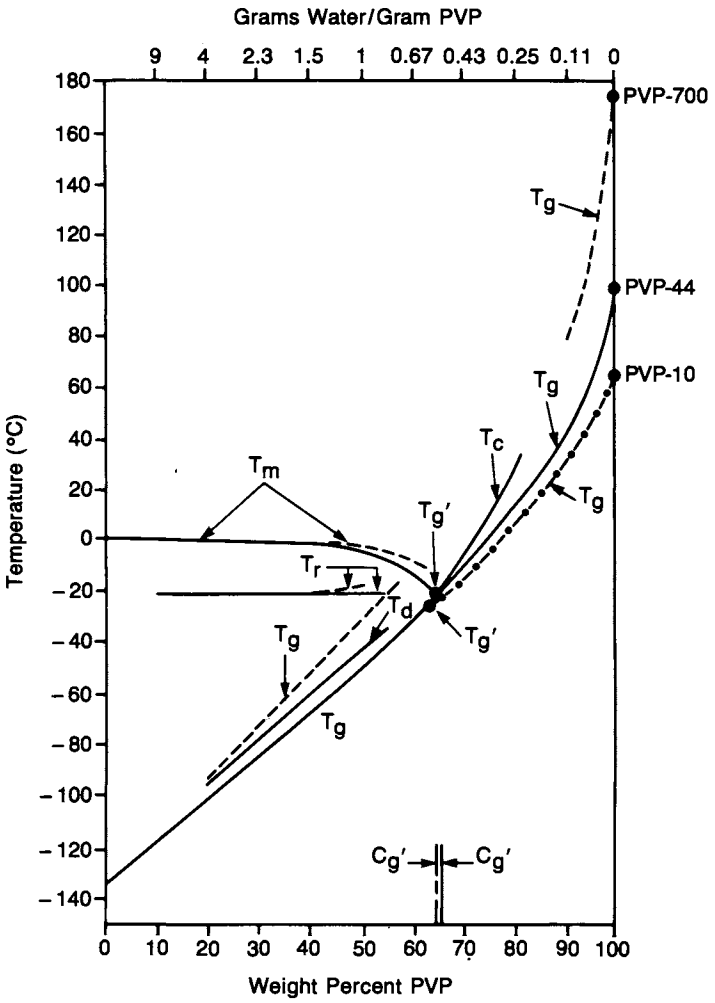

FIGURE 62. Solid-liquid state diagram for water-PVP, showing the following transitions: Tm, Tg, Tg', Td, Tr, Tc. (—— = PVP-44, - - - - - = PVP-700, -●-●-●-●-●-●-●-●- = PVP-10.) (From Levine, H. and Slade, L., *Water Science Reviews,* Vol. 3, Franks, F., Ed., Cambridge University Press, Cambridge, 1988, 79. With permission.)

MW, the Tg'-Cg' point moves up the temperature axis toward 0°C and to the right along the composition axis toward 100 w% solute.[8]

C. Cryostabilization Technology

"Cryostabilization technology"[8,27,31-34] represents a new conceptual approach to a practical industrial technology for the stabilization during processing and storage of frozen, freezer-stored, and freeze-dried foods. This technology emerged from our food polymer science research approach and developed from a fundamental understanding of the critical physicochemical and thermomechanical structure-property relationships that underlie the behavior of water in all non-equilibrium food systems at subzero temperatures.[4,6] Cryostabilization provides a means of protecting products, stored for long periods at typical freezer temperatures (e.g., Tf = −18°C), from deleterious changes in texture (e.g., "grain growth" of ice, solute crystallization), structure (e.g., collapse, shrinkage), and chemical composition (e.g., enzymatic activity, oxidative reactions such as fat rancidity, flavor/color degradation). Such changes are exacerbated in many typical fabricated foods whose formulas are dominated by low MW carbohydrates. The key to this protection, and resulting improvement in product qual-

ity and storage stability, lies in controlling the structural state, by controlling the physicochemical and thermomechanical properties, of the freeze-concentrated amorphous matrix surrounding the ice crystals in a frozen system. As alluded to earlier, the importance of the glassy state of this maximally freeze-concentrated solute-UFW matrix and the special technological significance of its particular Tg, i.e., Tg′, relative to Tf, have been described and illustrated by solute-water state diagrams such as the idealized one in Figure 63.[32] Upon a foundation of pioneering studies of the low-temperature thermal properties of frozen aqueous model systems by Luyet, MacKenzie, Rasmussen,[133,135,240-242,254,259,302] and Franks,[4-7,74] an extensive cryostabilization technology data base of DSC results for carbohydrate and protein food ingredients has been built.[8,25-34] As reviewed earlier, DSC results for the characteristic Tg′ values of individual carbohydrate and protein solutes have demonstrated that Tg′ is a function of MW for both homologous and quasi-homologous families of water-compatible monomers, oligomers, and high polymers. Examples of how the selection and use of appropriate ingredients in a fabricated product have allowed the food technologist to manipulate the composite Tg′, and thus deliberately formulate to elevate Tg′ relative to Tf and so enhance product stability, have been described,[8,25-34] as reviewed below.

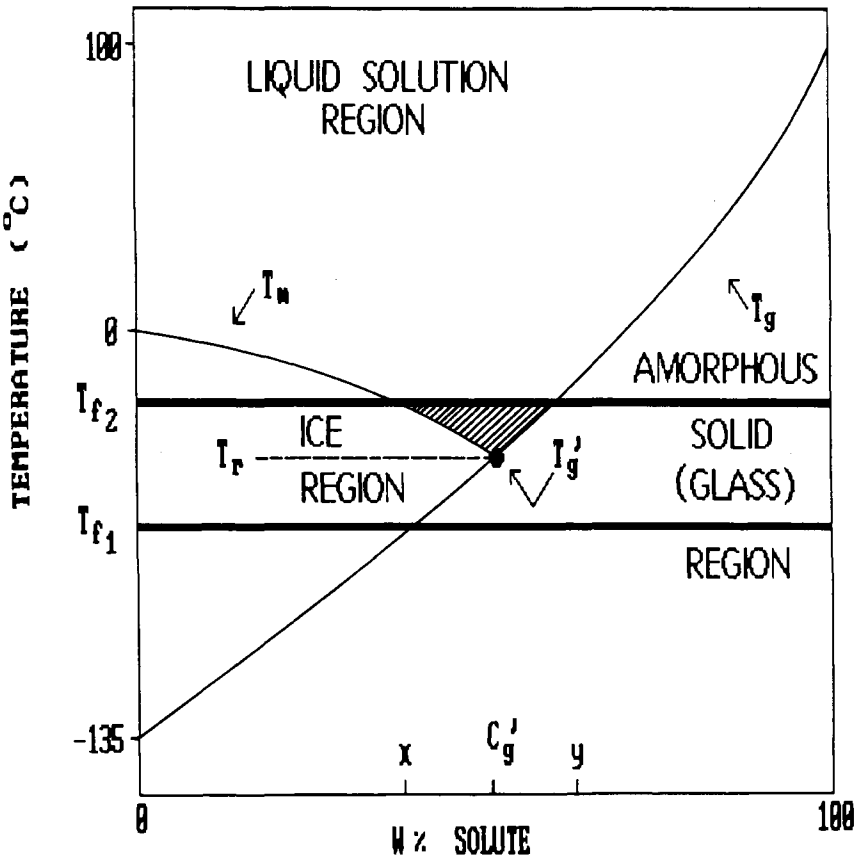

FIGURE 63. Idealized state diagram of temperature vs. w% solute for an aqueous solution of a hypothetical small carbohydrate (representing a model frozen food system), illustrating the critical relationship between Tg′ and freezer temperature (Tf), and the resulting impact on the physical state of the freeze-concentrated amorphous matrix. (From Levine, H. and Slade, L., *Cryo.-Lett.*, 9, 21, 1988. With permission.)